

**Design, synthesis and pharmacological
evaluation of novel fluorescent ligands
for the mu-opioid receptor**

William Marshall

BSc, MSc

Thesis submitted to the University of Nottingham
for the degree of Doctor of Philosophy

March 2021

Abstract

The mu opioid receptor (MOR) belongs to the superfamily of G-protein coupled receptors (GPCRs) and remains an important target in the management of pain and addiction, with an emerging role in promoting tumour growth. Understanding of the complex role of the MOR in these signalling pathways would be aided by further study of receptor-ligand interactions. Development of fluorescent ligands to target the MOR may provide the necessary tools to study such receptor pharmacology and localisation in healthy and diseased tissue.

Previously described high affinity fluorescent MOR ligands have been unsuitable for confocal imaging studies due to high levels of non-specific interactions with the cellular membrane. The introduction of amino acid-based linker moieties to separate the orthostere and fluorophore of fluorescent ligands has been reported to improve receptor binding affinity, receptor subtype selectivity and the confocal imaging properties of fluorescent ligands for various GPCRs.

This thesis describes the development of novel fluorescent MOR ligands based upon the opioid antagonists naltrexone and alvimopan which also contain amino acid-based linkers. Evaluation of the reported SAR of small molecule opioid receptor ligands was used to inform orthostere selection and location of linker attachment. Different amino acid linker compositions were investigated through the synthesis and evaluation of MOR binding affinity of non-fluorescent congeners in a series of TR-FRET competition binding assays. Coupling of the optimised congeners to red-emitting fluorophores (BODIPY 630/650 or sulfo-Cy5) afforded nine amino acid-linked fluorescent ligands for MOR. Assessment of MOR binding affinity of the fluorescent ligands was achieved in TR-FRET saturation binding assays.

Investigation of the linker composition of β -naltrexamine-based ligands did not identify any significant differences in MOR binding affinity between non-

fluorescent congeners containing different amino acid linkers. However, a subsequent series of BODIPY 630/650-containing fluorescent ligands were identified to possess sub-nanomolar MOR binding affinities ($pK_D = 9.20-9.58$).

Non-fluorescent derivatives of (3*R*,4*R*)-3,4-dimethyl-4-(3-hydroxyphenyl) piperidine displayed improved MOR binding affinity when a phenylalanine moiety was bound via an *N*-propanoate, but further elaboration of the linker was found not to improve binding further. High affinity fluorescent ligands for the MOR containing the BODIPY 630/650 fluorophore were once more identified utilising this design approach ($pK_D = 8.14-8.47$).

Acknowledgements

I would like to thank my supervisors Professor Barrie Kellam, Dr Shailesh Mistry, Dr Steve Briddon and Professor Peter Scammells for their guidance and support throughout the project.

I consider myself extremely lucky to have been able to meet so many friends across two continents throughout the course of this project, and I am extremely grateful for their insight and encouragement. To that end, I would like to thank the present and former members of the BDI medicinal chemistry groups, the Cell Signalling Research Group and the Scammells research group at MIPS.

I would particularly like to acknowledge Dr Tim Fyfe for his support and advice in numerous aspects of my chemistry, and Dr Leigh Stoddart for her guidance in pharmacological experiments. Both went above and beyond to help me on countless occasions, for which I am truly grateful.

I would also like to thank Lee Hibbett and Dr Jason Dang for their technical assistance and advice, as well as recognise all of the technicians at both the University of Nottingham and Monash University.

Without the support of my friends and family this project would simply not have been completed. I would like to thank my parents and sister for their continued encouragement and support through many challenging times. I would especially like to thank Dr Olivia Webster for her belief in me, for her many hours of proofreading, and for her kindness and patience in times of need.

Finally, I would like to thank the School of Pharmacy, University of Nottingham for funding this project.

Abbreviations

A ₁ AR	A ₁ adenosine receptor
A ₃ AR	A ₃ adenosine receptor
ANOVA	analysis of variance
ATP	adenosine triphosphate
β-FNA	β-funaltrexamine
BODIPY	boron-dipyrromethene
BBB	blood-brain barrier
cAMP	cyclic adenosine monophosphate
CBS catalyst	Corey-Bakshi-Shibata catalyst ((3 <i>aR</i>)-1-methyl-3,3-diphenyl-3 <i>a</i> ,4,5,6-tetrahydropyrrolo[1,2- <i>c</i>][1,3,2]oxazaborole)
CNS	central nervous system
CYP2D6	cytochrome P450 2D6
DAMGO	[<i>D</i> -Ala ² , <i>N</i> -MePhe ⁴ , Gly-ol]-enkephalin
DCM	dichloromethane
DIPEA	diisopropylethylamine
DMAP	4-dimethylaminopyridine
DMF	dimethylformamide
DMHPP	(3 <i>R</i> ,4 <i>R</i>)-3,4-dimethyl-4-(3-hydroxyphenyl) piperidine
DMSO	dimethyl sulfoxide
DMT	dimethyl tyrosine
DOR	delta opioid receptor
FCS	fluorescence correlation spectroscopy
FITC	fluorescein isothiocyanate
Fmoc	fluorenylmethyloxycarbonyl
FP	fluorescence polarisation
FRET	fluorescence resonance energy transfer
GDP	guanosine diphosphate
GI	gastrointestinal

GIRK	G protein–coupled inwardly rectifying potassium channel
GPCR	G protein-coupled receptor
GTP	guanosine triphosphate
H ₁ R	histamine H ₁ receptor
HBSS	HEPES-buffered saline solution
HBTU	(2-(1 <i>H</i> -benzotriazol-1-yl)-1,1,3,3-tetramethyluronium hexafluorophosphate
HCTU	<i>O</i> -(1 <i>H</i> -6-chlorobenzotriazole-1-yl)-1,1,3,3-tetramethyluronium hexafluorophosphate
HEK293	human embryonic kidney 293 cells
HOBt	hydroxybenzotriazole
HPLC	high performance liquid chromatography
KOR	kappa opioid receptor
LCMS	liquid chromatography-mass spectrometry
Lumi4-Tb	Lumi4-terbium cryptate
M ₃ R	M ₃ muscarinic receptor
<i>m</i> CPBA	<i>meta</i> -chloroperbenzoic acid
MNTX	methylnaltrexone
MOR	mu opioid receptor
MPTP	1-methyl-4-phenyl-1,2,3,6-tetrahydropyridine
N/OFFQ	nociception/orphanin FQ
NBD	nitrobenzofurazan
NHS	<i>N</i> -hydroxysuccinimide
NIR	near-infrared
NSCLC	non-small cell lung cancer
OIC	opioid-induced constipation
OR	opioid receptor
P-gp	P-glycoprotein
PAMORA	peripherally acting MOR antagonists
PEG	polyethylene glycol

PKC	phosphokinase C
PLC	phospholipase C
POI	postoperative ileus
PNS	peripheral nervous system
PyBOP	benzotriazol-1-yloxytripyrrolidinophosphonium hexafluorophosphate
S ₀	singlet ground state
S ₁	singlet excited state
SAR	structure-activity relationship
SEM	standard error of mean
STAB	Sodium triacetoxymethylborohydride
Sulfo-Cy5	sulfo-cyanine5
T ₁	triplet excited state
TBS	<i>tert</i> -butyldimethylsilyl
TEA	Triethylamine
TFA	trifluoroacetic acid
TFFH	tetramethylfluoroformamidinium hexafluorophosphate
Tic	tetrahydro-isoquinoline-3-carboxylic acid
TIPS	triisopropylsilane
TLC	thin layer chromatography
TR-FRET	time-resolved fluorescence resonance energy transfer
TRPV1	transient receptor potential cation channel subfamily V member 1
XAC	xanthine amine congener

Table of contents

Abstract.....	i
Acknowledgements	iii
Abbreviations.....	iv
Table of contents	vii
1. Introduction	1
1.1 G protein-coupled receptors	1
1.2 Opioid receptors	2
1.2.1 Opioid receptors as therapeutic targets.....	4
1.2.2 The mu opioid receptor in cancer.....	7
1.3 Studying ligand-receptor interactions	8
1.3.1 <i>In silico</i> modelling	8
1.3.2 Radioligand binding assays	9
1.3.3 Fluorescent ligands	10
1.4 Fluorescent opioid receptor ligands.....	22
1.5 Research aims	27
2. Design, synthesis and pharmacological evaluation of β -naltrexamine-based fluorescent ligands.....	30
2.1 Structure-activity relationships (SARs) of morphinan opioids.....	30
2.1.1 The morphinan core structure.....	31
2.1.2 The 4,5 α -epoxy bridge.....	32
2.1.3 The 3-hydroxyl group.....	33
2.1.4 Modification of the 6-position.....	36
2.1.5 Modification of the 7-position via a 6-14 bridge	40
2.1.6 <i>N</i> -Alkylation	42
2.1.7 Modification of the 14-position.....	44
2.2 Selection of a lead molecule and fluorescent ligand design	46
2.2.1 Lead molecule selection	46
2.2.2 Fluorescent ligand design	48
2.3 Non-fluorescent β -naltrexamine congeners.....	49
2.3.1 <i>In silico</i> modelling	50
2.3.2 Synthesis of β -naltrexamine single amino acid congeners.....	55
2.3.3 MOR binding affinity of the non-fluorescent β -naltrexamine congeners ..	61
2.4 Synthesis and pharmacological evaluation of fluorescent ligands.....	64

2.4.1	Synthesis of fluorescent β -naltrexamine compounds	65
2.4.2	MOR binding affinity of fluorescent β -naltrexamine compounds.....	66
2.5	Discussion	70
3	Design, synthesis and pharmacological evaluation of 3,4-dimethyl-4-(3-hydroxyphenyl) piperidine-based fluorescent ligands	74
3.1	Selection of a lead molecule.....	74
3.2	SARs of (3 <i>R</i> ,4 <i>R</i>)-3,4-dimethyl-4-(3-hydroxyphenyl) piperidine structures.....	76
3.2.1	Structural determinants of function	76
3.2.2	Modification of the aromatic ring.....	79
3.2.3	<i>N</i> -substitution	82
3.2.4	Modification of the piperidine ring	86
3.3	Fluorescent ligand and non-fluorescent congener design	87
3.4	Synthesis of 3,4-dimethyl-4-(3-hydroxyphenyl) piperidine	89
3.4.1	Enantioselective synthetic route	90
3.4.2	Non-enantioselective synthetic route	95
3.5	First generation non-fluorescent congeners	97
3.5.1	Synthesis of enantiomeric DMHPP congeners	98
3.5.2	MOR binding affinities of enantiomeric DMHPP congeners	99
3.5.3	Synthesis of further single amino acid congeners	101
3.5.4	MOR binding affinity of single amino acid congeners	102
3.6	Second generation non-fluorescent congeners	106
3.6.1	Synthesis of tripeptide congeners	107
3.6.2	MOR binding affinity of tripeptide congeners.....	113
3.7	Fluorescent 3,4-dimethyl-4-(3-hydroxyphenyl) piperidine-based compounds	115
3.7.1	Synthesis of fluorescent β -naltrexamine compounds.....	116
3.7.2	MOR binding affinity of fluorescent β -naltrexamine compounds.....	119
3.8	Discussion	122
4	General discussion and conclusion.....	125
4.1	General discussion	125
4.2	Further <i>in vitro</i> characterisation.....	126
4.3	Future works.....	127
4.4	General conclusions.....	130
5	Experimental.....	132
5.1	General chemistry.....	132
5.2	General pharmacology	208

5.3 <i>In silico</i> modelling	211
6. References	212

1. Introduction

1.1 G protein-coupled receptors

G protein-coupled receptors (GPCRs) represent the largest family of cell-surface receptors and the most frequently targeted receptor family for pharmaceutical intervention and research.^{1, 2} Its members display a vast and diverse range of functions, but all possess a conserved structure and primary mechanism of action. Structurally, GPCRs consist of seven transmembrane α -helices arranged in a non-linear barrel shape.^{1, 3} These helices are connected by less structured extracellular and intracellular loops with an extracellular *N*-terminal region and intracellular *C*-terminal region (**Figure 1-1**).^{1, 3} Regulation of GPCR signalling is activated endogenously by peptide, hormone and neurotransmitter agonists, but intervention by exogenous drugs allows signalling to be manipulated for medical and research purposes.

Receptor activation by orthosteric ligand binding typically occurs within the transmembrane bundle causing a conformational change in receptor structure that allows new cytoplasmic interactions to occur.¹ Binding of a heterotrimeric G protein to the intracellular region of a GPCR can occur before or after receptor activation, with activation resulting in the exchange of a bound guanosine diphosphate (GDP) molecule for guanosine triphosphate (GTP).⁴ The GTP-bound G protein is released from the receptor and the G protein subunits disperse. The GTP-bound α -subunit can interact with proteins elsewhere in the cell, with further signalling induced by hydrolysis of GTP to GDP. In this inactive state, the α -subunit can reunite with the $\beta\gamma$ -subunit complex - which can also engage in signalling pathways while separated - and reassociate with the GPCR (**Figure 1-1**).

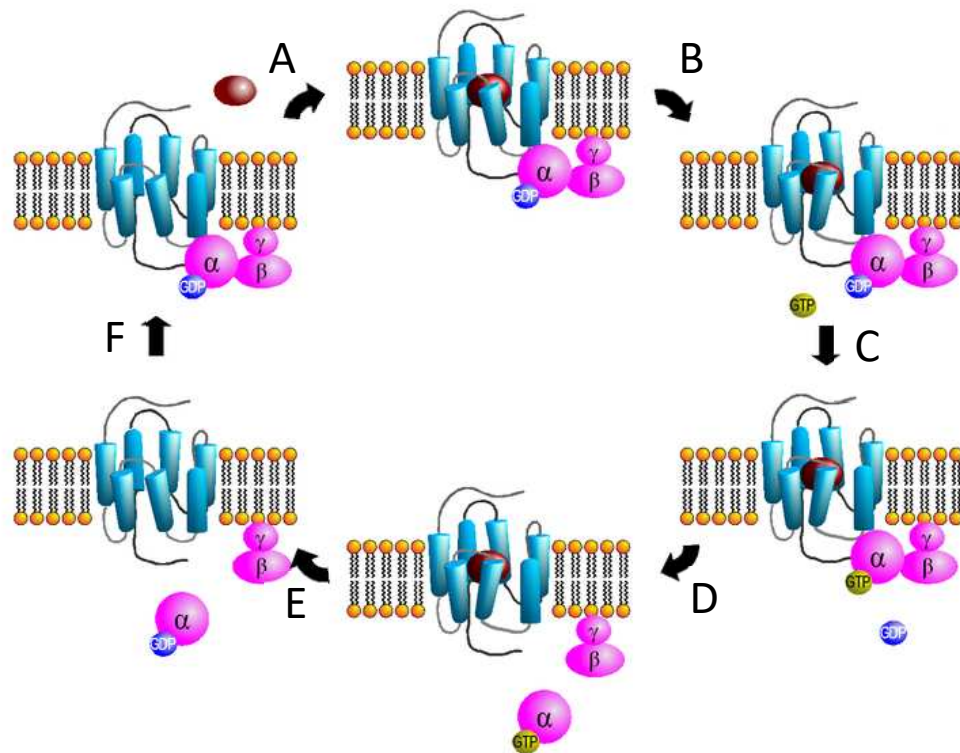


Figure 1-1: A representation of GPCR activation and G protein signalling.

Source: Sven Jahnichen, 24.04.2006.

The GPCR structure is composed of seven transmembrane helices joined by intracellular and extracellular loops. They are also characterised by an extracellular *N*-terminal region and an intracellular *C*-terminal region. (A) An orthosteric agonist can bind to the extracellular binding site. (B) The bound agonist switches the GPCR into an active conformation. (C) In this state, the G protein-bound GDP is exchanged for GTP. (D) With GTP bound, the α - and $\beta\gamma$ -subunits dissociate. (E) Signalling interactions made by the α -subunit result in hydrolysis of GTP to GDP. The agonist dissociates from the receptor binding site, returning it to the inactive conformation. (F) The inactive conformation of the GPCR is able to bind to a GDP-bound G protein heterotrimer.

1.2 Opioid receptors

The opioid family of receptors (ORs) are members of the class A gamma subgroup of GPCRs which bind a $G_{i/o}$ trimer via the C-terminus of the active receptor.⁵ The dissociated $\alpha_{i/o}$ subunit inhibits adenylyl cyclase activity, preventing production of cyclic adenosine monophosphate (cAMP) from adenosine triphosphate (ATP), leading to transient receptor potential cation

channel subfamily V member 1 (TRPV1) ion channel inhibition.⁶ The $\beta\gamma$ subunit complex can also interact with various membrane-bound ion channels, including pre- and post- synaptic Ca^{2+} ion channels and G protein-coupled inwardly rectifying K^+ (GIRK) channels.^{7, 8} It is in these ways that the ORs are able to modulate neuronal excitation and neuropeptide release, resulting in their antinociceptive effects (**Figure 1-2**).^{5, 9}

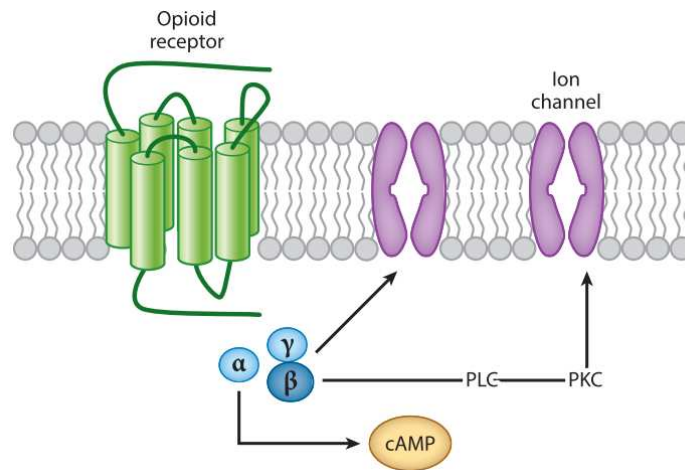


Figure 1-2: Opioid receptor signalling by activated G protein subunits.⁵

Source: Stein (2016)⁵

Activation of an OR results in the release of its G protein subunits. The $\alpha_{i/o}$ subunit inhibits adenylyl cyclase activity, leading to TRPV1 ion channel inhibition due to lower cAMP levels. The $\beta\gamma$ subunit complex can interact with various membrane-bound ion channels either directly, or via phospholipase C/phosphokinase C (PLC/PKC) pathways.⁵

ORs are also able to recruit various kinases to phosphorylate their cytoplasmic regions, including GPCR kinases (GRK), which can recruit arrestin.⁹ Once bound, arrestin desensitises the OR by preventing coupling to G proteins and initiates receptor internalisation and recycling or degradation.⁹

Sequence analysis of cDNA in mice with selective deletion of genes confirms only three OR genes exist: the mu (MOR), delta (DOR) and kappa (KOR) receptors.¹⁰ Other OR subtypes have been proposed, including the nociception/orphanin FQ (N/OFQ), epsilon and sigma receptors, but none are widely considered to be “true” ORs due to significant differences in gene sequence or receptor function.⁵ For this reason, these additional receptors

were not considered further in this project. There is some structural variety amongst the three major ORs due to post-translational modifications and gene splicing.¹⁰ Changes in functionality can also be obtained through the formation of dimers and oligomers.¹⁰ Additionally, different ligands can elicit different effects at the same receptor through allosteric modulation and biased signalling.^{10, 11}

ORs are implicated in the regulation of numerous signalling pathways and physiological responses. Though most commonly known for their role in nociception and analgesia, OR activation is additionally associated with constipation, respiratory depression, convulsions, anxiety, diuresis and reduction of inflammation.⁵ This results from the wide distribution of ORs in different cells of the body, including neurons of the peripheral (PNS) and central (CNS) nervous systems, neuroendocrine cells, immune cells and cells of the gastrointestinal (GI) tract.⁵

Endogenous peptidic OR ligands are known to regulate these effects. The endorphins, enkephalins and dynorphins share the “opioid motif”, a common *N*-terminal Tyr-Gly-Gly-Phe-Met/Leu sequence responsible for orthosteric OR binding. Receptor subtype selectivity is determined by the remaining *C*-terminal regions of these polypeptides: β -endorphin and the enkephalins act primarily at MOR and DOR, and the dynorphins selectively bind to KOR.⁵ Endomorphins do not contain the “opioid motif”, but are able to selectively bind MOR.⁵

1.2.1 Opioid receptors as therapeutic targets

A broad range of OR ligands have been developed to target the pathways regulated by ORs for clinical benefit. Some OR ligands, such as the natural products of *Papaver somniferum* (opium poppy), morphine (**1**) and codeine (**2**), have been used in medicine for millennia,¹² while novel OR ligands continue to be approved for medicinal use.¹³

A range of different opioid agonists are used therapeutically (**Figure 1-3**) with differences in prescribing based not only on the level of analgesia required, but also the route of administration, desired onset and duration, as well as the side effect profile of the drug.^{5, 14-16} OR agonists are primarily prescribed for pain; other effects are usually off-target interactions rather than desired outcomes.¹⁴⁻¹⁶ The most commonly prescribed opioid agonists - morphine (**1**), codeine (**2**), oxycodone (**3**), tramadol (**4**), fentanyl (**5**) and many of their derivatives - act primarily at the MOR.^{5, 14, 15}

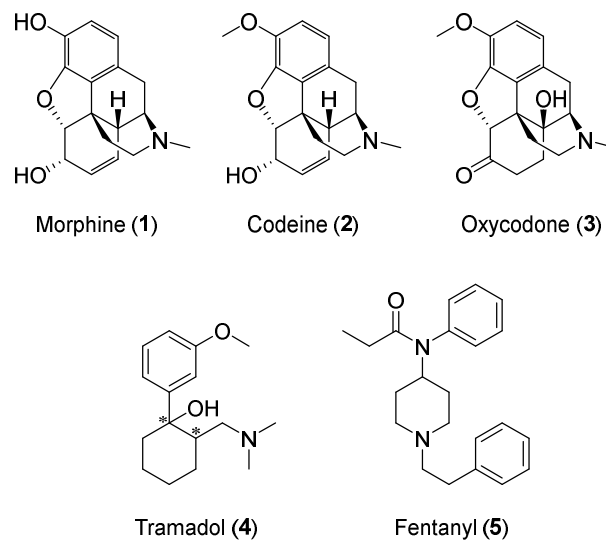


Figure 1-3: Structures of the most commonly prescribed opioid agonist.¹⁴

The structures of the most commonly prescribed OR agonist drugs in England. Tramadol is marketed as a racemic mixture of the 1*S*,2*S* and 1*R*,2*R* enantiomers.

OR antagonists are commonly prescribed to deal with the side effects of opioid use or overuse. Clinically approved OR antagonists (**Figure 1-4**) can be split into two groups: centrally acting MOR antagonists, which are able to penetrate the blood-brain barrier (BBB) and act throughout the body, and peripherally acting MOR antagonists (PAMORAs), whose activities are restricted to peripheral cells. The peripheral selectivity of PAMORAs results from physicochemical properties which limit GI absorption and result in poor BBB penetrability.

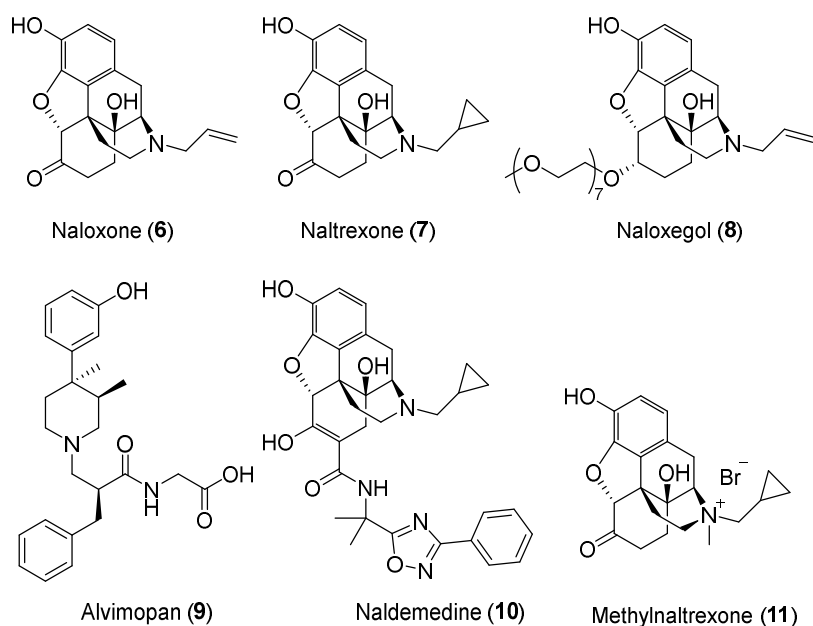
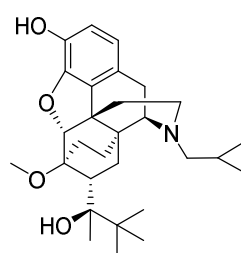


Figure 1-4: Structures of clinically approved opioid antagonists.

Bowel related issues are the most common side effects of opioid use, whether following surgery or from treatment of chronic cancer pain, and include opioid-induced constipation (OIC) and postoperative ileus (POI).¹⁷ OIC results from increased intestinal fluid absorption due to alterations to MOR- and DOR-regulated K⁺ channel activation in GI cells.¹⁷ Methylnaltrexone (MNTX) (**11**), naloxegol (**8**), and the recently approved naldemedine (**10**) are all approved opioid antagonists for the treatment of OIC. POI, the loss of coordinated bowel propulsion following surgery, can be treated by alvimopan (**9**), another peripherally acting MOR antagonist. Opioid agonists that are prescribed for surgical pain act through the MOR to block the release of neurotransmitters from excitatory motor neurons and stimulate the release of neurotransmitters from inhibitory motor neurons, causing this lack of GI motility.¹⁸ Antagonism of peripheral ORs can treat these conditions without impacting CNS analgesia by centrally-acting OR agonists.

Naloxone (**6**) and naltrexone (**7**) possess high bioavailability from the gut and are able to penetrate the BBB and act on the ORs of the CNS.¹⁵ They are used to treat overdose of opioid agonists and in addiction therapy, although antagonist treatment alone does not prevent the cravings associated with opioid withdrawal so has poor compliance.¹⁵

OR ligands with more complex pharmacological profiles have been developed, such as the mixed agonist/antagonist buprenorphine (**12**), which is a partial agonist of MOR that acts as an antagonist of KOR and DOR.^{19, 20} The high MOR binding affinity, slow dissociation kinetics, and partial MOR agonist profile of buprenorphine (**12**), make it suitable for treatment of opioid dependency, often in a fixed-dose formulation with naloxone (**6**), as it prevents other opioids from eliciting a full effect while decreasing cravings and withdrawal.²⁰



Buprenorphine (**12**)

Figure 1-5: Structure of the mixed agonist/antagonist buprenorphine (12)

1.2.2 The mu opioid receptor in cancer

Opioids are commonly used to treat chronic pain in cancer patients, but evidence has emerged in the past two decades linking the MOR with increased tumour growth. Morphine (**1**) has been found to stimulate phosphorylation and activation of the survival-promoting protein kinase Akt in MOR-expressing cells,^{21,22} stimulate angiogenic cell proliferation in MOR-expressing cells in both *in vitro* and *in vivo* models,²² and reduce time to tumour detection when treated with morphine (**1**) in a breast tumour xenograft model in mice.²² The co-administration of naloxone (**6**) reduces the rate of tumour growth, increasing the time to tumour detection by over 50%.²² MOR knockout mice injected with melanoma cells, present significantly reduced tumour growth, even in the absence of exogenous opioids.²³

Seven weeks of morphine (**1**) treatment was found to increase the density of tumour vasculature and cause tumours to increase in size and number, resulting in shorter survival in transgenic mouse models that developed breast

tumours from a tumour antigen fusion gene.²⁴ Importantly, morphine (1) treatment was not found to advance the onset of tumour development, indicating that opioid use does not increase the chance of an individual developing cancer.²⁴

Several studies have found that expression of the MOR is higher in both human tumours and mouse tumour models,²⁴⁻²⁶ that overexpression of MOR in non-small cell lung cancer (NSCLC) cells, and that treatment with various MOR agonists results in changes typical of increased epithelial mesenchymal transition as well as increased tumour growth rates.²⁷ Clinical studies into MOR-induced tumour growth, though largely limited to retrospective analyses and anecdotal evidence, support this hypothesis.^{28, 29} Furthermore, breast cancer patients possessing an MOR A118G polymorphism showed a decreased mortality rate compared to wildtype patients.^{30, 31}

The MOR-activated systems responsible for its role in tumour development are not yet well understood. Further study of these systems, and continued study of non-cancer MOR activation are therefore paramount to improve future treatment methods and aid next-generation drug design.

1.3 Studying ligand-receptor interactions

The study of ligand-receptor interactions, and the signalling pathways activated or inhibited as a result, is a key way in which cellular functions are understood in both healthy and diseased states. Different experimental and computational tools are available to study these interactions.

1.3.1 *In silico* modelling

Three-dimensional models of GPCRs solved via X-ray crystallography can be used to aid ligand design. The process of creating high quality crystals of membrane-bound receptors like GPCRs remains challenging, as the GPCR structure can become compromised when removed from the cell membrane.³²

However, advances in crystallisation techniques have allowed a growing number of high quality X-ray crystal structures of GPCRs (including the ORs in 2012³³⁻³⁵) to be solved. In some instances, active and inactive conformations of a receptor can be identified through co-crystallisation with a bound agonist or antagonist.³²

In silico modelling allows chemical structures to be docked into the active site of the solved x-ray crystal structure of a receptor, predicting individual interactions between the compound and receptor, as well as the overall binding affinity. *De novo* ligand design is then the process of modifying docked compounds to improve existing predicted interactions or to form new interactions with the receptor.^{32, 36} Alternatively, smaller structural fragments can be docked into optimal positions for receptor interaction. The docked fragments are then covalently linked into a single structure, while still maintaining these optimised positions.³⁶⁻³⁸ A *de novo* approach to ligand design is especially valuable when a high degree of concordance is found between *in silico* predictions and *in vitro* results.³⁶

In silico modelling is a useful and promising tool for ligand design which continues to be improved upon. However, experimental evaluation of synthesised ligands is still required to fully optimise ligand design.

1.3.2 Radioligand binding assays

Radioligands are simply radiolabelled versions of known ligands – a ligand which has an atom in its structure exchanged for a radioisotope equivalent, such as ³H, ¹²⁵I or ³²P. Radioligands have been widely used in pharmacology to determine receptor binding affinities of either the radioligand – and therefore the unlabelled version of the ligand – or an unlabelled competitor.³⁹ The receptor binding affinity (equilibrium dissociation constant - K_D) of a radioligand can be determined in a saturation binding assay by measuring the specific binding of the radioligand across a suitable range of concentrations in which specific binding reaches saturation (B_{max}). The binding affinity of an

unlabelled competitor ligand (K_i) can be determined by measuring the competitive displacement of a fixed concentration of radiolabelled ligand. Additionally, receptor kinetic assays using radioligands can be used to determine the association and dissociation rates of either the radioligand or an unlabelled competitor.^{39, 40}

However, radioligand binding assays require a large cell population (over 10,000 cells) per data point and, unlike fluorescent ligands, cannot be used to study interactions at a single cell level. Safety while handling radioligands alongside disposal of the subsequent radioactive waste are additional disadvantages to radioligand use. These issues are greatly magnified if the radioligand is not commercially available and must be synthesised.

1.3.3 Fluorescent ligands

Fluorescent ligands have increasingly replaced the use of radioligands in ligand-receptor binding studies, mostly due to safety and cost considerations – not only the cost of purchasing radioligands but also equipment for safe handling and storage. Fluorescent ligands can be used in the same pharmacological assays as radioligands to determine labelled or unlabelled ligand binding affinities and kinetics. However, the applications of fluorescent ligands are far more diverse than this, and through the use of different fluorophores, orthosteres and linker structures (described below), a diverse range of fluorescent ligands can be made with different physical and photophysical properties to study receptor binding, signalling and for cell visualisation. Radioligands remain useful in the study of specific ligands, as their binding profile is representative of the unlabelled version of the ligand. While fluorescent ligands have many benefits, they are considered to be unique pharmacological entities, which are not representative of their unlabelled parent compound.⁴¹

1.3.3.1 Principles of fluorescence

Fluorescence occurs in certain molecules in which an electron can be promoted from the singlet ground state (S_0) to the singlet excited state (S_1) by the absorption of a photon. The return of this electron to S_0 results in the emission of a photon as fluorescence. However, due to loss of energy by vibrational relaxation while in S_1 (Stokes shift), the emitted photon has lower energy than the absorbed photon, resulting in a longer wavelength of emitted light (**Figure 1-6**).

Intersystem crossing occurs when an excited electron transitions from S_1 to the triplet excited state (T_1). In S_1 the spin of the excited electron remains paired, but in T_1 these spins are parallel. In T_1 energy loss is slower and photon emission as phosphorescence is greatly delayed compared to fluorescence. Intersystem crossing is more favourable in molecules which have overlapping S_1 and T_1 levels, as less energy is required to move between them.

The fluorescence quantum yield (Φ_F) of a fluorescent molecule (fluorophore) is the frequency with which an absorbed photon results in fluorescent emission of a photon. A fluorophore with a high Φ_F will convert a high percentage of absorbed photons into fluorescence, while a lower Φ_F fluorophore will convert more absorbed photons into phosphorescence.

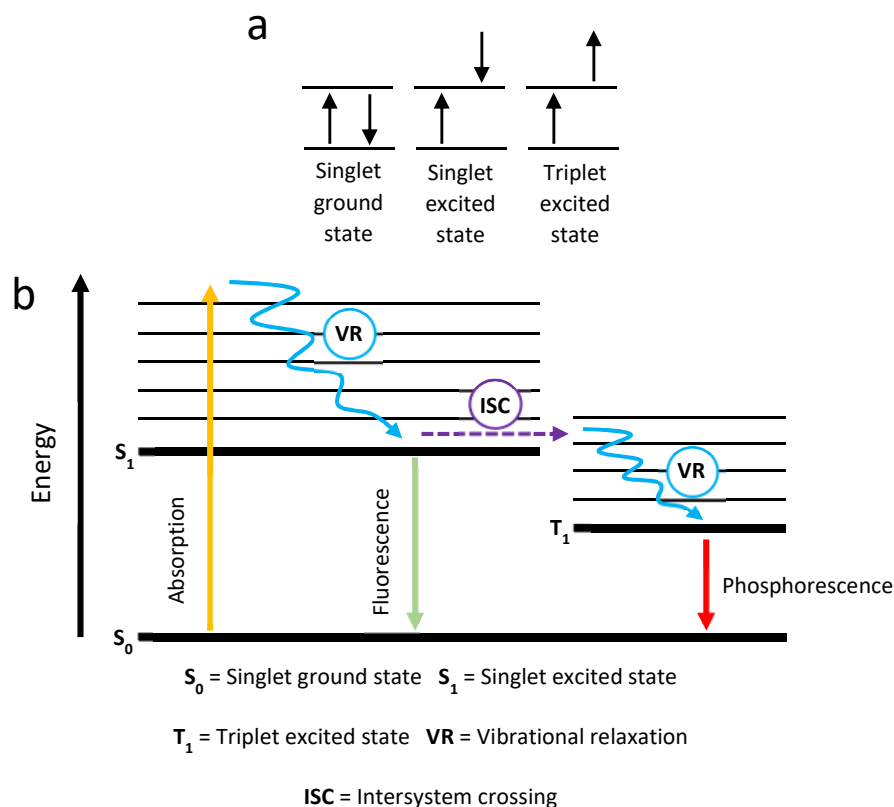


Figure 1-6: Jablonski diagram displaying the excitation states of electrons in fluorescent compounds.

(a) In the singlet ground state (S_0) electron spins are paired. When an electron is promoted to the singlet excited state (S_1) it remains paired. In the triplet excited state (T_1) the electrons are parallel. (b) Absorption of a photon by an electron in the singlet ground state (S_0) results in promotion of the electron to the singlet excited state (S_1). While in the singlet excited state vibrational relaxation results in energy loss (Stokes shift). When the excited electron returns to the singlet ground state, a photon of lower energy is emitted as fluorescence. Intersystem crossing occurs when an excited proton in S_1 transitions to T_1 . Electrons in T_1 can undergo further vibrational relaxation before returning to S_0 , emitting energy as phosphorescence.

1.3.3.2 Structure of a fluorescent ligand

In the most basic form, fluorescent ligands are composed of a known receptor ligand (typically an orthostere) labelled with a fluorophore. The first example of this was 9-aminoacridine-labelled propranolol (9-AAP) (**13**), with numerous other examples described in the literature (**Figure 1-7**).⁴²⁻⁴⁴ Unlike most radioligands, the labelling position is crucial, as fluorescent labelling can

significantly alter the structure of the ligand and its properties. It is important to avoid fluorophore conjugation onto key functional positions of the orthostere which would interfere with binding, but direct attachment of a bulky fluorophore anywhere on a ligand is likely to influence receptor binding.

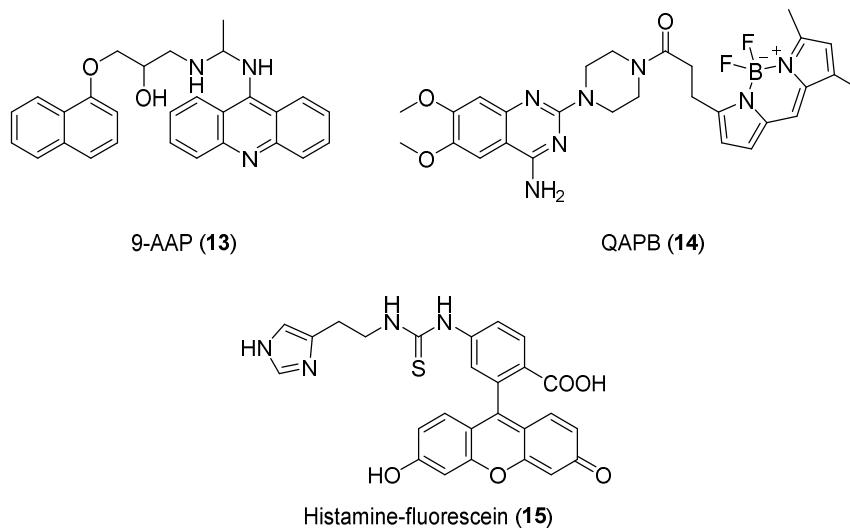


Figure 1-7: Examples of early directly labelled fluorescent ligands.⁴²⁻⁴⁴

Early examples of fluorescent ligands attached a fluorophore to an orthostere directly. Examples include the 9-aminoacridine-propranolol β -adrenoceptor antagonist 9-AAP (13), The prazosin-BODIPY FL α -adrenoceptor antagonist QAPB (14) and the histamine-fluorescein complex (15)

For this reason, the orthostere and fluorophore are now more commonly separated through a linker moiety. Linkers are typically linear chains, often composed of a repeated structural subunit, such as the polyethylene glycol (PEG) linker of 18 or the glycol linker of 16 (Figure 1-8).^{45, 46} Linkers typically possess few structural features to reduce disruption of orthostere binding. However, even with a well calculated point of attachment and linker design, fluorescent ligands will possess different properties from their unlabelled precursor. Detailed reviews covering the past five decades of fluorescent ligand designs have been published by Baindur *et al.*,⁴⁴ Middleton *et al.*⁴⁷ and Vernall *et al.*⁴¹

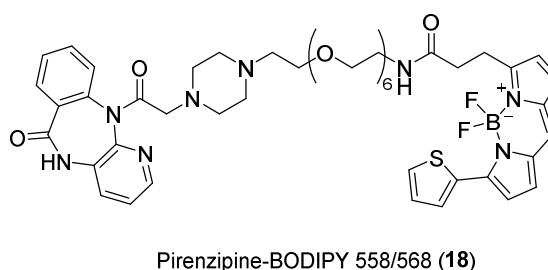
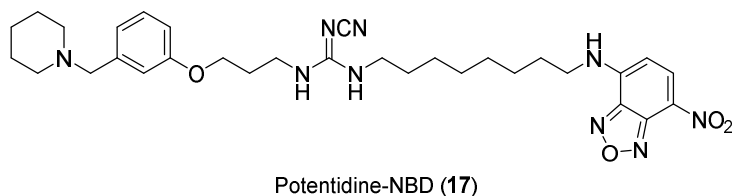
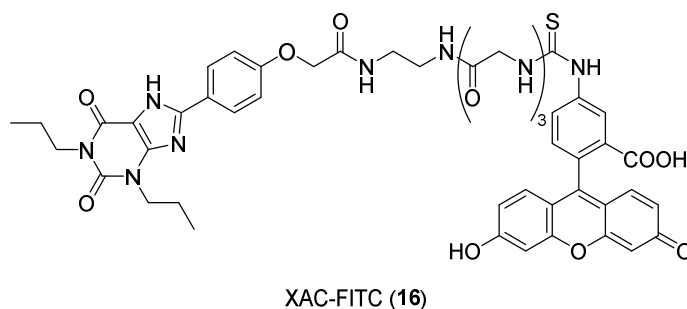


Figure 1-8: Examples of fluorescent ligands with differently composed linkers.^{45, 46, 48}

The XAC-based fluorescent ligand **(16)** utilises a glycol linker between the orthostere and fluorescein isothiocyanate (FITC) fluorophore.⁴⁶ An octanyl linker connects the potentidine orthostere and nitrobenzofurazan (NBD) fluorophore of **17**.⁴⁸ The BODIPY 558/568 fluorophore and pirenzepine orthostere of **18** are connected by a PEGyl hexamer linker.⁴⁵

Choice of fluorophore is a crucial aspect of fluorescent ligand design. Factors such as fluorophore polarity, solubility, emission wavelength, quantum yield and stability of fluorescent signal should be considered in relation to the purpose of the ligand and the experiments it will be used in. In general, low photobleaching (irreversible loss of fluorescence due to photon induced chemical damage), high fluorescence intensity, high quantum yield and near-infrared (NIR) emission spectra (to distinguish the signal from autofluorescence) are preferred in fluorophores, such as sulfo-Cy5 and some BODIPY variants.

When investigating a particular receptor system, it is useful to have multiple fluorescent ligands with different fluorophores available, so that the best

fluorescent ligand can be matched to the assay. For example, BODIPY 630/650 benefits from superior fluorescence intensity and a longer fluorescence lifetime compared with other red-emitting fluorophores, while sulfo-Cy5 is a hydrophilic fluorophore which achieves a better signal to noise ratio due to fewer non-specific membrane interactions.⁴⁹

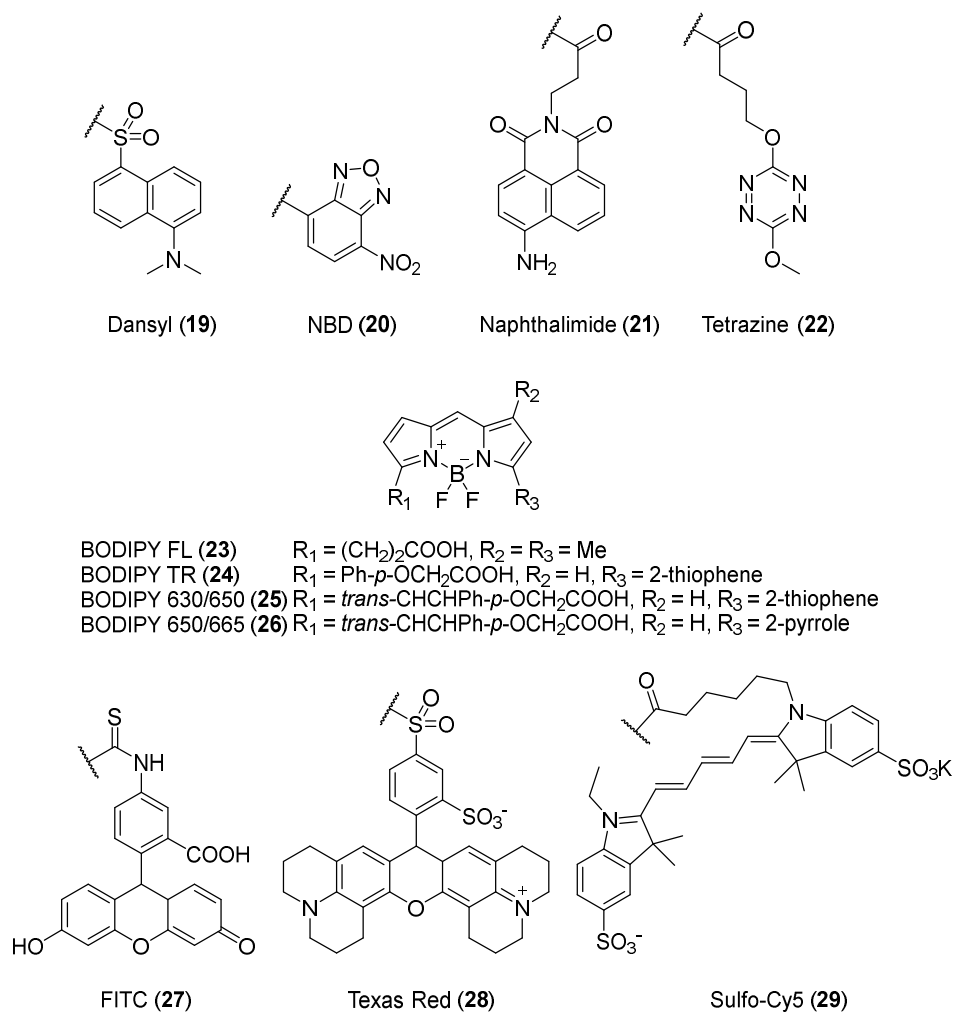


Figure 1-9: Structures of some commonly used fluorophores.

A new approach to linker design has recently been pioneered, incorporating more complex structural elements. Vernall *et al.*⁵⁰ synthesised fluorescent adenosine receptor ligands using a xanthine amine congener (XAC) orthostere bound to BODIPY 630/650-X via a peptidic linker. Previous examples of peptidic linker moieties are composed of unsubstituted glycyl subunits,⁴⁶ but the linkers in the Vernall *et al.*⁵⁰ study utilised different amino acids to optimise receptor-ligand interactions. This work expanded upon the observations of Jacobson *et*

*al.*⁵¹ that conjugation of amino acids to XAC could influence A₁ and A₃ adenosine receptor (A₁AR and A₃AR) binding affinity, with certain amino acid congeners conferring improvements in receptor subtype selectivity compared to the non-selective XAC. Vernall *et al.*⁵⁰ synthesised a series of terminally Fmoc-bound (fluorenylmethyloxycarbonyl) dipeptide congeners of XAC (**Figure 1-10**), incorporating different combinations of amino acids to optimise A₃AR binding and selectivity against A₁AR. There was some variation in the adenosine receptor binding profiles between the non-fluorescent congeners and the corresponding BODIPY 630/650-X fluorescent compounds, but the study yielded fluorescent ligands containing a Ser-Tyr dipeptide linker with greatly improved A₃AR binding affinity and receptor subtype selectivity compared to previous non-peptidic fluorescent ligands (**Figure 1-11**).⁵⁰

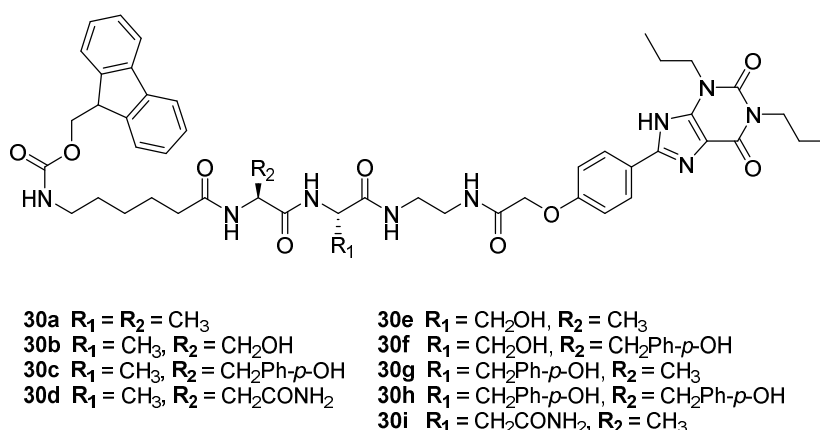
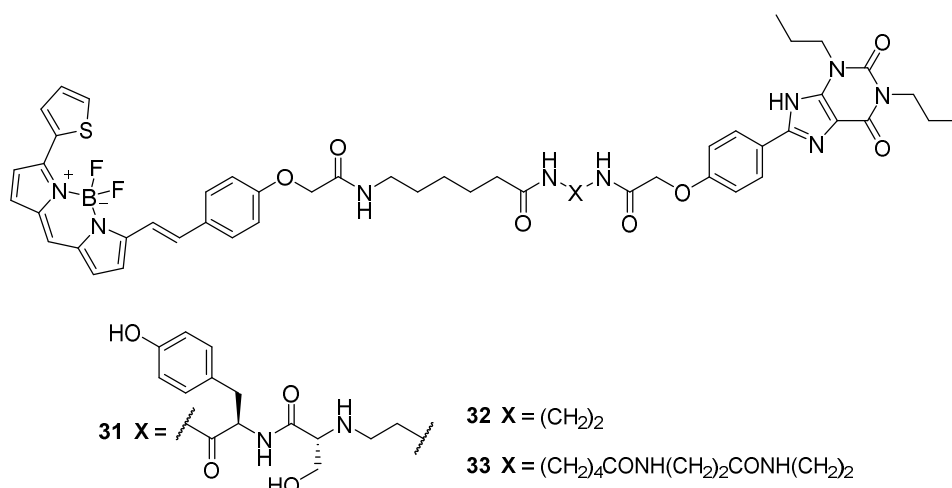


Figure 1-10: Structures of dipeptide Fmoc XAC congeners with different amino acid compositions synthesised by Vernall *et al.*⁵⁰

A similar approach was taken by this group to synthesise fluorescent ligands for the histamine H₁ receptor (H₁R).⁵² They developed a series of high affinity mepyramine- and VUF13816-based fluorescent H₁R ligands containing a peptidic linker. The high lipophilicity of the fluorescent mepyramine compound **34a** had made it unsuitable for confocal imaging.⁵³ Replacement of the pentyl linker of **34a** with di- or tripeptides yielded compounds **34b-d** which, while resulting in attenuation of binding affinity compared to **34a**, exhibited displaceable membrane binding at H₁R, indicating a high degree of specific binding ideal for confocal imaging.^{52, 53} Similar structures containing the

VUF13816 orthostere produced similarly high affinity fluorescent ligands with favourable imaging properties (**Figure 1-12**).⁵² The optimal amino acid linker composition of these fluorescent VUF13816 ligands continues to be studied (unpublished).



Compound	A ₃ AR pK _i	A ₁ AR pK _i	A ₃ AR K _i /A ₁ AR K _i
31	9.12	7.62	31.6
32	7.51	8.03	0.3
33	8.38	7.79	3.9

Figure 1-11: Structures and adenosine receptor binding affinities of XAC-BODIPY 630/650-X fluorescent ligands with different linker compositions.⁵⁰

The linker moiety of the fluorescent ligand **31** is composed of a Tyr-Ser dipeptide, resulting from optimisation of the amino acids in the linker to improve A₃AR binding affinity and receptor subtype selectivity compared to the non-selective fluorescent ligands **32** and **33**.⁵⁰

Recent projects which have developed fluorescent ligands containing peptidic linkers sought to improve the hydrophilicity and imaging properties of the ligands, rather than to improve binding affinity through new linker-receptor interactions. These projects have utilised only simple Ala-Ala linkers rather than more complex amino acid combinations.^{54, 55}

1.3.3.3 Applications of fluorescent ligands

Fluorescent ligands have been in use since the 1960s, mostly as histological stains.⁵⁶ The discovery of selective small molecule fluorescent ligands led to the development of a growing number of pharmacological assays, which will be described in this section.

Confocal microscopy

Use of fluorescent ligands in confocal microscopy can produce high-resolution images of receptor localisation on different scales - from a population of cells down to single cell level. Automated confocal microscopy has been used in receptor-ligand binding studies, similar to those described above using radioligands, to measure the binding affinity of labelled and unlabelled ligands (Figure 1-13).^{40, 57}

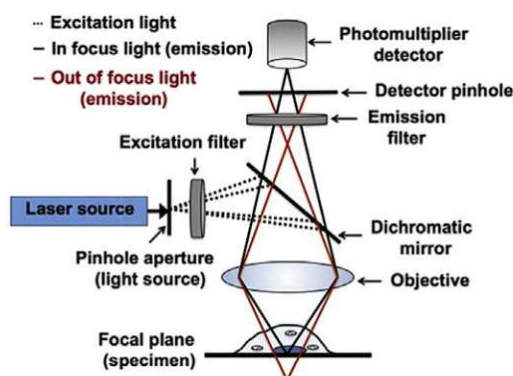


Figure 1-13: Confocal microscopy experiment using fluorescent ligands.

Source: Stoddart *et al.* (2015)⁴⁰

A laser beam passes through an adjustable pinhole and is reflected off a dichromatic mirror. It is then focused by the objective onto a focal plane of the fluorescent ligand-bound specimen. Emitted fluorescence travels back through the objective, where in focus light is focused through a different pinhole into the photomultiplier detector.⁴⁰

Fluorescence correlation spectroscopy

Fluorescence correlation spectroscopy (FCS) measures fluctuations in the emitted photons of excited fluorescent ligands as they pass through a small confocal volume. Time dependent measurement of these emissions using autocorrelation analysis provides information on the fluorescent ligand's mobility (and therefore binding state) and concentration within the confocal volume.^{40, 58} FCS can be used in low-expression systems, including native tissue. The small scale at which FCS operates under allows more detailed characterisation of receptors, such as the spatial organisation of receptors, detection of receptor oligomerisation into signalling complexes, and identification of different receptor conformations.^{40, 53, 58}

Fluorescence polarisation

Fluorescence polarisation (FP) is a simpler method which takes advantage of differences in the flexible linker region of fluorescent ligands by measuring the change in polarisation of light emitted from a fluorophore.³⁹ Upon excitation by polarised light, a receptor-bound fluorophore will emit light that is still polarised, while an unbound fluorescent ligand will emit depolarised light due to rapid rotation in the linker region. The differences in fluorescent ligand mobility and resulting depolarisation of light can be measured to determine binding affinity of the fluorescent ligand or an unlabelled competitor.³⁹ However, when working with low concentrations, FP suffers from poor precision compared with other quantitative methods.³⁹

Fluorescence resonance energy transfer

Fluorescence resonance energy transfer (FRET) is a measurement of the non-radiative transfer of energy between two fluorescent moieties. A lanthanide-containing donor fluorophore is excited by a photon of a particular wavelength and emits light at a different wavelength (or wavelengths). A successful transfer

of energy is dependent on the proximity of the donor and acceptor fluorophores. If the acceptor is in close proximity to the donor, the energy of the emitted photon can be transferred to the acceptor, allowing it to fluoresce at a different wavelength. In a FRET assay, a receptor is labelled with a donor fluorophore and a fluorescent ligand for that receptor contains an acceptor fluorophore which is able to absorb the emitted wavelength of the donor (Figure 1-14).^{40, 58}

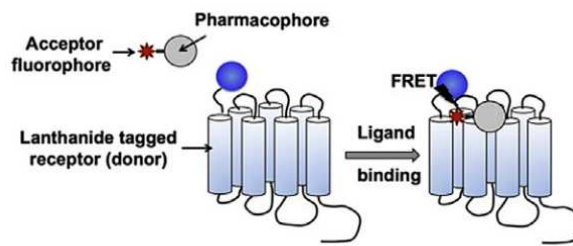


Figure 1-14: Principle of FRET using a fluorescently labelled receptor and ligand.⁴⁰

Source: Stoddart *et al.* (2015).⁴⁰

The lanthanide-based fluorophore (donor) of a tagged receptor is excited and emits light as fluorescence. FRET occurs when the acceptor fluorophore of a bound fluorescent ligand is excited energy transferred from the donor. FRET can only occur when the ligand is bound as it requires close proximity between the donor and acceptor fluorophores.^{40, 58}

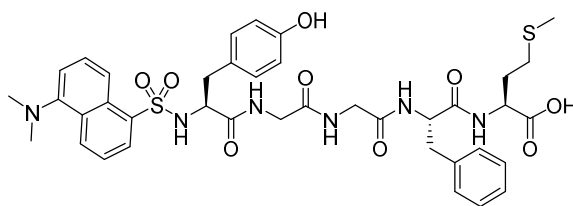
For example, Lumi4-terbium cryptate (Lumi4-Tb) can be used to fluorescently label receptors. The receptor is labelled with the donor fluorophore in such a position that only bound ligands are sufficiently close enough for FRET to take place. Lumi4-Tb absorbs light at a peak of around 340 nm and emits light at peaks of 490, 548, 587 and 621 nm. Emitted light in the 621 nm range can be absorbed by some fluorophores, such as BODIPY 630/650 which emits light at a wavelength peaking at around 650 nm. In this example, fluorescence is measured at 620 nm (from the donor) and 665 nm (for the acceptor) to ensure that there is minimal overlap in emission spectra. The ratio of these emissions indicates the frequency of FRET occurring, and therefore allows measurement the binding affinity of the fluorescent ligand.

Time-resolved FRET (TR-FRET) introduces a short gap (of 50-150 microseconds) between the energy input and measurement of emission. This allows short-lived fluorescence from sources other than the donor and receptor to decay, leaving a clearer signal from the donor and acceptor emissions, which have longer fluorescence lifetimes.

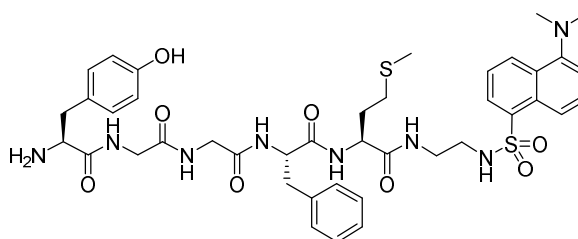
1.4 Fluorescent opioid receptor ligands

Development of fluorescent opioid ligands was initially limited to fluorescent conjugates of peptidic OR ligands, mostly enkephalins and their synthetic analogues.⁴⁴ Compared to small molecule fluorescent conjugates, the addition of a fluorophore represents a less significant increase in molecular weight and often positions the fluorophore further from the ligand binding site, reducing the likelihood of interfering with orthosteric binding.⁴⁷ Fournie-Zaluski *et al.*⁵⁹ discovered that attachment of a dansyl moiety to the *N*-terminus of met-enkephalin (**36a**) resulted in a loss of OR binding affinity, while *C*-terminal dansyl attachment (**36b**) retained the activity of the unlabelled enkephalin. Following this, several other *C*-terminally linked fluorescent peptides were synthesised, each possessing improved binding affinity compared to their parent ligands (**Figure 1-15**).⁶⁰⁻⁶²

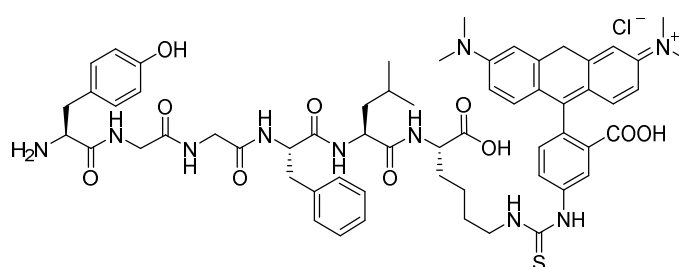
Peptidic fluorescent OR ligands have remained popular, with structures developed to incorporate non-naturally occurring amino acids, such as dimethyl tyrosine (DMT), tetrahydro-isoquinoline-3-carboxylic acid (Tic) and *N*-leucine (Nle) (**Figure 1-16**).⁶³⁻⁶⁶



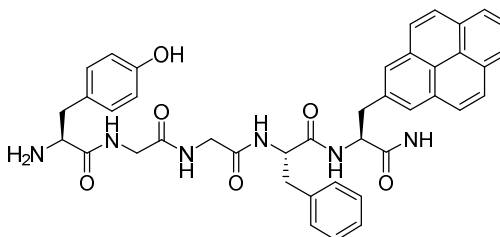
N-dansyl-met-enkephalin (**36a**)



C-(CH₂)₂-dansyl-met-enkephalin (**36b**)

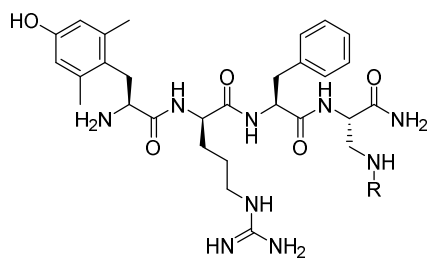


[*D*-Ala², Leu⁵]enkephalin-Lys-N^ε-rhodamine (**37**)

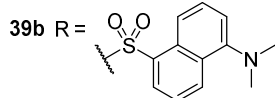


Pya⁵-Enkephalin (**38**)

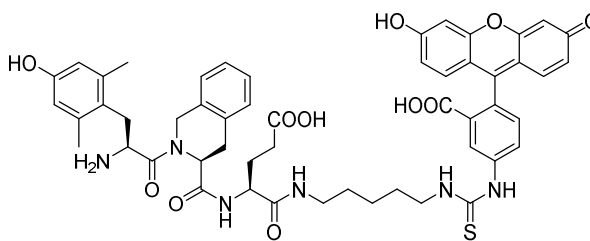
Figure 1-15: Structures of several early enkephalin-based fluorescent OR ligands.⁵⁹⁻⁶²



39a R = C(=O)Ph- α -NH₂



Fluorescent analogues of [DMT¹]DALDA



Dmt-Tic-Glu-FITC (**40**)

Figure 1-16: Structures of fluorescent peptidic ligands which utilise unnatural amino acids.^{63,}

The development of non-peptidic fluorescent OR ligands was initially slow, and those that had been discovered utilised morphinan scaffolds with directly bound fluorophores, such as the fluorescein-oxymorphone derivatives developed by Kolb and colleagues (**Figure 1-17**).^{67, 68} The close spatial relationship between the orthostere and fluorophore resulted in greatly diminished receptor binding, relative to their unlabelled parent compounds.^{67, 68}

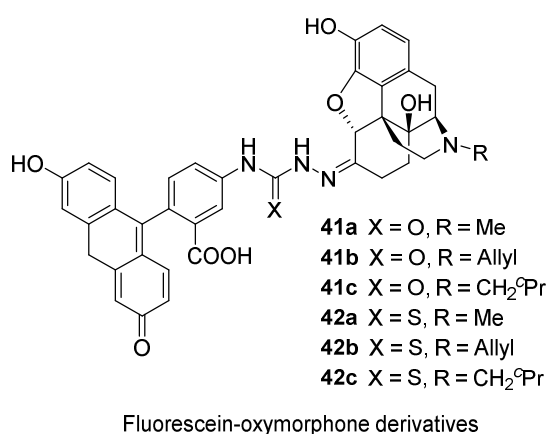


Figure 1-17: Fluorescent oxymorphone derivatives with directly bound fluorescein fluorophores.^{67, 68}

Progress was made by Archer *et al.*,⁶⁹ who incorporated a short sarcosine linker between different orthosteres and a NBD fluorophore (**Figure 1-18**). The same group produced a series of BODIPY-labelled ligands, including a MOR-selective irreversibly binding fluorescent ligand (**46**).⁷⁰ Unfortunately, some of these compounds suffered from significant hydrophobicity or exhibited absorption and emission wavelengths unsuitable for many modern pharmacological methods, which typically prefer NIR emitting fluorophores.^{57, 69, 70}

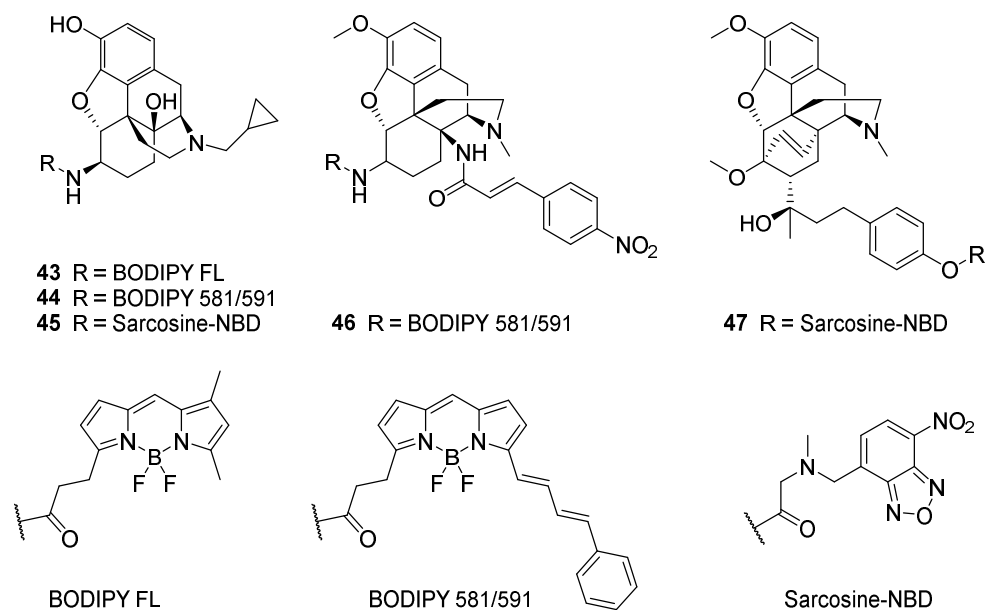


Figure 1-18: Selection of fluorescent OR ligands.^{69, 70}

6- and 7-position conjugated NBD fluorescent ligands **45** and **47** were synthesised by Archer *et al.*⁶⁹ containing a sarcosine linker. BODIPY-fluorescent OR ligands (**43**, **44** and **46**) were synthesised by Emmerson *et al.*⁷⁰ including the irreversible fluorescent ligand **46**.

Since the 1990s, development of fluorescent MOR ligands has been somewhat neglected compared to advances at other receptors.⁴¹ More recently however, Schembri *et al.*⁵⁷ reported the successful synthesis of several oripavine-derived fluorescent ligands (**Figure 1-19**). This project aimed to modernise fluorescent MOR ligands with more practically useful fluorophores and longer linker moieties to reduce the impact of fluorophore attachment on binding. Of the compounds synthesised, the sulfo-Cy5 (**51**) and BODIPY 630/650-X (**50**) compounds were particularly favoured: **50** for its high binding affinity, receptor subtype selectivity and bright fluorescence, and **51** for its rapid, reversible specific binding to MOR, making it well suited for confocal imaging.⁵⁷ Despite its favourable properties, **50** was found to exhibit more non-specific binding than **51**, making it less useful for confocal imaging.⁵⁷

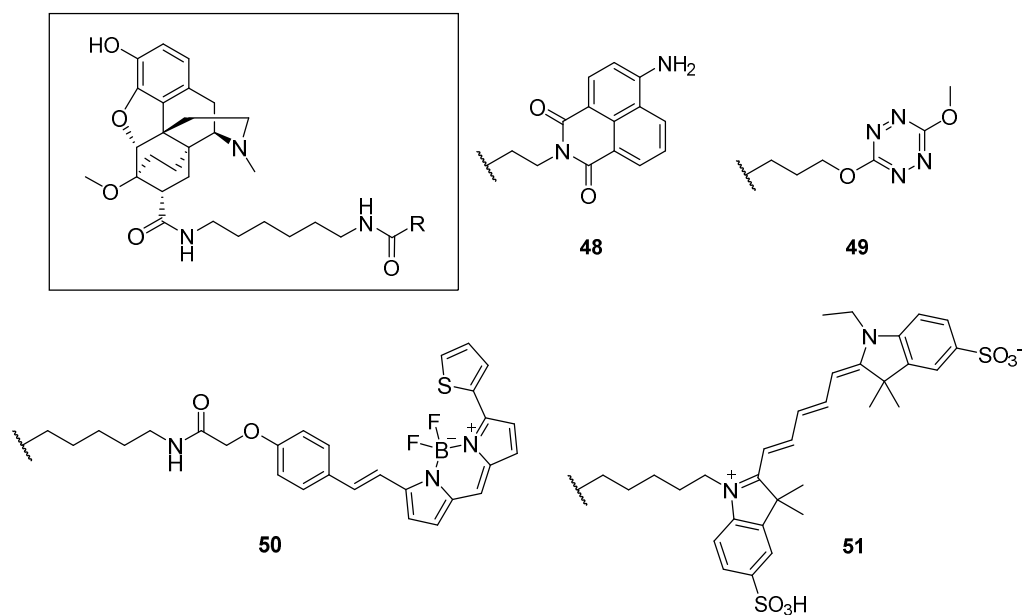


Figure 1-19: Fluorescent oripavine-derived OR ligands synthesised by Schembri *et al.*⁵⁷

Finally, in an attempt to broaden the range of available fluorescent OR ligands, Lam *et al.*⁷¹ synthesised fluorescent OR agonists using morphine (**1**) and a sulfo-Cy5 fluorophore (**Figure 1-20**). The fluorescent compound **52** was found to possess similar properties to the parent compound morphine (**1**) and was able to induce internalisation.⁷¹

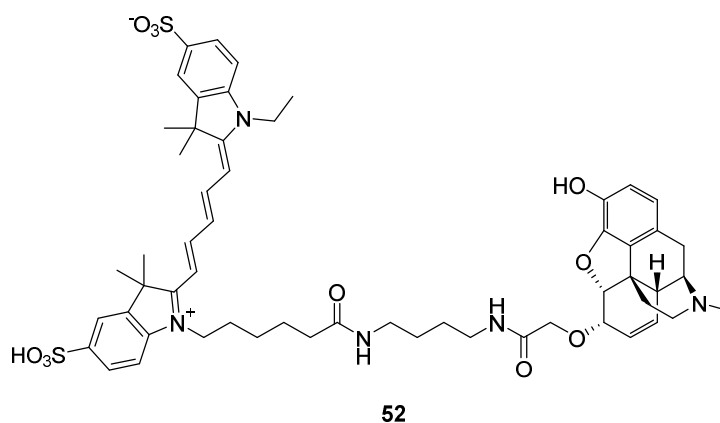


Figure 1-20: A fluorescent OR agonist composed of morphine and sulfo-Cy5, synthesised by Lam *et al.*⁷¹

For further information regarding fluorescent OR ligands, particularly those of the KOR and DOR, a thorough review of selective and non-selective fluorescent

opioid ligands synthesised to date has recently been published by Drakopoulos *et al.*⁷²

1.5 Research aims

Despite the progress which has been made in the development of diverse fluorescent MOR ligands, scope remains for novel compounds with previously unobtained properties. Perhaps most notably absent from the literature, are red-emitting BODIPY-labelled fluorescent MOR ligands which are suitable for confocal imaging studies. The BODIPY 630/650-X fluorescent MOR ligand **50** demonstrates the potential to produce a high affinity fluorescent ligand with highly desirable fluorescent properties, but further development is required to improve the specific binding profile of either this or similar fluorescent compounds.⁵⁷

A potential solution to this disadvantage of BODIPY 630/650 use can be found in the peptide-linked fluorescent A₃AR and H₁R ligands described by Vernall *et al.*⁵⁰ and Stoddart *et al.*⁵² respectively. In both instances, lipophilic BODIPY 630/650-X-containing fluorescent ligands with hydrocarbon linkers - which were considered unsuitable for confocal imaging - were modified with peptidic linker moieties.^{50, 52} Unlike the corresponding non-peptidic ligands, peptide-linked fluorescent ligands identified in these studies displayed displaceable membrane binding, making them far better suited for confocal imaging and broader pharmacological applications.^{50, 52} This same rationale, applied to MOR ligands, could result in BODIPY 630/650-containing fluorescent MOR ligands which retain the benefits of this fluorophore, while making it sufficiently hydrophilic for broader use in pharmacological assays.

Aside from altering the physicochemical properties of the fluorescent ligands, the incorporation of peptides into the linker of fluorescent ligands can improve receptor binding affinity and subtype specificity.⁵⁰ By progressively altering the amino acid side chains of the peptide linker, Vernall *et al.*⁵⁰ were able to improve A₃AR binding affinity and selectivity. It may also be possible to uncover

beneficial interactions for MOR binding through similar modifications of amino acids bound to a MOR ligand orthostere. Perhaps the closest example to this in OR ligands is the study by Lipkowski *et al.*,⁷³ which attempted to incorporate peptide sections from leu-enkephalin (**58**) and dynorphin A (**59**) into the 6-position of oxymorphone (**53**) and naltrexone (**7**) (**Figure 1-21**). These modifications did not result in improvement of MOR binding or receptor subtype selectivity, but the ligand design was based on several assumptions around how these synthetic morphinans and endogenous ligands bind to the MOR, and presumed overlap in the resulting ligands (**54-57**) which may not be accurate.⁷³

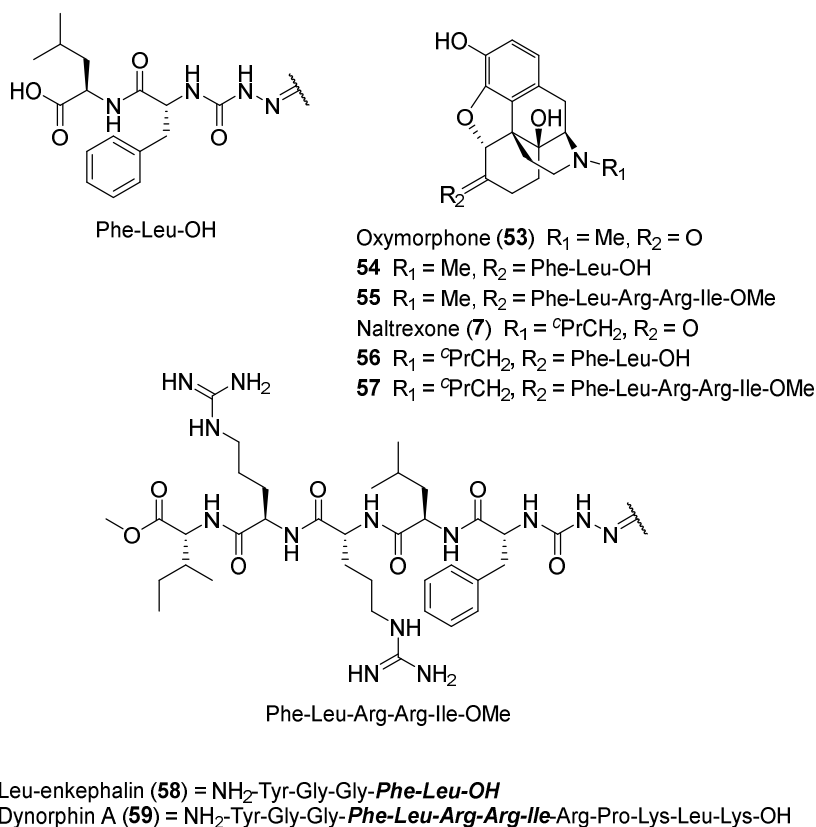


Figure 1-21: Oxymorphone- and naltrexone-bound derivatives of leu-enkephalin and dynorphin A, synthesised by Lipkowski *et al.*⁷³

Peptides bound to the 6-position of either oxymorphone (**53**) or naltrexone (**7**) were chosen to match those contained in the structures of leu-enkephalin (**58**) and dynorphin A (**59**) (shown in bold).⁷³

This project aimed to design, synthesise and pharmacologically evaluate novel fluorescent antagonist ligands for the MOR with several key features. To

enhance MOR binding through interactions between the linker and receptor, and to decrease non-specific interaction through increased hydrophilicity, fluorescent ligands were designed to include linkers containing an optimal number and composition of amino acids. With these modifications it was hoped that lipophilic fluorophores such as BODIPY 630/650 could be incorporated into the fluorescent ligand structure, while maintaining desirable properties for confocal imaging and broader pharmacological applications. It was decided that the compounds produced in this study should be MOR antagonists, as they are better suited for studying receptor-ligand interactions. Fluorescent agonist ligands, such as those synthesised by Lam *et al.*,⁷¹ are useful for studying aspects of receptor signalling but induce cellular changes through receptor activation which can make studying receptor-ligand interaction more difficult. The evaluation, synthesis and determination of MOR binding affinity of morphinan-based fluorescent ligands of this design are described in **Chapter 2**.

As described in this chapter, the receptor binding components (orthosteres) of fluorescent OR ligands can be divided into endogenous peptides (and their derivatives) and small molecule morphinan-based compounds. To truly expand the fluorescent tools available to pharmacologists studying ORs, it is important to consider designs outside of these existing paradigms. Therefore, a further aim of this project was to synthesise fluorescent small molecule MOR antagonist ligands using a non-morphinan orthostere, in addition to the inclusion of an amino acid-based linker. The evaluation, synthesis and determination of MOR binding affinity of such fluorescent ligands is described in **Chapter 3**.

2. Design, synthesis and pharmacological evaluation of β -naltrexamine-based fluorescent ligands

This chapter will describe an approach to fluorescent ligand design that was more similar to previously described fluorescent opioid ligands, as it utilised a morphinan-containing orthostere from which a linker to a fluorophore was attached. In contrast to previously reported fluorescent ligands based on the morphinan scaffold, this approach incorporated amino acids in the linker between the pharmacophore and fluorophore. As described in the previous chapter, this aimed to improve the physicochemical properties of the compound, as well as providing an opportunity for the residues in the linker to form interactions with the receptor binding site.

This chapter will discuss the design process undertaken for these fluorescent ligands, beginning with an evaluation of the SARs for ligands of this type and how this rationalises the choice of orthostere and point of linker attachment, before moving on to describe *in silico* modelling of the newly designed compounds. This is followed by a description of the synthesis and pharmacological evaluation of a series of non-fluorescent congeners, before finishing with the synthesis and pharmacology of the final fluorescent ligands.

2.1 Structure-activity relationships (SARs) of morphinan opioids

There is an extensive range of diverse scaffolds for opioid receptor ligands reported in the literature. The SAR of opioid ligands containing the morphinan structure will be discussed here, such as the agonists morphine (**1**) and buprenorphine (**12**), the antagonists naloxone (**6**) and naltrexone (**7**), and novel structures from SAR studies which are not used clinically. Other non-morphinan opioid ligand structures, such as that of the antagonist alvimopan (**9**), will be discussed in **Chapter 3**.

2.1.1 The morphinan core structure

Many frequently used opioids share a common morphinan (17-azatetracyclo[7.5.3.0^{1,10}.0^{2,7}]heptadeca-2,4,6-triene) structure. This consists of four connected rings (**Figure 2-1**): an aromatic ring (ring-A) and two further saturated carbon rings chained below (ring-B and ring-C) with a fourth ring (ring-D) containing a nitrogen protruding from carbons 9 and 13. As is often the case with structures bearing multiple chiral centres, the morphinan scaffold appears in a number of naturally occurring alkaloids such as morphine (**1**), codeine (**2**) and thebaine, all isolated from the opium plant. From these natural products, a great number of semi-synthetic derivatives have been reported.

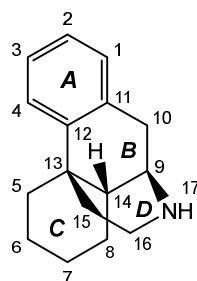


Figure 2-1: The morphinan structure.

The morphinan structure consists of an aromatic ring (A) with two saturated rings (B and C) linked below. A fourth ring (D) containing a secondary amine links carbons 9 and 13. Chiral centres are present at positions 9 R , 13 R and 14 R .

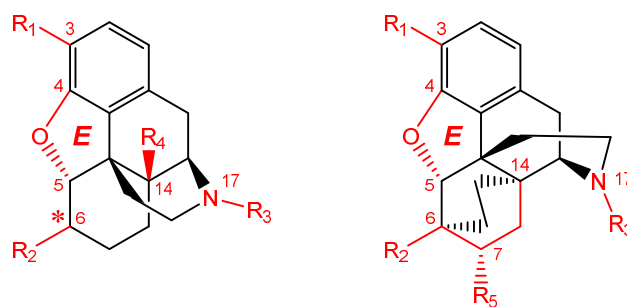
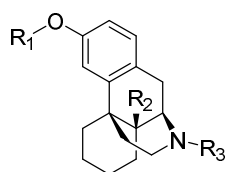


Figure 2-2: Common positions for modification of the morphinan structure found in opioid receptor ligands.

A 4,5 α -epoxy bridge (which forms **ring-E**) is commonly found in morphinan-based opioid receptor ligands. **R₁** is almost always a hydroxyl group in active compounds (such as in morphine **1**) but is a common site for prodrug modifications such as ethers (codeine **2**) and esters (diamorphine **68**). **R₂** is a highly variable site. Most opioid medicines of this type have a ketone (naloxone **6**) or chiral hydroxyl (morphine **1**) or methoxyl group (buprenorphine **12**) at the 6-position, but it is frequently used by medicinal chemists as a site to introduce variability or to alter pharmacokinetic properties (naloxegol **8**). **R₃** is methylated in most opioid agonists (morphine **1**, oxycodone **53**), but *N*-allyl (naloxone **6**) or *N*-cyclopropylmethyl (naltrexone **7**) substitution generates antagonists. In clinically used opioids, **R₄** is exclusively protonated or a hydroxyl, but further modification has produced some interesting irreversible ligands (clocinnamox **91**). A 6,14-bridge allows for a broad range of modifications to **R₅** in the literature but usually features a tertiary alcohol in clinical examples (buprenorphine **12**, etorphine **86**).

2.1.2 The 4,5 α -epoxy bridge

This large family of morphinan-containing opioid receptor ligands share many common features, notably, the 4,5 α -epoxy bridge which forms a fifth ring (ring-E) on the morphinan scaffold (**Figure 2-2**). This ring-E is found in the structures of naturally occurring alkaloids and their semi-synthetic derivatives. Crystal structure evidence suggests that this oxygen atom acts as a hydrogen bond acceptor for Y148^{3,33} of the MOR.³³ However, it is not essential for binding, as evidenced by the existence of morphinan opioid ligands which lack the 4,5 α -epoxy bridge (**Figure 2-3**).

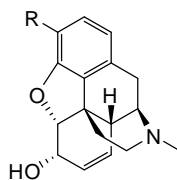


Compound	R ₁	R ₂	R ₃
Levorphanol (60)	H	H	CH ₃
Levomethorphan (61)	CH ₃	H	CH ₃
Butorphanol (62)	H	OH	^c BuCH ₂
Cyclorphan (63)	H	H	^c PrCH ₂
Levallorphan (64)	H	H	Allyl

Figure 2-3: Structures of several opioid receptor ligands which lack a 4,5 α -epoxy bridge.

2.1.3 The 3-hydroxyl group

Another frequent structural feature of this family is the 3-OH found on the aromatic ring-A. This phenolic group is a requirement for producing an active ligand, as attempts to install alternative groups at this position have resulted in loss of activity.^{74, 75} It is possible to replace the phenolic hydroxyl group with a carboxamide and maintain activity at the opioid receptors, albeit with significantly reduced binding affinity (**Figure 2-4**).⁷⁵ Extension from the amide results in further loss of binding affinity.⁷⁵ It is suggested that this phenol is able to form hydrogen bond interactions with H297^{6, 52} of the MOR, through a chain of two water molecules (**Figure 2-5**).³³



Compound	R	MOR p <i>K</i> _i
Morphine (1)	OH	9.1
65	CONH ₂	7.5
66	CONHCH ₃	6.4
67	CONH(CH ₃) ₂	5.8

Figure 2-4: The effect of 3-position substitution on the MOR binding affinity of morphine.⁷⁵

Binding affinities (p*K*_i) at MOR were determined by inhibition of [³H]-DAMGO in guinea pig brain membranes.⁷⁵

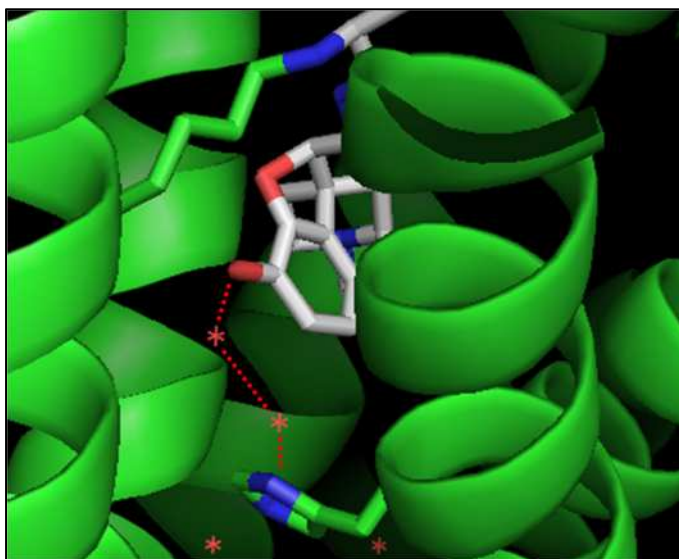


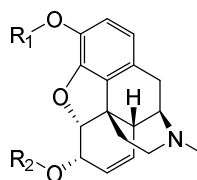
Figure 2-5: Hydrogen bonding in the crystal structure of MOR between the 3-hydroxyl group of β-FNA (74**) and H297^{6,52} via two water molecules.**

Adapted from Manglik *et al.* 2012.³³

The crystal structure of β-FNA bound to MOR (PDB: 4DKL) shows two water molecules (shown here as red stars) which could form a hydrogen bonding network (dotted red line) between the 3-hydroxyl of β-FNA and H297^{6,52,33}

Derivatives of the phenolic hydroxyl group are common in many medicines, including the natural product codeine (**2**), the 3-methyl ether of morphine (**1**).

However, codeine itself has relatively weak affinity for the MOR ($K_i = 0.35 \mu\text{M}$ versus [^3H]-DAMGO in guinea pig brain membranes), displaying a 200-fold reduction in binding affinity relative to morphine ($K_i = 1.8 \text{ nM}$).⁷⁶ Instead, it acts as a prodrug of morphine, requiring demethylation in the liver by cytochrome P450 2D6 (CYP2D6). The reduced analgesic effect of codeine, compared to that experienced by patients administered morphine, is a result of this necessary metabolism, which slows release of morphine into the body. Patients who carry allelic variants of *CYP2D6*, which reduce the enzyme's rate of metabolism, experience reduced efficacy from codeine owing to decreased morphine concentration.⁷⁷ Likewise, an allelic variant which increases CYP2D6 metabolism results in increased efficacy and morphine concentration.⁷⁷



Compound	R ₁	R ₂
Morphine (1)	H	H
Codeine (2)	CH ₃	H
Diamorphine (68)	Ac	Ac

Figure 2-6: Structures of morphine and its metabolic precursors.

Both codeine (**2**) and diamorphine (**68**) are prodrugs of morphine. Codeine (**2**) requires liver metabolism by CYP2D6 to yield morphine, resulting in a slower release and lower morphine concentration in the blood.⁷⁷ The 3- and 6-acetyl groups of diamorphine (**68**) can be hydrolysed by plasma esterase enzymes to produce morphine.⁷⁸

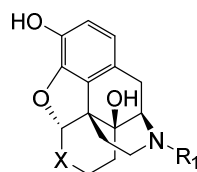
The other common alteration to the 3-hydroxyl group is esterification, with the best-known example of this being diamorphine (diacetylmorphine, heroin, **68**) - the 3,6-diacetoxy analogue of morphine (**1**). Unlike etherified analogues, such as codeine (**2**), esters do not require liver metabolism to be converted to the active morphine, as they can be hydrolysed by plasma esterases. When administered intravenously, the increased lipophilicity of these esters allows

swift passage across the blood-brain barrier, resulting in its rapid effect after administration.⁷⁸ Esterification of the phenolic hydroxyl has been used to develop opioids with differing rates of action and for alternative delivery methods.^{79, 80}

2.1.4 Modification of the 6-position

The 6-position on ring-C is the most varied site for modification amongst both clinical and non-clinical compounds. In some examples, such as oxymorphone (**53**), naloxone (**6**) and naltrexone (**7**), the 6-position is sp² hybridised and occupied by a ketone. In morphine (**1**), buprenorphine (**12**) and numerous other examples, the 6-position is saturated, resulting in an additional chiral centre (**Figure 2-7**).

As with the 3-hydroxyl group, the 6-position can be functionalised with simple ethers and esters to alter the pharmacokinetic properties of the compound. Larger functional groups have been substituted onto this site in numerous SAR studies and in some drugs, to introduce greater pharmacokinetic and pharmacodynamic changes to the ligand. The MOR antagonist naloxegol (**8**) contains a methoxylated PEGyl heptamer attached to the 6-position via an ether. The resulting increased hydrophilicity prevents it from penetrating the blood-brain barrier.⁸¹ In addition, the PEGylation makes **8** a substrate for P-glycoprotein (P-gp), further limiting its BBB permeability.⁸¹ Naloxegol (**8**) therefore acts as a peripheral opioid antagonist and is used in the treatment of opioid-induced constipation, having no interaction with central opioid receptors.⁸¹



Compound	R ₁	R ₂	6-position stereochemistry
6 Naloxone	Allyl	C=O	N/A
69a α-Naloxanol	Allyl	CHOH	6 <i>S</i>
69b β-Naloxanol	Allyl	CHOH	6 <i>R</i>
70a α-Naloxamine	Allyl	CHNH ₂	6 <i>S</i>
70b β-Naloxamine	Allyl	CHNH ₂	6 <i>R</i>
7 Naltrexone	^c PrCH ₂	C=O	N/A
71a α-Naltrexanol	^c PrCH ₂	CHOH	6 <i>S</i>
71b β-Naltrexanol	^c PrCH ₂	CHOH	6 <i>R</i>
72a α-Naltrexamine	^c PrCH ₂	CHNH ₂	6 <i>S</i>
72b β-Naltrexamine	^c PrCH ₂	CHNH ₂	6 <i>R</i>
8 Naloxegol	Allyl	CHO(CH ₂ CH ₂ O) ₇ CH ₃	6 <i>S</i>

Figure 2-7: The structures of naloxone and naltrexone and their chiral derivatives.

The chiral configuration of the 6-position influences several ligand properties. In the case of morphine (**1**), binding affinity and function at MOR are not greatly affected by altering the chiral configuration at position-6.⁸² In contrast, the epimeric products resulting from the reduction of the 6-keto moiety of naloxone (**6**) and naltrexone (**7**) display diverse properties; the corresponding β-alcohols (**69b** and **71b**) share similar antagonist properties to the parent ketones, however the α-alcohols (**69a** and **71a**) exhibit mixed agonist-antagonist activity for different opioid receptors.⁸³ The 6-amino analogues of naloxone and naltrexone are all MOR antagonists with reduced antagonist binding affinity, relative to the parent compounds, although this difference was greater *in vivo* compared to *in vitro* studies, suggesting pharmacokinetic factors

This is demonstrated in the example of naltrindole (**73**), a δ -selective antagonist whose indole is proposed to prevent MOR binding, due to a steric clash with W318^{7,35}.³³ A leucine residue (L300^{7,35}) occupies the same position in the crystal structure of the DOR, which does not result in a clash and allows binding and therefore selectivity (**Figure 2-9**).^{33, 34}

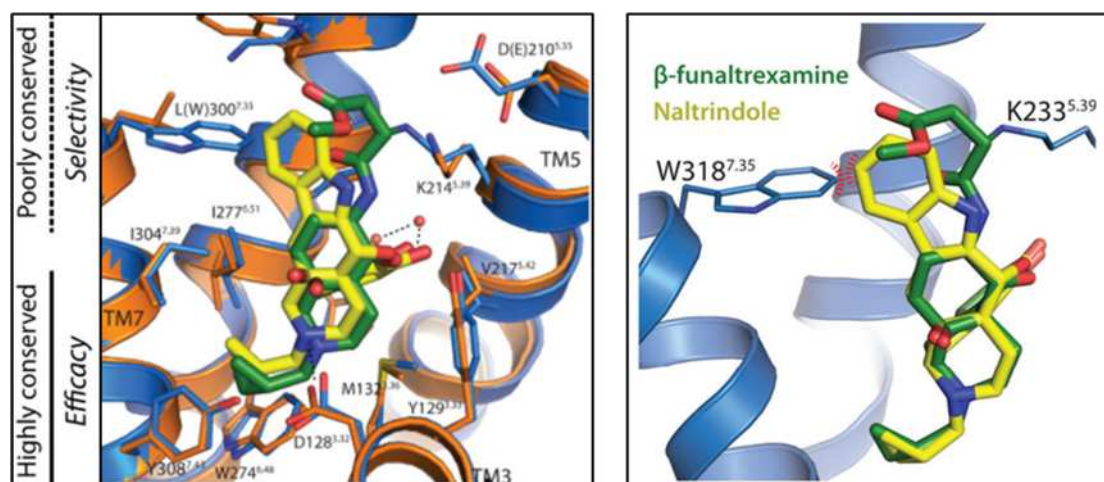


Figure 2-9: Overlays of naltrindole and β -FNA in the crystal structures of the mu and delta opioid receptor.^{33, 34}

Source: (left) Grenier *et al.* 2012,³⁴ (right) Manglik *et al.* 2012.³³

Left: The crystal structures of DOR (PDB: 4EJ4, orange) and MOR (PDB: 4DKL, blue) are overlaid displaying the high conservation of amino acids deeper in the binding pocket, but greater variation in the extracellular regions of the helices. Particularly of note is L300^{7,35} in DOR which is replaced by W318^{7,35} in MOR. The structure of naltrindole (**73**, yellow) is overlaid on the crystal structure of β -FNA (**74**, green) covalently bound to MOR.³⁴ **Right:** Naltrindole (**73**) is predicted to clash with W318^{7,35} in the MOR, preventing its binding and conferring selectivity for DOR.³³

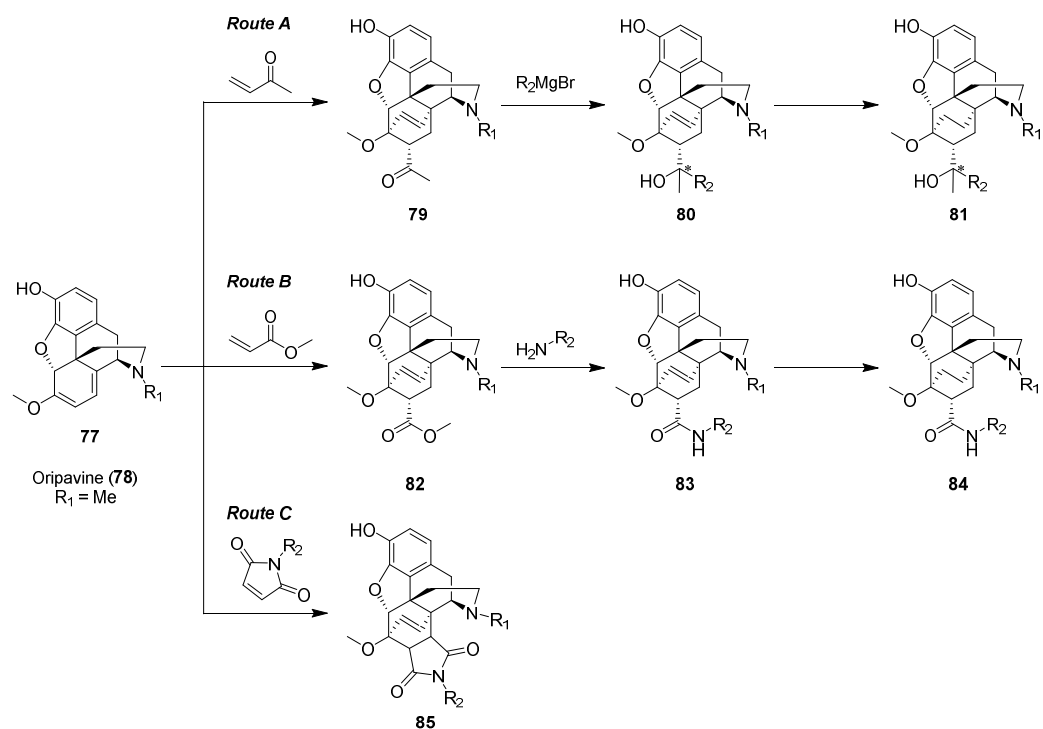
While modification of the 6-position of β -naltrexamine-based structures may confer changes to MOR, DOR, and KOR selectivity, ligand function at KOR has also been manipulated by 6-position substitution. One such example is nalfurafine (**75**), the 6-*N*-methyl-*trans*-3-(3-furyl)acrylamido analogue of β -naltrexamine (**72b**).⁸⁸ Despite featuring an *N*-cyclopropylmethyl group in the β -naltrexamine structure, which is typically antagonism-inducing (see **2.1.6**), nalfurafine (**75**) is a KOR agonist with weak partial agonist activity at MOR.⁸⁸ While the high KOR-selectivity of **75** seems to be dependent on the 6-*N*-methyl

group,⁸⁷ KOR agonism is often found in other β -naltrexamine-based compounds. For example, KOR agonist activity was found in the series of 6-cinnamoyl derivatives (**76a-d**) described by Derrick *et al.*^{89,90} and low level KOR agonism is displayed by the irreversible MOR antagonist β -FNA (**74**).^{87, 91, 92} β -naltrexamine-based ligands should therefore be tested for KOR binding affinity, as the SAR of how KOR agonism is induced is not well understood.

2.1.5 Modification of the 7-position via a 6-14 bridge

The introduction of an ethylene bridge between carbons 6 and 14 on ring-C has been utilised in ligands such as buprenorphine (**12**) and etorphine (**86**), to introduce additional structural modifications and improve binding affinity.¹⁹ The bridge is installed via Diels-Alder chemistry between a diene-containing morphinan (e.g. oripavine (**78**)), and methylvinyl ketone (**Figure 2-10**, route A). This is typically followed by a Grignard reaction to introduce additional functional groups (*tert*-butyl in the case of buprenorphine (**12**), *n*-propyl for etorphine (**86**)).⁹³ The ring-C olefin is often reduced as this can lead to higher MOR binding affinity, perhaps due to the resulting increase in flexibility in this region.^{57, 93}

The high affinity of 6-14 bridged opioid ligands is well known, as is their often poor subtype selectivity.⁹⁴ For example, diprenorphine (**87**) is a non-selective, weak partial agonist at all three ORs, that is used to displace other high affinity ligands, such as the powerful tranquilizer etorphine (**86**), which cannot be displaced by more frequently used antagonists like naloxone (**6**). These 6-14 bridged opioid ligands typically possess a mixture of partial agonism and antagonism at different opioid receptors.⁹⁴ Numerous compounds of this type have been synthesised and characterised, displaying only minor changes in binding affinity at the three ORs.⁹⁵⁻⁹⁸ However, manipulation of N/OFQ receptor affinity is possible through modifications to this region.^{95, 98}



Compound	Scaffold	R ₁	R ₂
12 Buprenorphine	81	^c PrCH ₂	<i>t</i> -Bu
86 Etorphine	80	Me	<i>n</i> -Pr
87 Diprenorphine	81	^c PrCH ₂	Me

Figure 2-10: Three approaches to the synthesis of 6-14 bridged opioid ligands.^{57, 93, 97, 99, 100}

Using oripavine (**78**) or another diene-containing morphinan as the starting material, Diels-Alder chemistry can be carried out with either methylvinyl ketone, methylacrylate or a substituted maleimide.^{57, 93, 97, 99, 100} **79** can be further reacted with a Grignard reagent to introduce an additional functional group (**80**).⁹³ Ester hydrolysis of **82** and subsequent amide coupling can also be used to functionalise the position (**83**).^{57, 97} The ring-C olefin in **80** and **83** can be reduced to give the more flexible **81** and **84** respectively.^{57, 93} In the synthesis of **81**, the reduction step is sometimes carried out prior to the Grignard reaction.⁹³ This reduction has been found not to work in imide compounds (**85**), possibly due to hinderance of the palladium from accessing the site by the bulky maleimide.⁵⁷

The structures of several common 6-14 bridged opioid receptor ligands are shown in the table, referencing the R-groups and structure of the general scaffold that they are derived from.

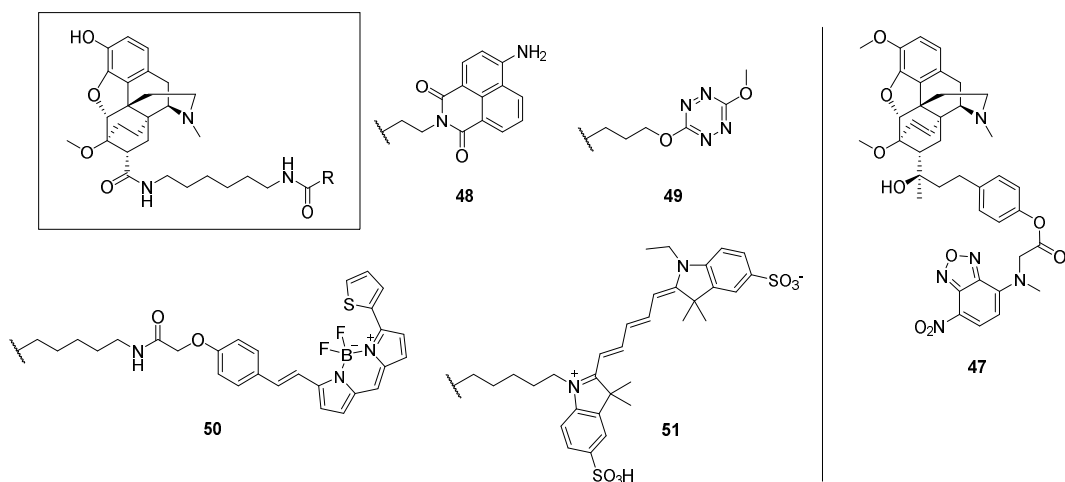


Figure 2-11: The structures of fluorescent opioid receptor ligands containing 6-14 bridged morphinan orthosteres.^{57, 69}

Left: Schembri *et al.*⁵⁷ utilised a 7-position amide to couple an oripavine-derived orthostere to several fluorophores (**48-51**). **Right:** One of the fluorescent ligands synthesised by Archer *et al.*⁶⁹ is a thebaine-derived structure similar to etorphine (**86**), where the fluorescent 7-nitrobenzo-2-oxa-1,3-diazole (NBD) moiety is connected to the 7-position (**47**).

An alternative method for introducing variation to this region is by using an alkyl acrylate, rather than methylvinyl ketone (**Figure 2-10**, route B).⁹⁷ This approach has been used extensively to introduce new chemical groups through hydrolysis of the installed ester, followed by amidation.^{57, 97, 99} These approaches have previously been used to link to a fluorophore, producing various fluorescent ligands for the opioid receptors (**Figure 2-11**).^{57, 69} A third method of expansion from ring-C uses a substituted maleimide in place of methylvinyl ketone as the dienophile (**Figure 2-10**, route C).^{57, 99, 100}

2.1.6 N-Alkylation

The 17-position amine of the morphinan structure is known to be highly influential over opioid receptor ligand properties in multiple ways. Whilst a simple *N*-methyl group is present in morphine and many other well-known opioids, different alkyl groups at this position generate a notable array of functional and pharmacodynamic properties in ligands.

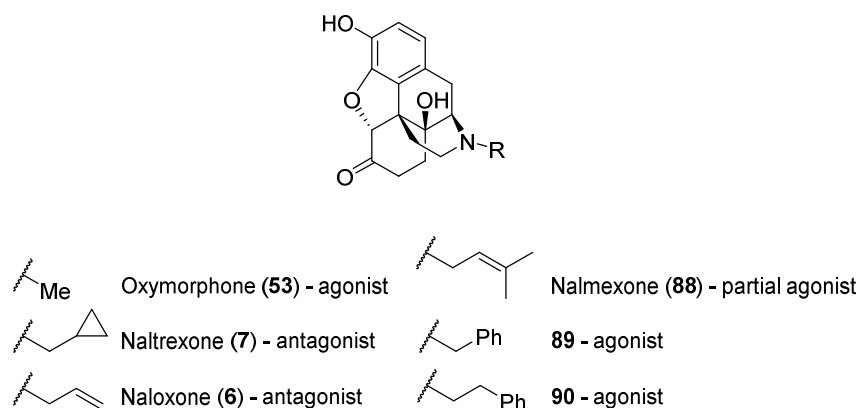


Figure 2-12: The effect of the *N*-substituent of different compounds in the oxymorphone family on function.^{101, 102}

The oxymorphone family of opioid ligands exemplifies this variety of function with changes in *N*-substituent (**Figure 2-12**). Two of the better known opioid antagonists, naloxone (**6**) and naltrexone (**7**), bear *N*-allyl and *N*-cyclopropylmethyl substituents respectively to confer MOR antagonist activity, unlike the *N*-methyl parent compound oxymorphone (**53**), which is an agonist.¹⁰¹ However, the *N*-benzyl (**89**) and *N*-phenethyl (**90**) analogues are both potent agonists and *N*-dimethylallyl substitution produces the partial agonist nalmexone (**88**).^{101, 102}

This demonstrates the complex role of *N*-substituents in the SAR of morphinan opioid ligands. The 2012 crystal structure of the MOR (PDB: 4DKL)³³ suggests potential interactions between the *N*-cyclopropylmethyl group of the covalently bound β -FNA (**74**) and neighbouring aromatic amino acids (**Figure 2-13**). However, given the differences between the *N*-substituents described above, it is challenging to predict what effect *N*-substitution with untested functional groups would have on ligand binding and function. The precise SAR of this *N*-substituted region still requires further investigation.

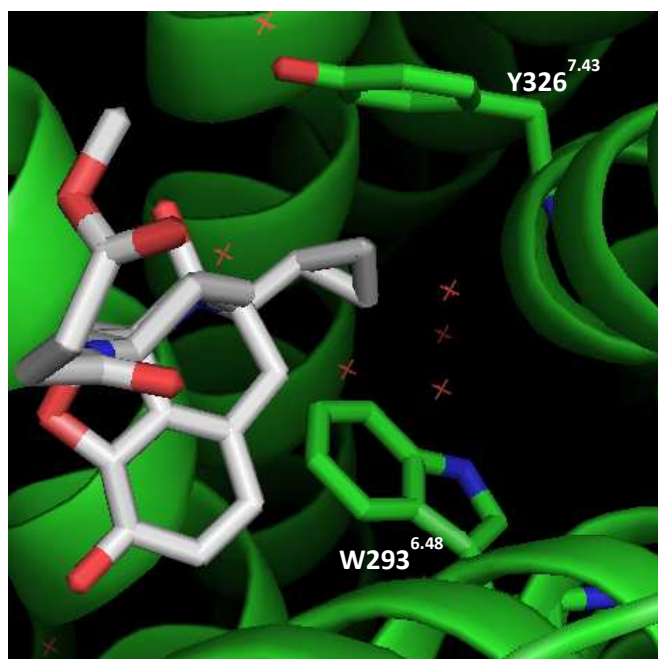


Figure 2-13: A potential π - π stacking interaction between the *N*-cyclopropylmethyl group of β -FNA, and aromatic amino acids in the binding pocket of MOR.³³

Adapted from Manglik *et al.* 2012.³³

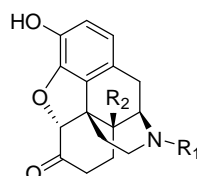
The proximity and orientation of the *N*-cyclopropylmethyl group of β -FNA (**74**) between Y326^{7.43} and W293^{6.48} in the crystal structure of MOR (PDB: 4DKL) suggest a π - π stacking interaction.

Another way in which the 17-position amine has been exploited is through quaternisation. Alkylation (typically methylation) of the tertiary amine produces a permanently charged quaternary species, giving it unique properties compared to its tertiary counterparts. This charge does not interfere greatly with binding as it is the protonated (and therefore charged) amine which forms an ionic interaction with D147^{3.32} in the MOR binding pocket.³³ One such example is methylnaltrexone (MNTX, **11**), a peripherally-acting opioid antagonist whose permanent charge prevents absorption across the blood brain barrier.¹⁰³

2.1.7 Modification of the 14-position

Variation at this position is fairly limited amongst most common opioid ligands and is typically a proton or hydroxyl group. Manglik *et al.*³³ did not propose a

specific interaction for the 14-hydroxyl group in their crystal structure of the MOR (PDB: 4DKL) based on its proximity to amino acids within receptor binding pocket. It has been suggested that the presence of the hydroxyl group in the oxymorphone-derived antagonists naloxone (**6**) and naltrexone (**7**) may restrict the freedom of rotation of the *N*-substituent, and subsequently eliminates low level agonism, making them antagonists.¹⁰⁴



Compound	MOR p <i>K</i> _i	R ₁	R ₂	Function
Oxymorphone (53)	9.0 ¹⁰⁵	Me	OH	Agonist
53a	10.0 ¹⁰⁵	Me	OMe	Agonist
53b	9.9 ¹⁰⁵	Me	OBn	Agonist
Naloxone (6)	7.3-9.0 ^a	^c PrCH ₂	OH	Antagonist
6a	9.7 ¹⁰⁶	^c PrCH ₂	O(CH ₂) ₃ Ph	Agonist
Naltrexone (7)	8.1-9.7 ^b	allyl	OH	Antagonist
7a	9.5 ¹⁰⁶	allyl	O(CH ₂) ₃ Ph	Agonist
Clocinnamox (91)	8.0 ¹⁰⁷	^c PrCH ₂	<i>p</i> CCA	Antagonist (irreversible)

*p*CCA – *p*-chlorocinnamoylamino. *a* – refs^{57, 108-112} *b* – refs^{57, 99, 108-110, 113, 114}

Figure 2-14: Modifications to the 14-position and their effect on MOR binding and ligand function.

The structures of 14-substituted opioid receptor ligands are shown, with binding data (p*K*_i) at MOR. Binding affinities at MOR were determined by inhibition of [³H]-DAMGO in rat brain membranes.¹⁰⁵⁻¹⁰⁷

Several recent studies have investigated 14-alkoxymorphinans to better establish SAR in this region (**Figure 2-14**). 14-*O*-Methylation of oxymorphone (**53**) was found to produce a compound (**53a**) with improved binding affinity at

all 3 opioid receptors.¹⁰⁵ The 14-*O*-benzyl analogue (**53b**) produced similar MOR affinity, but with reduced receptor subtype selectivity.¹⁰⁵ The 14-*O*-phenylpropyl analogues of both naloxone (**6**) and naltrexone (**7**) are full agonists (**6a** and **7a** respectively), in contrast to the antagonist activity of their 14-hydroxyl parent compounds.¹⁰⁶ Even the removal of the 3-hydroxyl group from **7a** yielded a ligand with sub-nanomolar MOR affinity.¹¹⁵ It is unclear whether new interactions formed by the phenylpropyl group simply overcome the loss of the 3-hydroxyl group, or if it adopts an entirely different binding position. A 14-amino group can also be used to functionalise this position, usually to form the corresponding amide analogues, such as those of the irreversible antagonist clocinnomox (**91**) and its derivatives.¹¹⁶⁻¹¹⁸

2.2 Selection of a lead molecule and fluorescent ligand design

There were several key criteria chosen to select a lead molecule. The lead molecule needed to be an antagonist, increasing the likelihood that any analogues synthesised would also be antagonists. A high binding affinity at MOR was desirable, as it would be more likely to produce high affinity fluorescent ligands. The lead molecule was also desired to be able to accommodate a linker in a position which is not critical for binding or function – linker attachment should not replace an important functional group. Therefore, a lead molecule with a well-understood structure-activity relationship (SAR) profile was sought, to minimise the disruption of key interactions and give the most predictable outcome in terms of binding and function.

2.2.1 Lead molecule selection

Known opioid receptor ligands were assessed using these criteria, with two molecules identified as candidates. Both naloxone (**6**) and naltrexone (**7**) are opioid receptor antagonists, with similarly well-established SAR profiles. Both

are high affinity ligands which have been utilised in numerous SAR studies, displaying tolerance for a broad range of modifications.

The well-established SAR profiles of naloxone (**6**) and naltrexone (**7**) guided the attachment point of the linker moiety. As described above, the 3-position and *N*-substituent of morphinan-based opioid ligands are important for binding and ligand function. The 14-position is capable of supporting larger substituents, but can also affect ligand function and receptor binding, making these unsuitable sites for ligand attachment.

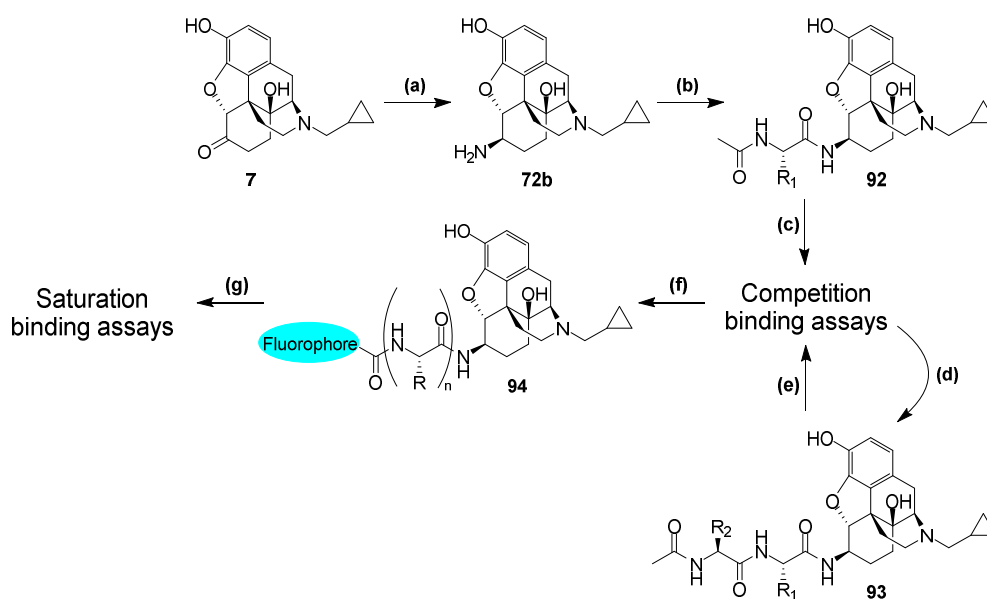
Subsequently, the 6-position was selected as the most suitable site for linker attachment. Introduction of an amine to the 6-position was ideal for attachment of the amino acid-based linker by direct amide coupling. Procedures for the reductive amination of the 6-keto moiety of both naloxone and naltrexone are well established.^{84, 119} However, the vast majority of literature examples employ β -naltrexamine (**72b**) as the orthostere, with few examples of either epimer of naloxamine (**70a** and **70b**) used. It is likely that this is due to the higher binding affinity of **72b**, providing the best starting point to produce high affinity ligands. For these reasons, β -naltrexamine (**72b**) was selected as the lead molecule for fluorescent ligand design.

Structures discounted from consideration include agonists and compounds containing prodrug modifications, such as ethers or esters at the 3-position. Buprenorphine (**12**) and other 6-14 bridged orthosteres were considered, as these structures have been previously used in fluorescent ligands. The fluorescent ligands described by Schembri *et al.*⁵⁷ (**Figure 2-11**) were antagonists, despite buprenorphine (**12**) itself being a partial agonist. Structurally, what drives this switch from partial agonism to antagonism is unclear. The oripavine starting material required to synthesise these compounds is an agonist, and therefore a controlled substance with greater legal barriers to use in synthesis. Due to these concerns, these 6-14 bridged compounds were deemed to be unsuitable orthosteres.

2.2.2 Fluorescent ligand design

The final fluorescent ligands were planned to consist of the β -naltrexamine orthostere connected to a fluorophore via a 6-position linker consisting of one or more amino acids. The number of amino acids and their composition would be determined through the synthesis and pharmacological evaluation of non-fluorescent congeners, as shown in the design scheme in **Scheme 2-1**.

An initial set of congeners were tested, consisting of the β -naltrexamine (**72b**) orthostere coupled to a single α -acetamido acid. The results from competition binding studies, alongside *in silico* modelling data, were used to inform further linker alterations. Once the optimal linker composition was established, a number of different fluorophores were coupled to the linker, with the resulting fluorescent compounds evaluated for MOR binding affinity in saturation binding experiments.



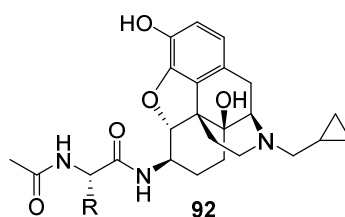
Scheme 2-1: Design scheme for the synthesis of β -naltrexamine-based fluorescent ligands.

The approach taken to design, synthesize and pharmacologically evaluate β -naltrexamine-based fluorescent ligands is shown: (a) reductive amination of naltrexone to naltrexamine and purification of epimers; (b) peptide coupling to a selection of different α -acetamido acids; (c) competition binding assay against a fluorescent ligand; (d) if the results suggested that a longer linker would be beneficial, coupling of a selection of different amino acids at the second position; (e) competition binding assay against a fluorescent ligand; (f) if the results suggested

that linker length is optimal, coupling of a selection of fluorophores to the linker; (g) saturation binding assay against an unlabelled ligand.

2.3 Non-fluorescent β -naltrexamine congeners

The first generation of congeners (**92**) were composed of variants of a single α -acetamido acid coupled to the 6-position of β -naltrexamine. The *N*-acetyl group was included to represent the further expansion of the linker, either to another amino acid or to a fluorophore. This acetamide would be expected to possess properties more similar to the final fluorescent ligands, than to the corresponding free primary amine. A selection of eight amino acids were chosen to reflect all types of amino acid (polar, non-polar, acidic, basic) as shown in **Figure 2-15**.



Compound	Amino acid	R
92a	Gly	H
92b	Ala	CH ₃
92c	Val	CH(CH ₃) ₂
92d	Phe	CH ₂ Ph
92e	Ser	CH ₂ OH
92f	Asn	CH ₂ CONH ₂
92g	Asp	CH ₂ COOH
92h	Lys	(CH ₂) ₄ NH ₂

Figure 2-15: Structures of the single amino acid non-fluorescent congeners.

2.3.1 *In silico* modelling

In silico modelling of the proposed ligands was undertaken to better understand the potential interactions of these β -naltrexamine congeners with the MOR, and as a tool to predict the optimal length and chemical composition of the linker region. The modelling was carried out using the online modelling software DockingServer (<http://www.dockingserver.com/web>). The crystal structure of the MOR (PDB: 4DKL) produced by Manglik *et al.*³³ was uploaded to the online software and the proposed ligand structures (those shown in **Figure 2-15**) were drawn and docked into the binding site of the receptor.

It was immediately clear that the predicted numerical values for binding affinity (pK_i) were inaccurate. Compounds with well-established literature pK_i values, such as naloxone (**6**) and naltrexone (**7**), were several log units lower than typical reported values. Instead, the positions of the docked β -naltrexamine orthostere were analysed and the relative differences in predicted pK_i were noted.

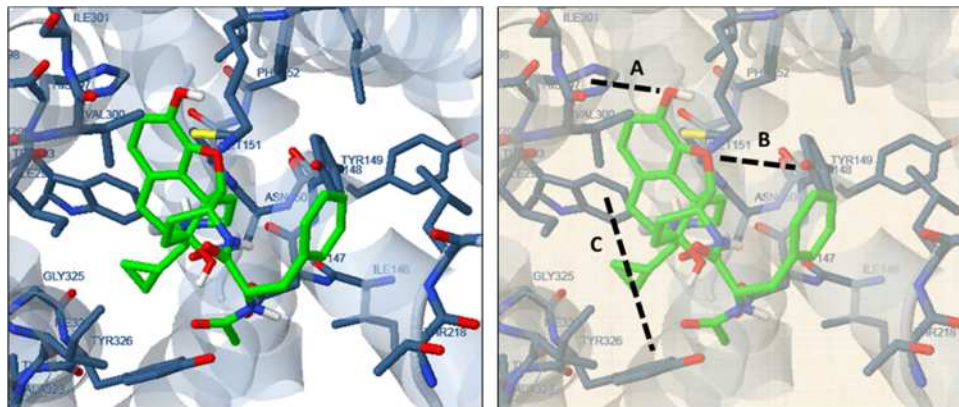


Figure 2-16: Positional criteria for the β -naltrexamine congeners within the MOR binding site.

Three key interactions that were easy to identify quickly were used to confirm the binding position of the β -naltrexamine orthostere. These are highlighted for the Phe congener **92d** in the right-hand image: **A** - the alignment of the 3-hydroxy to H297^{6,52}; **B** - the 4,5-epoxy in close proximity to Y148^{3,33}; **C** - the cyclopropylmethyl group positioned between Y326^{7,43} and W293^{6,48}.

The examples which predicted the highest relative binding affinity typically adopted a similar position to that of the covalently bound β -FNA. Building on

this observation, each congener was repeatedly docked, looking for several key positional criteria: the positioning of the cyclopropylmethyl group between Y326^{7.43} and W293^{6.48}, 4,5-epoxy in close proximity to Y148^{3.33} and the alignment of the 3-hydroxyl group to H297^{6.52} (as shown in **Figure 2-16**).

Twenty examples of each ligand were collected in which the bound ligand fitted this positional criteria. Further analysis of these examples showed that predicted interactions of the linker moieties were highly varied for each docked congener. Often the linker did not display any interactions or come into close proximity with any part of the receptor. Instead, the 6-position moiety projected into the extracellular space. However, there were several noteworthy interactions specific to individual congeners which appeared across multiple docking predictions.

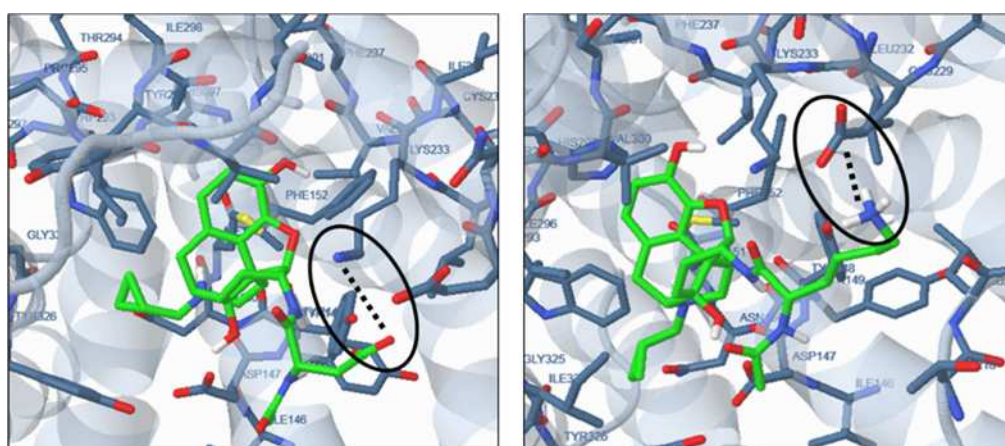


Figure 2-17: Docked ligands with highlighted linker side chain interactions.

Left: In some predictions, the aspartate congener (**92f**) was shown to form an ionic interaction with K233^{5.39}. **Right:** The Lys congener (**92h**) was sometimes predicted to interact ionically with E229^{5.35} but this resulted in disruption of some of the desirable interactions between the pharmacophore and receptor described in **Figure 2-13**.

In some iterations, the Asp congener (**92g**) was predicted to form an ionic interaction with K233^{5.39} (**Figure 2-17**) - the same lysine to which β -FNA is covalently bound in the crystal structure (PDB: 4DKL).³³ When docked, a glutamate congener was not able to form an interaction with K233^{5.39}, suggesting that the shorter side chain present on Asp was more ideally placed to do so.

An ionic interaction was also predicted between the Lys congener (**92h**) and E229^{5,35}, but this interaction distorted the docking pose of the rest of the ligand (**Figure 2-17**). An interaction of this kind could be more favourable without distortion if ornithine, or another basic amino acid with a shorter sidechain, replaced lysine.

The non-polar Ala (**92b**), Val (**92c**) and Phe (**92d**) congeners were predicted to form a non-polar interaction with Leu²¹⁹. However, this residue appears in the extracellular loop region of the receptor so it may not be available for binding due to the flexibility of this region. Similarly, the Asn congener (**92f**) was, in some instances, predicted to hydrogen bond with the backbone of this intracellular region.

The frequency of interactions with the extracellular loop region, as well as the trend of 6-position moieties showing no interaction with the receptor, are likely due to two key features of the MOR ligand binding site: the binding pocket is both shallow and polar. Manglik *et al.*³³ noted that the binding pocket of the MOR is particularly exposed and shallow, observing the difference between MOR and the M₃ muscarinic receptor (M₃R) which is deeper and narrower (**Figure 2-18**). The openness of the MOR ligand binding site means it is exposed to the extracellular fluid, and therefore contains a high concentration of polar amino acids. β -naltrexamine congeners containing non-polar amino acids might therefore be unable to find sites to make hydrophobic interactions.

The relatively short 6-position substituent of the bound β -FNA in the crystal structure can be seen protruding from the receptor, indicating its shallowness within the helical bundle (**Figure 2-19**). The proximity of the congeners to the surface may be why the modelling predicted interactions with the extracellular loop regions of the receptor.

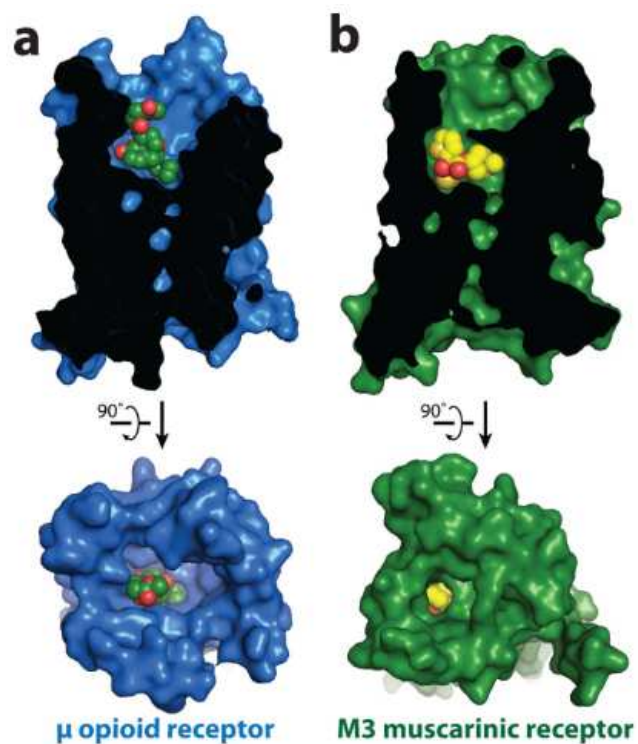


Figure 2-18: Comparison of the ligand binding pockets of MOR and M₃R.

Source: Manglik *et al.* 2012.³³

The MOR (a) binding pocket is both wide and exposed in comparison to the M3 muscarinic receptor (b) which has a narrow opening for ligand entry.

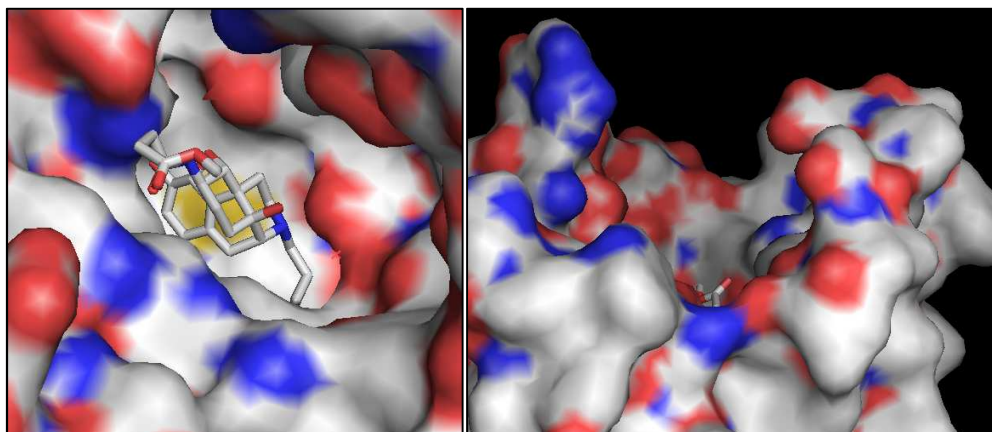


Figure 2-19: The MOR with bound β -FNA.

Crystal structure taken from Manglik *et al.* 2012.³³ Displayed in PyMOL.

A high density of polar amino acid side chains is present in the exposed binding pocket of the MOR. The oxygen (red), nitrogen (blue) and sulfur (yellow) atoms are coloured to indicate polar regions. The 6-position substituent is clearly visible extending to the surface of the binding pocket (right).

These observations were supported by the docking of two further sets of congeners, each containing two amino acids in their linker (**Figure 2-20**). One set contained Asp at the first position adjacent to the orthostere, as **92g** had the most consistent predicted interactions. The second position was varied, with the same eight amino acids used in the single amino acid congeners (**Figure 2-15**). The second set contained Ala at the first position with the same variation at the second position. This was intended to allow the amino acid at the second position to form interactions with reduced conformational restriction from any interactions made by the amino acid at the first position.

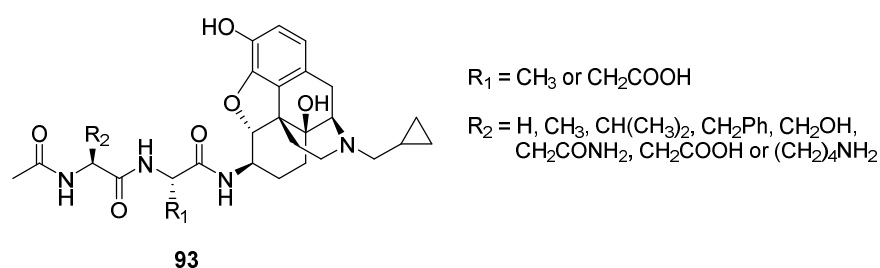


Figure 2-20: General formula for docked congeners containing 6-position dipeptides.

The 16 docked compounds were composed of either Ala or Asp at the first position and one of eight amino acids shown in **Figure 2-15** at the second position.

Gathering sufficient data to reach a firm conclusion was challenging, as the predicted binding positions of the dipeptide congeners were highly variable. In instances where the positioning of the orthostere met the criteria described above, the 6-position substituent was still varied in its positioning and proposed interactions. The only common theme observed amongst most examples was that the linker would coil back into the receptor rather than extending toward the extracellular regions of the receptor (**Figure 2-21**), possibly indicating that the linker was unable to find points of interaction further from the binding site.

The predicted docking positions of the tested congeners indicated that the first amino acid coupled to the 6-position of naltrexamine may be able to interact with the ligand binding pocket. Specifically, a polar amino acid at the first position could form the strongest interactions with the polar residues of the

binding pocket - particularly acidic or basic side chains. However, any further elaboration of the linker may exceed the limits of the binding pocket and was predicted to not form beneficial interactions.

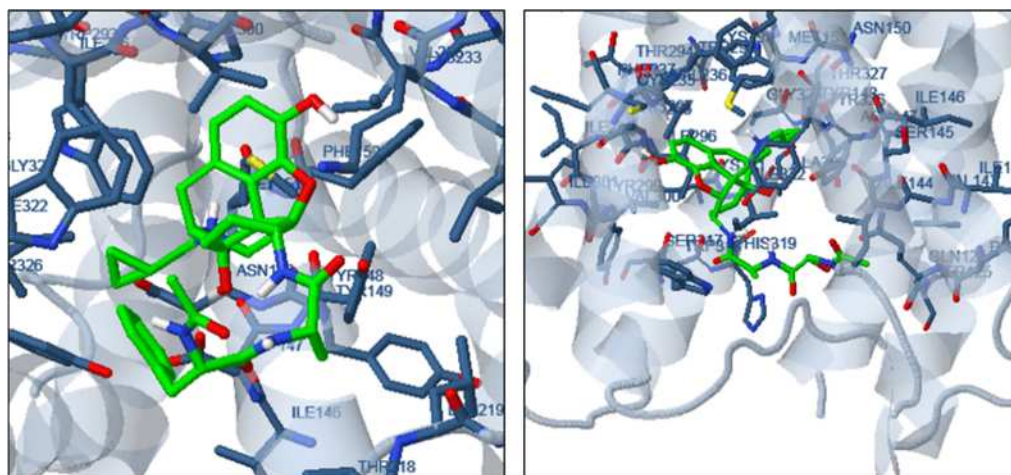


Figure 2-21: Predicted binding poses for congeners with linkers containing two amino acids.

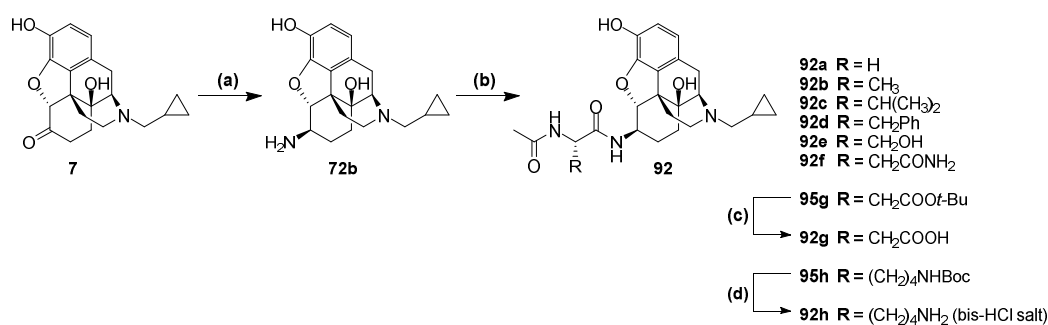
Left: The congener containing Ala (position 1) and Phe (position 2) is docked showing the linker coiling within the binding pocket rather than extending towards the extracellular regions of the receptor. **Right:** The congener with Ala (position 1) and Ser (position 2) extends across the entrance of the bind site rather than out of it.

The modal outcome of the docking was for the 6-position moiety to not form any interactions or, less plausibly, interact with an extracellular loop region. This suggests that there are few possible interactions for functional groups at the 6-position, or perhaps that this model may not be a good predictor of *in vitro* outcomes.

2.3.2 Synthesis of β -naltrexamine single amino acid congeners

The synthesis of β -naltrexamine from naltrexone has been described previously in the literature.^{84, 119} The synthetic route used in this project (**Scheme 2-2**) was a modified version of the route described by Filer *et al.*,¹¹⁹ with the tritiated naltrexone used in the procedure substituted for the ¹H isotope. This was followed by peptide coupling to the array of α -acetamido acids shown in **Figure 2-15**. Congeners containing a side chain protective group were deprotected prior to pharmacological testing.

Sodium triacetoxyborohydride (STAB) is typically preferred as a mild reducing agent, particularly in reductive amination reactions, due to its safety profile.¹²⁰ Sodium cyanoborohydride is often avoided as it can produce the toxic byproducts HCN and NaCN.¹²⁰ However, a literature search yields no examples of STAB use in the reductive amination of naltrexone (**7**) to β -naltrexamine (**72b**), with NaBH₃CN preferred in every case. An unpublished synthesis by a lab group member attempted a reductive amination of the chemically similar naloxone (**6**) using STAB as the reducing agent, but this almost exclusively yielded the α -epimer (**70a**). This may be due to the larger acetoxy groups of STAB, which may sterically hinder and prevent it from accessing the imine from the face that would produce the β -epimer (**70b**). Alternatively, it may result from differences in the strengths of these reducing agents, due to the electron-withdrawing effects of their respective cyano and acetoxy groups. However, the frequency with which STAB and NaBH₃CN are interchangeable in other reactions suggest that this is not the case.



Scheme 2-2: Synthesis of single amino acid congeners of β -naltrexamine (92**).**

Reagents and conditions: (a) i. NH₄OAc, MeOH, rt; ii. NaBH₃CN, MeOH, rt, 25%; (b) α -acetamido acid, PyBOP, DIPEA, DMF, rt, 73-90%; (c) TFA, TIPS, water, CH₂Cl₂, rt, 90%; (d) 4M HCl in 1,4-dioxane, rt, 99%.

Even when NaBH₃CN is used, the α -epimer (**72a**) remains the major product.⁸⁴ Use of substituted amines, such as dibenzyl amine, can direct the reduction towards greater β -epimer (**72b**) yield.⁸⁵ However, this approach introduces an additional hydrogenation step which would also decrease the final yield.

A pilot reaction using NH₄OAc with NaBH₃CN yielded four products. The β -epimer (**72b**) composed 25% of the total products, alongside the α -epimer

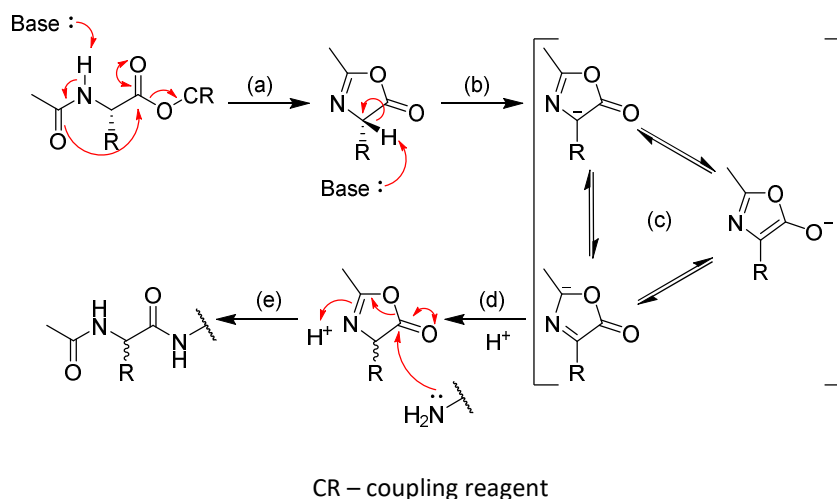
guanidinylated by-product (**97**) and 3-esterified, 6-guanidinylated by-product (**96**) were also present in large quantities.

To confirm that 6-position guanidinylation was occurring, two small scale investigative reactions were carried out; β -naltrexamine (**72b**) and naltrexone (**7**) were both separately mixed with HCTU and DIPEA in dimethylformamide (DMF). Unaltered naltrexone (**7**) was identified by liquid chromatography-mass spectrometry (LCMS), whereas the β -naltrexamine (**72b**) was entirely consumed and the 6-guanidinylated product (**97**) was identified by LCMS. At this time, a similar issue of guanidinylation had been encountered with the alvimopan-based compounds (**Chapter 3**), so the non-uronium-based PyBOP was chosen as an alternative coupling reagent. The stoichiometry was also altered from a 1:3:3 ratio (β -naltrexamine/coupling reagent/ α -acetamido acid) to 1:1:1 to discourage esterification of the 3-OH. These conditions generated the desired products in acceptable yields (39-74%) with neither by-product **96** nor **97** detectable in the reaction mixture.

$^1\text{H-NMR}$ analysis of the products of the peptide couplings revealed varying levels of epimerisation at the amino acid chiral centres. Racemisation of α -acetamido acids during peptide coupling is known to occur via a 5(4*H*)-oxazolone intermediate as shown in **Scheme 2-3**. The degree to which the chiral centre is racemised depends on the acidity of the α -proton, which varies for different amino acids. For example, the chiral centres of the Asn (**92f**) and Asp(*t*Bu) (**95g**) β -naltrexamine congeners were highly racemised (**Figure 2-23**). The electron withdrawing side chains of these amino acids can stabilise the α -carbocation, making the α -proton more acidic.¹²¹ The electron donating alkyl chain in the Lys(Boc) congener (**95h**) is less stabilising over the α -carbocation, and so produced very little racemisation (**Figure 2-23**).¹²¹

After separation by HPLC, three of the eight congeners produced sufficient chirally pure material that both *L*- and *D*-epimers could be pharmacologically tested. The chirality of the diastereomeric pair was assigned to each compound based on the relative size of identifiable peaks in the $^1\text{H NMR}$ of the mixture (**Figure 2-23**). The compound associated with the larger peak in the mixed ^1H

NMR was designated as the *L*-epimer, and the smaller peak was assigned to the *D*-epimer. In most cases this was a clear distinction, however, the ^1H NMR peaks for both epimers of the Asp(*t*Bu) congener were very similar, suggesting almost complete epimerisation of the chiral centre.



Scheme 2-3: The mechanism of α -acetamido acid racemisation via a 5(4*H*)-oxazolone intermediate.

(a) The acetyl carbonyl oxygen acts as a nucleophile in conjunction with deprotonation of the amide nitrogen, forming a lactone (5(4*H*)-oxazolone) and eliminating the coupling reagent (CR); (b) Deprotonation of the 5(4*H*)-oxazolone α -carbon causes it to become sp^2 hybridised; (c) The negative charge from deprotonation is stabilised across several positions in the oxazolone ring; (d) Protonation returns the α -carbon to the sp^3 hybridised state, generating an equal distribution of the two oxazolone enantiomers; (e) Nucleophilic attack of the oxazolone ester by a primary amine reopens the ring giving the same product as a non-cyclised peptide coupling, but with racemisation of the stereo centre.

Finally, the *tert*-butyl ester protecting group of both Asp congeners, and the Boc protecting group of the Lys congener were removed. *tert*-Butyl ester deprotection was carried out using an 18:1:1 mixture of trifluoroacetic acid (TFA)/triisopropylsilane (TIPS)/ H_2O in CH_2Cl_2 . Boc deprotection was achieved using a 4M HCl/1,4-dioxane.

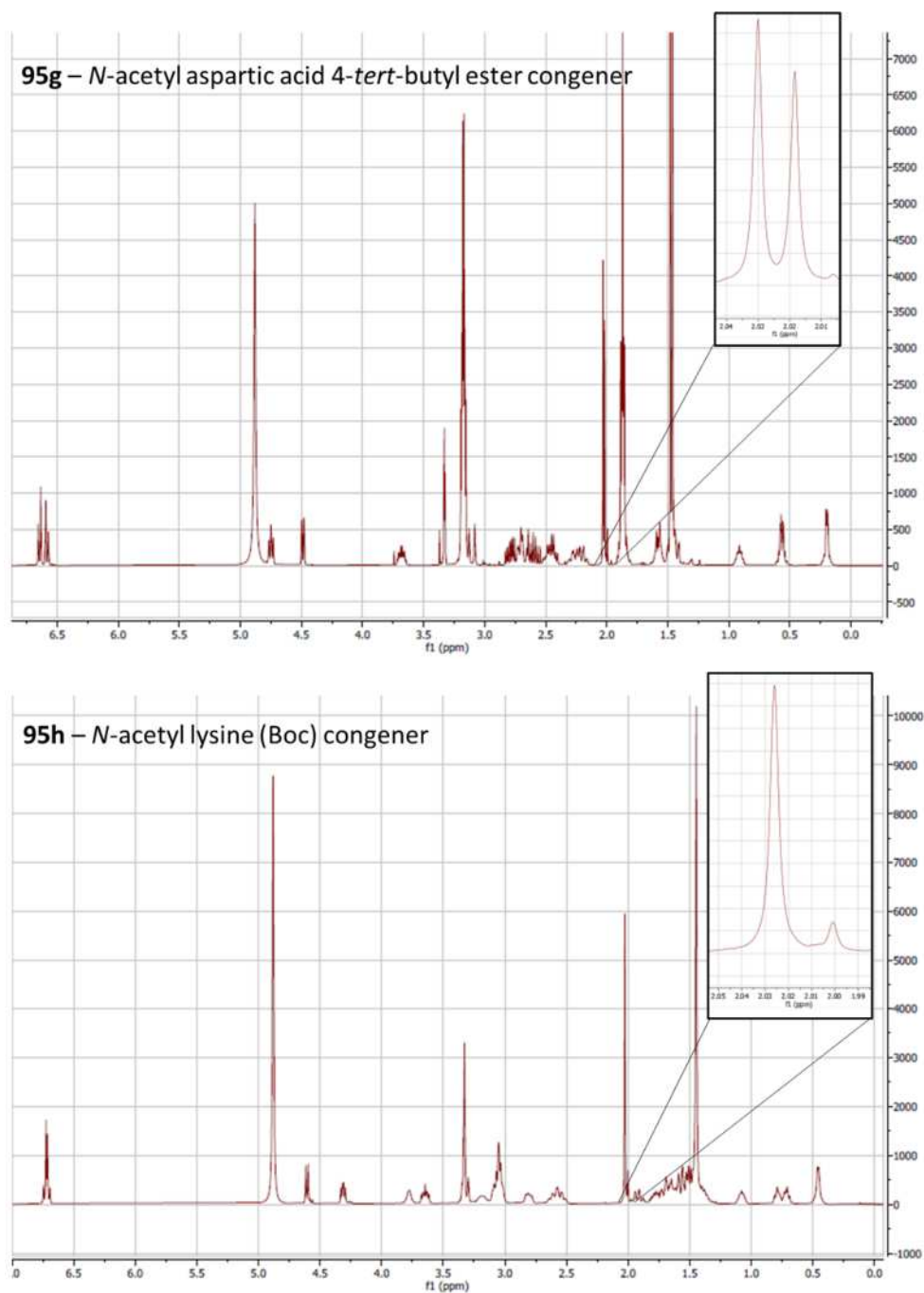


Figure 2-23: $^1\text{H-NMR}$ spectra for two β -naltrexamine congeners showing differing amounts of racemisation for each amino acid.

The proportion of product which has been converted to the *D*-epimer can be seen in the respective peaks of several functional groups of each β -naltrexamine congener. The clearest view of the level of epimerisation can be seen by looking at the acetyl CH_3 singlet peak (typically around 2.0 ppm). **(above)** The Asp(*t*Bu) congener (**95g**) was highly racemised, as seen in the acetyl CH_3 peaks (inset) where there are two peaks of similar height. **(below)** There was very little racemisation of the Lys(Boc) congener (**95h**), as shown at the acetyl CH_3 peaks (inset) where one peak is much larger than the other.

2.3.3 MOR binding affinity of the non-fluorescent β -naltrexamine congeners

Before evaluating the β -naltrexamine congeners, the K_D of the BODIPY 630/650-labelled oripavine derivative **50** (synthesised and characterised by Schembri *et al.*⁵⁷) was determined using TR-FRET in a saturation binding assay. **50** showed saturable high affinity binding to the SNAP-MOR in HEK293 cell membranes with a pK_D measured as 8.88 ± 0.36 (mean \pm SEM, $n = 3$) (Figure 2-24).

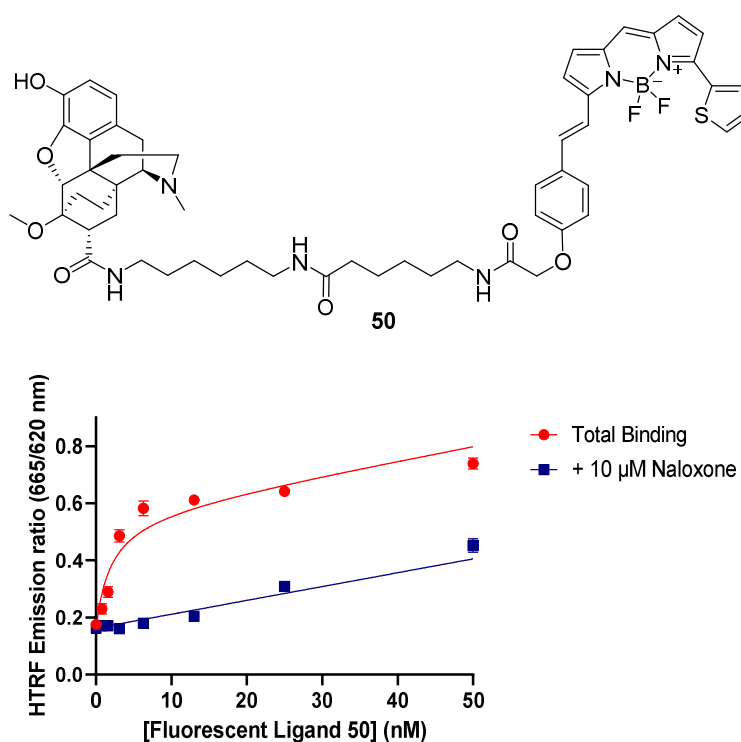


Figure 2-24: Structure and saturation binding of the fluorescent ligand **50 to the SNAP-MOR in HEK293 membranes.**

Membranes from Lumi4-Tb-labelled SNAP-MOR-expressing HEK293 cells were incubated with varying concentrations of the fluorescent ligand **50** (synthesised by Schembri *et al.*⁵⁷). Non-specific binding (blue) was determined in the presence of 10 μ M naloxone. Total binding (red) was determined in the absence of naloxone. Data points are the mean of a single experiment (mean \pm SEM) carried out in triplicate which are representative of three separate experiments, from each of which a value for K_D was determined.

The MOR binding affinities of the non-fluorescent congeners were then assessed by TR-FRET in a competition binding assay against **50**. The results were

plotted as competition binding curves (**Figure 2-25**) from which pK_i values were determined (**Table 2-1**).

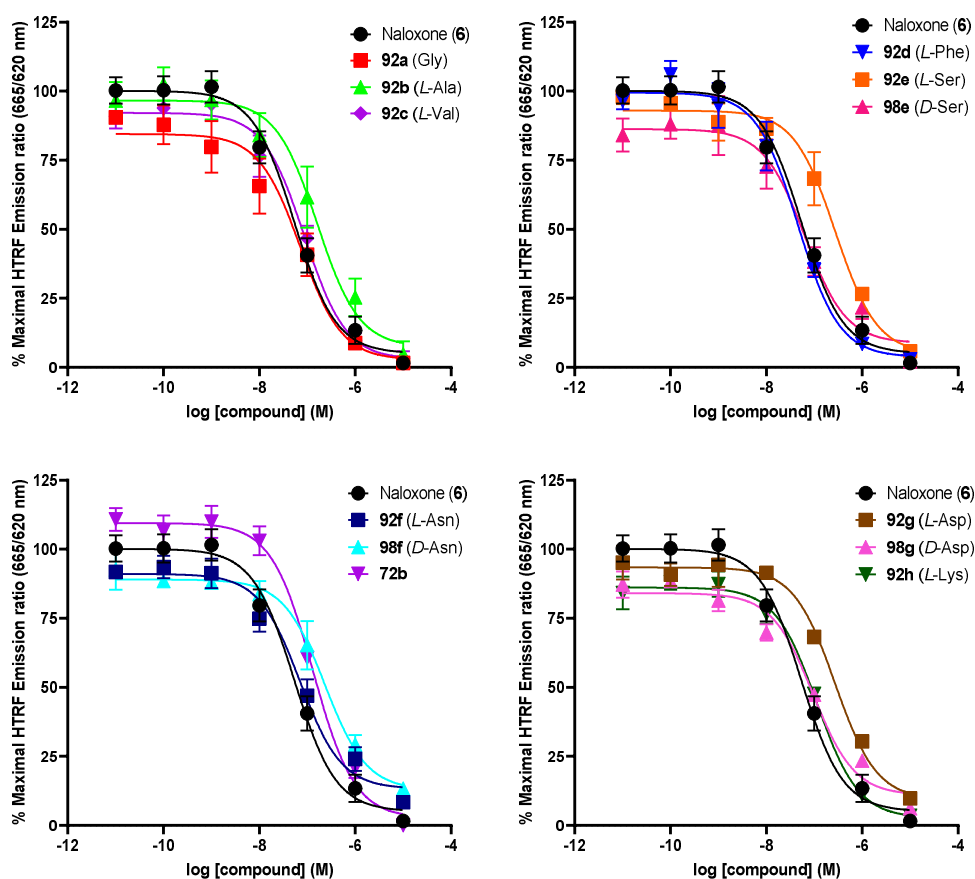


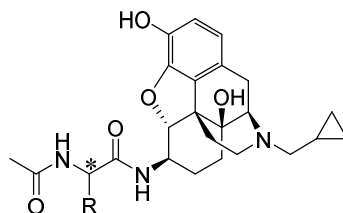
Figure 2-25: Competition binding assay using the non-fluorescent β -naltrexamine congeners.

Lumi4-Tb-labelled SNAP-MOR-expressing HEK293 cell membranes were incubated with 2 nM of the fluorescent ligand **50** (synthesised by Schembri *et al.*⁵⁷) and increasing concentrations of each of the β -naltrexamine congeners described in **Figure 2-15**. Where sufficient material of the respective D-isomer of a congener was isolated it was also tested. Data points are the mean of 3 or 4 separate experiments (mean \pm SEM), each carried out in duplicate.

All congeners reduced binding to non-specific binding levels. Competition binding experiments indicated that, although changes to linker composition produced a range of affinities (one-way ANOVA, $P = 0.01$), none of the linkers resulted in a significant change in MOR binding affinity compared to the unsubstituted β -naltrexamine (**72b**).

Similarly, no significant increase in binding affinity was seen with any congener compared to the glycine congener (**92a**), although congeners **92e** and **92g** (L-

isomers) showed a significant reduction in binding affinity from **92a** ($P < 0.05$, post-hoc Dunnett's multiple comparisons test). However, there was no significant difference between **92a** and the *D*-isomers **98e** and **98g**.



Compound	Config.	R	MOR $pK_i \pm SEM$	n
Naloxone (6)			7.69 ± 0.11	4
β -Naltrexamine (72b)			7.30 ± 0.08	4
92a	<i>R</i>	H	7.56 ± 0.16	3
92b	<i>R</i>	CH ₃	7.19 ± 0.28	3
92c	<i>R</i>	CH(CH ₃) ₂	7.50 ± 0.11	4
92d	<i>R</i>	CH ₂ Ph	7.76 ± 0.11	4
92e	<i>R</i>	CH ₂ OH	6.93 ± 0.12	3
98e	<i>S</i>	CH ₂ OH	7.61 ± 0.17	3
92f	<i>R</i>	CH ₂ CONH ₂	7.57 ± 0.12	3
98f	<i>S</i>	CH ₂ CONH ₂	7.05 ± 0.13	3
92g	<i>R</i>	CH ₂ COOH	6.98 ± 0.11	3
92g	<i>S</i>	CH ₂ COOH	7.44 ± 0.19	3
92h	<i>R</i>	(CH ₂) ₄ NH ₂	7.37 ± 0.08	3

Table 2-1: MOR binding affinities of α -acetamido acid β -naltrexamine congeners.

pK_i values at MOR were calculated from experimental IC_{50} values using the Cheng-Prusoff equation.¹²² Experimental IC_{50} values were determined by competitive displacement of the fluorescent ligand **50** (synthesised by Schembri *et al.*⁵⁷) in Lumi4-Tb-labelled SNAP-MOR-expressing HEK293 cell membranes. Values are the mean of 3 or 4 separate experiments (mean \pm SEM), each carried out in duplicate.

In light of these findings, along with the *in silico* modelling results, it was decided that there was no basis for further elaboration of the linker. Importantly, attachment of the linker at the 6-position did not diminish the

binding affinity of the unsubstituted β -naltrexamine (**72b**), indicating that the amino acid linker was well tolerated, regardless of side chain group. Synthesis of the final fluorescent ligands was carried out without further investigation of non-fluorescent congeners.

2.4 Synthesis and pharmacological evaluation of fluorescent ligands

The synthesised fluorescent ligands were composed of the β -naltrexamide bound to one of three fluorophore moieties via either an α -acetamidolysyl or β -alanyl linker (**Figure 2-26**). The fluorophores used were BODIPY 630/650-X, BODIPY 630/650 (without the hexanoyl spacer) and sulfo-Cy5.

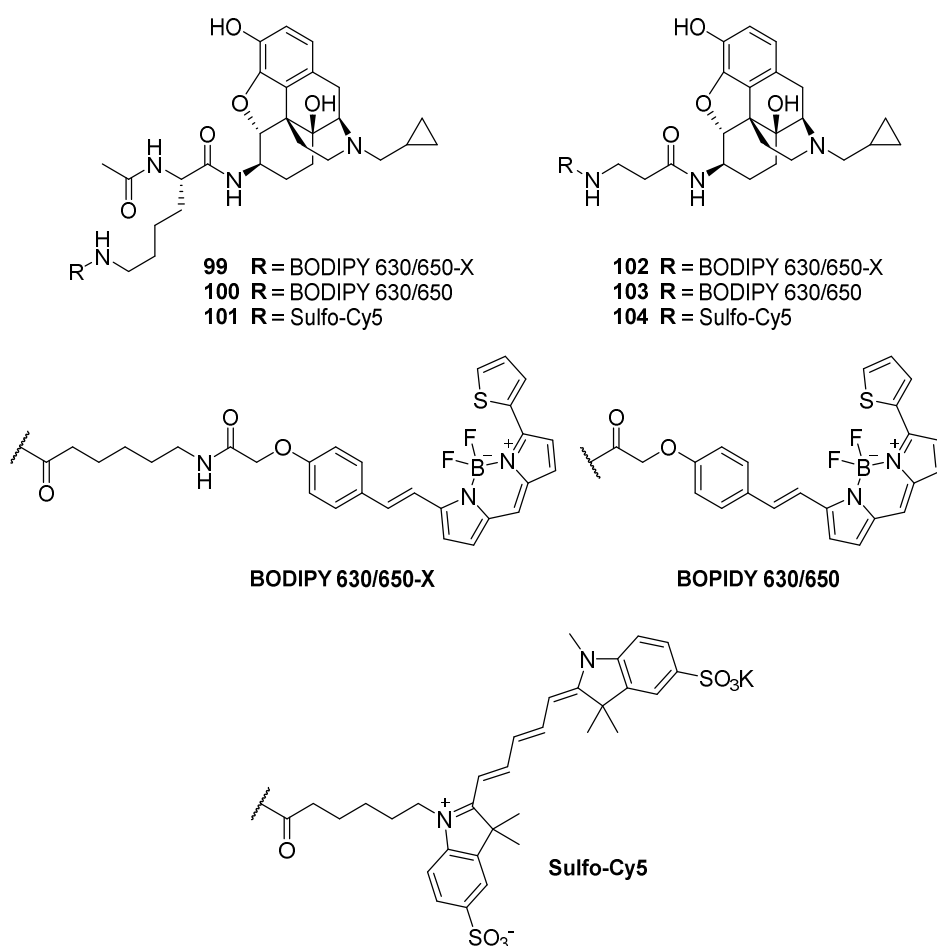


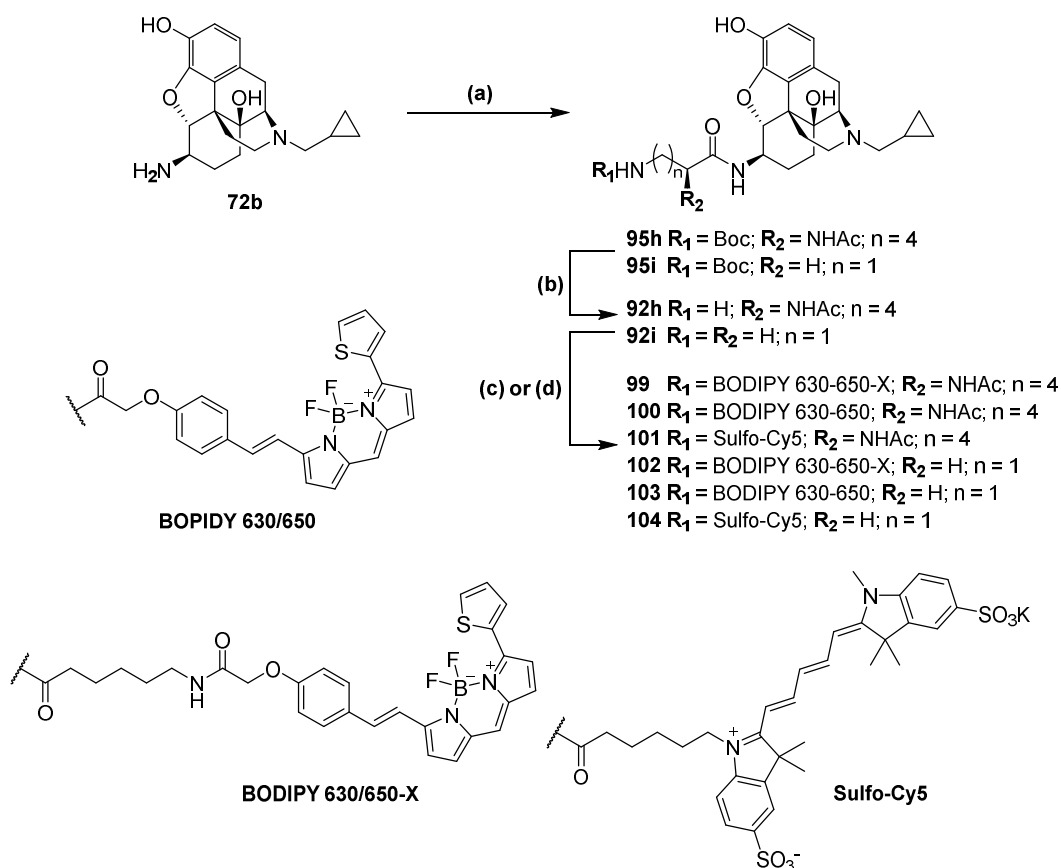
Figure 2-26: Structures of β -naltrexamine fluorescent compounds.

Two β -naltrexamine scaffolds bound to different linker moieties were combined with three fluorophores to give six novel fluorescent ligands. The two scaffolds utilise α -acetamidolysyl or β -alanyl linkers, which are bound to either BODIPY 630/650-X, BODIPY 630/650 or sulfo-Cy5.

The inclusion of an amino acid-based linker in these fluorescent ligands aimed to increase hydrophilicity and reduce non-specific binding, potentially making these fluorescent ligands more suitable for different imaging applications. The sulfo-Cy5 fluorescent ligand (**51**) synthesised by Schembri *et al.*⁵⁷ was preferred due to improved confocal imaging properties compared to the BODIPY 630/650-X compound (**50**), which displayed incomplete displacement of binding in the presence of an excess of unlabelled competitor, suggesting a higher level of non-specific binding. Fluorescent ligands composed of two different BODIPY 630/650 variants, with differing distances between orthostere and fluorophore, were synthesised to test the effect of this spacer on MOR binding affinity and potentially non-specific binding. However, fluorescent ligands containing sulfo-Cy5 (**101** and **104**) were also synthesised as they potentially possessed properties that were better suited to different pharmacological applications.

2.4.1 Synthesis of fluorescent β -naltrexamine compounds

Amino acid coupling of β -naltrexamine to the two amino acids was carried out using PyBOP and DIPEA in a 1:1:1:1 stoichiometric ratio (β -naltrexamine (**72b**)/PyBOP/DIPEA/acetamido acid), followed by Boc-deprotection of both compounds in 4M HCl/1,4-dioxane. BODIPY 630/650-X and sulfo-Cy5 were both pre-formed *N*-hydroxysuccinimide (NHS) esters, which were reacted with the β -naltrexamine congeners in the presence of DIPEA to produce the final fluorescent BODIPY 630/650-X (**99** and **102**) and sulfo-Cy5 (**101** and **104**) compounds. Coupling to the shorter BODIPY 630/650 compound differed, as it was a free acid rather than an NHS ester, requiring the use of PyBOP with DIPEA in a 1:1:1 ratio (PyBOP/BODIPY/ β -naltrexamine congener) to discourage 3-position ester formation.



Scheme 2-4: Synthesis of fluorescent β -naltrexamine-based compounds.

Reagents and conditions: (a) N^2 -acetyl- N^6 -Boc-lysine or N -Boc- β -alanine, PyBOP, DIPEA, DMF, rt, 73-90%; (b) 4M HCl in dioxane, rt, 99%; (c) BODIPY 630/650-X-OSu or sulfo-Cy5-OSu, DIPEA, DMF, rt, 35-83%; (d) BODIPY 630/650-OH, PyBOP, DIPEA, DMF, rt, 42-47%.

2.4.2 MOR binding affinity of fluorescent β -naltrexamine compounds

MOR binding affinities (pK_D) of the fluorescent compounds **99-104** were determined in saturation binding experiments (**Figure 2-27**, **Figure 2-27a** and **Table 2-2**). The four BODIPY 630/650-containing ligands (**99**, **100**, **102** and **103**) all exhibited sub-nanomolar binding affinities for MOR. Differences in linker composition or length were found to not significantly change MOR binding affinity (One-way ANOVA, $P = 0.32$). However, the sulfo-Cy5-containing **101** displayed a near-100-fold loss in pK_D compared to the BODIPY 630/650-containing (**99** and **100**) lysine-linked compounds.

The total binding curve for compound **104** at this concentration did not appear to reach saturation, meaning that a reliable pK_D value could not be determined. This suggests a significantly lower MOR binding affinity for **104** than the other measurable compounds.

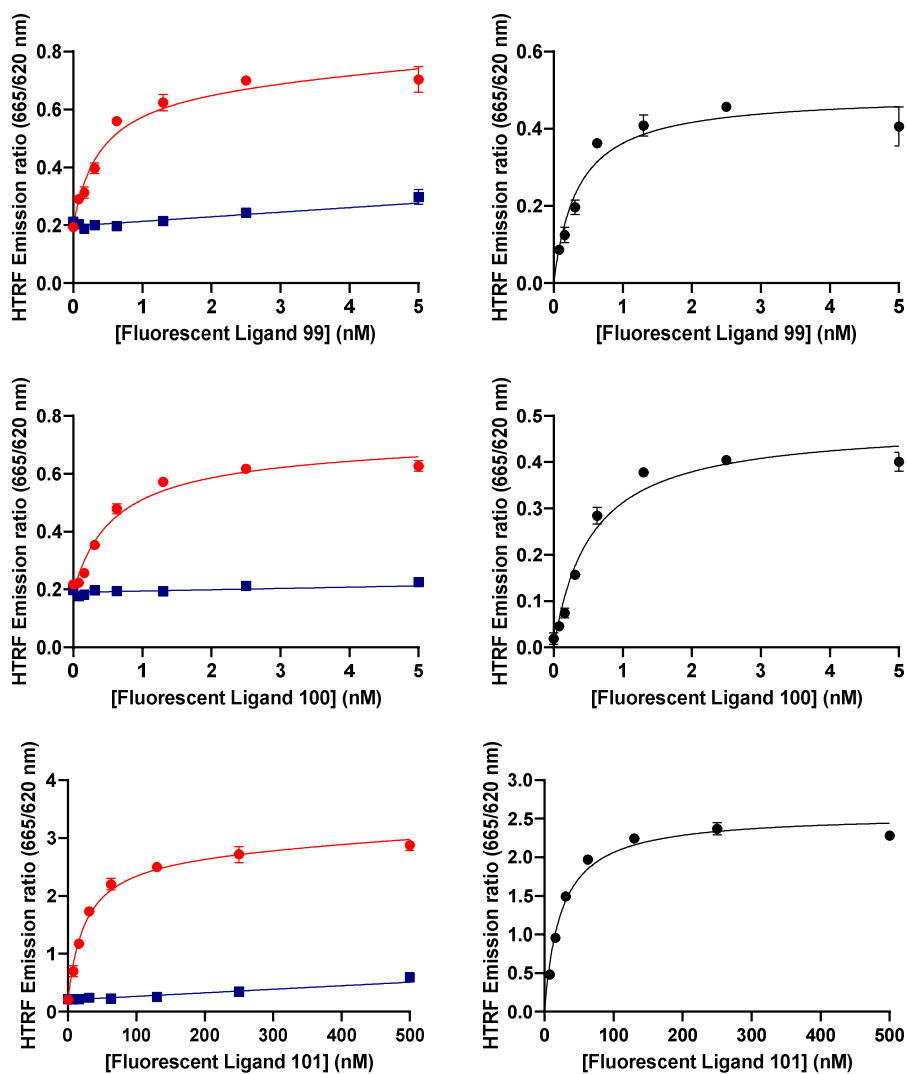


Figure 2-27: Saturation binding assay results for the lysine-linked fluorescent β -naltrexamine compounds.

Lumi4-Tb-labelled SNAP-MOR-expressing HEK293 cell membranes were incubated with increasing concentrations of the fluorescent compounds **99-101**. Non-specific binding (blue) was determined in the presence of 10 μ M naloxone. Total binding (red) was determined in the absence of naloxone. Specific binding (black) was calculated from total binding minus non-specific binding. Data points are the mean of a single experiment (mean \pm range) carried out in duplicate which are representative of four separate experiments from which a value for K_D was determined.

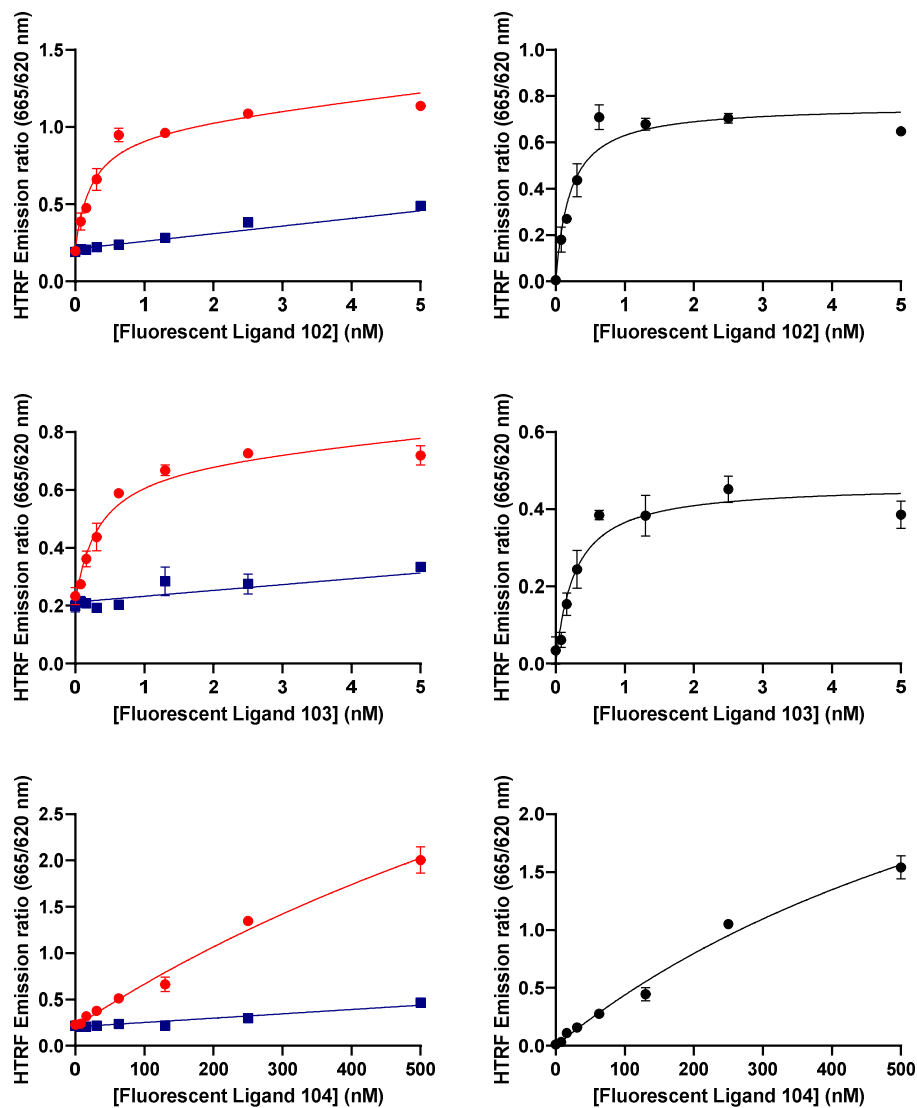


Figure 2-27a: Saturation binding assay results for the β -alanine-linked fluorescent β -naltrexamine compounds.

Lumi4-Tb-labelled SNAP-MOR-expressing HEK293 cell membranes were incubated with varying concentrations of the fluorescent compounds **102-104**. Non-specific binding (blue) was determined in the presence of 10 μ M naloxone. Total binding (red) was determined in the absence of naloxone. Specific binding (black) was calculated from total binding minus non-specific binding. Data points are the mean of a single experiment (mean \pm range) carried out in duplicate which are representative of three separate experiments from which a value for K_D was determined.

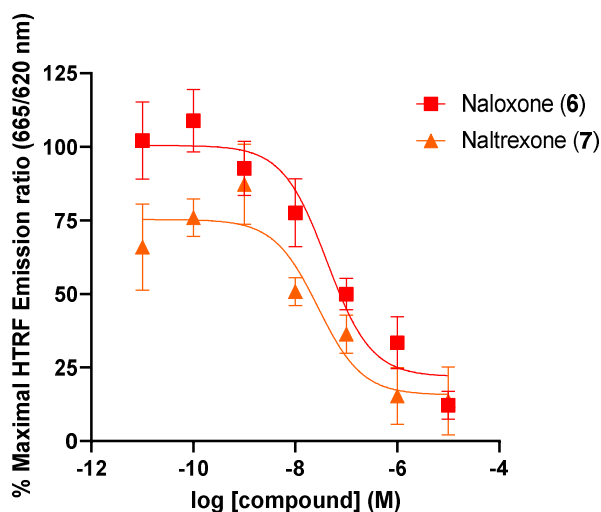
Compound	MOR $pK_D \pm SEM$	n
99	9.22 \pm 0.16	4
100	9.20 \pm 0.15	4
101	7.43 \pm 0.12	4
102	9.58 \pm 0.10	3
103	9.22 \pm 0.16	3
104	N/A ^a	3

^a – could not determine K_D within the tested concentration range

Table 2-2: MOR binding affinities of β -naltrexamine-based fluorescent ligands.

pK_D values were determined for the specific binding of each fluorescent ligand from the total binding and non-specific binding (+ 10 μ M naloxone) curves generated in Lumi4-Tb-labelled SNAP-MOR-expressing HEK293 cell membranes. pK_D values are the mean of a 3-4 experiments (\pm SEM), each carried out in duplicate.

Following this, compound **102** was selected for further competition binding assays against naloxone (**6**) and naltrexone (**7**) to confirm it was specifically labelling the MOR (**Figure 2-28**).



Compound	Obs. $pK_i \pm SEM$	Lit. pK_i range
Naloxone (6)	7.68 ± 0.26	7.3-9.0 ^a
Naltrexone (7)	7.86 ± 0.37	8.1-9.7 ^b

a – refs^{57, 108-112} *b* – refs^{57, 99, 108-110, 113, 114}

Figure 2-28: Competition binding assay results for naloxone and naltrexone against the fluorescent ligand **102.**

Lumi4-Tb-labelled SNAP-MOR-expressing HEK293 cell membranes were incubated with 2 nM of the fluorescent ligand **102** and varying concentrations of naloxone (**6**) and naltrexone (**7**). Data points and the observed pK_i values are the means of 4 separate experiments (mean \pm SEM), each carried out in triplicate. Values for pK_i were determined from the experimental IC_{50} and the fluorescent ligand K_D and concentration using the Cheng-Prusoff equation.¹²² Ranges of reported pK_i values for these compounds at MOR are included.

2.5 Discussion

Six fluorescent ligands with amino acid-based linkers joining the β -naltrexamine (**72b**) orthostere to a fluorophore were successfully synthesised and pharmacologically evaluated for binding affinity at MOR.

The 6-position of the morphinan scaffold of β -naltrexamine (**72b**) was identified as a suitable site for linker attachment, and subsequent substitution of this position with *N*-acetylated amino acids resulted in no significant loss of

MOR binding affinity from **72b**, indicating that substitution at this position is well tolerated.

It was hoped that interactions made between the amino acid substituent side chain groups and the receptor might improve MOR binding affinity. *In silico* modelling suggested that some beneficial interactions may be possible with certain amino acid side chains, but most docking predictions indicated a lack of interactions at this position. Competition binding experiments showed few significant differences in MOR binding affinity between amino acid congeners, mostly in agreement with the *in silico* predictions. These findings may be an example of the “message-address” concept described for morphinan opioid ligands, which suggests that ring-C substituents can affect receptor subtype selectivity but are not beneficial for binding affinity.³⁴

The only amino acid side chains which resulted in significant differences in MOR binding affinity from the Gly-congener **92a** were the *L*-Ser (**92e**) and *L*-Asp (**92g**) congeners, which had significantly lower MOR binding. However, the respective *D*-isomers **98e** and **98g** showed similar MOR binding affinities to **92a**, suggesting that particular conformations of these polar side chains are detrimental to MOR binding. In accordance with the “message-address” concept of OR binding, it may be that these side chain groups are able to confer some degree of receptor subtype selectivity against MOR binding. This could be illuminated by KOR and DOR competition binding experiments for these compounds.

In order to calculate the pK_i values for these non-fluorescent congeners, it was necessary to determine the K_D of the fluorescent competitor ligand **50**. The pK_D of **50** was measured as 8.88, slightly higher than the reported pA_2 value (8.37 - determined from antagonist concentration response curves fitted to a Gaddum-Schild equation in an ERK1/2 phosphorylation assay against the MOR agonist DAMGO and carried out in CHO cells expressing MOR).⁵⁷ Given the practical differences in determining these receptor binding values, it is unsurprising that the values differ. However, these values are similar enough

to give confidence to the measured values obtained from the saturation binding experiments.

The inclusion of amino acids in the linker aimed to increase the hydrophilicity of the compounds, to reduced non-specific binding. This had previously been proposed as a drawback of the BODIPY-based fluorescent MOR ligand **50**, which had displayed incomplete loss of fluorescence in the presence of an excess of unlabelled competitor, suggesting a higher level of non-specific binding.⁵⁷ Prior to carrying out the assays, there was some indication of success in meeting this aim. When preparing for the competition binding studies of non-fluorescent congeners, the 10 mM stock solution of **50** in dimethyl sulfoxide (DMSO) was found to be insoluble in HEPES-buffered saline solution (HBSS). The 10mM solution of **50** had to be further diluted in DMSO to 1 mM before it could be solubilised in HBSS. By comparison, the BODIPY 630/650-containing compounds from this study were soluble in HBSS buffer solution from a 10mM stock solution in DMSO. This suggests an improved hydrophilicity profile in these BODIPY 630/650-containing ligands compared to **50**, which may lead to fewer non-specific interactions away from the orthosteric binding site. Further testing will be required in order to confirm to what degree the compounds synthesised in this study participate in non-specific binding.

The four BODIPY 630/650-containing compounds (**99**, **100**, **102** and **103**) all exhibited sub-nanomolar binding affinities for MOR (**Table 2-2**), which was unchanged by variation in linker design (*N*-acetyl lysine or β -alanine) and length (the inclusion or absence of a hexanoyl spacer moiety). The lysine-linked sulfo-Cy5 compound (**101**) displayed a binding affinity for MOR comparable to the sulfo-Cy5 fluorescent MOR ligand (**51**) synthesised by Schembri *et al.*,⁵⁷ but the total binding curve for **104** did not reach saturation in the tested range so a reliable pK_D value could not be determined.

To confirm it was specifically labelling the MOR, **102** was selected for further competition binding assays against naloxone (**6**) and naltrexone (**7**). There was a high degree of variation in the results of these experiments (**Figure 2-28**), which could be attributed to the concentration of fluorescent ligand used. It is

common for the fluorescent ligand (or radioligand) concentration used in a competition binding assay to be equal to its K_D . However, due to the high MOR binding affinity of compound **102**, this concentration is very low. More consistent results would likely be achieved if a higher concentration of fluorescent ligand **102** was used.

The observed pK_i value for naltrexone (**7**) is slightly lower than previously reported, and the pK_i value for naloxone (**6**) is only comparable to some of the lower reported values. This also may have resulted from the inconsistency of the results. However, the pK_i value obtained for naloxone (**6**) in the competition binding experiments, which used the fluorescent ligand **50** (Table 2-1), was comparable to the value obtained with **102**. To ensure that receptor occupancy was at equilibrium, the experiment using **50** was repeated with a longer incubation period, but this produced a similar outcome. This suggests that this difference in obtained pK_i values is a result of methodological differences from the literature values.

3 Design, synthesis and pharmacological evaluation of 3,4-dimethyl-4-(3-hydroxyphenyl) piperidine-based fluorescent ligands

Existing fluorescent opioid receptor ligands are typically composed of a fluorophore bound to either an endogenous opioid peptide, or a morphinan-based opioid ligand, such as the fluorescent compounds synthesised in **Chapter 2**. The biological applications of fluorescent ligands continue to grow, as does the need for fluorescent ligands of different structures and properties. In order to escape the existing paradigm of fluorescent opioid ligand design, non-morphinan structures were considered to form the basis of a new class of fluorescent opioid ligands.

A problem associated with morphinan-based fluorescent ligand design is the legal barriers associated with the acquisition and synthetic use of narcotic starting materials. Even antagonist starting materials, such as the naltrexone (**7**) used in the synthesis of β -naltrexamine-based fluorescent ligands described in **Chapter 2**, require additional oversight during synthesis. Therefore, a fluorescent ligand synthesised from non-biologically active, commercially available starting materials would be desirable.

3.1 Selection of a lead molecule

The same criteria used to select a morphinan orthostere in **Chapter 2** were also used to select a non-morphinan lead molecule. The chosen characteristics of a lead molecule were an MOR antagonist with high MOR binding affinity and a well-established SAR profile. The range of well-described opioid ligands which are neither morphinan-based, nor developed from an endogenous peptide, is quite limited. The 2007 review of opioid antagonists by Goodman *et al.*¹²³ includes a diverse array of novel opioid receptor ligand structures from patent literature (**Figure 3-1**). Many of these structures are reported to possess sub-nanomolar binding affinities for MOR which would be highly desirable for

fluorescent ligand design.¹²³ However, publications describing the SAR of these compounds are rare and, whilst some aspects of SAR can be inferred from the structures covered under the patent, it is unclear where might be suitable on these structures for linker attachment with minimal impact on MOR binding affinity.

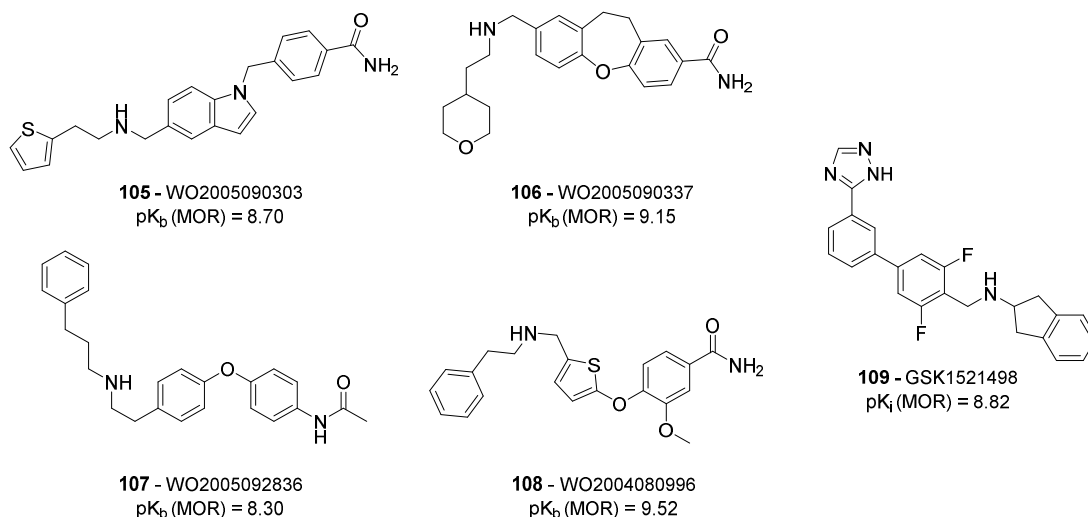


Figure 3-1: Structures of novel MOR antagonists or inverse agonists.

105-108 are a selection of MOR antagonist structures with the reported MOR binding affinities taken from patents.¹²³ These structures have not been reported outside of these patents, so their SAR profiles are not well understood. **109** is better described in the literature, but is an inverse agonist, rather than an antagonist, and was therefore unsuitable as a lead molecule.

Many of these compounds have been targeted towards treatment of compulsive consumption of food, alcohol and drugs.¹²³ Similarly, GSK1521498 (**109**) has been the subject of numerous published studies on compulsive reward-related behaviours.^{109, 124, 125} Though often described as an antagonist, this compound has shown inverse agonism of MOR, KOR and DOR.¹²⁵ In this project, the lead molecule for fluorescent ligand design should be an antagonist, rather than a reverse agonist, as it is desirable that the fluorescent ligand does not elicit a response upon receptor binding. The functional profiles of many of these novel opioid ligands is not well described, so the outcome of using them as the orthostere in a fluorescent ligand is unpredictable. Due to this uncertainty, these compounds were not considered appropriate for use in this study. While it may be possible to synthesise a fluorescent opioid

antagonist from these structures, a thorough study of their SAR would first be required, which falls outside the scope of this project.

Alvimopan (**9**) was chosen as the lead molecule for this study, fulfilling the criteria as a high affinity MOR antagonist, which has also been the subject of numerous SAR studies. The structure of alvimopan (**9**) was published by Zimmerman *et al.*¹¹⁰ in 1994 but the (3*R*,4*R*)-3,4-dimethyl-4-(3-hydroxyphenyl) piperidine (DMHPP) orthostere it contains was first reported in 1978.¹²⁶ Numerous SAR studies of DMHPP-containing ligands led to the discovery of alvimopan (**9**) and have defined much of the structure's SAR. This made it an ideal candidate for fluorescent ligand design, as this existing SAR could be used to select a point of attachment for the linker moiety and guide linker design.

3.2 SARs of (3*R*,4*R*)-3,4-dimethyl-4-(3-hydroxyphenyl) piperidine structures

Unlike other non-morphinan opioid antagonists, alvimopan (**9**) has a well-established SAR which has been explored in numerous published studies. The antagonist function of alvimopan (**9**) and other related compounds is derived from the DMHPP orthostere which is described below. SAR studies exploring the effect of modifications to DMHPP on MOR binding affinity, receptor subtype selectivity and function, are also described in this section.

3.2.1 Structural determinants of function

Zimmerman *et al.*¹²⁶ first described the discovery of the DMHPP structure, focusing on the chiral relationship between the 3- and 4-position substituents. They describe the change in function of known agonist **110** to antagonism when methylated at the 3-position, with antagonist activity found to be greater in the (*R*)-methyl diastereomer **111** than the (*S*)-methyl **112**. Further study of the relationship between these methyl groups has shown a trend of slightly lower MOR binding by the 3*S*,4*S*-enantiomer, with the 3*R*,4*R*-enantiomer (**111**) preferred in most studies using this scaffold.¹²⁷

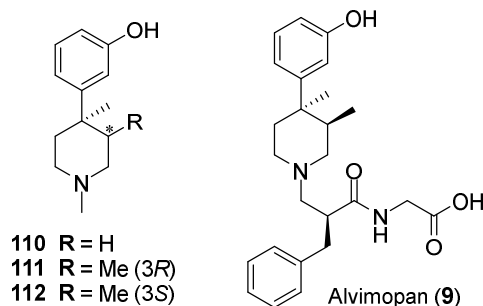


Figure 3-2: Variants of the 3,4-dimethyl-4-(3-hydroxyphenyl) piperidine structure.

The antagonist DMHPP structure **111** discovered by Zimmerman *et al.* is the 3*R*-methyl variant of the agonist **110**. The 3*S*-methyl variant **112** showed a weaker antagonist activity in rat and mouse responses than **111**.¹²⁶ These findings led to the discovery of the opioid antagonist alvimopan (**9**).¹¹⁰

It has been hypothesised that this change in function is not the result of interactions made by the 3-methyl group in the receptor, but rather the effect that this group has on the piperidine ring conformation.¹²³ Unlike the more rigid structures of morphinan opioids, there is some flexibility for the phenol to adopt either an axial or equatorial position relative to the piperidine. The proposed equatorial positioning of alvimopan (**9**) is supported by crystal structure data¹²⁷ as well as the antagonist activity of the equatorially locked structure **113** (**Figure 3-3**).¹²⁸ Even removal of the 3-methyl group of this equatorially locked species produced an antagonist (**114**),¹²⁹ supporting the role of 3*R*-methyl as being responsible for conformational change, rather than interacting with the receptor.

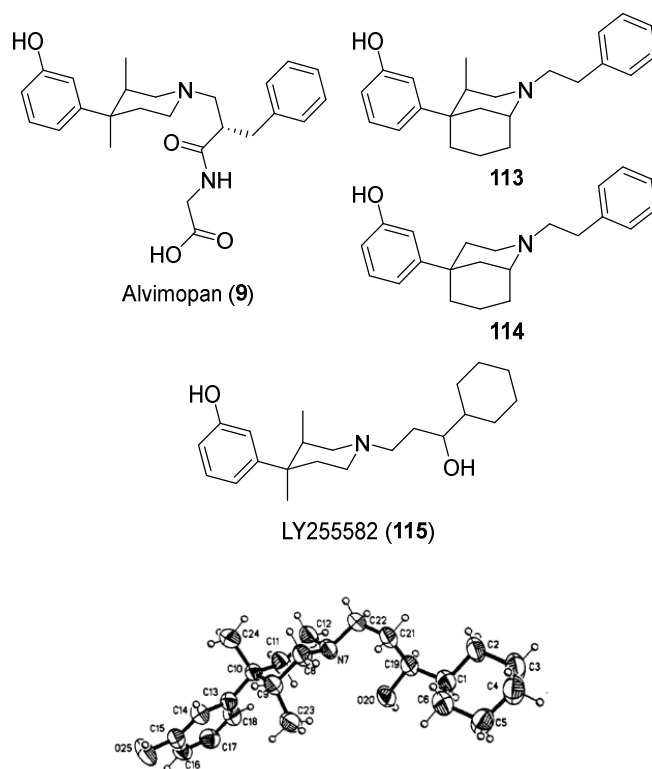


Figure 3-3: The proposed equatorial phenol positioning in DMHPP antagonists.

The phenol of alvimopan (**9**) is hypothesised to adopt an equatorial position relative to the piperidine ring as a result of 3-position methylation.¹²³ The equatorially locked compounds **113** and **114** support this claim, as they are both antagonists.^{128, 129} The DMHPP-containing opioid antagonist LY255582 (**115**) is shown above its crystal structure, adopting an equatorial position.¹²⁷

The opioid antagonist axelopran (**116**) was initially believed to adopt a similar conformation to that of alvimopan (**9**),¹³⁰ but separation of the precursor isomers **117a** and **117b** revealed **117b** to be a weakly binding partial agonist, while **117a** was a high affinity antagonist (**Figure 3-4**).¹³¹ To produce this antagonism, it is possible that the piperidine ring of **117a** switches to a boat conformation for the phenol to adopt an equatorial conformation, but x-ray crystallography of **117a** shows it adopting the axial chair conformation.¹³¹ The absence of the 3- and 4-methyl groups may cause the phenol to prefer this axial conformation. The antagonism of axelopran (**116**) may result from a steric clash between the axial phenol and the 2-6 ethylene bridge, preventing it from adopting an agonist binding pose.

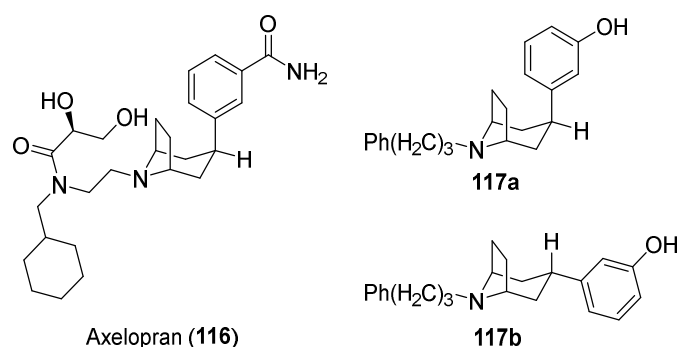


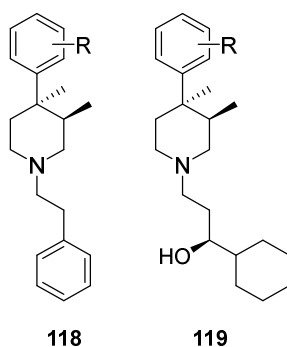
Figure 3-4: The structures of axelopran (116) and its precursor isomers.^{130, 131}

The opioid ligand axelopran (116) and its precursor 117a are both antagonists, despite appearing to position their 4-aryl rings axially.^{130, 131} 117b, the isomer of 117a possesses partial agonist activity, though its active conformation has not been investigated.¹³¹

3.2.2 Modification of the aromatic ring

Outside of the conserved chirality of the piperidine 3- and 4-position substituents, SAR studies have sought to evaluate the suitability of different positions on the DMHPP structure for substitution and elaboration. The aromatic ring has been investigated by modification of substituent position and composition.

The phenol ring of DMHPP structures is understood to interact with the receptor similarly to the phenol ring-A of morphinan opioid ligands, but DMHPP-based ligands appear to have a higher tolerance for functionalisation. While the substitution of an amide onto the aromatic ring of morphine results in a dramatic loss in binding affinity (**Figure 2-4**),⁷⁵ the same change in the DMHPP compounds 118a and 115 results in a minor change in MOR binding affinity (**Figure 3-5**).^{111, 132} This is exemplified by the MOR antagonist axelopran (116), a ligand possessing similar properties to alvimopan (9), which is achieved through numerous bioisosteric replacements, including a *meta*-amide group.



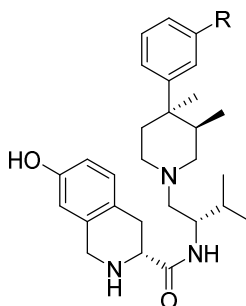
R	Scaffold 118	MOR p <i>K</i> _i	Scaffold 119	MOR p <i>K</i> _i
3-OH	118a	8.72	LY255582 (115)	10.00
3-CONH ₂	118b	8.33	119b	9.7
3-CONHMe	118c	7.15		
3-CON(Me) ₂	118d	5.92		
3-CO ₂ Me	118e	6.07	119e	7.36
3-CO ₂ H			119f	6.84
3-CH ₂ OH	118g	7.96		
3-NH ₂	118h	6.82	119h	8.72
3-NHCOMe	118i	7.17	119i	8.62
3-H			119j	8.11
2-OH			119k	6.39
4-OH			119m	7.52

Figure 3-5: Comparison of different aryl ring substituents and their effect on MOR binding affinity.^{111, 132}

Small, polar functional groups such as an amide (**118b**, **119b**) can be substituted onto DMHPP scaffolds such as **118** and **119** with relatively small changes to MOR binding affinity compared to the corresponding hydroxyl-containing compounds (**118a** and **115**).^{111, 132} Larger groups typically see a reduction in p*K*_i, but not to the degree seen in morphinan ligands (as shown in **Figure 2-4**). Ionisable groups are also less favoured, but removal of the hydroxyl (**119j**) can still produce a high affinity ligand.¹³² Relocation of the hydroxyl group to either the *para*- or *meta*-position results in a large loss of MOR binding affinity (**119k** and **119m**).¹³²

Other small polar groups at this position can also be tolerated, and can even be used to improve receptor subtype selectivity, albeit with a lower affinity for

MOR.^{111, 132} Removal of the hydroxyl group from **115**, while resulting in a loss of MOR binding affinity, still produced a high affinity ligand (**119j**) due to the exceptional MOR binding affinity of the parent compound. MOR binding affinity of the KOR-selective ligand JDtic (**120**) is actually improved by removal of the hydroxyl, with no effect shown over KOR binding (**Figure 3-6**).¹³³ A *meta*-amide group on this structure produces no change in MOR affinity, but rather a loss in binding affinity at KOR.^{133, 134}



Compound	R	pK _e (MOR)	pK _e (DOR)	pK _e (KOR)
JDtic (120) ^a	OH	7.60	7.13	10.70
121 ^a	H	8.05	6.35	10.62
122 ^b	CONH ₂	7.68	6.32	9.92

a - ref¹³³, *b* - ref¹³⁴

Figure 3-6: Opioid receptor binding affinities for JDtic (120**) and its *meta*-substituted variants.**^{133, 134}

Removal of the aryl hydroxyl group from the KOR-selective antagonist JDtic (**120**) results in a gain in MOR binding affinity with little effect on KOR binding affinity. Replacement of the hydroxyl group with an amide does not affect MOR binding but reduces KOR binding affinity.^{133, 134}

Relocation of the hydroxyl group of **115** can result in a more drastic loss of binding affinity. The *para*-hydroxyl variant (**119m**) binds with similar MOR affinity to some of the less well-tolerated *meta*-substituents shown in **Figure 3-5**, but the *ortho*-hydroxyl compound **119k** suffers a 4000-fold loss in MOR binding affinity compared to **115**.¹³²

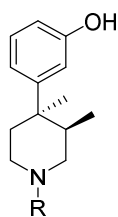
The fact that some changes to the composition and position of the aryl ring substituent are tolerated, whilst other changes cause an extreme reduction in

MOR binding affinity, demonstrates that this region of the orthostere is highly influential over receptor binding. Despite the variety of tolerated substituents, the aryl ring is clearly tightly bound within the receptor binding site, leaving room for only subtle structural modifications, without suffering unacceptable losses to binding affinity.

3.2.3 *N*-substitution

In morphinan opioid ligands, the *N*-substituent is crucial in determining ligand function, with minor structural changes causing the ligand to switch its agonist/antagonist activity (see **Figure 2-12**). As previously discussed, the functionality of DMHPP ligands is determined by the stereoisomerism of the 3- and 4-methyl groups, and *N*-substitution has not been found to influence ligand function. Instead, the *N*-substituent can influence receptor subtype selectivity, as demonstrated by the DMHPP-based KOR antagonist JD_{Tic} (**120**). In this regard, the role of DMHPP *N*-substituents is similar to the 6-position substituents of morphinan-based opioid ligands. However, the “message-address” concept described for morphinan opioid ligands (**2.1.4**) cannot be applied to DMHPP compounds, as *N*-substitution is also able to modulate receptor binding affinity.

SAR studies investigating *N*-substitution of DMHPP determined that a phenyl or cyclohexyl group bound to the amine via an ethylene or propylene spacer was optimal for MOR binding;^{127, 135} *N*-substitution of a phenylpropyl group (**125**) resulted in a 100-fold increase in MOR affinity compared to the *N*-methyl compound (**111**) (**Figure 3-7**).¹³⁵ This phenyl positioning is conserved in the structure of alvimopan (**9**), alongside a 2-amide-bound glycine moiety, which alters the compound’s physicochemical properties to restrict its absorption from the GI tract.¹¹⁰

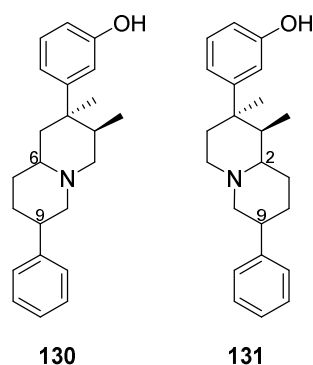


Compound	R	p <i>K</i> _i or % inh. At 100 nM
111	Me	7.1
123	CH ₂ Ph	89%
124	(CH ₂) ₂ Ph	8.82
125	(CH ₂) ₃ Ph	9.16
126	(CH ₂) ₄ Ph	8.70
127	CH ₂ ^c Hex	7.77
128	(CH ₂) ₂ ^c Hex	9.19
129	(CH ₂) ₃ ^c Hex	9.31

Figure 3-7: The effect of differences in *N*-alkylene-phenyl substituent spacing on MOR binding affinity.^{127, 135}

Binding affinities were determined by displacement of [³H]-naloxone from MOR in rat brain homogenate.^{127, 135}

The *N*-substituent conformation which facilitates this increased binding affinity has been investigated through restriction of the *N*-alkyl spacer. A study by Le Bourdonnec *et al.*¹³⁶ synthesised and tested a series of conformationally locked congeners of the *N*-phenylethyl DMHPP compound **124** (**Figure 3-8**). Two of these quinolizidine compounds possessed higher binding affinities than the unrestricted **124**. Functional assays revealed **131b** to be an agonist, while **130b** remained an antagonist. *In silico* analysis of their respective lowest energy conformations showed that **124** and **130b** maintained equatorial phenols, while an axial phenol conformation was generated for **131b**. The same group investigated further substitution of the quinolizidine ring of **130b**, but this was found to be detrimental to MOR binding.¹³⁷



Compound	Scaffold	Conformation	MOR p <i>K</i> _i
124	-	-	8.74
130a	130	6 <i>R</i> ,9 <i>R</i>	6.37
130b	130	6 <i>S</i> ,9 <i>S</i>	9.21
130c	130	6 <i>R</i> ,9 <i>S</i>	6.96
130d	130	6 <i>S</i> ,9 <i>R</i>	6.96
131a	131	2 <i>R</i> ,9 <i>R</i>	7.59
131b	131	2 <i>S</i> ,9 <i>S</i>	9.05
131c	131	2 <i>R</i> ,9 <i>S</i>	7.43
131d	131	2 <i>S</i> ,9 <i>R</i>	7.14

Figure 3-8: MOR binding affinities of DMHPP compounds with conformationally restricted *N*-substituents.¹³⁶

A series of fused ring compounds were investigated to determine the active conformation of the phenylethyl DMHPP compound **124**.¹³⁶ Every isomeric combination of the quinolizidines **130** and **131** were tested, with two analogues identified to possess higher binding affinities than the unrestricted **124**. **131b** was found to be an agonist, likely due to distortion of the piperidine ring. **130b** displayed antagonist activity and was determined to represent the active conformation of **124**.

Another approach to conformational restriction of *N*-substituents introduced functional groups into the propylene spacer of compound **125** (Figure 3-9).¹³⁸ MOR binding affinity was impaired when the spacer was forced to adopt a *cis*-conformation through the introduction of a double bond (**133**), but the *trans*-isomer (**132**) displayed a similar MOR affinity to **125**, suggesting that they share similar binding poses. Substitution of a benzofuran (**134**) also resulted in a loss

of MOR binding affinity, indicating that rotational freedom of the phenyl ring is necessary for it to be optimally positioned for binding.¹³⁸

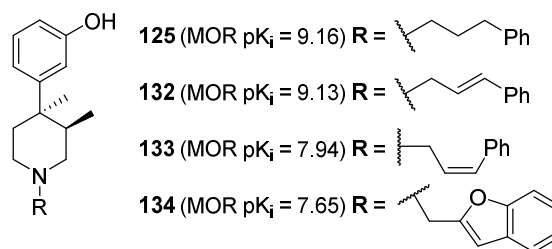
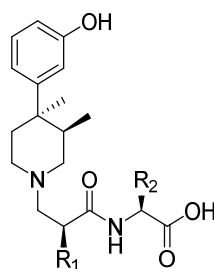


Figure 3-9: DMHPP compounds with conformationally restricted N-substituents.¹³⁸

A series of conformationally restricted variants of the phenylpropyl DMHPP compound **125** were synthesised. The MOR binding affinity of the *trans*-propenyl isomer **132** was unchanged from the unrestricted **125**. The *cis*-propenyl isomer **133** exhibited a lower MOR binding affinity, suggesting that the *trans*-conformation is representative of the binding pose of **125**. The loss of MOR binding affinity displayed by the benzofuran congener (**134**) reveals that rotational freedom of the phenyl ring is necessary to be optimally positioned for binding.¹³⁸

Functionalisation of the amino acid side chain of alvimopan (**9**) has also been explored, with several different amino acids utilised to replace glycine (**Figure 3-10**).¹³⁹ Most of these modifications were found to reduce MOR binding affinity, except the lysine variant (**135d**), which had a similar MOR binding affinity to alvimopan but possessed far greater receptor subtype selectivity. Removal of the benzyl group from alvimopan resulted in a larger loss of binding affinity, but this could be partially recovered when different amino acids were substituted for glycine.¹³⁹ It is noteworthy that addition of a phenyl group to alvimopan (**135b**) resulted in a loss in MOR binding affinity, but the same modification in the *des*-benzyl structure improved binding affinity (**136e**). This may suggest that these functional groups compete for the same binding site, making the amino acid side chain detrimental for MOR binding when the benzyl group is present, but favourable for binding when the benzyl group is absent.



Compound	R ₁	R ₂	MOR pK _i or % inh. at 10 μM
Alvimopan (9)	Bn	H	9.33
135a	Bn	Me	9.20
135b	Bn	Bn	8.77
135c	Bn	CH ₂ COOH	8.14
135d	Bn	(CH ₂) ₄ NH ₂	9.30
136a	H	H	20%
136e	H	Bn	7.44
136f	H	CH ₂ ^c Hex	7.70
136g	H	(CH ₂) ₂ Ph	7.24
136i	H	(CH ₂) ₄ NH ₂	45%

Figure 3-10: Modifications to the structure of alvimopan (9).¹³⁹

Modification of the amino acid utilised in the structure of alvimopan (9) resulted in loss of MOR binding affinity (**135a-c**) except the lysine congener (**135d**) which showed similar binding affinity to alvimopan (9). Removal of the benzyl group from alvimopan (9) resulted in a loss of MOR binding affinity (**136a**), which was partially recovered by the inclusion of amino acids containing a phenyl or cyclohexyl group (**136e-g**).

3.2.4 Modification of the piperidine ring

The crucial role that 3- and 4-position substituents play in determining ligand function limits how the piperidine ring can be functionalised. Outside of the fused ring structures described above, modifications to the piperidine ring have been more limited than those seen in other regions. Most elaboration of the piperidine ring had been through internal bridging to investigate piperidine ring

conformation, such as **113** and **114** (**Figure 3-3**),^{128, 129} and the 2-6 ethylene bridge seen in axelopran (**116**).^{130, 131}

Substitution onto the 6-position of **124** showed that modification of this position with even small alkyl groups was detrimental to opioid receptor binding, with further loss of binding affinity associated with larger substituents.¹⁴⁰ Substitution of the piperidine ring should therefore be avoided, except to confer specific positioning of the *N*-substituent (as seen in **Figure 3-8**).

3.3 Fluorescent ligand and non-fluorescent congener design

The SAR studies of the DMHPP structure reveal its potential to produce high affinity antagonist ligands for MOR. Modification of the piperidine ring is best avoided due to the potential for function-altering conformation shifts and, while aryl ring substitution can be tolerated, a *meta*-hydroxyl or amide group should be utilised for optimal MOR binding affinity. Contrastingly, *N*-substitution could provide an ideal location for linker and fluorophore attachment.

Elaboration of the linker from the existing glycine moiety of alvimopan (**9**) could achieve this project's aim of utilising amino acids in the linker of a DMHPP-based fluorescent ligand to improve physiochemical properties. The study by Le Bourdonnec *et al.*¹³⁹ into amino acid substitution of alvimopan (**9**) supports the potential for incorporating different amino acids at this site, but only in the absence of the benzyl group (**Figure 3-10**). While loss of this group is detrimental to MOR binding affinity, it has been shown that certain amino acids are able to recover some of the lost binding affinity.¹³⁹ Benzyl removal also has synthetic benefits, as the epimers generated by benzylation must be separated, resulting in a loss of useful material.^{110, 141}

It was decided that fluorescent compounds of the design shown in **Figure 3-11** would be synthesised. The composition of the first bound amino acid (referred to as "the first position") would be determined using synthesised non-

fluorescent single amino acid congeners (**136**) through measurement of MOR binding affinity. These results would be used to inform any further elaboration of the linker. It was planned that click chemistry would be used to attach the alkynyl group of a modified fluorophore to a terminal azidoalanine moiety, forming a 1,2,3-triazole ring (**Scheme 3-1**). Some non-fluorescent congeners would incorporate a terminal phenylalanine moiety as a bioisostere of the 1,2,3-triazole amino acid (**138**).

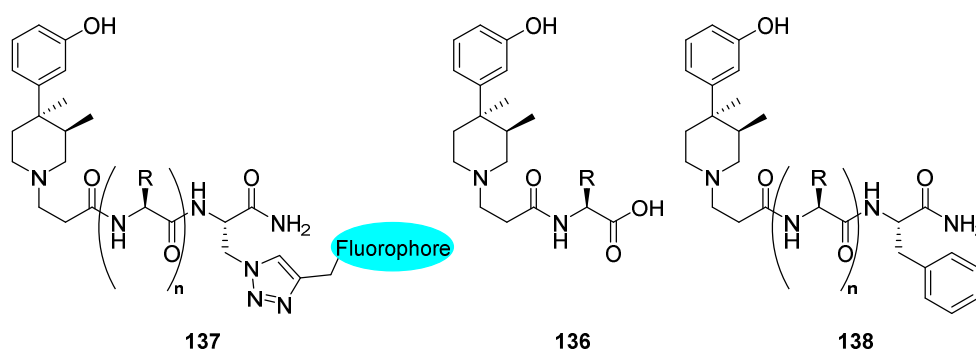
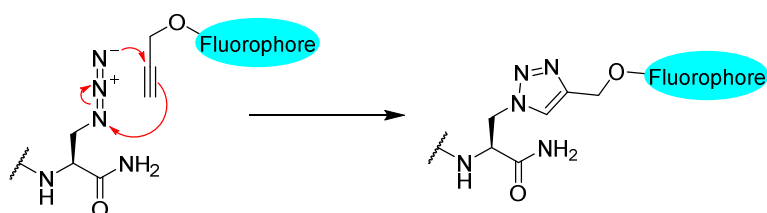


Figure 3-11: General design of DMHPP-based fluorescent ligands.

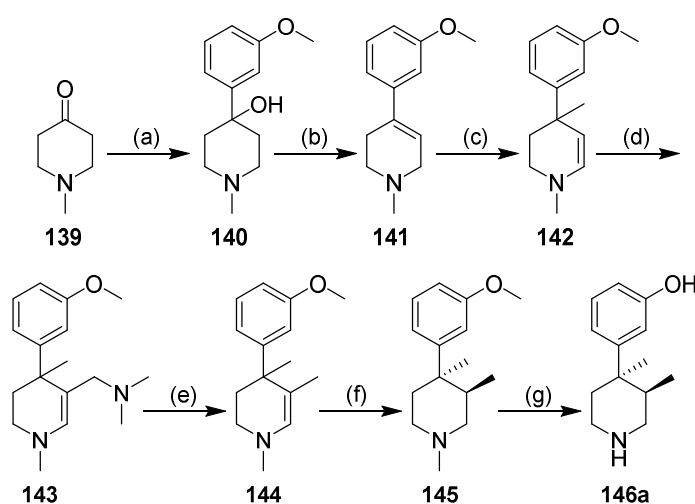
The planned structure of the fluorescent ligands designed in this chapter consisted of the 3,4-dimethyl-4-(3-hydroxyphenyl) piperidine orthostere connected to a peptidic linker region (**137**). The composition of this linker region was refined by the synthesis and pharmacological evaluation of non-fluorescent congeners (**136** and **138**). Click chemistry was planned to be used to attach the alkynyl group of a modified fluorophore to an azidoalanine moiety, forming a 1,2,3-triazole ring (**Scheme 3-1**). This was represented in non-fluorescent congeners by incorporating a phenylalanine bioisostere (**138**).



Scheme 3-1: Mechanism of the azide-alkyne cycloaddition between azidoalanine and the alkyne of a modified fluorophore.

3.4 Synthesis of 3,4-dimethyl-4-(3-hydroxyphenyl) piperidine

A benefit of the DMHPP structure as a lead molecule is that it can be synthesised from commercially available, non-narcotic starting materials. Synthesis of DMHPP **146a** was first described by Mitch *et al.*¹⁴² (**Scheme 3-2**) but suffered from low yield and included the neurotoxic intermediate **141**, the *m*-methoxy-variant of 1-methyl-4-phenyl-1,2,3,6-tetrahydropyridine (MPTP) which is known to induce Parkinsonism.¹⁴³ A safer, higher yielding route with fewer synthetic steps was published by Werner *et al.*¹⁴¹ five years later (**Scheme 3-7**) and has served as the standard route to **146a** synthesis since, on both laboratory and industrial scales.



Scheme 3-2: Synthetic scheme for (3*R*,4*R*) 3,4-dimethyl-4-(3-hydroxyphenyl) piperidine by Mitch *et al.*¹⁴²

Reported reagents and conditions: (a) (3-methoxyphenyl)lithium, THF, -70°C; (b) *p*-TsOH, PhMe, reflux; (c) *n*-BuLi, MeI, THF, -10°C; (d) H₂CO, (Me)₂NH, H₂SO₄, H₂O, 70°C; (e) H₂, Pd/Ba₂SO₄, EtOH, rt; (f) i) NaBH₃CN, MeOH, rt; ii) dibenzoyl *L*-tartrate, EtOH; (g) i) vinyl chloroformate, DCE, reflux; ii) HCl, EtOH, reflux, iii) HBr, AcOH, reflux.

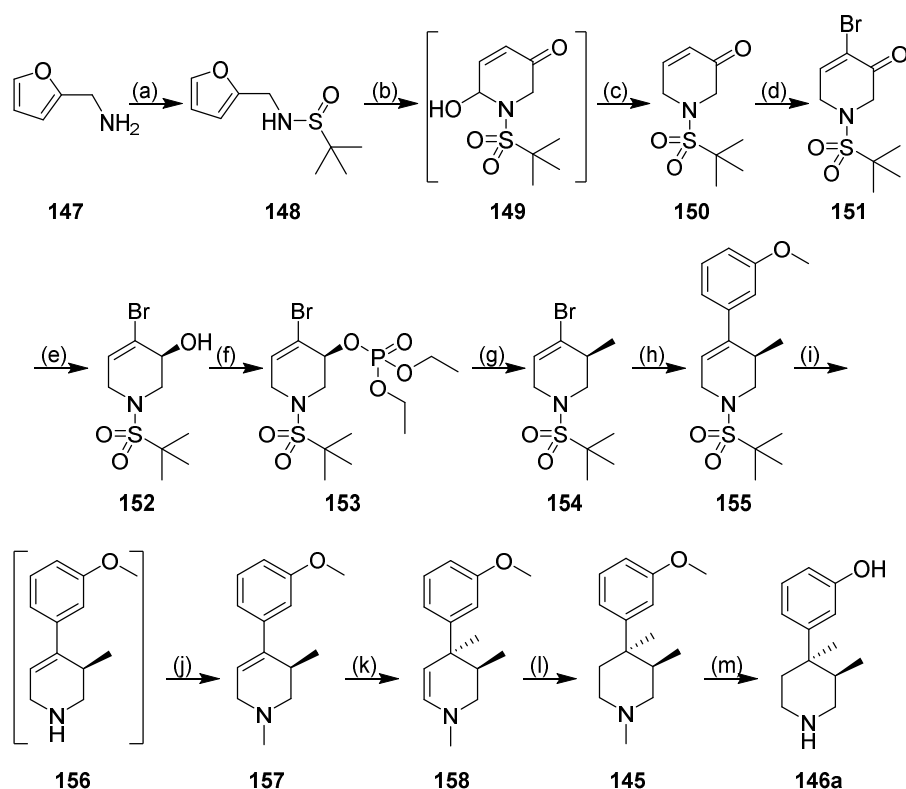
Both of these racemic synthetic routes produce undesired isomers which require chiral purification and result in significant losses in mass of useful product. In response to this problem, an enantioselective synthetic route to **146a** was developed by Furkert *et al.*¹⁴⁴ which almost exclusively produced the desirable 3*R*,4*R*-isomer (**Scheme 3-3**). The reported overall yields of both the

Werner *et al.*¹⁴¹ and Furkert *et al.*¹⁴⁴ routes were similar (15-16%), although the latter involved more synthetic steps.

Unlike the commonly utilised Mitch *et al.* and Werner *et al.* syntheses, there are no reports of the enantioselective synthetic route being repeated since the paper was published in 2007. Therefore, it was initially decided that the route described by Furkert *et al.*¹⁴⁴ would be followed in this project, as an external assessment of the utility of this synthetic route. The chemistry following the Furkert *et al.*¹⁴⁴ route is reported in section **3.4.1** below. Unfortunately, the enantioselectivity described by the authors could not be replicated in this project. Instead, the synthetic route described by Werner *et al.*¹⁴¹ was pursued, and is reported on in section **3.4.2**.

3.4.1 Enantioselective synthetic route

The reported enantioselective synthetic route by Furkert *et al.*¹⁴⁴ is shown in **Scheme 3-3**. Unfortunately, the described enantioselectivity could not be replicated in this project, and thus the synthetic route was not followed to completion. The completed chemistry from this project is shown in **Scheme 3-4**.

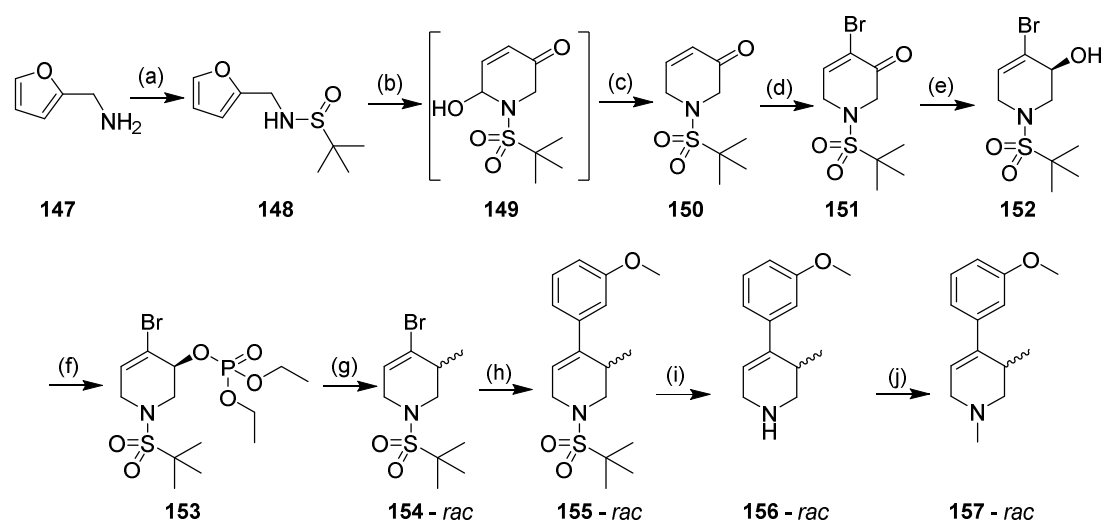


Scheme 3-3: Synthetic scheme for chirally-selective route to (*R*),(*R*)-3,4-dimethyl-4-(3-hydroxyphenyl)piperidine by Furkert *et al.*¹⁴⁴

Reported reagents and conditions: a) *t*-BuSOCl, NEt₃, DCM, 2 h, 0°C; b) *m*-CPBA, DCM, 3 h, RT; c) Et₃SiH, BF₃·OEt₂, DCM, 3 h, 0°C; d) Br₂, NEt₃, DCM, 1 h, 0°C; e) CBS catalyst, BH₃·PhNEt₂, THF, 16 h, 0°C; f) (EtO)₂P(O)Cl, DMAP, NEt₃, DCM, 24 h, 0°C; g) MeMgBr, CuBr·SMe₂, dry THF, 5 h, -40°C; h) 3-OMe-PhB(OH)₂, Pd(Ph₃P)₄, Na₂CO₃, 1:1 ethanol/toluene, 100°C, 30 min; i) TfoH, anisole, DCM, 30 min, 0°C; j) CH₂O, NaBH₃CN, MeCN, 30 min, RT; k) *n*-BuLi, Me₂SO₄, THF, 30 min, -50°C; l) NaBH₄, methanol, 3 h, 0°C; m) 1) NaOH, PhOCOCl, toluene, 2 h, reflux; 2) HBr, AcOH, 18 h, reflux.

In contrast to the literature method, the coupling of *tert*-butylsulfonyl chloride (*t*BuSOCl) to α -furfurylamine (**147**) was carried out using a stoichiometric amount *t*BuSOCl, added dropwise as a dilute solution in dichloromethane (DCM) to prevent di-substitution of the amine. The reaction of sulfinamide **148** with *meta*-chloroperbenzoic acid (*m*CPBA) had two effects. Upon addition of *m*CPBA, oxidation of the sulfinamide to produce the sulfonamide was quickly observed by TLC. A Prilezhaev reaction then introduced an epoxide onto the furan ring, with a subsequent *aza*-Achmatowitz rearrangement to produce the 6-membered ring **149** (Scheme 3-5). Alcohol reduction using boron trifluoride

diethyl etherate and triethylsilane resulted in a poor yield of **150** (22% over two steps), vastly different from the reported 78% yield.¹⁴⁴ Attempts to modify the reaction conditions (temperature, stoichiometry, order of reagent addition) produced only minor changes to overall yield. A key discovery was that the reaction did not scale up well, with the best yield of 36% achieved using 100 mg of **150**. The remaining material was reacted in twelve separate reaction vessels in parallel to optimise the yield over these steps.

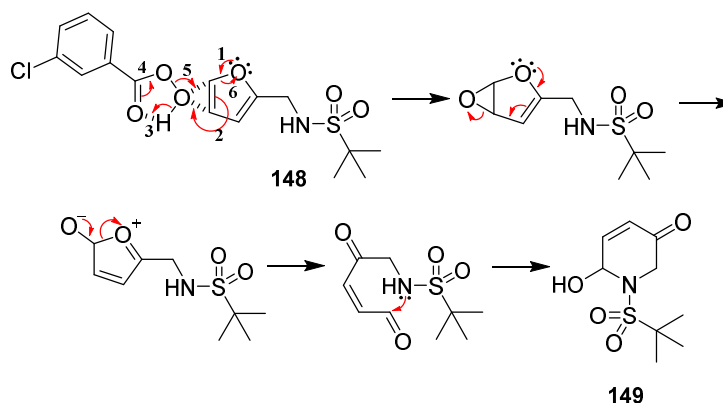


Scheme 3-4: Synthesis of (R),(R)-3,4-dimethyl-4-(3-hydroxyphenyl)piperidine precursors.¹⁴⁴

Based on the synthesis described by Furkert *et al.*¹⁴⁴ shown in **Scheme 3-3**. Reagents and conditions: (a) *t*-BuSOCl, NEt₃, DCM, 2 h, 0°C, 90%; (b) *m*-CPBA, DCM, 3 h, RT; (c) Et₃SiH, BF₃·OEt₂, DCM, 3 h, 0°C, 36% (2 steps); (d) Br₂, NEt₃, DCM, 1 h, 0°C, 77%; (e) CBS catalyst, BH₃·PhNEt₂, THF, 16 h, 0°C, 77%; (f) (EtO)₂P(O)Cl, DMAP, NEt₃, DCM, 24 h, 0°C, 82%; (g) MeMgBr, CuBr·SMe₂, dry THF, 5 h, -40°C, 34%; (h) 3-OMe-PhB(OH)₂, Pd(Ph₃P)₄, Na₂CO₃, 1:1 ethanol/toluene, 100°C, 30 min, 73%; (i) TfOH, anisole, DCM, 30 min, 0°C, 94%; (j) CH₂O, NaBH₃CN, MeCN, 30 min, RT, 89%.

Bromination of **150** by Br₂ in the presence of triethylamine (TEA) produced the 4-bromo compound **151** in good yield. The ketone was then enantioselectively reduced to the (*S*)-alcohol using a CBS catalyst ((*3aR*)-1-methyl-3,3-diphenyl-3*a*,4,5,6-tetrahydropyrrolo[1,2-*c*][1,3,2]oxazaborole). The chiral purity of **152** was confirmed by determination of [α]_D which was comparable to the literature value.¹⁴⁴ The alcohol of **152** was then esterified by diethyl chlorophosphate and 4-dimethylaminopyridine (DMAP) in high yield, although the reaction did not

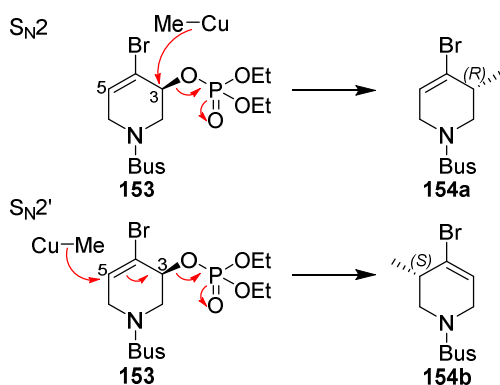
go to completion under the tested conditions, with a small amount of starting material recovered each time.



Scheme 3-5: Oxidation and rearrangement of *N*-furfurylsulfonamide by *m*CPBA.

Oxidation of **148** results in epoxide formation, which occurs via a Prilezhaev reaction. An *aza*-Achmatowicz rearrangement converts the 5-membered epoxide intermediate into the 6-membered intermediate **149**.

The procedure developed by Furkert *et al.*¹⁴⁴ had optimised the reaction conditions for the enantioselective methylation of **153**, using different methylating agents and copper catalysts. It was therefore disappointing to find, when using the described methyl Grignard and copper (I) bromide dimethyl sulphide complex, that the product **154** was a mixture of enantiomers, in contrast to the near-complete enantioselectivity reported in the protocol.¹⁴⁴ The authors described the reaction as occurring via an S_N2' mechanism, with methylation occurring at the unsaturated 5-position to produce the desired (*R*)-isomer (**154a**). They report that the (*S*)-isomer (**154b**) was produced by the S_N2 mechanism through direct displacement of the phosphate (**Scheme 3-6**). The conditions used were proposed to direct the methylation almost exclusively to the S_N2' route, but the experiments carried out in this study did not replicate the literature results, producing a mixture of **154a** and **154b**.



Scheme 3-6: Reaction mechanisms to produce the two 3-methyl enantiomers of 154.

Above: The S_N2 mechanism results in direct substitution at the 3-position of the piperidine ring, producing the (*R*)-isomer **154a**. **Below:** The (*S*)-isomer is produced by an S_N2' mechanism, substituting onto the 5-position and eliminating the phosphate from the sp^2 -hybridised 3-position.

After several attempts to direct the methylation towards the desired product were unsuccessful, it was decided that the synthetic route should be switched to the route developed by Werner *et al.*¹⁴¹ (**Scheme 3-7**). Since this method would require separation of enantiomers, the Furkert *et al.*¹⁴⁴ synthesis was continued, using the mixed methylation products (**154**) to produce **157**. Since **157** differs only from compound **161** in the Werner *et al.*¹⁴¹ synthesis in their respective O-phenol substituents, testing the separability of the enantiomers of **157** would indicate if the enantiomers of **161** were also separable.

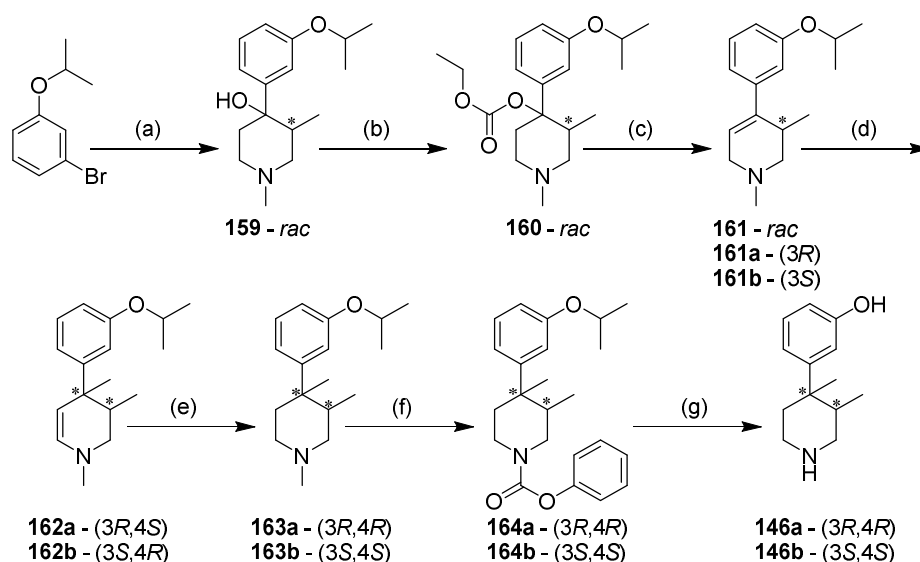
For that purpose, a Suzuki coupling was carried out between the mixed enantiomers of **154** and 3-methoxybenzeneboronic acid in the presence of tetrakis(triphenylphosphine)-palladium (0) and sodium carbonate to give the product **155**. This was then treated with triflic acid and anisole to remove the *tert*-butylsulfonyl (bus) protecting group to give the secondary amine **156**. Reductive amination of formaldehyde by **156**, using STAB as the reducing agent, yielded the *N*-methyl piperidine **157**.

The 3*R* (**157a**) and 3*S* (**157b**) isomers were successfully isolated by high performance liquid chromatography (HPLC), indicating that the *iso*-propyl derivative **161** could also be purified using this method. **157a** made up 61% of the isolated product, with **157b** composing the remaining 39%. It is assumed

that this ratio is unchanged for compounds **154-157** and that this is representative of the ratio of S_N2' to S_N2 products **154a** and **154b** in **Scheme 3-6**.

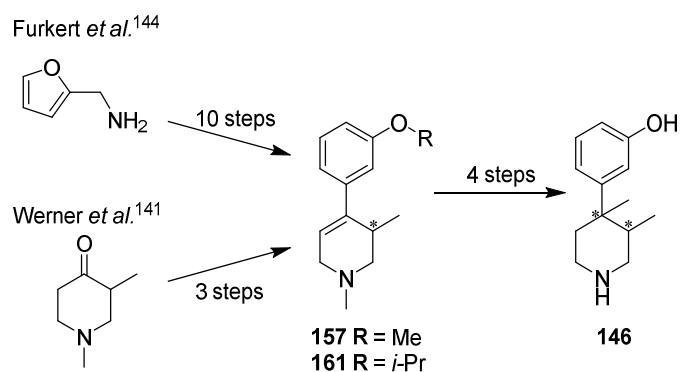
3.4.2 Non-enantioselective synthetic route

As discussed above, once it was established that chirally-pure products would not be achievable using the method developed by Furkert *et al.*,¹⁴⁴ it was decided that the protocol described by Werner *et al.*¹⁴¹ would be a more suitable route to synthesis of **146a** (**Scheme 3-7**). In the absence of any benefit over chiral selectivity, this approach was more desirable as it halved the number of synthetic steps from fourteen to seven (shown in **Figure 3-8**).



Scheme 3-7: Non-chirally-selective synthesis of 3,4-dimethyl-4-(3-hydroxyphenyl)piperidine.¹⁴¹

Based on the synthesis described by Werner *et al.*¹⁴¹ with shown yields achieved in this project. Reagents and conditions: (a) i) *n*-BuLi, THF, -75°C, 1 h; ii) 1,3-dimethylpiperid-4-one, -75°C, 94%; (b) EtO₂CCl, EtOAc, 24 h, 79%; (c) decalin, 24 h, reflux, 99%; (d) *n*-BuLi, Me₂SO₄, THF, 1 h, -50°C, 77%; (e) NaBH₄, MeOH, 0°C, 71%; (f) NaOH, PhOCOCl, toluene, 2 h, reflux, 74%; (g) HBr, AcOH, 18 h, reflux, 86%.



Scheme 3-8: Comparison of synthetic routes to produce DMHPP 146.

The longer synthetic route developed by Furkert *et al.*¹⁴⁴ describes enantiomeric selectivity in favour of the (*R*)-isomer of **157**. However, this result could not be replicated in this study. In the absence of chiral selectivity, the shorter route developed by Werner *et al.*¹⁴¹ to synthesise **161** was preferred. Both methods incorporate the same final four steps to produce **146**.

1-Bromo-3-*iso*-propoxybenzene was stirred with *n*-BuLi, converting it to the more reactive aryllithium, to which dimethylpiperid-4-one was added, resulting in addition of the phenol into the ketone. This produced a mixture of all four stereoisomers of the tertiary alcohol **159** in high yield. Ethylchloroformate was coupled to the alcohol to give the carbonate ester **160**. Heating **160** to 195°C in decalin resulted in thermal elimination of ethanol and carbon dioxide, leaving the unsaturated 1,2,3,6-tetrahydropyridine **161** and trace amounts of **159**.

At this stage the enantiomers of **161** were separated by HPLC using the same method developed to purify the enantiomers of **157**. As expected, **161a** and **161b** were easily separated using this method. Following separation, the remaining chemistry was carried out on both enantiomers separately and in parallel, using the same conditions.

Deprotonation of the 6-position of **161** by *n*-BuLi and 4-position methylation by dimethyl sulfide yielded chirally-pure **162a** and **162b** in separate reactions. The presence of the chiral 3-methyl group resulted in exclusively *trans*-methylation of the 4-position. A stoichiometric amount of dimethyl sulfide was used to avoid previously reported amine quaternisation.¹⁴¹ Due to initial difficulties in sourcing dimethyl sulfide, methyl iodide was also investigated as a methylating agent in this reaction. However, this approach produced only small quantities

of product, with mostly unreacted starting material and a mixture of unidentified by-product recovered. A similar result had also been reported when using methyl iodide or methyl bromide as methylating agents.¹⁴¹

The unsaturated bond of the 1,2,3,4-tetrahydropyridine ring was reduced by sodium borohydride to produce **163**. Displacement of the *N*-methyl group by phenylchloroformate (**164**) and subsequent removal of both the *N*- and *O*-substituents by hydrogen bromide in acetic acid completed the syntheses of **146a** and **146b**.

3.5 First generation non-fluorescent congeners

Following the successful synthesis of the DMHPP orthostere, a series of single amino acid congeners bound to DMHPP by a *N*-propanamide moiety were synthesised, and their MOR binding affinity determined over two phases (**Figure 3-12**). An initial set of glycine congeners using both the *3R,4R*-isomer **146a** and the *3S,4S*-isomer **146b** were synthesised and tested. This was carried out to both confirm **146a** as the higher MOR affinity isomer, and to substantiate the reported loss of MOR binding affinity when the benzyl group is removed from alvimopan (**9**).¹³⁹ The second set of congeners were exclusively synthesised from **146a**, with various amino acids substituted onto the *N*-propanamide. This set included several of the congeners synthesised and tested by Le Bourdonnec *et al.*¹³⁹ and some previously untested structures.

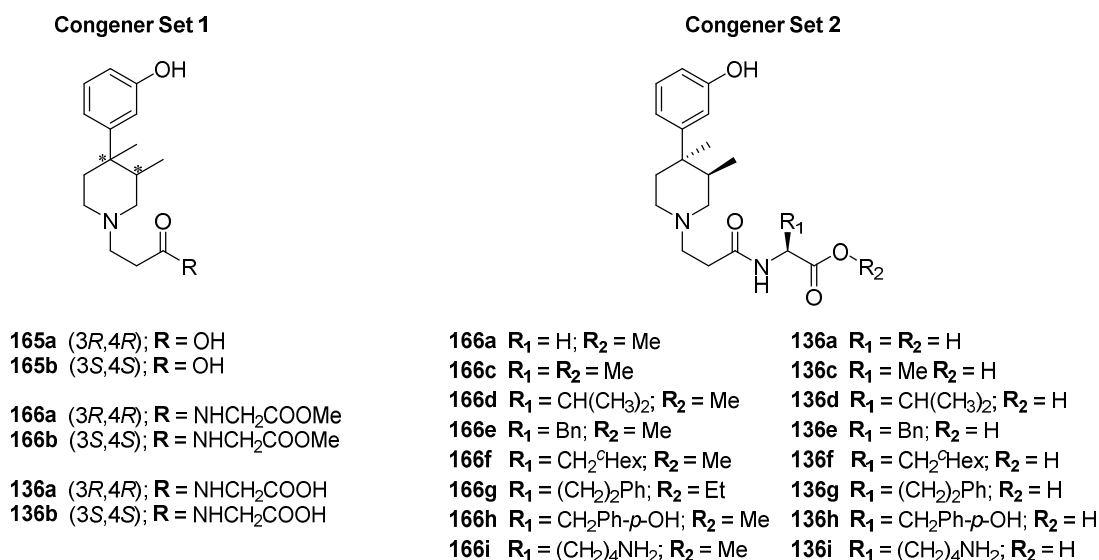
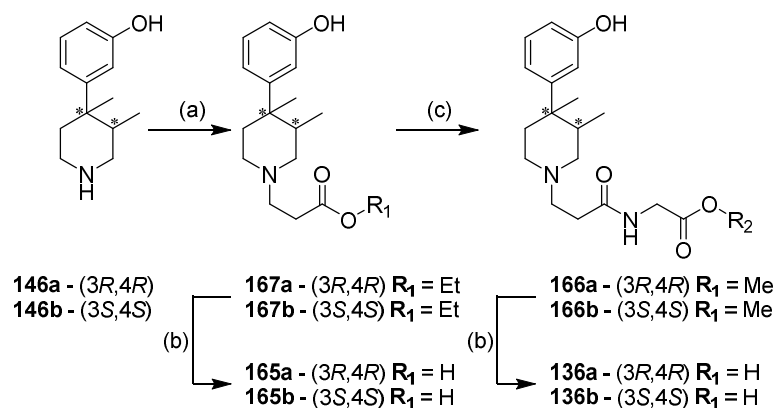


Figure 3-12: Structures of the tested single amino acid congener sets.

The first set of tested congeners included both the 3*R*,4*R*-orthostere **146a** and its 3*S*,4*S*-isomer **146b**. For each orthostere structure a glycine acid, glycine methyl ester and unsubstituted *N*-propionic acid congener were tested. In the second set, a series of different amino acid congeners bound to **146a** were tested as both the methyl ester and acid forms.

3.5.1 Synthesis of enantiomeric DMHPP congeners

The synthesis shown in **Scheme 3-9** follows a route similar to the one proposed by Zimmerman *et al.*¹¹⁰ in their paper describing the discovery of alvimopan (**9**). A propanoate moiety was introduced to the piperidine amine by Michael addition of **146a** to ethyl acrylate. This ethyl ester (**167a**) was hydrolysed under acidic conditions to produce the acid **165a**. Coupling to glycine methyl ester using the coupling reagent (2-(1*H*-benzotriazol-1-yl)-1,1,3,3-tetramethyluronium hexafluorophosphate (HBTU) with hydroxybenzotriazole (HOBT) and DIPEA, produced **166a** in a surprisingly low yield. The purity of the base used in the reaction was questionable, so the reaction was repeated with fresh DIPEA. This change did not result in an improved yield, but sufficient material had been produced for testing and for further ester hydrolysis to give the free acid **136a**. Synthesis of the 3*S*,4*S* congeners was carried out using the same method, as shown in **Scheme 3-9**.



Scheme 3-9: Synthesis of non-fluorescent glycine DMHPP congeners.

Reagents and conditions: (a) ethyl acrylate, DMF, 20 h, 50°C, 84%; (b) 4M HCl, dioxane, 2 h, reflux, 99%; (c) glycine-OMe.HCl, HBTU, HOBT, DIPEA, THF, 24 h, 16%.

3.5.2 MOR binding affinities of enantiomeric DMHPP congeners

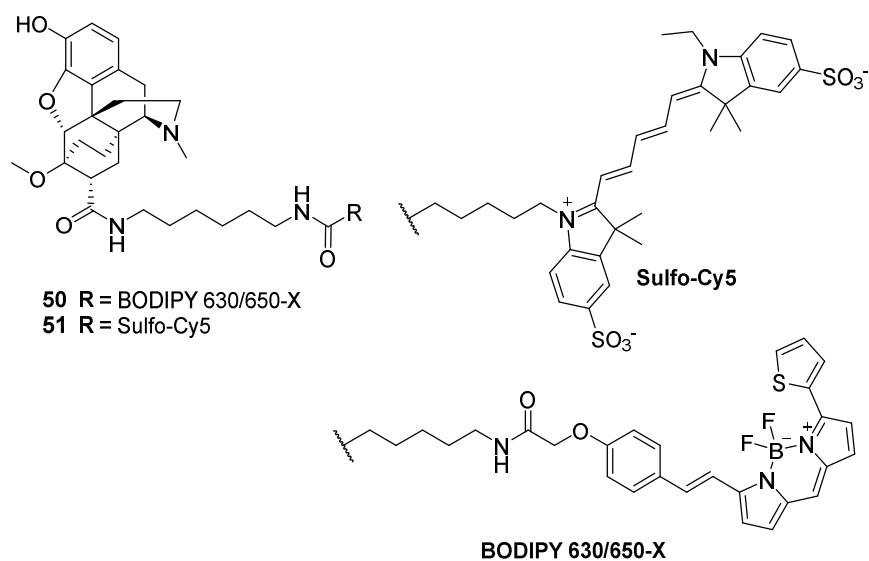


Figure 3-13: The structures of the oripavine-derived fluorescent ligands used in this study, synthesised and characterised by Schembri *et al.*⁵⁷

These fluorescent MOR ligands were used as labelled competitor ligands in competition binding studies to determine the MOR binding affinities of unlabelled compounds. The Sulfo-Cy5 fluorescent ligand **51** was most appropriate to be used in the competition binding studies measured by automated confocal imaging (described in 3.5.2), due to its low levels of non-specific binding.⁵⁷ The BODIPY 630/650-X fluorescent ligand **50** was found to be better suited for the TR-FRET competition binding studies due to its higher MOR binding affinity (described in 3.5.4).

The MOR binding affinities of the first set of congeners was determined using automated confocal microscopy in a competition binding assay against the sulfo-Cy5-labelled oripavine derivative **51** (synthesised and characterised by Schembri *et al.*⁵⁷). The results were plotted as competition binding curves (**Figure 3-14**) from which pK_i values were determined.

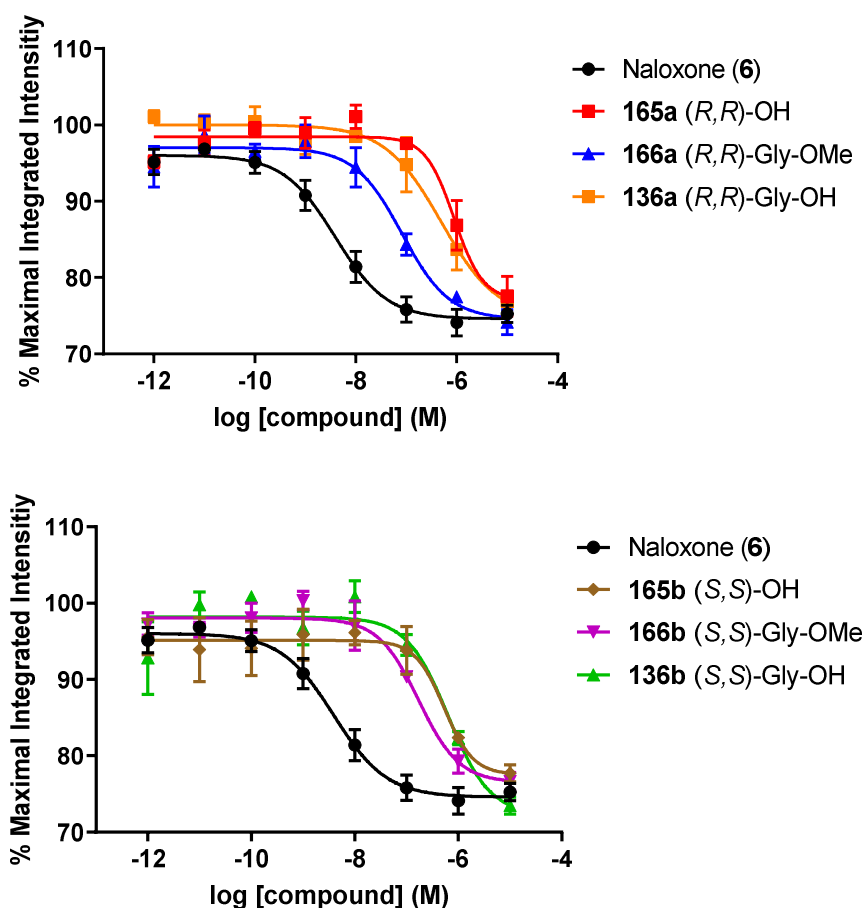
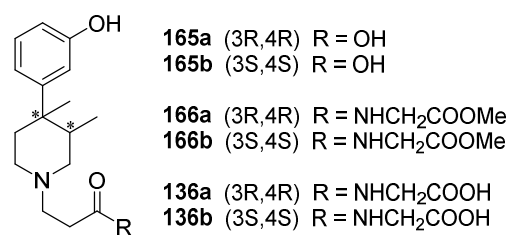


Figure 3-14: Competition binding assay for enantiomeric DMHPP congeners.

MOR-expressing HEK293 cells were incubated with 50 nM of the fluorescent ligand **51** (synthesised by Schembri *et al.*⁵⁷) and increasing concentrations of each of the enantiomeric congeners described in **Figure 3-15**. Data points are the mean of 3 or 4 separate experiments (mean \pm SEM), each carried out in duplicate.



Compound	MOR pK _i ± SEM	n
Naloxone (6)	8.70 ± 0.15	4
165a - (<i>R,R</i>)-OH	6.28 ± 0.20	3
165b - (<i>S,S</i>)-OH	6.55 ± 0.31	3
166a - (<i>R,R</i>)-Gly-OMe	7.40 ± 0.17	3
166b - (<i>S,S</i>)-Gly-OMe	7.04 ± 0.16	3
136a - (<i>R,R</i>)-Gly-OH	6.68 ± 0.17	3
136b - (<i>S,S</i>)-Gly-OH	6.48 ± 0.23	3

Figure 3-15: MOR binding affinities of enantiomeric DMHPP congeners.

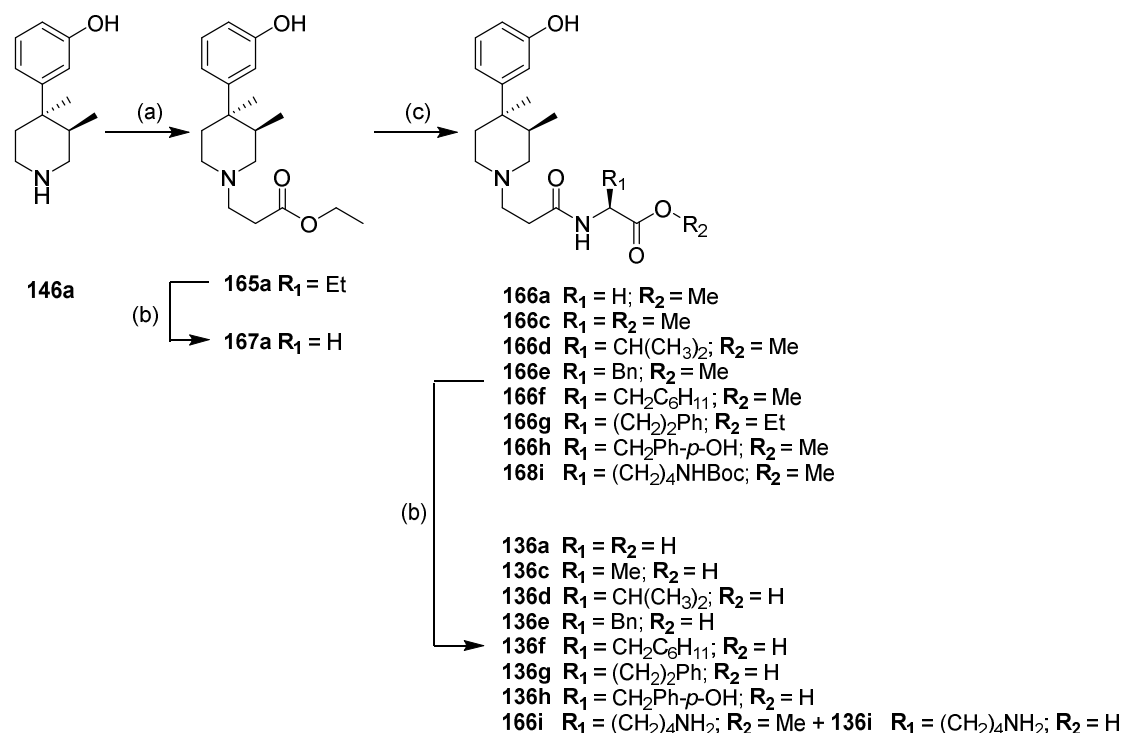
pK_i values at MOR were calculated from experimental IC₅₀ values using the Cheng-Prusoff equation.¹²² Experimental IC₅₀ values were determined by competitive displacement of the fluorescent ligand **51** (synthesised by Schembri *et al.*⁵⁷) in MOR-expressing HEK293 cells. Values are the mean of 3 or 4 separate experiments (mean ± SEM), each carried out in duplicate.

All congeners reduced binding to non-specific binding levels. Competition binding experiments indicated significant differences within the range of affinities (one-way ANOVA, P = 0.004) and between the Gly-OMe congeners **166a** and **166b** and the remaining acidic congeners (P < 0.05, post-hoc Tukey's multiple comparisons test). Significant differences in MOR binding affinity were not found between any of enantiomeric pairs, with only minor differences in pK_i exhibited.

3.5.3 Synthesis of further single amino acid congeners

In the second set of single amino acid congeners, the composition of the amino acid coupled to the propanamide of the 3*R*,4*R*-isomer **165a** was altered with a selection of different amino acids (**Scheme 3-10**). A previous study by Le Bourdonnec *et al.*¹³⁹ had tested a limited selection of congeners sharing the

structure **136** (Figure 3-10). Some of these described compounds were synthesised, along with a selection of other amino acid congeners.



Scheme 3-10: Synthesis of single amino acid DMHPP congeners.

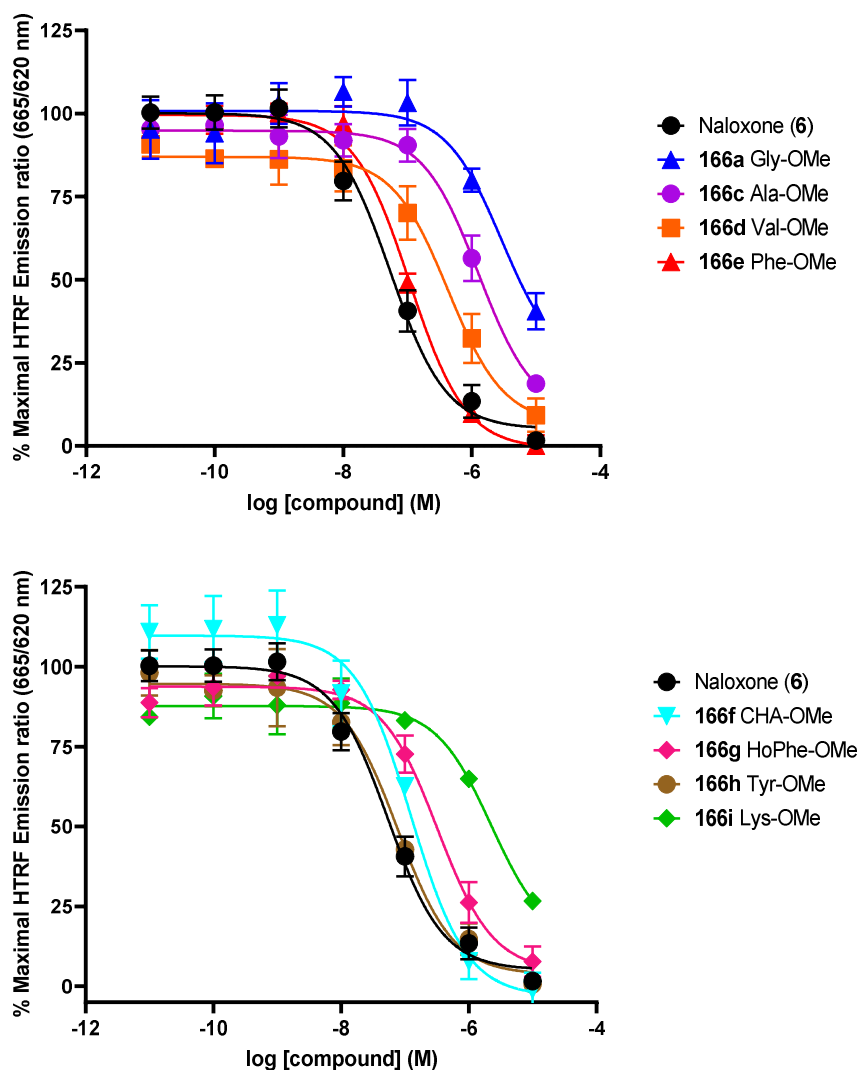
Reagents and conditions: (a) ethyl acrylate, DMF, 50°C, 84%; (b) 4M HCl, dioxane, reflux, 99%; (c) amino acid alkyl ester hydrochloride, HBTU, HOBT, DIPEA, THF, 12-17%.

The method used to synthesise these congeners was unaltered from the method described for the first set of single amino acid congeners (3.5.2) and again resulted in low reaction yields. However, sufficient material had been produced for testing (166a,c-i) and for further ester hydrolysis to give the free acids (136a,c-i).

3.5.4 MOR binding affinity of single amino acid congeners

Given the large number of compounds, the higher throughput TR-FRET-based method of competition binding assay against the BODIPY 630/650-labelled oripavine derivative **50** (synthesised and characterised by Schembri *et al.*⁵⁷), was used to determine the MOR binding affinities of the second set of single amino acid congeners. The results were plotted as competition binding curves

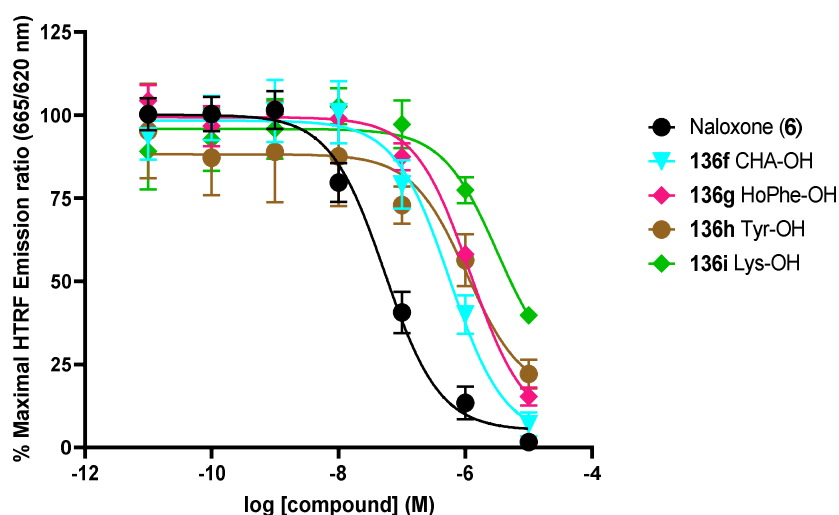
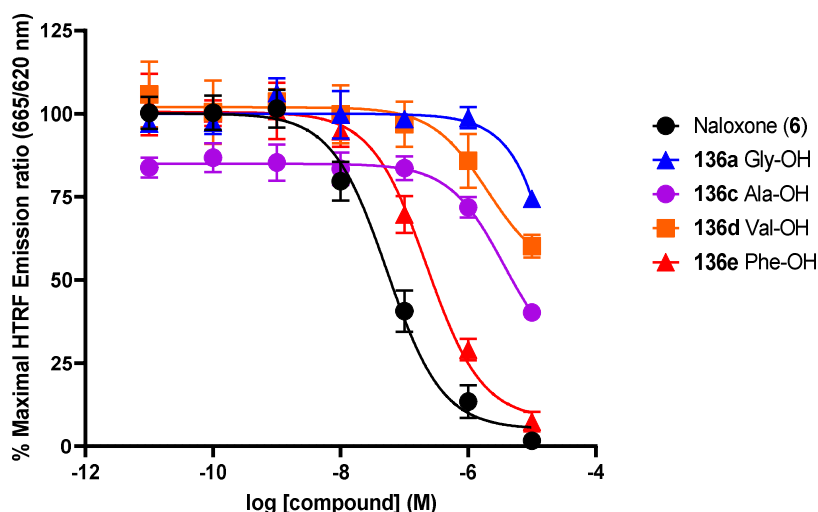
(Figure 3-16 and Figure 3-17), from which pK_i values were determined for compounds which reduced binding to non-specific levels (Table 3-1). Percentage inhibition at the highest tested concentration (10 μ M) is given for compounds which did not produce full competition binding curves.



CHA – cyclohexylalanine, HoPhe - homophenylalanine

Figure 3-16: Competition binding assay results for single amino acid DMHPP congeners.

Lumi4-Tb-labelled SNAP-MOR-expressing HEK293 cell membranes were incubated with 2 nM of the fluorescent ligand **50** (synthesised by Schembri *et al.*⁵⁷) and increasing concentrations of each of the amido ester congeners described in Scheme 3-10. Data points are the mean of 3 or 4 separate experiments (mean \pm SEM), each carried out in duplicate.



CHA – cyclohexylalanine, HoPhe - homophenylalanine

Figure 3-17: Competition binding assay results for single amino acid DMHPP congeners.

Lumi4-Tb-labelled SNAP-MOR-expressing HEK293 cell membranes were incubated with 2 nM of the fluorescent ligand **50** (synthesised by Schembri *et al.*⁵⁷) and increasing concentrations of each of the amido acid congeners described in **Scheme 3-10**. Data points are the mean of 3 or 4 separate experiments (mean \pm SEM), each carried out in duplicate.

Amongst the methyl ester compounds that displayed full inhibition of fluorescent ligand **50**, a significant range of pK_i values were observed (one-way ANOVA, $P = 0.001$). **166e** and **166h** were found to possess significantly higher MOR binding affinities than **166d** and **166g** ($P < 0.05$, post-hoc Tukey's multiple comparisons test). Fewer acidic congeners were able to produce full competition binding curves, but of those that did, **136e** showed significantly

higher MOR binding affinity than **136g** ($P < 0.05$, post-hoc Tukey's multiple comparisons test).

Compound		MOR $pK_i \pm SEM$ or % inh.			Compound		MOR $pK_i \pm SEM$ or % inh. at 10 μM	
		at 10 μM (lit. value ^a)		n			% inh. at 10 μM	n
136a	Gly	28%	(20%)	4	166a	Gly	59%	4
136c	Ala	60%		3	166c	Ala	82%	3
136d	Val	40%		3	166d	Val	6.79 \pm 0.17	3
136e	Phe	7.07 \pm 0.13	(7.44)	4	166e	Phe	7.39 \pm 0.07	4
136f	CHA	6.67 \pm 0.17	(7.70)	3	166f	CHA	7.32 \pm 0.14	3
136g	HoPhe	6.34 \pm 0.10	(7.24)	3	166g	HoPhe	6.91 \pm 0.12	3
136h	Tyr	78%		3	166h	Tyr	7.53 \pm 0.14	3
136i	Lys	60%	(45%)	3	166i	Lys	73%	3

CHA – cyclohexylalanine, HoPhe - homophenylalanine

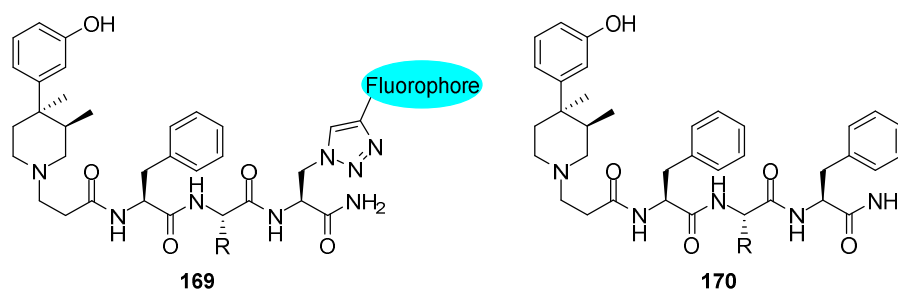
Table 3-1: MOR binding affinities of single amino acid DMHPP congeners.

pK_i values at MOR were calculated from experimental IC_{50} values using the Cheng-Prusoff equation.¹²² Experimental IC_{50} values were determined by competitive displacement of the fluorescent ligand **50** (synthesised by Schembri *et al.*⁵⁷) in Lumi4-Tb-labelled SNAP-MOR-expressing HEK293 cell membranes. Where a complete dose-response curve could not be established, percentage inhibition of the fluorescent ligand **50** by unlabelled congener at 10 μM is given. Values are the mean of 3 or 4 separate experiments (mean \pm SEM), each carried out in duplicate.

^a – Reported pK_i values by Le Bourdonnec *et al.*¹³⁹ measured by competitive displacement of [³H]-diprenorphine from MOR-expressing CHO cells.

Based on these results, phenylalanine was identified as the optimal amino acid to occupy the first position of a DMHPP-based fluorescent ligand linker. The higher MOR binding affinities displayed by the methyl ester congeners, compared to the corresponding acids, suggested that this was a suitable position for linker elaboration.

3.6 Second generation non-fluorescent congeners



Compound	R
170a Gly	H
170b Ala	CH ₃
170c Val	CH(CH ₃) ₂
170d Ser	CH ₂ OH
170e Asn	CH ₂ CONH ₂
170f Asp	CH ₂ COOH
170g Lys	(CH ₂) ₄ NH ₂
170h Arg	(CH ₂) ₃ NHC(NH ₂)NH

Figure 3-18: DMHPP-containing fluorescent ligand and non-fluorescent congener design.

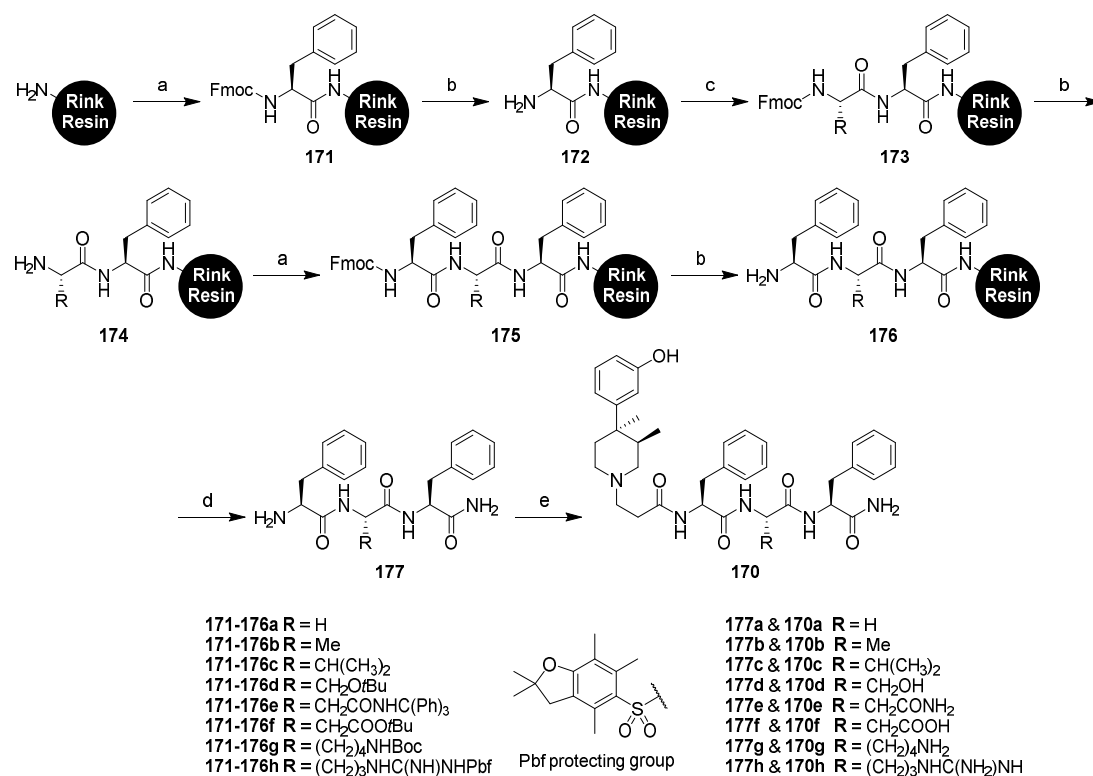
Left: General formula for the planned DMHPP-containing fluorescent ligands. The peptidic linker region would contain a phenylalanine moiety at the first position based on previous pharmacological testing. The second position would be occupied by one of the amino acids shown in the table. The third position was planned to be a 1,2,3-triazole with a fluorophore attached via the 4-position. **Right:** To determine the optimal amino acid composition at the second position, a series of non-fluorescent congeners were synthesised with each of the amino acids shown in the table. In these congeners, a phenylalanine moiety was substituted into the third position as a bioisostere of the 1,2,3-triazole.

It was decided that the composition of an amino acid at the second position should be explored, but, unlike the single amino acid congeners (**136**), there was no existing literature data for compounds of this kind with two or more amino acids. A range of amino acids representative of all amino acid types were selected to be used at the second position in this set of congeners (**Figure 3-18**). It was planned that a fluorophore could be attached to the linker via an

azide-alkyne cycloaddition between the alkyne of a modified fluorophore and an azidoalanine amino acid (**Scheme 3-1**). Rather than using the more expensive azidoalanine in the non-fluorescent congeners, a phenylalanine was incorporated at the third position as a bioisostere of the 1,2,3-triazole which results from this click reaction. Eight compounds with the final structures **170** shown in **Figure 3-18** were synthesised and their MOR binding affinities determined to identify the optimal composition of the linker.

3.6.1 Synthesis of tripeptide congeners

The longer tripeptide linkers were assembled by solid phase peptide synthesis prior to coupling to **165a**. This resulted in a much faster synthetic route to produce the tripeptide congeners, which could be carried out in parallel reactions. Solid phase synthesis proceeded as shown in **Scheme 3-11** using a rink amide resin. The initial (C-terminal) Fmoc-protected phenylalanine was coupled to the resin amine using an excess of amino acid, HCTU and DIPEA in DMF. The resin was washed with DMF, followed by Fmoc deprotection with a 20% solution of piperidine in DMF. The resin was washed again in DMF and the coupling and deprotection steps were repeated twice more with the appropriate amino acids in order to give the final products (**176**). After each coupling step (before deprotection), a 3:2 mixture of acetic anhydride/pyridine was added to the resin to “cap” (acetylate) any unreacted amino groups. Once the tripeptides (**176**) were assembled and Fmoc-deprotected, they were cleaved from the resin using an 18:1:1 mixture of TFA/TIPS/water. Any amino acid side chain protective groups were also removed by the cleavage mixture. It was planned that the purified tripeptide would then be coupled to **165a** to give the final tripeptide congeners.



Scheme 3-11: Proposed solid phase synthesis of the linker tripeptides and coupling to the DMHPP orthostere.

Solid phase peptide synthesis was carried out using a rink amide resin. Three cycles of Fmoc-amino acid coupling followed by Fmoc deprotection were carried out. Cleavage from the resin and amino acid side chain deprotection was carried out simultaneously. The final compounds **170a-h** were proposed to be synthesised by coupling to **165a**, but this method yielded no identifiable products. Reagents and conditions: (a) Fmoc-phenylalanine, HCTU, DIPEA, DMF, rt; (b) Pyridine, DMF, rt; (c) Fmoc-amino acid, HCTU, DIPEA, DMF, rt; (d) TFA, TIPS, water, rt; (e) **165a**, HCTU, DIPEA, DMF.

Use of newer rink amide resin was found to improve the yield of solid-phase tripeptide synthesis, suggesting degradation in some of the older samples used. The cleavage products (**177a-h**) were typically mixed with large quantities of unidentified by-products, which may have been a mixture of resin fragments and acetyl-capped incomplete peptides. The desired products were easily separable from this mixture by column chromatography. Despite having isolated 10-20 mg of each tripeptide, a coupling reaction with **165a** produced no identifiable products (**170**). A small amount of uncoupled tripeptide was recovered but the starting **165a** could not be identified in the reaction mixture.

It was proposed that **165a** could be forming esters with the phenolic hydroxyl group (**Figure 3-19**), so several protecting groups for the phenol were investigated to avoid this potential esterification. Initially a *tert*-butyldimethylsilyl (TBS) group was coupled to the phenol using TBS chloride with an imidazole catalyst (**Scheme 3-12**). TBS is known to be stable under basic conditions and easily cleaved by acid, so ester hydrolysis of **179** was carried out using 1M NaOH. However, the phenol is a better leaving group than an aliphatic alcohol, making the TBS-phenol-ether more susceptible to basic cleavage and, as a result, this reaction yielded only **165a**, without any remaining TBS-protected product.

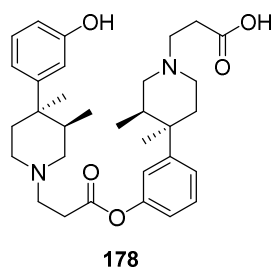
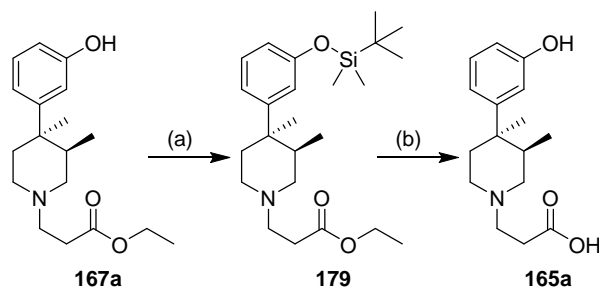


Figure 3-19: The proposed structure of a di-DMHPP ester.

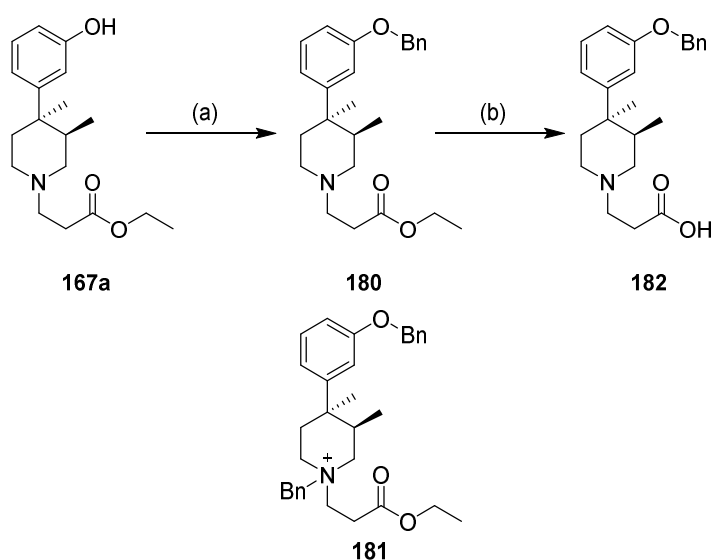
The low yields observed in the peptide coupling reactions described in **3.5.1**, **3.5.3** and **3.6.1** between the *N*-propionic acid DMHPP **165a** and an amino ester or tripeptide were proposed to have resulted from esterification between the *N*-substituent and the phenolic hydroxyl group, giving the structure shown (**178**). Further coupling between **178** and additional units of **165a** or an amino acid amine could also have occurred.



Scheme 3-12: TBS-protection of the phenol of 167a followed by an unsuccessful ester hydrolysis.

The phenolic hydroxyl group of **167a** was successfully protected with a *tert*-butyldimethylsilyl (TBS) group, but basic hydrolysis of the ethyl ester of **179** also removed the TBS group. Reagents and conditions: (a) TBS chloride, imidazole, DMF, rt; (b) 1M NaOH, EtOH, H₂O, rt.

The phenol was instead benzyl-protected using benzyl bromide with potassium carbonate (**Scheme 3-13**). It was found that equal amounts of benzyl bromide and **167a** were necessary in order to avoid benzylation of the tertiary amine (**181**). This stoichiometry resulted in a 70% yield with incomplete consumption of both reagents, but heating the reaction promoted quaternisation of the amine (**181**). Instead, the reaction was stopped after stirring overnight at room temperature and the product (**180**) and unreacted starting material (**167a**) were recovered. Ester hydrolysis of **180** was successfully carried out under acidic conditions.



Scheme 3-13: Benzyl-protection of the phenol of 167a followed by ester hydrolysis.

The phenolic hydroxyl group of **167a** was successfully benzyl-protected with a stoichiometric amount of benzyl bromide at room temperature to avoid producing the dibenzyl quaternised species **181**. Acidic hydrolysis of the ethyl ester of **180** produced the acid **182**. Reagents and conditions: (a) BnBr, K₂CO₃, DMF, rt; (b) 2M HCl, dioxane, H₂O, rt.

Coupling of **182** to the tripeptide was again unsuccessful, with disappearance of **182** and limited recovery of unreacted tripeptide. Alternative reaction conditions were trialled for this coupling reaction, replacing HCTU with tetramethylfluoroformamidinium hexafluorophosphate (TFFH) to generate an in-situ acid fluoride to couple to the tripeptide. Once again, this reaction was unsuccessful, but a noteworthy outcome was the identification by LCMS of a common by-product of both the HCTU and TFFH reactions. The by-product had

a molecular weight of 394, a number which could not be fitted to any LCMS adduct of the starting materials or desired product. ¹H NMR analysis of the purified by-product revealed a profile typical of a DMHPP-based compound and it was determined that the structure was likely to be the guanidinylated DMHPP **183** (Figure 3-20).

Uronium-based coupling reagents are known to “cap” peptide amines, forming a guanidinium and preventing further amide formation. It is therefore plausible that this could occur on the secondary amine of this piperidine ring. Formation of **183** is surprising though, as it would have to result from a reverse Michael reaction, followed by attack by the piperidine on the HCTU uronium. However, the matching molecular weight by LCMS and ¹H NMR evidence (Figure 3-20) strongly suggest that this was the case.

Since both HCTU and TFFH contain the uronium group, it was decided that substitution of these coupling reagents for the phosphonium-based PyBOP would illuminate the issue. The coupling reaction between **165a** and the asparagine-containing tripeptide (**177e**) with PyBOP successfully produced the product **170e**, albeit in a low yield (15%). **146a** was identified in the reaction mixture, confirming that a reverse Michael reaction had occurred under these basic coupling conditions. It seems that the α -proton of the *N*-propanoate was more acidic than anticipated and was removed by the DIPEA under these conditions, resulting in the reverse Michael reaction.

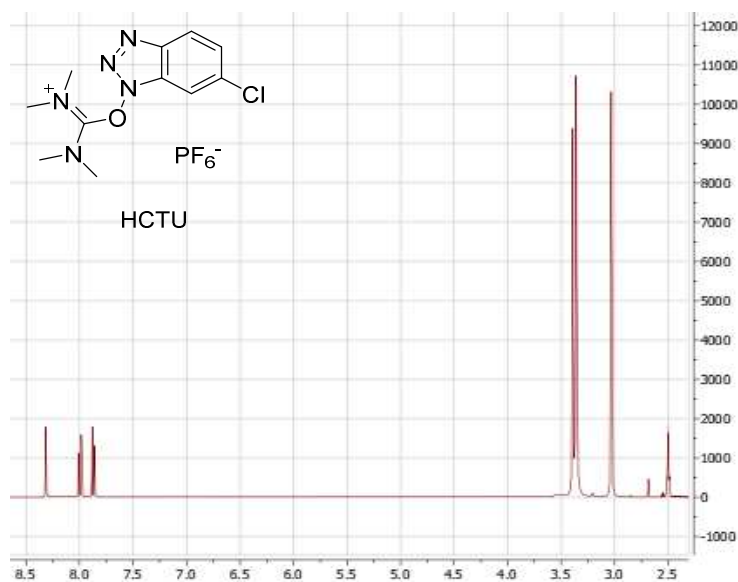
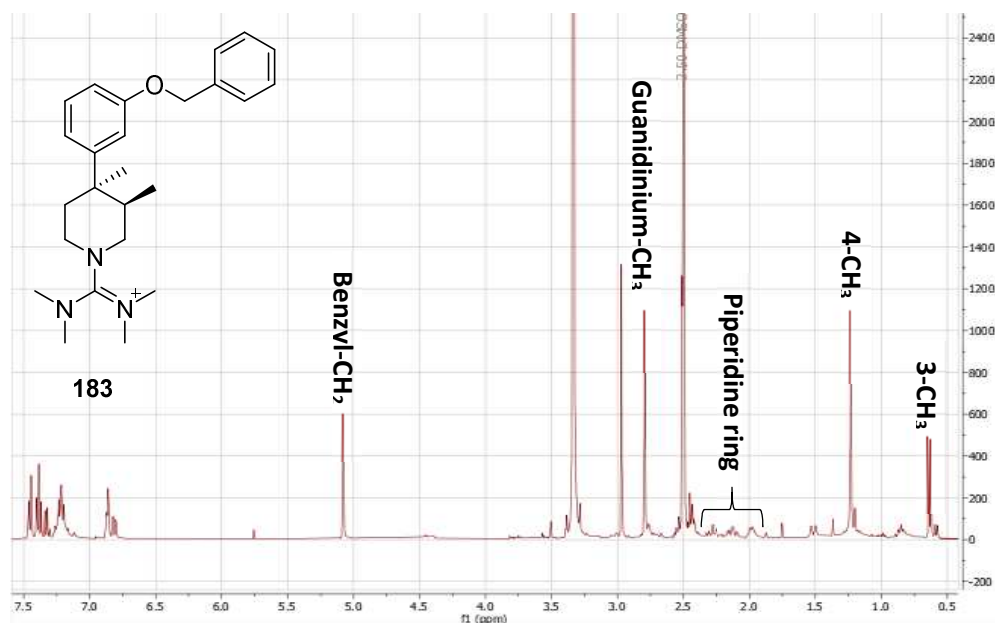
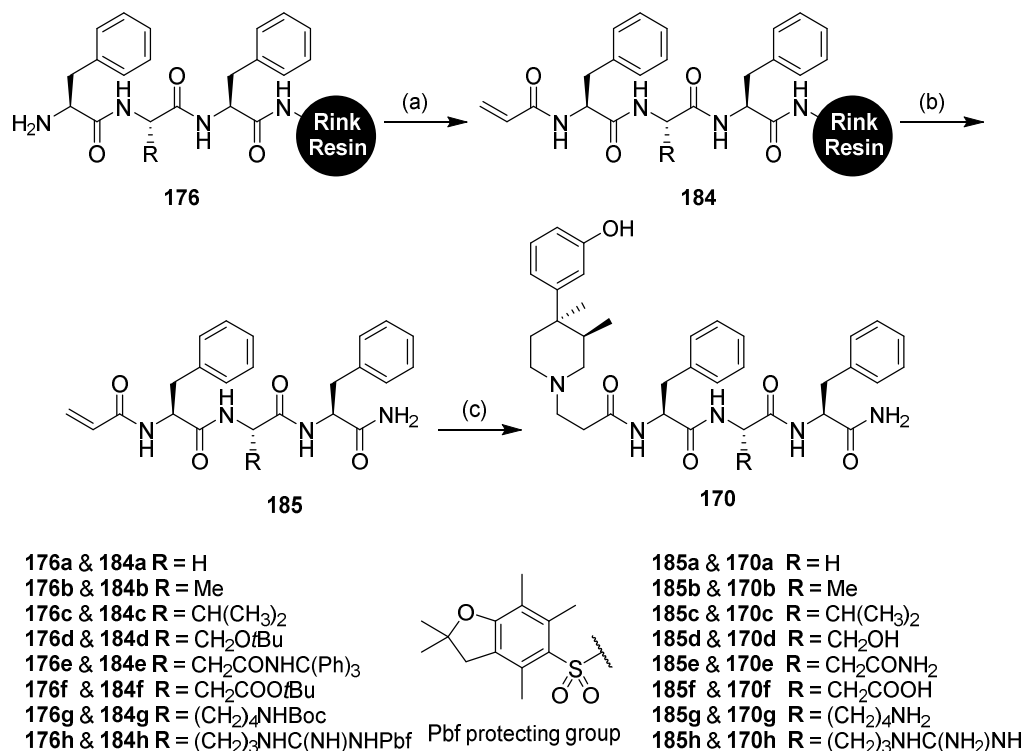


Figure 3-20: ^1H NMR of the guanidylated DMHPP 183.

Above: The structure is clearly identifiable as containing the DMHPP structure from features such as the 3-CH₃ 3H doublet at 0.63 ppm, the 4-CH₃ 3H singlet at 1.23 ppm, the characteristic piperidine peaks between 1.90 and 2.35 ppm, the benzyl CH₂ peak at 5.08 ppm, and the arrangement of aromatic peaks. The noteworthy additions to this spectra are the two large singlet peaks at 2.79 and 2.97 ppm. The ^1H NMR predictions generated by the MestReNova and ChemDraw software both -predicted two large singlet peaks for the guanidinium methyl groups, but differed dramatically in their predicted locations, likely due to interpretation of the permanent charge in this region. **Below:** The ^1H NMR of HCTU also showed two large singlet peaks in a similar region (3.03 and 3.39 ppm, the latter overlaps with a water peak) which adds further evidence to the formation of this species.

The PyBOP-coupled reaction could have been further optimised to improve the yield, however an alternative solution was pursued in which acrylic acid was coupled to the resin-bound peptide. Michael addition of **146a** to the cleaved acrylamide **185** yielded the products **170a-h** (Scheme 3-14), without the need for phenol hydroxyl protection.



Scheme 3-14: Alternative route to synthesis of DMHPP tripeptide congeners.

Reagents and conditions: (a) Acrylic acid, HCTU, DIPEA, DMF, rt; (b) TFA, TIPS, water, rt; (c) **146a**, NMP, 85°C.

3.6.2 MOR binding affinity of tripeptide congeners

The MOR binding affinities of the non-fluorescent congeners were then assessed by TR-FRET in a competition binding assay against the fluorescent compound **50**. The results were plotted as competition binding curves (Figure 3-21), from which p*K*_i values were determined (Table 3-2). All congeners reduced binding to non-specific levels.

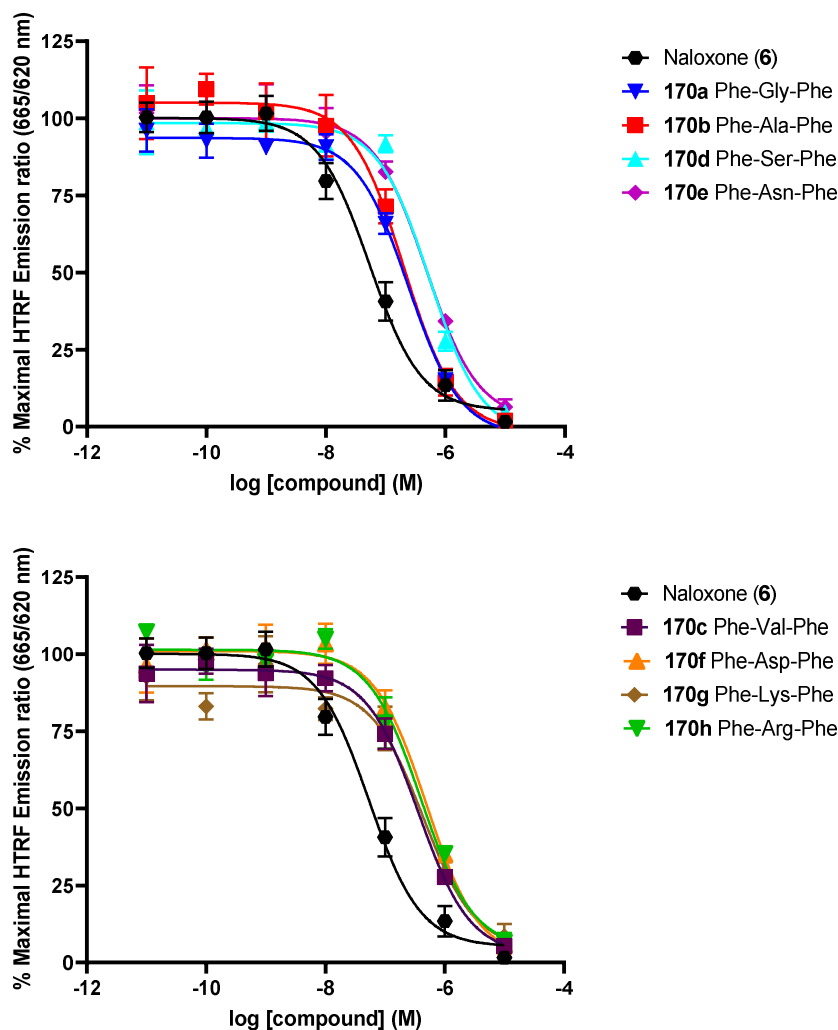


Figure 3-21: Competition binding assay results for tripeptide DMHPP congeners.

Lumi4-Tb-labelled SNAP-MOR-expressing HEK293 cell membranes were incubated with 2 nM of the fluorescent ligand **50** (synthesised by Schembri *et al.*⁵⁷) and increasing concentrations of each of the tripeptide congeners described in **Figure 3-18**. Data points are the mean of 3 or 4 separate experiments (mean \pm SEM), each carried out in duplicate.

The competition binding assay results for the tripeptide congeners produced a significant range of pK_i values (one-way ANOVA, $P = 0.009$), although only **170b** exhibited a significantly higher pK_i value than **170d**, **170e** and **170f** ($P < 0.05$, post-hoc Tukey's multiple comparisons test), with no other significant differences found. Comparison of these results with the Phe-OH congener **136e** showed no significant change in binding affinity from **136e** ($P > 0.05$, post-hoc Dunnett's multiple comparisons test). However, all of these congeners produced significantly lower binding affinities than the Phe-OMe congener

166e ($P < 0.05$, post-hoc Dunnett's multiple comparisons test) except for **170a** and **170b**.

Compound	MOR $pK_i \pm SEM$	n
Naloxone (6)	7.69 ± 0.11	4
170a Phe-Gly-Phe	7.03 ± 0.09	3
170b Phe-Ala-Phe	7.11 ± 0.14	3
170c Phe-Val-Phe	6.86 ± 0.12	3
170d Phe-Ser-Phe	6.68 ± 0.12	3
170e Phe-Asn-Phe	6.74 ± 0.16	3
170f Phe-Asp-Phe	6.72 ± 0.13	3
170g Phe-Lys-Phe	6.78 ± 0.17	3
170h Phe-Arg-Phe	6.82 ± 0.11	3

Table 3-2: MOR binding affinities of tripeptide DMHPP congeners.

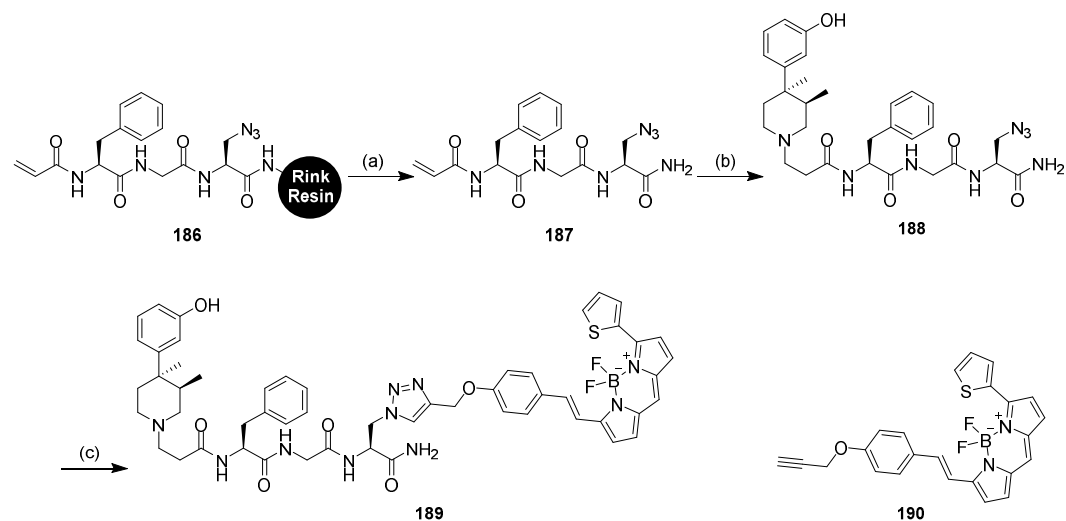
pK_i values at MOR were calculated from experimental IC_{50} values using the Cheng-Prusoff equation.¹²² Experimental IC_{50} values were determined by competitive displacement of the fluorescent ligand **50** (synthesised by Schembri *et al.*⁵⁷) in Lumi4-Tb-labelled SNAP-MOR-expressing HEK293 cell membranes. Values are the mean of 3 or 4 separate experiments (mean \pm SEM), each carried out in duplicate.

The absence of improvement in MOR binding affinity shown by these tripeptide congeners indicated that the introduction of further amino acids to the linker was unlikely to improve binding affinity. Therefore, the decision was made for the project to proceed to synthesis of the fluorescent ligands.

3.7 Fluorescent 3,4-dimethyl-4-(3-hydroxyphenyl) piperidine-based compounds

Since amino acid composition at the second position was shown not to significantly influence MOR binding affinity, it was decided that a glycine moiety would be used at this position, giving a fluorescent ligand of the design **189** shown in **Scheme 3-15**. It was planned that an azidoalanine would occupy the third position of the tripeptide linker, and once bound to the DMHPP

orthostere, would undergo a click reaction with an alkyne-bound BODIPY 630/650 (**190**) to produce the 1,2,3-triazole-linked fluorescent product **189**.



Scheme 3-15: Synthesis of the click-BODIPY 630/650 DMHPP fluorescent ligand.

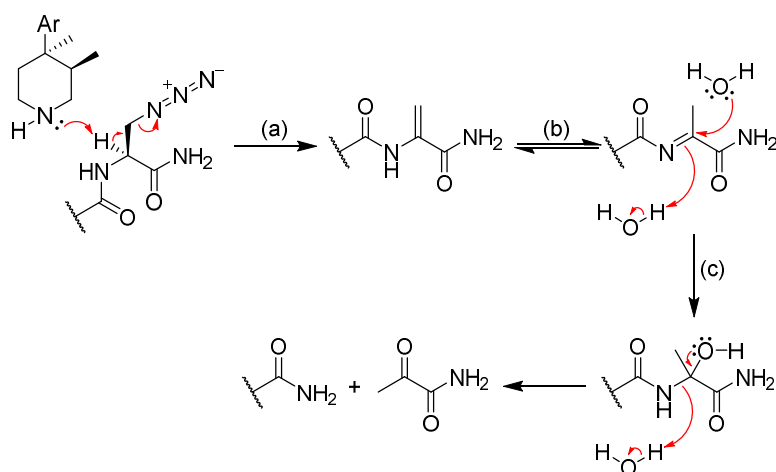
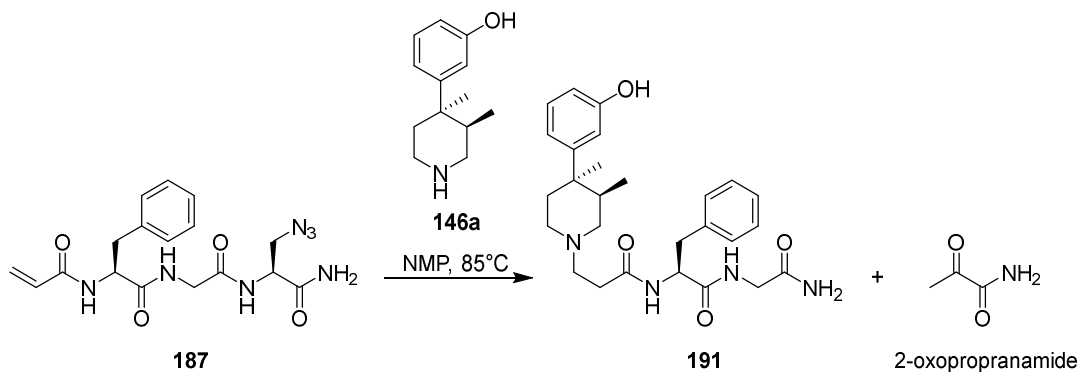
The proposed synthetic scheme for synthesis of the fluorescent compound **189**. Reagents and conditions: (a) TFA, TIPS, H₂O, rt; (b) **146a**, NMP, 85°C; (c) **190**, H₂O, rt.

3.7.1 Synthesis of fluorescent β -naltrexamine compounds

Solid-phase synthesis of the azido-containing tripeptide (**186**) was unchanged from the method described in **Scheme 3-11**. Following TFA cleavage of the peptide from the resin, the purified peptide **187** was reacted with **146a** in NMP at 85°C. Formation of a new product was observed by TLC, however, LCMS analysis revealed that it was not the desired product (**188**). The limited amount of material recovered made it difficult to definitively determine what occurred in the reaction, but ¹H NMR and LCMS evidence suggested that the dipeptide **191** had been produced, with loss of the azidoalanine.

A proposed mechanism for the formation of this product is shown in **Scheme 3-16**. The excess of **146a** in this highly concentrated reaction would create a basic environment which could have resulted in deprotonation of the α -carbon of azidoalanine. Literature examples describe β -elimination of azidoalanine under basic, high temperature conditions to produce dehydroalanine.^{145, 146}

Tautomerism of the dehydroalanine from the alkene to the imine would then provide a site for nucleophilic attack by water molecules present in the hygroscopic solvent.^{147, 148} Further research is required in order to confirm the presence of both the dipeptide congener with a terminal amide (**191**) and 2-oxopropanamide following this reaction.

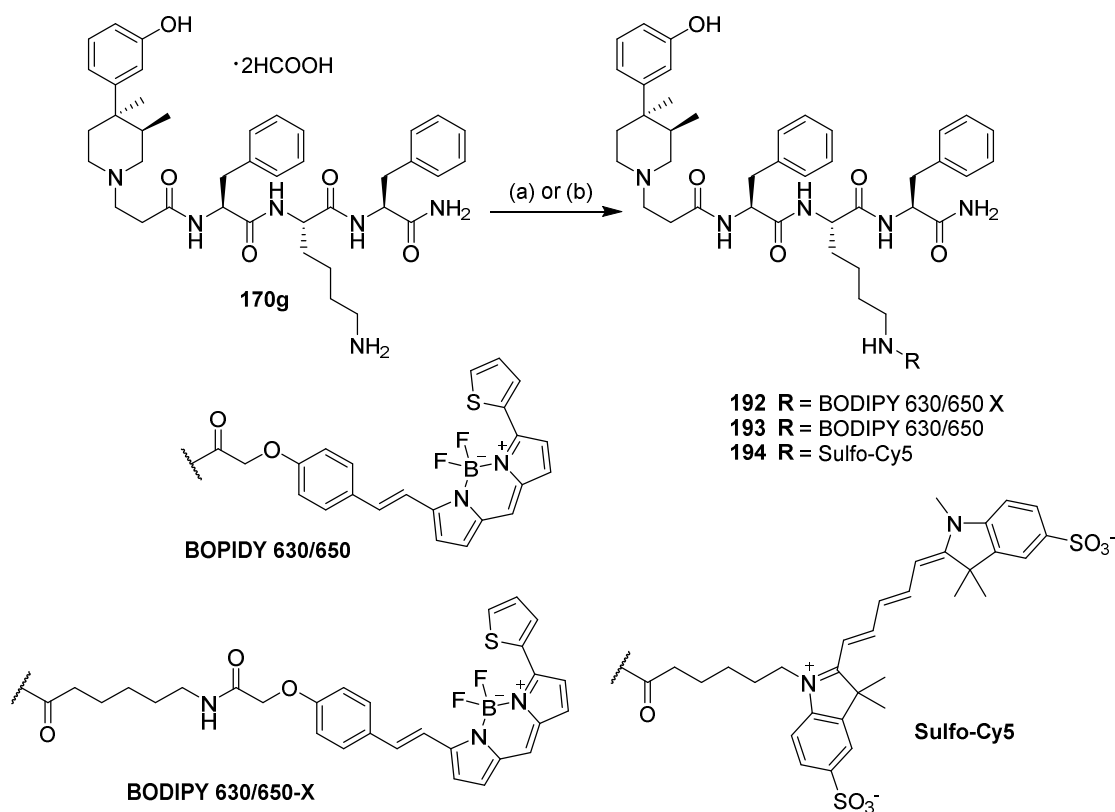


Scheme 3-16: The proposed reaction and mechanism for the β -elimination of azidoalanine and subsequent imine hydrolysis.

(a) The piperidine amine of **146a** deprotonates the α -carbon of azidoalanine, resulting in elimination of an azide ion and forming dehydroalanine; (b) Tautomerization of dehydroalanine converts it to the imine; (c) Hydrolysis of the imine results in a new primary amide and the loss of 2-oxopropanamide.

This reaction may have been possible at a lower temperature and reduced concentration of **146a** without loss of the azidoalanine, but this would require the reaction to be left for several weeks. Even at 85°C and in a highly concentrated solution, these Michael reactions typically took 2-3 days to reach

completion. At this stage of the project there was insufficient time remaining to experiment with different conditions to form the azido product **188**, so a different approach was decided upon.



Scheme 3-17: Synthesis of fluorescent DMHPP compounds from 170g.

Reagents and conditions: (a) BODIPY 630/650-X-OSu or sulfo-Cy5-OSu, DIPEA, DMF, rt, 40-53%; (b) BODIPY 630/650-OH, PyBOP, DIPEA, DMF, rt, 35%.

The Phe-Lys-Phe congener **170g** had been produced in sufficient quantity that it could be used to produce fluorescent ligands by coupling a fluorophore carboxylic acid to the lysine amine (**Scheme 3-17**). This approach benefitted from both speed of synthesis and that a greater variety of fluorophores could now be attached, as an alkynyl group on the fluorophore was no longer necessary for attachment. Similar to the fluorescent compounds described in **Chapter 2**, three fluorophores were coupled to **170g**: BODIPY 630/650-X, BODIPY 630/650 and sulfo-Cy5.

Due to the apparent acidity of the propanamide α -proton, the use of base in these fluorophore couplings was problematic. BODIPY 630/650-X and sulfo-Cy5

were both pre-formed NHS esters, which theoretically did not require base to react. However, the ^1H NMR of **170g** showed that it was a di-formic acid salt, due to formic acid used during HPLC purification. It was decided that these reactions would be carried out in the absence of base, and, should the reaction not proceed, dilute base could be added slowly until the reaction was complete. This caution was unnecessary in practice, as the reaction proceeded without base to produce the products **192** and **194**. Coupling to the shorter BODIPY 630/650 compound differed, as it was a free acid rather than an NHS ester. In this reaction, the coupling reagent PyBOP and BODIPY 630/650 were mixed in DMF with one equivalent of DIPEA to form the active ester before the addition of **170g**. It was hoped that the base would be consumed during this first step, with none remaining to deprotonate the propanamide. These conditions successfully produced the fluorescent compound **193**.

3.7.2 MOR binding affinity of fluorescent β -naltrexamine compounds

MOR binding affinities (pK_D) of the fluorescent compounds **192-194** were determined in saturation binding experiments (**Figure 3-22** and **Table 3-3**). The specific binding curves of the BODIPY 630/650-containing ligands (**192** and **193**) were both saturated, displaying similar pK_D values. However, the specific binding curve for compound **194** at this concentration did not appear to reach saturation, meaning that a reliable pK_D value could not be determined. This suggests a significantly lower MOR binding affinity for **194** than **192** and **193**.

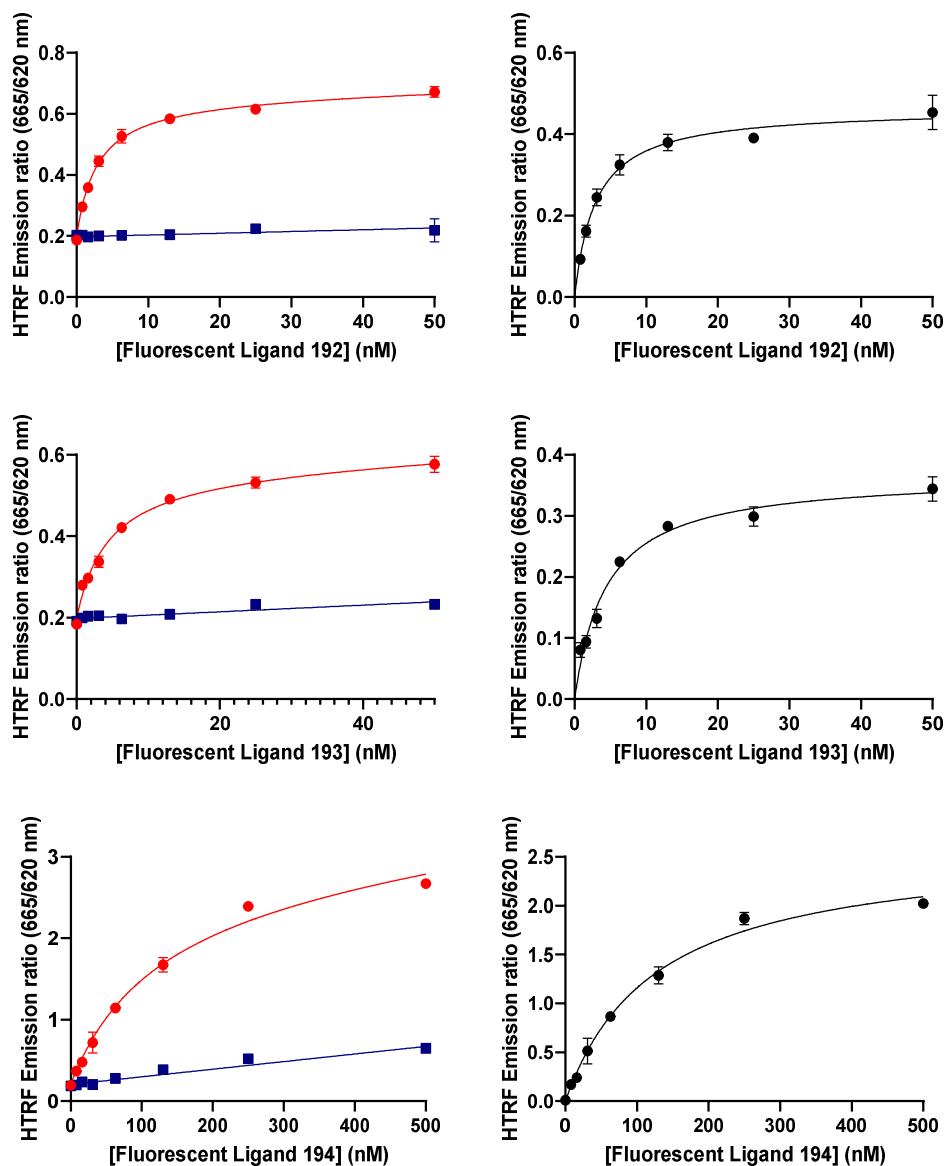


Figure 3-22: Saturation binding assay results for fluorescent DMHPP compounds.

Lumi4-Tb-labelled SNAP-MOR-expressing HEK293 cell membranes were incubated with increasing concentrations of the fluorescent compounds **192-194**. Non-specific binding (blue) was determined in the presence of 10 μ M naloxone. Total binding (red) was determined in the absence of naloxone. Specific binding (black) was calculated from total binding minus non-specific binding. Data points are the mean of a single experiment (mean \pm range) carried out in duplicate which are representative of four separate experiments from which a value for K_D was determined.

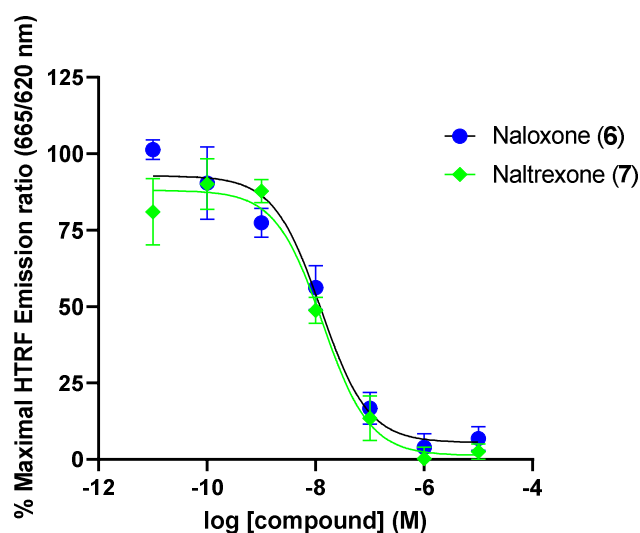
Following this, compound **192** was selected for further competition binding assays against naloxone (**6**) and naltrexone (**7**) to confirm it was specifically labelling the MOR (**Figure 3-23**).

Compound	$pK_D \pm SEM$	n
192 - BODIPY 630/650-X	8.47 ± 0.04	3
193 - BODIPY 630/650	8.18 ± 0.09	3
194 - sulfo-Cy5	N/A ^a	3

^a – could not determine K_D within the tested concentration range

Table 3-3: MOR binding affinities of fluorescent DMHPP ligands.

pK_D values were determined for the specific binding of each fluorescent ligand from the total binding and non-specific binding (+ 10 μ M naloxone) curves generated in Lumi4-Tb-labelled SNAP-MOR-expressing HEK293 cell membranes. pK_D values are the mean of a 3-4 experiments (mean \pm SEM), each carried out in duplicate.



Compound	Obs. MOR $pK_i \pm SEM$	Lit. MOR pK_i range
Naloxone (6)	8.20 ± 0.15	7.3-9.0 ^a
Naltrexone (7)	8.18 ± 0.14	8.1-9.7 ^b

^a – refs^{57, 108-112} ^b – refs^{57, 99, 108-110, 113, 114}

Figure 3-23: Competition binding assay results for naloxone and naltrexone against the fluorescent ligand 192.

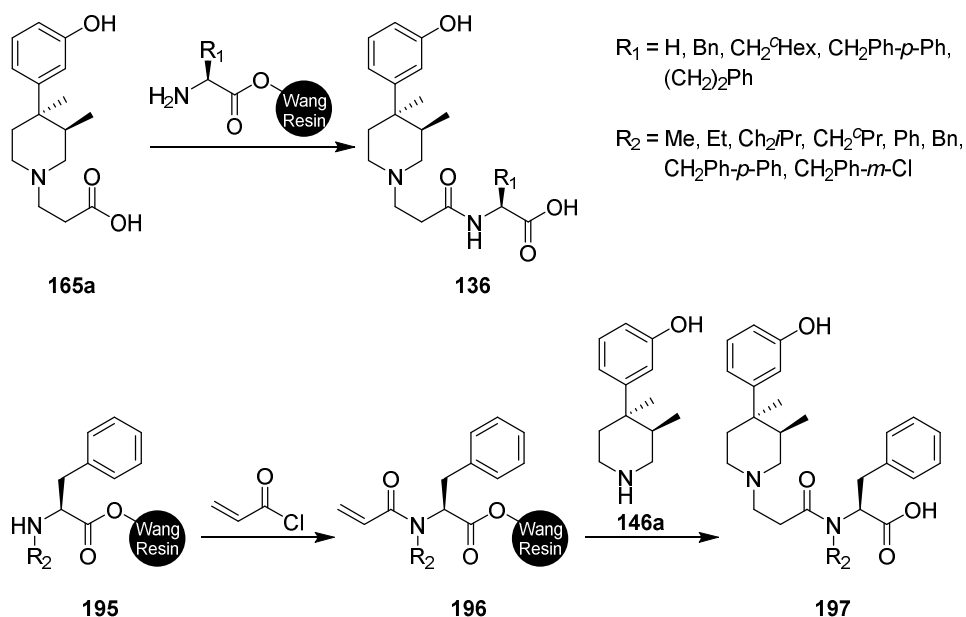
Lumi4-Tb-labelled SNAP-MOR-expressing HEK293 cell membranes were incubated with 2 nM of the fluorescent ligand **192** and varying concentrations of naloxone (**6**) and naltrexone (**7**). Data points and the observed pK_i values are the mean of 4 separate experiments (mean \pm SEM), each carried out in triplicate. Values for pK_i were determined from the experimental IC_{50} and the fluorescent ligand K_D and concentration using the Cheng-Prusoff equation.¹²² Ranges of reported pK_i values for these compounds at MOR are included.

3.8 Discussion

Three fluorescent peptide-linked MOR ligands were successfully synthesised and pharmacologically evaluated for binding affinity at MOR using the DMHPP orthostere.

The synthesis of the DMHPP structure itself and its *N*-substituted congeners encountered several challenges. The initial synthetic route pursued to synthesise **146a** was carried out in accordance with the method described by Furkert *et al.*,¹⁴⁴ but did not result in the described enantioselectivity of products. The observed ratio of enantiomers **157a** and **157b**, which were quantified following chiral purification, suggests a synthetic bias in favour of the desired 3*R* enantiomer **154a** during methylation, but not the near-complete enantioselectivity previously reported. Without the benefit of enantioselectivity, the non-selective synthetic route described by Werner *et al.*¹⁴¹ was preferred, and was completed without complication to produce **146a** and **146b**.

The discovery that the *N*-propanoic acid congener **165a** undergoes both a reverse Michael reaction, and subsequent guanidinylation of the piperidine amine, was unexpected. This is only the second reported instance of amide couplings to **165a**, the first being Le Bourdonnec *et al.*¹³⁹ in 2008, in which **165a** was coupled to a Wang resin-bound amino acid with no reported synthetic issues (**Scheme 3-18**). However, the absence of reported yields for these reactions make them difficult to compare.¹³⁹ In the same study, it was reported that *N*-substituted amino acids (**195**) could not be coupled to **165a** using, “a wide range of coupling reagents and reaction conditions”, but a similar approach to the one described in **Scheme 3-14** to form acrylamides (**185**) before carrying out a Michael addition to **146a** was successful (**Scheme 3-18**).¹³⁹ Without further development of the findings of Le Bourdonnec *et al.*,¹³⁹ it is not possible to determine if similar issues were encountered or resolved.



Scheme 3-18: Synthetic routes used by Le Bourdonnec *et al.*¹³⁹ to synthesis single amino acid DMHPP congeners.

Above: Synthesis of congeners of the formula **136** were reported by Le Bourdonnec *et al.*¹³⁹ to have been successfully synthesised by coupling **165a** to Wang resin-bound amino acids. **Below:** Le Bourdonnec *et al.*¹³⁹ reported that *N*-substituted resin-bound amino acids (**195**) could not be coupled to **165a** by the same method. Instead the *N*-substituted resin-bound amino acids (**195**) were coupled to acryloyl chloride and the subsequent acrylamides (**196**) were reacted with **146a** to give **197** after resin cleavage.

Only minor differences in binding affinity were observed between the tested *3R,4R* and *3S,4S* enantiomers of **136a-b**, **165a-b** and **166a-b**, but differences of this magnitude can be found in other DMHPP-based compounds, with *3R,4R* enantiomers typically displaying a slightly higher MOR binding affinity than the respective *3S,4S* enantiomer.¹²⁷ The enantiomers of both of the acidic compounds **136** and **165** displayed similar MOR binding affinities, suggesting that the glycine moiety does not play a crucial role in MOR binding. These acidic congeners displayed lower MOR binding affinities than the corresponding methyl esters, indicating that the free acid, while beneficial for imparting important pharmacokinetic properties on alvimopan (**9**) as a clinical drug, may not be beneficial for MOR binding.

A loss in MOR binding affinity was observed for all methyl ester congeners (**166**) when hydrolysed to their respective acids (**136**), but the magnitude of MOR

affinity attenuation differed between congeners. Congeners containing an aromatic or cyclohexyl amino acid side chain displayed the highest MOR binding affinities, although some of the calculated pK_i values were lower than previously reported, but these difference may be due to the different methods used to measure MOR binding affinity (see **Table 3-1**).¹³⁹ Phe was identified as the optimal amino acid to occupy the first position of the linker due to the high pK_i values of both the methyl ester **166e** and acid **136e**, the similarity between the observed and literature pK_i values of **136e**, and the high receptor subtype selectivity reported for **136e**, which is desirable, despite not being an explicit aim of the project.¹³⁹

No significant differences in MOR binding affinity were found between the tripeptide congeners **170a-h**, suggesting that no further benefit would be gained from linker elaboration. Much like the β -naltrexamine congeners described in **Chapter 2**, it is likely that the functional groups of the second position amino acid are too far from the shallow binding pocket of MOR to positively influence binding affinity. These tripeptide congeners produced a similar MOR binding affinity to the phenylalanine congener **136e**, showing that elaboration of the linker through a longer peptide chain was well tolerated, providing a suitable site for linker and fluorophore attachment.

The BODIPY 630/650-containing compounds (**192** and **193**) exhibited similar MOR binding affinities to the BODIPY 630/650 compound **50** described by Schembri *et al.*⁵⁷ The total binding curve for the sulfo-Cy5-containing compound **194** did not reach saturation in the tested range, so a reliable pK_D value could not be determined. To confirm it was specifically labelling the MOR, **192** was selected for further competition binding assays against naloxone (**6**) and naltrexone (**7**). The observed pK_i values for naloxone (**6**) and naltrexone (**7**) were within the range reported in the literature (see **Figure 3-23**).

4 General discussion and conclusion

A series of fluorescent ligands based on the MOR antagonists naltrexone (**7**) and alvimopan (**9**) were successfully synthesised and evaluated for their MOR binding affinity. Common outcomes were observed in the MOR binding affinities of both β -naltrexamine- and DMHPP-based fluorescent ligands, and the corresponding non-fluorescent congeners, which are discussed below, as well as identification of further pharmacological experimentation necessary to better characterise these ligands. Additionally, opportunities for future projects based on the results of this study are proposed.

4.1 General discussion

Across all tested orthostere and linker combinations, the BODIPY 630/650-containing compounds possessed higher MOR binding affinities than the corresponding sulfo-Cy5 compounds. Of the sulfo-Cy5-containing compounds, only **101** exhibited saturated specific MOR binding at 500 nM, so pK_D values for **104** and **194** could not be determined. The MOR binding affinity of **104** ($pK_D = 7.43$) is similar to the single amino acid congeners (**92a-h**, **98g-h**) ($pK_i = 6.93$ - 7.76) and the unsubstituted β -naltrexamine (**72b**) ($pK_i = 7.30$). A similar trend was found for the sulfo-Cy5 compound **51** synthesised by Schembri *et al.*,⁵⁷ which also had a similar MOR binding affinity to its non-fluorescent congener. The pA_2 value of **51** ($pA_2 = 7.31$ by displacement of DAMGO in MOR-expressing CHO cells) was similar to the pK_i value of the unsubstituted precursor ($pK_i = 6.97$ by displacement of [³H]-diprenorphine in MOR-expressing CHO cell membranes).

In contrast, BODIPY 630/650 attachment to these congeners was beneficial for MOR binding, resulting in significant increases in MOR binding compared to their non-fluorescent congeners. *In silico* modelling of other BODIPY 630/650-containing fluorescent ligands has predicted that the BODIPY 630/650

fluorophore can become embedded in the cellular membrane, benefitting ligand binding through hydrophobic interactions.⁵⁰ This could explain the difference in MOR binding affinity observed between BODIPY 630/650- and sulfo-Cy5-containing compounds in this study, as the hydrophilic sulfo-Cy5 fluorophore would not gain the same benefit from these hydrophobic interactions.

4.2 Further *in vitro* characterisation

Due to significant interruption to laboratory access during the 2020/21 COVID-19 pandemic, there were aspects of this project which could not be completed in full. Further pharmacological investigation of the fluorescent ligands synthesised in this project is required to better understand their properties and applications. Given the promising results displayed by these ligands in the assays undertaken so far, it is anticipated that these subsequent assays will soon be completed.

The non-specific binding profiles of these compounds should be established, particularly for the BODIPY 630/650-containing ligands. The high binding affinities of these compound must be contextualised by establishing to what degree non-specific binding contributes to these values. The non-specific binding values determined in the TR-FRET saturation binding assays, whilst insightful, do not fully express the non-specific binding of the tested compounds. The non-specific binding measured in these assays were based on proximity and alignment with the Lumi4-Tb-tagged receptor, and non-specific binding which occurred further away from a tagged receptor was not reflected in the saturation binding assay results. The non-specific binding profiles of these compounds could be determined through live cell confocal imaging, both with and without an excess of an unlabelled orthosteric competitor. Colocalization of the fluorescent ligands with the fluorescently labelled receptors, and the degree of displacement of the fluorescent ligand by the

competitor, would clarify whether non-specific binding is influential over the obtained binding affinities.

It would also be valuable to establish the receptor subtype selectivity of the fluorescent ligands, which could be achieved by conducting similar saturation binding experiments to those carried out in this study. Fluorescently labelled DOR- and KOR-expressing cell lines would be used, and the non-specific binding curve would be established through coincubation with known DOR and KOR antagonists in place of naloxone (**6**). While high receptor subtype selectivity is not a requirement for these fluorescent ligands to be pharmacologically useful, understanding the selectivity would give clearer guidance for how these fluorescent ligands could be used.

This project specifically aimed to produce fluorescent antagonists for MOR. Given the literature precedent of 6-substituted β -naltrexamine compounds which have retained antagonist activity, and the conserved antagonist profile of the DMHPP orthostere, it is likely that these synthesised fluorescent ligands will remain antagonists of MOR. However, a functional assay will be necessary to confirm this. Antagonism of the fluorescent compounds could be determined by measuring the inhibition of a functional response, such as ERK phosphorylation or cAMP production, when the fluorescent ligand is in competition with a MOR agonist such as DAMGO. Furthermore, it could be useful to carry out similar experiments at DOR and KOR, as some opioid ligands are known to possess mixed functional activities at different ORs.

4.3 Future works

In addition to the characterisation of these synthesised fluorescent compounds, this study could form the foundation for future investigations into fluorescent opioid ligands with optimised physicochemical and receptor binding properties. Further improvements to MOR binding affinity of the β -naltrexamine-based compounds could be developed through modifications to other regions of the morphinan scaffold. In particular, 14-position

modifications provide intriguing possibilities for improvements to binding affinity, while balancing these improvements against changes to ligand function (**Figure 2-14**). As further research is carried out to better establish the SAR of this region, the results could be used to inform better fluorescent ligand design.

While modifications to the 6-position of β -naltrexamine (**72b**) did not yield benefits to MOR binding affinity, the “message-address” concept suggests that the 6-linker region could be investigated for receptor subtype selectivity. The *N*-acetylated single amino acid β -naltrexamine congeners synthesised in this study could form the starting point of such an investigation, from which larger functional groups could be introduced to refine any existing subtype selectivity.

The DMHPP-based fluorescent ligands described in this study display that this orthostere can be fluorescently labelled to produce high affinity fluorescent MOR ligands, but further refinement of these structures may be possible. Fluorescent ligands of the design **189** could not be synthesised due to decomposition of the azidoalanine precursor **187**, possibly via the proposed mechanism described in **Scheme 3-16**. Further investigation is required to confirm the by-products of this reaction and to determine appropriate reaction conditions to synthesise **189**, but it would likely require a significant decrease in reaction concentration and temperature, resulting in a far longer reaction time. Instead, optimisation of the existing fluorescent ligands might be preferable. It is unclear whether the terminal phenylalanine moiety, which had been used as a bioisostere of 1,2,3-triazole, is beneficial for binding. The lack of significant differences in MOR binding affinity between the congeners **170a-h** suggest that that modification of amino acids in the linker beyond the first position are not influential over MOR binding affinity. Therefore, removal or replacement of the phenylalanine, as shown in the designs **198** and **199** (**Figure 4-1**), may result in increased hydrophilicity and better confocal imaging properties, without reducing MOR binding affinity.

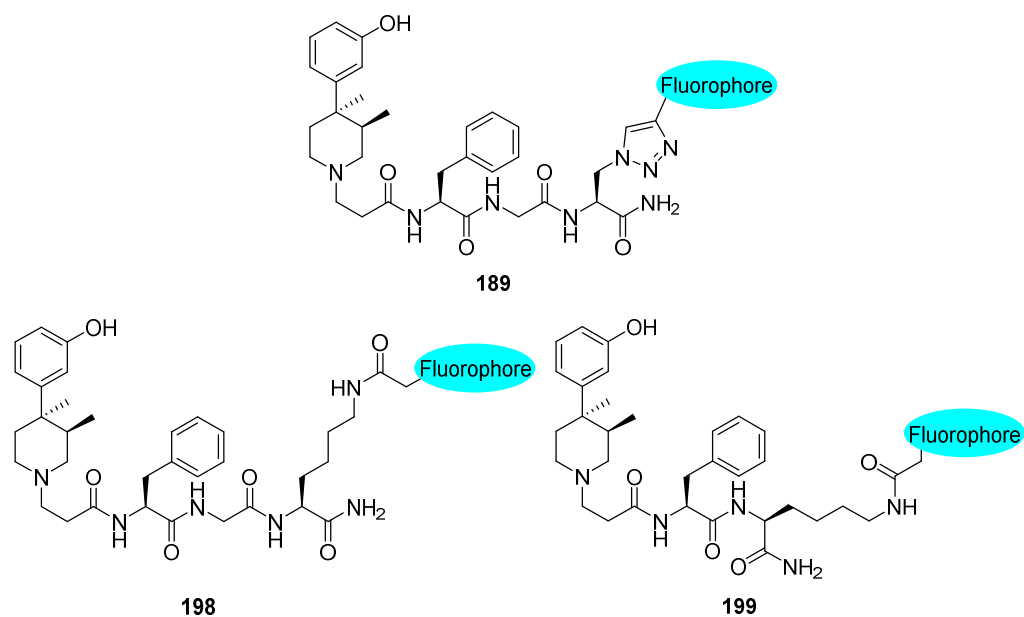
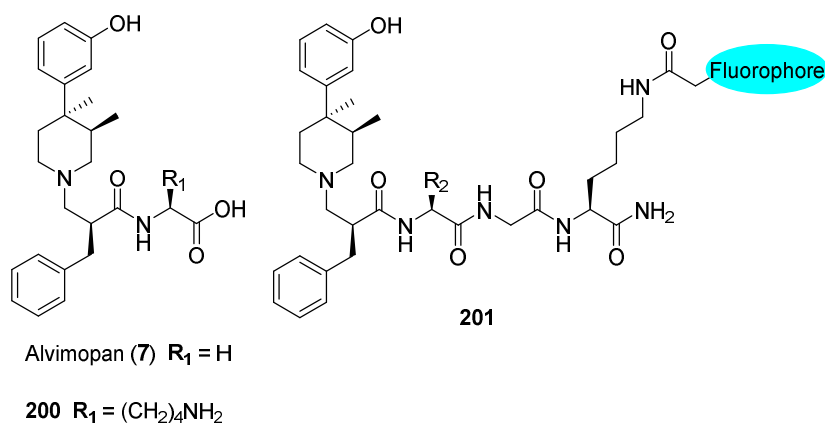


Figure 4-1: The planned DMHPP based ligand design of this project and proposed alternative fluorescent ligand designs.

Fluorescent ligands of the design **189** could not be synthesised due to decomposition of the precursor **187** under reaction conditions. **198** and **199** are proposed as alternative fluorescent ligand designs which could maintain the binding profile of **192**, while potentially increasing hydrophilicity and improving photophysical properties.

Removal of the benzyl group from alvimopan results in a large drop in MOR binding affinity,¹³⁹ but the fluorescent ligands synthesised in this project show that high affinity fluorescent ligands can be produced in the absence of this benzyl group. Reintroduction of the benzyl group could lead to further gains in binding affinity, although the study by Le Bourdonnec *et al.*¹³⁹ demonstrates that substitution of glycine from the structure of alvimopan with other amino acids does not improve MOR binding affinity. However, the lysine congener (**200**) possessed a similar MOR binding affinity to alvimopan (**7**) with greater receptor subtype selectivity (**Figure 4-2**). Incorporation of **7** or **200** into fluorescent ligands of the design **201** could produce fluorescent ligands that possess high binding affinity and selectivity for MOR.



Compound	MOR pK_i	KOR pK_i	DOR pK_i
Alvimopan (7)	9.33	7.00	7.92
200	9.30	6.24	5.82

Figure 4-2: Design for alvimopan-based fluorescent ligands containing a peptidic linker.

Le Bourdonnec *et al.*¹³⁹ identified that replacement of the glycine moiety of alvimopan (**7**) with lysine resulted in a compound (**200**) possessing similar MOR binding affinity to **7** but with greatly improved receptor subtype selectivity. Investigation of fluorescent ligands of the structure **201** could produce fluorescent compounds with high binding affinity and selectivity for MOR, where $R_2 = H$ or $(CH_2)_4NH_2$.

4.4 General conclusions

This project succeeded in synthesising high affinity fluorescent ligands for the MOR containing amino acid-based linkers. Fluorescent ligands composed of a β -naltrexamine (**72b**) orthostere fluorescently labelled with a BODIPY 630/650 fluorophore via an amino acid linker, displayed sub-nanomolar binding affinity for MOR. Additionally, the first fluorescent ligands based on the MOR antagonist alvimopan (**7**) are reported, with two BODIPY 630/650-containing fluorescent ligands displaying high MOR binding affinities.

Although improvement in MOR binding affinity through the introduction of amino acid-based linkers was limited, these fluorescent ligands may possess improved confocal imaging properties from increased hydrophilicity, compared to previously reported high affinity fluorescent MOR ligands. Further

pharmacological evaluation is required to fully assess the receptor subtype selectivity, binding specificity, and imaging properties of these ligands.

5. Experimental

5.1 General chemistry

Chemicals and solvents were purchased from standard commercial suppliers without further purification. Deuterated solvents were purchased from Fisher Scientific UK Ltd and VWR International LLC. Flash column chromatography was performed using Fluorochem silica gel 60A 40-63 μ . Thin-layer chromatography (TLC) was performed using Merck silica gel 60F 254 plates and examination was carried out under UV light (254 nm).

Reactions were monitored by liquid chromatography-mass spectrometry (LCMS) or TLC. Staining was carried out using potassium permanganate, vanillin, ninhydrin and 2,4-dinitrophenylhydrazine (2,4-DNP). Unless otherwise stated, reactions were carried out at room temperature. Organic extracts following aqueous work up procedures were dried using MgSO₄ or Na₂SO₄ before gravity filtration and evaporation. Evaporation of organic solvents was done *in vacuo* at 40°C in a water bath.

LCMS results were collected on a Shimadzu UFLCXR HPLC system with an Applied Biosystems MDS SCIEX API2000 electrospray ionisation mass spectrometer. The coupled column was a Phenomenex Gemini-NX 3 μ m-110 Å C18, 50x2mm column thermostated at 40°C. The flow rate was 0.5 mL/min and the UV detection was at 220 nm and 254 nm. The eluent used was a MeCN/H₂O mix containing 0.1% formic acid at a gradient of 1:19 to 19:1 (v/v) over 5 minutes.

High resolution mass spectrometry (HRMS) time of flight, electrospray (TOF ES +/-) were recorded on a Waters 2795 separation module/micromass LCT platform.

Specific rotation was measured using a Bellingham + Stanley Ltd ADP220 Polarimeter with a 1 ml sample tube with a 0.5 dm pathway length. $[\alpha]_D^T$ was calculated using the following equation:

$$[\alpha]_D^T = \frac{100 \times \alpha}{l \times c}$$

Where α = measured rotation in degrees. l = length of the pathway in decimetres. c = concentration in g/ml. T = temperature at which the measurement was taken (Celsius).

$^1\text{H-NMR}$ spectra were recorded on a Bruker-AV 400 at 400.13 MHz and $^{13}\text{C-NMR}$ was recorded at 101.62 MHz. Chemical shifts (δ) were recorded in ppm with reference to the chemical shift from the deuterated solvent. Coupling constants (J) were recorded in Hz.

Analytical HPLC was performed using either system 1 or 2 to confirm purity.

System 1: Phenomenex Gemini reverse phase 5 μm C_{18} column (250 x 4.6 mm), a flow rate of 1.00 mL/min and UV detection at 214 and 254 nm. Linear gradient 5% - 95% solvent B over 30 minutes. Solvent A: 0.1% formic acid (FA) in water; Solvent B: 0.1% FA in MeCN.

System 2: Phenomenex Gemini reverse phase 5 μm C_{18} column (250 x 4.6 mm), a flow rate of 1.00 mL/min and UV detection at 214 and 254 nm. Linear gradient 5% - 95% solvent B over 30 minutes. Solvent A: water; Solvent B: MeOH.

Semi-preparative HPLC was performed using either system 3 or 4.

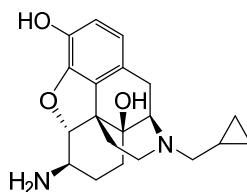
System 3: Phenomenex Gemini reverse phase 5 μm C_{18} column (250 x 10 mm), a flow rate of 5.00 mL/min and UV detection at 214 and 254 nm. Linear gradient 5% - 95% solvent B over 30 minutes. Solvent A: 0.1% formic acid (FA) in water; Solvent B: 0.1% FA in MeCN.

System 4: Phenomenex Gemini reverse phase 5 μm C_{18} column (250 x 10 mm), a flow rate of 5.00 mL/min and UV detection at 214 and 254 nm. Linear gradient 5% - 95% solvent B over 30 minutes. Solvent A: water; Solvent B: MeOH.

Chirally-selective HPLC (analytical and semi-preparative) was performed using either system 5 (analytical) or 6 (semi-preparative).

System 5: Phenomenex Lux 3 μm Cellulose-1 column (250 x 4.6 mm), a flow rate of 1.00 mL/min and UV detection at 214 and 254 nm. Isocratic 1% solvent B over 10 minutes. Solvent A: n-Hexane; Solvent B: EtOH.

System 6: Phenomenex Lux 5 μm Cellulose-1 column (250 x 10 mm), a flow rate of 5.00 mL/min and UV detection at 214 and 254 nm. Isocratic 1% solvent B over 10 minutes. Solvent A: n-Hexane; Solvent B: EtOH.



(4R,4aS,7R,7aR,12bS)-7-amino-3-(cyclopropylmethyl)-1,2,3,4,5,6,7,7a-octahydro-4aH-4,12-methanobenzofuro[3,2-e]isoquinoline-4a,9-diol (72b)

Naltrexone (**7**) (100 mg, 0.29 mmol, 1.0 eq) and ammonium acetate (224 mg, 2.90 mmol, 10.0 eq) were dissolved in dry MeOH (5 ml) under N_2 and stirred at room temperature for 30 min. A solution of sodium cyanoborohydride (20 mg, 0.32 mmol, 1.2 eq) in MeOH (2 ml) was added dropwise to the reaction mixture and stirred at room temperature for 2 hr. The reaction mixture was then diluted with water (50 ml) and the pH adjusted to 9 using 1M NaOH. It was then extracted with chloroform (3 x 20 ml) and the combined organic extracts were dried over MgSO_4 . The solvent was evaporated *in vacuo* and column chromatography (1-5% 1M NH_4OH in $\text{MeOH}/\text{CH}_2\text{Cl}_2$) afforded **72b** as a yellow oil (25 mg, 25%).

$[\alpha]_{\text{D}}^{19}$: -131.9 (H_2O , c 1.00)

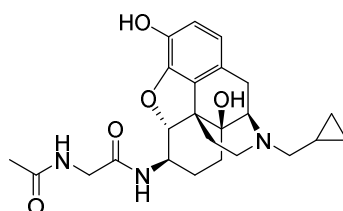
^1H NMR (MeOD): δ 0.09 – 0.22 (m, 2H, cyclopropyl 2- CH_2 and 3- CH_2), 0.47 – 0.60 (m, 2H, cyclopropyl 2- CH_2 and 3- CH_2), 0.82 – 0.95 (m, 1H, cyclopropyl 1-CH), 1.34 – 1.45 (m, 2H, 8- CH_2 , 15- CH_2), 1.49 – 1.60 (m, 2H, 7- CH_2 , 8- CH_2), 1.79 (td, J = 12.9, 10.3 Hz, 1H, 7- CH_2), 2.14 (td, J = 10.0, 3.2 Hz, 1H, 16- CH_2), 2.22 (td, J = 12.0, 4.3 Hz, 1H, 15- CH_2), 2.38 (dd, J = 12.1, 5.9 Hz, 1H, N- CH_2 - C_3H_5), 2.42 (dd, J = 12.1, 6.0 Hz, 1H, N- CH_2 - C_3H_5), 2.51 (ddd, J = 12.1, 7.3, 4.4 Hz, 1H, 6-CH), 2.63 (td, J = 12.4, 6.0 Hz, 1H, 16- CH_2), 2.63 – 2.69 (m, 1H, 10- CH_2), 3.06 (d, J =

18.4 Hz, 1H, 10-CH₂), 3.10 (d, *J* = 5.7 Hz, 1H, 9-CH), 4.22 (d, *J* = 7.3 Hz, 1H, 5-CH), 6.54 (d, *J* = 8.1 Hz, 1H, 1-CH), 6.61 (d, *J* = 8.0 Hz, 1H, 2-CH)

¹³C NMR (MeOD): δ 3.9, 4.1, 9.6, 18.6, 22.7, 25.7, 30.7, 31.0, 44.1, 47.5, 53.5, 59.3, 62.4, 70.5, 97.4, 118.6, 119.6, 123.1, 131.2, 141.0, 141.7.

General procedure 1 – amide coupling of β-naltrexamine and *N*-acetylated amino acid

Amino acid (0.06 mmol) and HBTU (22 mg, 0.06 mmol, 1.0 eq) were dissolved in DMF (2.5 mL). DIPEA (10.5 μL, 0.06 mmol, 1.0 eq) was added and the reaction mixture was stirred for 20 minutes. β-naltrexamine (20 mg, 0.06 mmol, 1.0 eq) was separately dissolved in DMF (2.5 mL) and added dropwise to the main reaction mixture. The reaction mixture was stirred for two hours. The solvent was removed under high vacuum and the residue was purified by column chromatography (1:19 MeOH: CH₂Cl₂). Where necessary, further purification was carried out using reverse phase HPLC (system 4).



2-Acetamido-*N*-((4*R*,4*aS*,7*R*,7*aR*,12*bS*)-3-(cyclopropylmethyl)-4*a*,9-dihydroxy-2,3,4,4*a*,5,6,7,7*a*-octahydro-1*H*-4,12-methanobenzofuro[3,2-*e*]isoquinolin-7-yl)acetamide (92a)

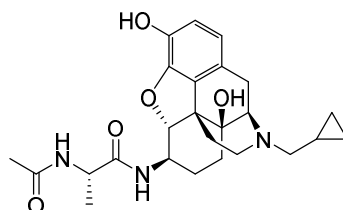
The title compound was synthesised as described in general procedure 1, using *N*-acetyl-glycine (7 mg, 0.06 mmol) to give **92a**, a white solid (19 mg, 73%).

¹H NMR (MeOD): δ 0.25 (d, *J* = 4.9 Hz, 2H, cyclopropyl 2-CH₂ and 3-CH₂), 0.60 (p, *J* = 9.3 Hz, 2H, cyclopropyl 2-CH₂ and 3-CH₂), 0.93 (h, *J* = 8.7, 7.9 Hz, 1H, cyclopropyl 1-CH), 1.42-1.53 (m, 2H, 8-CH₂ and 15-CH₂), 1.55-1.64 (m, 2H, 7-CH₂ and 8-CH₂), 1.86 (qd, *J* = 13.5, 12.5, 3.9 Hz, 1H, 7-CH₂), 2.23-2.39 (m, 2H, 15-CH₂ and 16-CH₂), 2.46-2.56 (m, 1H, N-CH₂-C₃H₅), 2.60-2.84 (m, 3H, 10-CH₂

and 16-CH₂ and N-CH₂-C₃H₅), 3.15 (d, *J* = 18.5 Hz, 1H, 10-CH₂), f3.69 (ddd, *J* = 12.4, 7.7, 4.5 Hz, 1H, 6-CH), 3.85 (d, *J* = 1.5 Hz, 2H, glycine-CH₂), 4.48 (d, *J* = 7.7 Hz, 1H, 5-CH), 6.60 (d, *J* = 8.2 Hz, 1H, 2-CH), 6.65 (d, *J* = 8.1 Hz, 1H, 1-CH).

¹³C NMR (MeOD): δ 2.6, 3.5, 13.1, 19.5, 21.1, 22.4, 23.8, 29.7, 42.3, 48.5, 51.3, 58.5, 60.1, 62.5, 70.2, 91.4, 117.4, 118.9, 140.7, 142.3, 170.0, 172.5.

m/z: HRMS C₂₄H₃₁N₃O₅ [MH]⁺ calcd 442.2336; found 442.2341



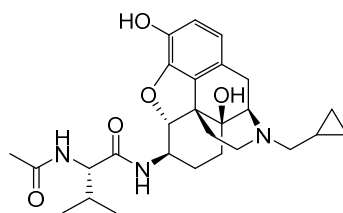
(S)-2-Acetamido-N-((4R,4aS,7R,7aR,12bS)-3-(cyclopropylmethyl)-4a,9-dihydroxy-2,3,4,4a,5,6,7,7a-octahydro-1H-4,12-methanobenzofuro[3,2-e]isoquinolin-7-yl)propanamide (92b)

The title compound was synthesised as described in general procedure 1, using *N*-acetyl-*L*-alanine (8 mg, 0.06 mmol) to give **92b**, a white solid (20 mg, 74%).

¹H NMR (DMSO-*d*₆): δ 0.05-0.07 (m, 2H, cyclopropyl 2-CH₂ and 3-CH₂), 0.29-0.45 (m, 2H, cyclopropyl 2-CH₂ and 3-CH₂), 0.67-0.82 (m, H, cyclopropyl 1-CH), 1.07 (d, *J* = 7.1 Hz, 3H, alanine CH₃), 1.10 – 1.21 (m, 2H, 8-CH₂ and 15-CH₂), 1.28 – 1.40 (m, 2H, 7-CH₂ and 8-CH₂), 1.55 (qd, *J* = 12.7, 2.5 Hz, 1H, 7-CH₂), 1.75 (s, 3H, acetyl CH₃), 1.87 (td, *J* = 12.0, 3.8 Hz, 1H, 16-CH₂), 2.03 (td, *J* = 12.3, 5.0 Hz, 1H, 15-CH₂), 2.17 – 2.29 (m, 2H, N-CH₂-C₃H₅), 2.51 – 2.59 (m, 1H, 10-CH₂), 2.55 – 2.62 (m, 1H, 16-CH₂), 2.86 (d, *J* = 18.4 Hz, 1H, 10-CH₂), 2.90 (d, *J* = 5.6 Hz, 1H, 9-CH), 4.19 (p, *J* = 7.2 Hz, 1H, alanine α-CH), 4.37 (d, *J* = 7.7 Hz, 1H, 5-CH), 6.42 (d, *J* = 8.1 Hz, 1H, 1-CH), 6.48 (d, *J* = 8.0 Hz, 1H, 2-CH), 7.91 (d, *J* = 8.2 Hz, 1H, acetamide NH), 8.04 (d, *J* = 7.9 Hz, 1H, 6-NH), 8.27 (s, 1H, 3-OH).

¹³C NMR (DMSO-*d*₆): δ 3.5, 3.7, 9.3, 19.0, 22.2, 22.7, 24.3, 29.8, 30.4, 43.7, 47.0, 47.8, 51.1, 58.4, 61.7, 69.6, 90.5, 117.0, 118.4, 123.5, 131.3, 140.4, 142.1, 168.8, 172.0.

m/z: HRMS C₂₅H₃₃N₃O₅ [MH]⁺ calcd 456.2493; found 456.2493



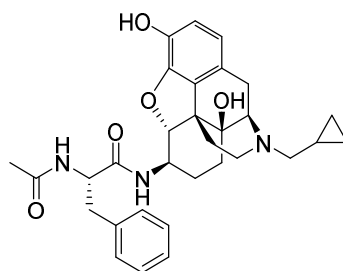
(S)-2-Acetamido-N-((4R,4aS,7R,7aR,12bS)-3-(cyclopropylmethyl)-4a,9-dihydroxy-2,3,4,4a,5,6,7,7a-octahydro-1H-4,12-methanobenzofuro[3,2-e]isoquinolin-7-yl)-3-methylbutanamide (92c)

The title compound was synthesised as described in general procedure 1, using *N*-acetyl-*L*-valine (10 mg, 0.06 mmol) to give **92c**, a white solid (16 mg, 55%).

^1H NMR (DMSO- d_6): δ 0.07 – 0.17 (m, 2H, cyclopropyl 2-CH₂ and 3-CH₂), 0.40 – 0.54 (m, 2H, cyclopropyl 2-CH₂ and 3-CH₂), 0.82 (dd, J = 8.4, 6.8 Hz, 6H, valine CH(CH₃)₂), 0.78 – 0.91 (m, 1H, cyclopropyl 1-CH), 1.24 (dd, J = 11.6, 2.8 Hz, 1H, 15-CH₂), 1.26 (td, J = 13.8, 3.0 Hz, 1H, 8-CH₂), 1.42 (dt, J = 13.5, 3.3 Hz, 1H, 8-CH₂), 1.48 - 1.57 (m, 1H, 7-CH₂), 1.64 (qd, J = 13.0, 2.8 Hz, 1H, 7-CH₂), 1.82 – 1.93 (m, 1H, valine CH(CH₃)₂), 1.88 (s, 3H, acetyl CH₃), 1.98 (td, J = 11.9, 3.7 Hz, 1H, 16-CH₂), 2.13 (td, J = 12.4, 5.0 Hz, 1H, 15-CH₂), 2.28 – 2.42 (m, 2H, N-CH₂-C₃H₅), 2.51 – 2.59 (m, 1H, 10-CH₂), 2.60 (dd, J = 7.2, 4.1 Hz, 1H, 16-CH₂), 2.97 (d, J = 18.4 Hz, 1H, 10-CH₂), 3.02 (d, J = 5.5 Hz, 1H, 9-CH₂), 3.35 – 3.48 (m, 1H, 6-CH), 4.18 (dd, J = 9.3, 6.9 Hz, 1H, valine α -CH), 4.46 (d, J = 7.8 Hz, 1H, 5-CH), 6.52 (d, J = 8.1 Hz, 1H, 1-CH), 6.58 (d, J = 8.1 Hz, 1H, 2-CH), 7.86 (d, J = 9.3 Hz, 1H, acetamide NH), 8.22 (s, 1H, 3-OH), 8.26 (d, J = 7.8 Hz, 1H, 6-NH).

^{13}C NMR (DMSO- d_6): δ 4.0, 4.2, 9.6, 18.7, 19.5, 22.6, 23.0, 24.8, 30.3, 30.7, 31.6, 44.3, 47.4, 1.6, 57.6, 58.8, 62.2, 70.0, 90.9, 117.5, 118.9, 123.8, 131.7, 140.9, 142.5, 169.6, 171.0.

m/z : HRMS C₂₇H₃₇N₃O₅ [MH]⁺ calcd 484.2806; found 484.2815



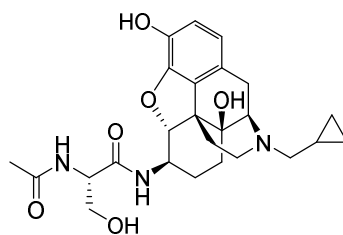
(S)-2-Acetamido-N-((4R,4aS,7R,7aR,12bS)-3-(cyclopropylmethyl)-4a,9-dihydroxy-2,3,4,4a,5,6,7,7a-octahydro-1H-4,12-methanobenzofuro[3,2-e]isoquinolin-7-yl)-3-phenylpropanamide (92d)

The title compound was synthesised as described in general procedure 1, using *N*-acetyl-*L*-phenylalanine (12 mg, 0.06 mmol) to give **92d**, a white solid (20 mg, 63%).

^1H NMR (DMSO- d_6): δ 0.13 (d, $J = 4.9$ Hz, 2H, cyclopropyl 2- CH_2 and 3- CH_2), 0.35 – 0.63 (m, 2H, cyclopropyl 2- CH_2 and 3- CH_2), 0.74 – 0.97 (m, 1H, cyclopropyl 1-CH), 1.18 – 1.30 (m, 2H, 8- CH_2 and 15- CH_2), 1.33 – 1.44 (m, 2H, 7- CH_2 and 8- CH_2), 1.49 (td, $J = 12.6, 2.7$ Hz, 1H, 7- CH_2), 1.79 (s, 3H, acetyl CH_3), 2.00 (td, $J = 12.2, 3.9$ Hz, 1H, 16- CH_2), 2.14 (td, $J = 12.5, 5.1$ Hz, 1H, 15- CH_2), 2.29 – 2.46 (m, 2H, $\text{N-CH}_2\text{-C}_3\text{H}_5$), 2.53 – 2.67 (m, 1H, 16- CH_2), 2.73 (dd, $J = 13.5, 8.9$ Hz, 1H, phenylalanine CH_2), 2.92 (dd, $J = 13.5, 5.6$ Hz, 1H, phenylalanine CH_2), 2.98 (d, $J = 18.4$ Hz, 1H, 10- CH_2), 3.05 (d, $J = 5.5$ Hz, 1H, 9-CH), 3.38 – 3.45 (m, 1H, 6-CH), 4.45 (d, $J = 7.7$ Hz, 1H, 5-CH), 4.51 (td, $J = 8.8, 5.7$ Hz, 1H, phenylalanine $\alpha\text{-CH}$), 6.53 (d, $J = 8.1$ Hz, 1H, 1-CH), 6.59 (d, $J = 8.0$ Hz, 1H, 2-CH), 7.15 – 7.31 (m, 5H, phenylalanine aromatic protons), 8.10 (d, $J = 8.7$ Hz, 1H, acetamide NH), 8.17 (s, 1H, 3-OH), 8.26 (d, $J = 8.0$ Hz, 1H, 6-NH).

^{13}C NMR (DMSO- d_6): δ 3.5, 3.8, 9.0, 22.2, 22.6, 24.1, 29.7, 30.2, 38.6, 43.9, 46.9, 51.1, 53.8, 58.3, 61.7, 69.6, 90.4, 117.1, 118.5, 123.3, 126.2, 128.0, 129.2, 131.2, 137.8, 140.4, 142.0, 168.9, 170.6.

m/z : HRMS $\text{C}_{31}\text{H}_{37}\text{N}_3\text{O}_5$ $[\text{MH}]^+$ calcd 532.2806; found 532.2810



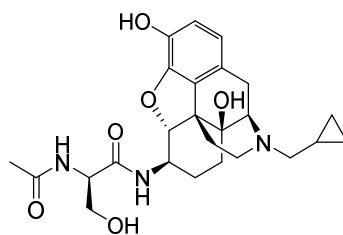
(S)-2-Acetamido-N-((4R,4aS,7R,7aR,12bS)-3-(cyclopropylmethyl)-4a,9-dihydroxy-2,3,4,4a,5,6,7,7a-octahydro-1H-4,12-methanobenzofuro[3,2-e]isoquinolin-7-yl)-3-hydroxypropanamide (92e)

The title compound was synthesised as described in general procedure 1, using *N*-acetyl-*L*-serine (9 mg, 0.06 mmol) to give **92e**, a white solid (12 mg, 43%).

^1H NMR (DMSO- d_6): δ 0.04 – 0.21 (m, 2H, cyclopropyl 2- CH_2 and 3- CH_2), 0.41 – 0.51 (m, 2H, cyclopropyl 2- CH_2 and 3- CH_2), 0.75 – 0.92 (m, 1H, cyclopropyl 1-CH), 1.17 – 1.30 (m, 2H, 8- CH_2 and 15- CH_2), 1.41 (dt, $J = 13.2, 3.3$ Hz, 1H, 8- CH_2), 1.49 (dq, $J = 12.5, 3.6$ Hz, 1H, 7- CH_2), 1.66 (qd, $J = 12.9, 2.9$ Hz, 1H, 7- CH_2), 1.88 (s, 3H, acetyl CH_3), 1.98 (td, $J = 12.0, 3.7$ Hz, 1H, 16- CH_2), 2.14 (td, $J = 12.4, 5.1$ Hz, 1H, 15- CH_2), 2.33 (h, $J = 6.1$ Hz, 2H, N- CH_2 - C_3H_5), 2.59 (td, $J = 11.5, 5.2$ Hz, 1H, 16- CH_2), 2.96 (d, $J = 18.3$ Hz, 1H, 10- CH_2), 3.01 (d, $J = 5.6$ Hz, 1H, 9-CH), 3.38 – 3.58 (m, 1H, 6-CH), 3.51 (dd, $J = 5.9, 2.2$ Hz, 2H, serine CH_2), 4.30 (dt, $J = 8.5, 5.9$ Hz, 1H, serine α -CH), 4.52 (d, $J = 7.6$ Hz, 1H, 5-CH), 6.52 (d, $J = 8.1$ Hz, 1H, 1-CH), 6.58 (d, $J = 8.0$ Hz, 1H, 2-CH), 7.86 (d, $J = 8.4$ Hz, 1H, acetamide NH), 8.15 (d, $J = 8.1$ Hz, 1H, 6-NH), 8.26 (s, 1H, 3-OH).

^{13}C NMR (DMSO- d_6): δ 3.5, 3.7, 9.2, 22.1, 22.7, 24.4, 29.8, 30.4, 43.7, 47.0, 51.2, 54.8, 58.4, 61.7, 62.1, 69.6, 90.5, 117.0, 118.4, 123.4, 131.3, 140.4, 142.1, 169.2, 169.7.

m/z : HRMS $\text{C}_{25}\text{H}_{33}\text{N}_3\text{O}_6$ $[\text{MH}]^+$ calcd 472.2442; found 472.2440



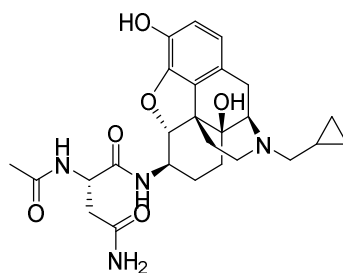
(R)-2-Acetamido-N-((4R,4aS,7R,7aR,12bS)-3-(cyclopropylmethyl)-4a,9-dihydroxy-2,3,4,4a,5,6,7,7a-octahydro-1H-4,12-methanobenzofuro[3,2-e]isoquinolin-7-yl)-3-hydroxypropanamide (98e)

The title compound was synthesised as described in general procedure 1, using *N*-acetyl-*L*-serine (9 mg, 0.06 mmol) to give **98e** (a white solid) as a biproduct of **92e** (7 mg, 25%).

^1H NMR (DMSO- d_6): δ 0.06 – 0.17 (m, 2H, cyclopropyl 2-CH₂ and 3-CH₂), 0.42 – 0.53 (m, 2H, cyclopropyl 2-CH₂ and 3-CH₂), 0.79 – 0.91 (m, 1H, cyclopropyl 1-CH), 1.18 – 1.33 (m, 2H, 8-CH₂ and 15-CH₂), 1.38 – 1.49 (m, 2H, 7-CH₂ and 8-CH₂), 1.72 (qd, J = 13.1, 3.3 Hz, 1H, 7-CH₂), 1.90 (s, 3H, acetyl CH₃), 1.97 (td, J = 12.0, 3.7 Hz, 1H, 16-CH₂), 2.13 (td, J = 12.5, 5.1 Hz, 1H, 15-CH₂), 2.32 (h, J = 6.1 Hz, 2H, N-CH₂-C₃H₅), 2.58 (td, J = 12.3, 5.5 Hz, 1H, 16-CH₂), 2.96 (d, J = 18.3 Hz, 1H, 10-CH₂), 3.01 (d, J = 5.6 Hz, 1H, 9-CH), 3.39 – 3.59 (m, 1H, 6-CH), 3.56 (d, J = 5.4 Hz, 2H, serine CH₂), 4.23 (dt, J = 8.4, 5.4 Hz, 1H, serine α -CH), 4.53 (d, J = 7.6 Hz, 1H, 5-CH), 6.51 (d, J = 8.1 Hz, 1H, 1-CH), 6.57 (d, J = 8.0 Hz, 1H, 2-CH), 7.87 (d, J = 8.4 Hz, 1H, acetamide NH), 8.08 (d, J = 8.4 Hz, 1H, 6-NH), 8.37 (s, 1H, 3-OH).

^{13}C NMR (DMSO- d_6): δ 3.5, 3.7, 9.2, 22.1, 22.8, 24.5, 29.9, 30.4, 43.7, 47.0, 51.2, 55.4, 58.4, 61.7, 61.8, 69.6, 90.6, 117.0, 118.3, 123.4, 131.3, 140.4, 142.1, 169.4, 169.9.

m/z : HRMS C₂₅H₃₃N₃O₆ [MH]⁺ calcd 472.2442; found 472.2443



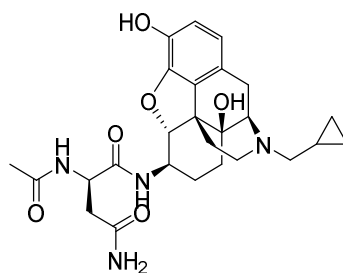
(S)-2-Acetamido-*N*¹-((4*R*,4*aS*,7*R*,7*aR*,12*bS*)-3-(cyclopropylmethyl)-4*a*,9-dihydroxy-2,3,4,4*a*,5,6,7,7*a*-octahydro-1*H*-4,12-methanobenzofuro[3,2-*e*]isoquinolin-7-yl)succinimide (92f)

The title compound was synthesised as described in general procedure 1, using *N*-acetyl-*L*-asparagine (10 mg, 0.06 mmol) to give **92f**, a white solid (13 mg, 44%).

¹H NMR (DMSO-*d*₆): δ 0.05 – 0.20 (m, 2H, cyclopropyl 2-CH₂ and 3-CH₂), 0.40 – 0.58 (m, 2H, cyclopropyl 2-CH₂ and 3-CH₂), 0.74 – 0.94 (m, 1H, cyclopropyl 1-CH), 1.17 – 1.32 (m, 2H, 8-CH₂ and 15-CH₂), 1.37 – 1.48 (m, 2H, 7-CH₂ and 8-CH₂), 1.71 (td, *J* = 13.1, 12.6, 10.0 Hz, 1H, 7-CH₂), 1.87 (s, 3H, acetyl CH₃), 1.97 (td, *J* = 12.0, 3.7 Hz, 1H, 16-CH₂), 2.13 (td, *J* = 12.4, 5.1 Hz, 1H, 15-CH₂), 2.32 (dd, *J* = 12.7, 6.5 Hz, 1H, N-CH₂-C₃H₅), 2.36 (dd, *J* = 12.7, 6.5 Hz, 1H, N-CH₂-C₃H₅), 2.39 (dd, *J* = 15.4, 8.1 Hz, 1H, asparagine CH₂), 2.46 (dd, *J* = 15.4, 4.8 Hz, 1H, asparagine CH₂), 2.59 (td, *J* = 12.6, 12.0, 5.0 Hz, 1H, 16-CH₂), 2.96 (d, *J* = 18.4 Hz, 1H, 10-CH₂), 3.01 (d, *J* = 5.6 Hz, 1H, 9-CH), 3.35 – 3.46 (m, 1H, 6-CH), 4.50 (td, *J* = 8.2, 4.8 Hz, 1H, asparagine α-CH), 4.55 (d, *J* = 7.7 Hz, 1H, 5-CH), 6.51 (d, *J* = 8.0 Hz, 1H, 1-CH), 6.57 (d, *J* = 8.1 Hz, 1H, 2-CH), 6.85 (s, 1H, asparagine CONH₂), 7.27 (s, 1H, asparagine CONH₂), 7.94 (d, *J* = 8.4 Hz, 1H, acetamide NH), 8.03 (d, *J* = 8.4 Hz, 1H, 6-NH), 8.31 (s, 1H, 3-OH).

¹³C NMR (DMSO-*d*₆): δ 3.5, 3.7, 9.2, 22.1, 22.9, 24.4, 29.9, 30.4, 37.5, 43.7, 47.0, 49.8, 51.3, 58.4, 61.7, 69.6, 90.5, 117.0, 118.3, 123.4, 131.3, 140.4, 142.1, 169.1, 170.9, 171.6.

m/z: HRMS C₂₆H₃₄N₄O₆ [MH]⁺ calcd 499.2551; found 499.2551



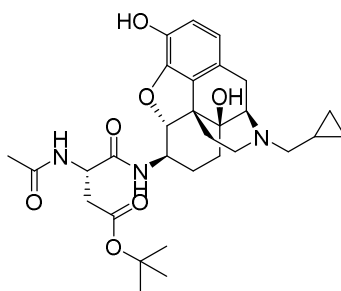
(S)-2-Acetamido-*N*¹-((4*R*,4*aS*,7*R*,7*aR*,12*bS*)-3-(cyclopropylmethyl)-4*a*,9-dihydroxy-2,3,4,4*a*,5,6,7,7*a*-octahydro-1*H*-4,12-methanobenzofuro[3,2-*e*]isoquinolin-7-yl)succinimide (98f)

The title compound was synthesised as described in general procedure 1, using *N*-acetyl-*L*-asparagine (10 mg, 0.06 mmol) to give **98f** (a white solid) as a biproduct of **92f** (8 mg, 27%).

¹H NMR (DMSO-*d*₆): δ 0.08 – 0.19 (m, 2H, cyclopropyl 2-CH₂ and 3-CH₂), 0.42 – 0.54 (m, 2H, cyclopropyl 2-CH₂ and 3-CH₂), 0.75 – 0.92 (m, 1H, cyclopropyl 1-CH), 1.20 – 1.30 (m, 2H, 8-CH₂ and 15-CH₂), 1.37 – 1.50 (m, 2H, 7-CH₂ and 8-CH₂), 1.67 (qd, *J* = 14.0, 13.5, 3.4 Hz, 1H, 7-CH₂), 1.85 (s, 3H, acetyl CH₃), 1.99 (td, *J* = 12.1, 3.8 Hz, 1H, 16-CH₂), 2.14 (td, *J* = 12.4, 5.0 Hz, 1H, 15-CH₂), 2.31 (dd, *J* = 15.1, 8.2 Hz, 1H, N-CH₂-C₃H₅), 2.31 – 2.43 (m, 2H, N-CH₂-C₃H₅ and asparagine CH₂), 2.46 (dd, *J* = 15.1, 5.8 Hz, 1H, asparagine CH₂), 2.59 (td, 18.4, 5.7 Hz, 1H, 16-CH₂), 2.98 (d, *J* = 18.4 Hz, 1H, 10-CH₂), 3.04 (d, *J* = 5.6 Hz, 1H, 9-CH), 3.37 – 3.45 (m, 1H, 6-CH), 4.54 (d, *J* = 7.6 Hz, 1H, 5-CH), 4.57 (td, *J* = 8.3, 5.8 Hz, 1H, asparagine α-CH), 6.52 (d, *J* = 8.1 Hz, 1H, 1-CH), 6.59 (d, *J* = 8.0 Hz, 1H, 2-CH), 6.85 (s, 1H, asparagine CONH₂), 7.24 (s, 1H, asparagine CONH₂), 7.99 (d, *J* = 8.4 Hz, 1H, acetamide NH), 8.09 (d, *J* = 8.1 Hz, 1H, 6-NH), 8.20 (s, 1H, 3-OH).

¹³C NMR (DMSO-*d*₆): δ 3.5, 3.8, 9.1, 22.2, 22.8, 24.1, 29.8, 30.3, 38.1, 43.9, 46.9, 49.7, 51.3, 58.3, 61.7, 69.6, 90.4, 117.1, 118.4, 123.4, 131.2, 140.4, 142.1, 169.1, 170.8, 171.3.

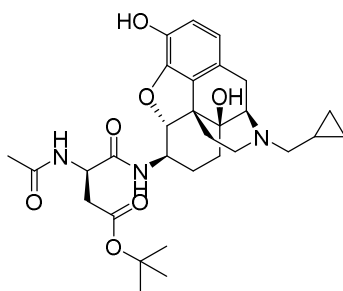
m/z: HRMS C₂₆H₃₄N₄O₆ [MH]⁺ calcd 499.2551; found 499.2554



***tert*-Butyl (S)-3-acetamido-4-(((4R,4aS,7R,7aR,12bS)-3-(cyclopropylmethyl)-4a,9-dihydroxy-2,3,4,4a,5,6,7,7a-octahydro-1H-4,12-methanobenzofuro[3,2-e]isoquinolin-7-yl)amino)-4-oxobutanoate (95g)**

The title compound was synthesised as described in general procedure 1, using *N*-acetyl-*L*-aspartic acid 4-*tert*-butyl ester (14 mg, 0.06 mmol) to give **95g**, a white solid (13 mg, 39%).

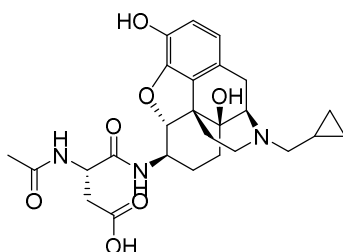
¹H NMR (MeOD): δ 0.42 – 0.57 (m, 2H, cyclopropyl 2-CH₂ and 3-CH₂), 0.68 – 0.87 (m, 2H, cyclopropyl 2-CH₂ and 3-CH₂), 1.02 – 1.16 (m, 1H, cyclopropyl 1-CH), 1.46 (s, 9H, *t*-Bu CH₃), 1.51 – 1.68 (m, 3H, 7-CH₂, 8-CH₂, 15-CH₂), 1.71 (dt, *J* = 13.8, 3.1 Hz, 1H, 8-CH₂), 1.94 (qd, *J* = 12.9, 2.8 Hz, 1H, 7-CH₂), 1.99 (s, 3H, acetyl CH₃), 2.48 – 2.66 (m, 1H, 16-CH₂), 2.60 (dd, *J* = 16.3, 8.5 Hz, 1H, aspartate CH₂), 2.69 (td, *J* = 12.6, 3.7 Hz, 1H, 15-CH₂), 2.78 (dd, *J* = 16.3, 5.3 Hz, 1H, aspartate CH₂), 2.86 (dd, *J* = 13.5, 7.5 Hz, 1H, N-CH₂-C₃H₅), 3.08 (dd, *J* = 12.5, 4.3 Hz, 1H, 16-CH₂), 3.14 (dd, *J* = 19.5, 6.0 Hz, 1H, 10-CH₂), 3.30 – 3.40 (m, 2H, 10-CH₂, N-CH₂-C₃H₅), 3.60 (ddd, *J* = 12.7, 7.8, 5.0 Hz, 1H, 6-CH), 3.89 (d, *J* = 5.7 Hz, 1H, 9-CH), 4.62 (d, *J* = 7.9 Hz, 1H, 5-CH), 4.70 (dd, *J* = 8.4, 5.4 Hz, 1H, aspartate α-CH), 6.71 (d, *J* = 8.3 Hz, 1H, 1-CH), 6.74 (d, *J* = 8.3 Hz, 1H, 2-CH).



***tert*-Butyl (*R*)-3-acetamido-4-(((*4R,4aS,7R,7aR,12bS*)-3-(cyclopropylmethyl)-4a,9-dihydroxy-2,3,4,4a,5,6,7,7a-octahydro-1*H*-4,12-methanobenzofuro[3,2-*e*]isoquinolin-7-yl)amino)-4-oxobutanoate (**95d**)**

The title compound was synthesised as described in general procedure 1, using *N*-acetyl-*L*-aspartic acid 4-*tert*-butyl ester (14 mg, 0.06 mmol) to give **95d** (a white solid) as a biproduct of **95g** (10 mg, 30%).

¹H NMR (MeOD): δ 0.40 – 0.57 (m, 2H, cyclopropyl 2-CH₂ and 3-CH₂), 0.63 – 0.91 (m, 2H, cyclopropyl 2-CH₂ and 3-CH₂), 1.02 – 1.15 (m, 1H, cyclopropyl 1-CH), 1.44 (s, 9H, *t*-Bu CH₃), 1.51 – 1.67 (m, 3H, 7-CH₂, 8-CH₂, 15-CH₂), 1.70 (dt, *J* = 13.8, 3.1 Hz, 1H, 8-CH₂), 1.92 (qd, *J* = 12.9, 2.8 Hz, 1H, 7-CH₂), 2.01 (s, 3H, acetyl CH₃), 2.48 – 2.66 (m, 1H, 16-CH₂), 2.55 (dd, *J* = 16.0, 7.7 Hz, 1H, aspartate CH₂), 2.68 (td, *J* = 12.5, 3.5 Hz, 1H, 15-CH₂), 2.77 (dd, *J* = 16.1, 6.4 Hz, 1H, aspartate CH₂), 2.85 (dd, *J* = 13.5, 7.5 Hz, 1H, N-CH₂-C₃H₅), 3.01 – 3.18 (m, 2H, 10-CH₂, 16-CH₂), 3.34 – 3.39 (m, 2H, 10-CH₂, N-CH₂-C₃H₅), 3.61 (ddd, *J* = 12.7, 7.8, 4.8 Hz, 1H, 6-CH), 3.87 (d, *J* = 5.7 Hz, 1H, 9-CH), 4.62 (d, *J* = 7.8 Hz, 1H, 5-CH), 4.72 (dd, *J* = 7.7, 6.4 Hz, 1H, aspartate α-CH), 6.71 (d, *J* = 8.3 Hz, 1H, 1-CH), 6.74 (d, *J* = 8.2 Hz, 1H, 2-CH).

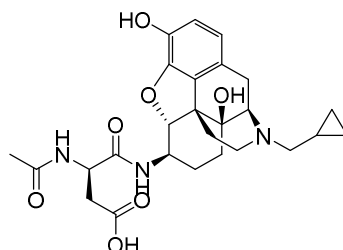


(*S*)-3-Acetamido-4-(((*4R,4aS,7R,7aR,12bS*)-3-(cyclopropylmethyl)-4a,9-dihydroxy-2,3,4,4a,5,6,7,7a-octahydro-1*H*-4,12-methanobenzofuro[3,2-*e*]isoquinolin-7-yl)amino)-4-oxobutanoic acid (92g**)**

To *tert*-butyl (*S*)-3-acetamido-4-(((4*R*,4*aS*,7*R*,7*aR*,12*bS*)-3-(cyclopropylmethyl)-4*a*,9-dihydroxy-2,3,4,4*a*,5,6,7,7*a*-octahydro-1*H*-4,12-methanobenzofuro[3,2-*e*]isoquinolin-7-yl)amino)-4-oxobutanoate (**95g**) (1 mg, 0.002 mmol) in DMF (1 ml) was added an 18:1:1 mixture of TFA (0.9 ml), TIPS (0.05 ml) and water (0.05 ml). The reaction mixture was stirred at room temperature until complete by TLC. Solvent was removed under high vacuum and purification by reverse phase HPLC (system 4) yielded **92g**, a white solid (1 mg, 99%).

¹H NMR (DMSO-*d*₆): δ 0.26 – 0.51 (m, 2H, cyclopropyl 2-CH₂ and 3-CH₂), 0.51 – 0.74 (m, 2H, cyclopropyl 2-CH₂ and 3-CH₂), 0.92 – 1.09 (m, 1H, cyclopropyl 1-CH), 1.86 (s, 3H, acetyl CH₃), 2.42 (dd, *J* = 16.1, 8.0 Hz, 1H, aspartic acid CH₂), 2.62 (dd, *J* = 16.1, 5.8 Hz, 1H, aspartic acid CH₂), 3.35 – 3.44 (m, 1H, 6-CH), 4.59 (td, *J* = 8.1, 5.9 Hz, 1H, aspartic acid α-CH), 4.65 (d, *J* = 7.5 Hz, 1H, 5-CH), 6.62 (d, *J* = 8.0 Hz, 1H, 1-CH), 6.68 (d, *J* = 8.2 Hz, 1H, 2-CH), 8.12 (s, 1H, acetamide NH), 8.14 (s, 1H, 6-NH).

m/z: HRMS C₂₆H₃₃N₃O₇ [MH]⁺ calcd 500.2391; found 500.2395

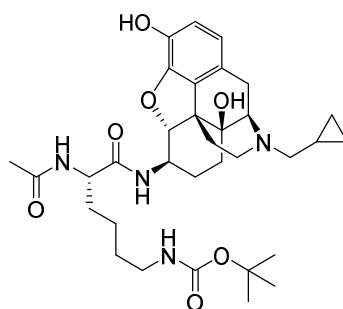


(*R*)-3-Acetamido-4-(((4*R*,4*aS*,7*R*,7*aR*,12*bS*)-3-(cyclopropylmethyl)-4*a*,9-dihydroxy-2,3,4,4*a*,5,6,7,7*a*-octahydro-1*H*-4,12-methanobenzofuro[3,2-*e*]isoquinolin-7-yl)amino)-4-oxobutanoic acid (98g**)**

To *tert*-butyl (*R*)-3-acetamido-4-(((4*R*,4*aS*,7*R*,7*aR*,12*bS*)-3-(cyclopropylmethyl)-4*a*,9-dihydroxy-2,3,4,4*a*,5,6,7,7*a*-octahydro-1*H*-4,12-methanobenzofuro[3,2-*e*]isoquinolin-7-yl)amino)-4-oxobutanoate (**95e**) (1 mg, 0.002 mmol) in DMF (1 ml) was added an 18:1:1 mixture of TFA (0.9 ml), TIPS (0.05 ml) and water (0.05 ml). The reaction mixture was stirred at room temperature until complete by TLC. Solvent was removed under high vacuum and purification by reverse phase HPLC (system 4) yielded **98g**, a white solid (1 mg, 99%).

^1H NMR (DMSO- d_6): δ 0.27 – 0.51 (m, 2H, cyclopropyl 2- CH_2 and 3- CH_2), 0.50 – 0.75 (m, 2H, cyclopropyl 2- CH_2 and 3- CH_2), 0.93 – 1.10 (m, 1H, cyclopropyl 1-CH), 1.86 (s, 3H, acetyl CH_3), 2.63 (dd, $J = 16.4, 4.9$ Hz, 1H, aspartic acid CH_2), 3.34 – 3.44 (m, 1H, 6-CH), 4.54 (td, $J = 8.3, 5.1$ Hz, 1H, aspartic acid α -CH), 4.66 (d, $J = 7.5$ Hz, 1H, 5-CH), 6.61 (d, $J = 8.2$ Hz, 1H, 1-CH), 6.67 (d, $J = 8.2$ Hz, 1H, 2-CH).

m/z : HRMS $\text{C}_{26}\text{H}_{33}\text{N}_3\text{O}_7$ $[\text{MH}]^+$ calcd 500.2391; found 500.2403

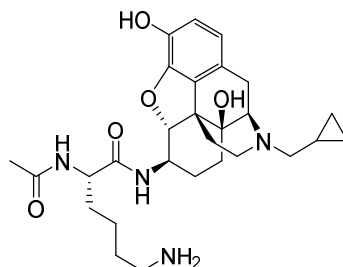


tert-Butyl ((S)-5-acetamido-6-(((4R,4aS,7R,7aR,12bS)-3-(cyclopropylmethyl)-4a,9-dihydroxy-2,3,4,4a,5,6,7,7a-octahydro-1H-4,12-methanobenzofuro[3,2-e]isoquinolin-7-yl)amino)-6-oxohexyl)carbamate (95h)

The title compound was synthesised as described in general procedure 1, using N^2 -acetyl- N^6 -Boc- L -lysine (17 mg, 0.06 mmol) to give **95h**, a white solid (27 mg, 73%).

^1H NMR (MeOD): δ 0.08 – 0.26 (m, 2H, cyclopropyl 2- CH_2 and 3- CH_2), 0.47 – 0.62 (m, 2H, cyclopropyl 2- CH_2 and 3- CH_2), 0.82 – 0.95 (m, 1H, cyclopropyl 1-CH), 1.24 – 1.70 (m, 8H, 7- CH_2 , 8- CH_2 , 15- CH_2 , lysine β - CH_2 , lysine γ - CH_2 , lysine δ - CH_2), 1.43 (s, 9H, Boc CH_3), 1.69 – 1.92 (m, 2H, 8- CH_2 , lysine β - CH_2), 2.01 (s, 3H, acetyl CH_3), 2.15 (td, $J = 12.1, 11.6, 3.2$ Hz, 1H, 16- CH_2), 2.24 (td, $J = 12.1, 4.5$ Hz, 1H, 15- CH_2), 2.40 (h, $J = 6.4$ Hz, 2H, N- CH_2 - C_3H_5), 2.63 - 2.68 (m, 1H, 10- CH_2), 2.65 (td, $J = 18.8, 6.0$ Hz, 1H, 16- CH_2), 2.96 – 3.19 (m, 4H, 9- CH_2 , 10- CH_2 , lysine ϵ - CH_2), 3.67 (ddd, $J = 12.3, 7.4, 4.6$ Hz, 1H, 6-CH), 4.31 (dd, $J = 8.4, 5.6$ Hz, 1H, lysine α -CH), 4.46 (d, $J = 7.5$ Hz, 1H, 5-CH), 6.56 (d, $J = 8.1$ Hz, 1H, 1-CH), 6.62 (d, $J = 8.1$ Hz, 1H, 2-CH).

^{13}C NMR (MeOD): δ 4.2, 4.5, 10.2, 22.6, 23.5, 24.1, 25.4, 28.8, 30.6, 31.1, 32.0, 33.2, 41.1, 45.3, 52.8, 54.9, 60.2, 63.7, 71.7, 79.7, 93.0, 118.6, 120.0, 125.4, 132.4, 141.7, 143.7, 158.5, 173.2, 174.0.



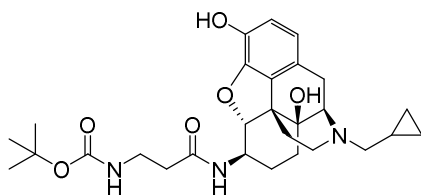
(S)-2-Acetamido-6-amino-N-(((4R,4aS,7R,7aR,12bS)-3-(cyclopropylmethyl)-4a,9-dihydroxy-2,3,4,4a,5,6,7,7a-octahydro-1H-4,12-methanobenzofuro[3,2-e]isoquinolin-7-yl)hexanamide (92h)

To tert-butyl ((S)-5-acetamido-6-(((4R,4aS,7R,7aR,12bS)-3-(cyclopropylmethyl)-4a,9-dihydroxy-2,3,4,4a,5,6,7,7a-octahydro-1H-4,12-methanobenzofuro[3,2-e]isoquinolin-7-yl)amino)-6-oxohexyl)carbamate (**95h**) (25mg, 0.041 mmol) in dioxane (1 ml) under N_2 was added 4M HCl in dioxane (1 ml). The reaction mixture was stirred at room temperature until complete by TLC. Solvent was removed under high vacuum and purification by reverse phase HPLC (system 4) yielded **92h**, a white solid (24 mg, 100%).

^1H NMR (MeOD): δ 0.46 – 0.59 (m, 2H, cyclopropyl 2- CH_2 and 3- CH_2), 0.69 – 0.87 (m, 2H, cyclopropyl 2- CH_2 and 3- CH_2), 1.05 – 1.18 (m, 1H, cyclopropyl 1-CH), 1.35 – 2.02 (m, 10H, 7- CH_2 , 8- CH_2 , 15- CH_2 , lysine β - CH_2 , lysine γ - CH_2 , lysine δ - CH_2), 2.04 (s, 3H, acetyl CH_3), 2.62 (td, $J = 13.1, 6.2$ Hz, 1H, 16- CH_2), 2.70 (td, $J = 10.0, 3.2$ Hz, 1H, 15- CH_2), 2.87 – 2.99 (m, 3H, N- CH_2 - C_3H_5 , lysine ϵ - CH_2), 3.08 – 3.23 (m, 2H, 10- CH_2 , 16- CH_2), 3.30 – 3.42 (m, 2H, 10- CH_2 , N- CH_2 - C_3H_5), 3.60 – 3.71 (m, 1H, 6-CH), 3.95 (d, $J = 5.4$ Hz, 1H, 9-CH), 4.33 (dd, $J = 8.5, 5.3$ Hz, 1H, lysine α -CH), 4.69 (d, $J = 7.8$ Hz, 1H, 5-CH), 6.71 – 6.77 (m, 2H, 1-CH, 2-CH).

^{13}C NMR (MeOD): δ 3.4, 6.2, 6.9, 22.6, 23.7, 24.5, 24.6, 28.1, 28.9, 31.1, 32.7, 40.5, 43.8, 47.6, 52.7, 54.8, 58.7, 62.2, 68.1, 91.9, 119.6, 120.9, 121.9, 130.7, 143.0, 143.7, 173.5, 174.1.

m/z : HRMS $C_{28}H_{40}N_4O_5$ $[MH]^+$ calcd 513.3071; found 513.3066

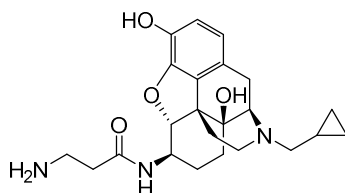


tert-Butyl (3-(((4R,4aS,7R,7aR,12bS)-3-(cyclopropylmethyl)-4a,9-dihydroxy-2,3,4,4a,5,6,7,7a-octahydro-1H-4,12-methanobenzofuro[3,2-e]isoquinolin-7-yl)amino)-3-oxopropyl)carbamate (95i)

The title compound was synthesised as described in general procedure 1, using *N*-Boc- β -alanine (11 mg, 0.06 mmol) to give **95i**, a white solid (28 mg, 90%).

1H NMR (MeOD): δ 0.09 – 0.22 (m, 2H, cyclopropyl 2-CH₂ and 3-CH₂), 0.45 – 0.59 (m, 2H, cyclopropyl 2-CH₂ and 3-CH₂), 0.81 – 0.92 (m, 1H, cyclopropyl 1-CH), 1.34 – 1.48 (m, 2H, 8-CH₂, 15-CH₂), 1.40 (s, 9H, Boc CH₃), 1.49 – 1.61 (m, 2H, 7-CH₂, 8-CH₂), 1.78 (qd, J = 13.8, 12.6, 3.4 Hz, 1H, 8-CH₂), 2.16 (td, J = 9.2, 3.6 Hz, 1H, 16-CH₂), 2.23 (td, J = 11.9, 4.1 Hz, 1H, 15-CH₂), 2.34 (t, J = 6.8 Hz, 2H, β -alanine NH-CH₂-CH₂-CO), 2.34 – 2.54 (m, 1H, N-CH₂-C₃H₅), 2.58 – 2.73 (m, 2H, 10-CH₂, 16-CH₂), 3.06 (d, J = 18.5 Hz, 1H, 10-CH₂), 3.15 (d, J = 5.5 Hz, 1H, 9-CH), 3.24 – 3.30 (m, 2H, β -alanine NH-CH₂-CH₂-CO), 3.62 (ddd, J = 12.7, 7.8, 4.8 Hz, 1H, 6-CH), 4.37 (d, J = 7.7 Hz, 1H, 5-CH), 6.54 (d, J = 8.2 Hz, 1H, 1-CH), 6.60 (d, J = 8.1 Hz, 1H, 2-CH).

^{13}C NMR (MeOD): δ 4.1, 4.6, 9.9, 23.6, 25.5, 28.8, 31.2, 31.6, 37.5, 37.9, 45.6, 49.9, 52.7, 60.1, 63.8, 71.7, 80.2, 93.2, 118.6, 120.1, 125.1, 132.4, 142.0, 143.7, 158.4, 173.6.

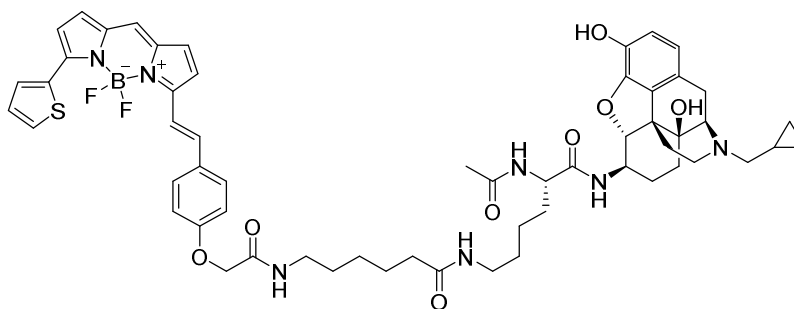


3-Amino-N-(((4R,4aS,7R,7aR,12bS)-3-(cyclopropylmethyl)-4a,9-dihydroxy-2,3,4,4a,5,6,7,7a-octahydro-1H-4,12-methanobenzofuro[3,2-e]isoquinolin-7-yl)propanamide (92i)

To tert-butyl (3-(((4*R*,4*aS*,7*R*,7*aR*,12*bS*)-3-(cyclopropylmethyl)-4*a*,9-dihydroxy-2,3,4,4*a*,5,6,7,7*a*-octahydro-1*H*-4,12-methanobenzofuro[3,2-*e*]isoquinolin-7-yl)amino)-3-oxopropyl)carbamate (**95i**) (26mg, 0.050 mmol) in dioxane (1 ml) under N₂ was added 4M HCl in dioxane (1 ml). The reaction mixture was stirred at room temperature until complete by TLC. Solvent was removed under high vacuum and purification by reverse phase HPLC (system 4) yielded **92i**, a white solid (25 mg, 100%).

¹H NMR (MeOD): δ 0.45 – 0.60 (m, 2H, cyclopropyl 2-CH₂ and 3-CH₂), 0.66 – 0.88 (m, 2H, cyclopropyl 2-CH₂ and 3-CH₂), 1.04 – 1.19 (m, 1H, cyclopropyl 1-CH), 1.51 – 1.67 (m, 2H, 8-CH₂, 16-CH₂), 1.67 – 1.81 (m, 2H, 7-CH₂, 8-CH₂), 1.88 (qd, *J* = 12.8, 2.0 Hz, 1H, 7-CH₂), 2.61 (td, *J* = 13.2, 4.8 Hz, 1H, 16-CH₂), 2.59 – 2.72 (m, 2H, NH-CH₂-CH₂-CO), 2.70 (td, *J* = 12.8, 3.6 Hz, 1H, 15-CH₂), 2.91 (dd, *J* = 13.6, 7.6 Hz, 1H, N-CH₂-C₃H₅), 3.08 – 3.25 (m, 4H, 10-CH₂, 16-CH₂, NH-CH₂-CH₂-CO), 3.33 – 3.43 (m, 2H, 10-CH₂, N-CH₂-C₃H₅), 3.62 – 3.72 (m, 1H, 6-CH), 3.95 (d, *J* = 5.8 Hz, 1H, 9-CH), 4.58 (d, *J* = 7.9 Hz, 1H, 5-CH), 6.73 (d, *J* = 8.2 Hz, 1H, 1-CH), 6.76 (d, *J* = 8.3 Hz, 1H, 2-CH).

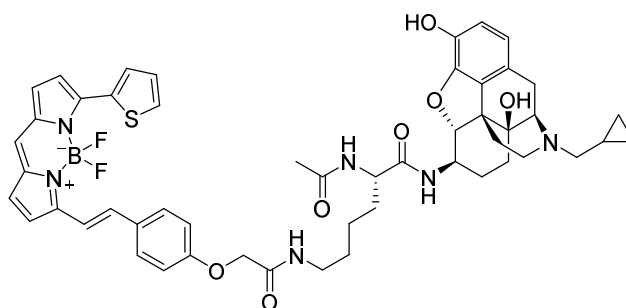
¹³C NMR (MeOD): δ 3.4, 6.2, 6.8, 24.4, 24.7, 28.8, 31.1, 33.0, 37.0, 43.7, 47.6, 52.4, 58.7, 64.2, 71.3, 92.2, 119.4, 121.0, 121.9, 130.8, 143.1, 143.7, 171.9.



(S)-2-Acetamido-N-(((4*R*,4*aS*,7*R*,7*aR*,12*bS*)-3-(cyclopropylmethyl)-4*a*,9-dihydroxy-2,3,4,4*a*,5,6,7,7*a*-octahydro-1*H*-4,12-methanobenzofuro[3,2-*e*]isoquinolin-7-yl)-6-(6-(2-(4-((*E*)-2-(5,5-difluoro-7-(thiophen-2-yl)-5*H*-4*λ*⁴,5*λ*⁴-dipyrrolo[1,2-*c*:2',1'-*f*][1,3,2]diazaborinin-3-yl)vinyl)phenoxy)acetamido)hexanamido)hexanamide (99**)**

To (S)-2-acetamido-6-amino-N-((4R,4aS,7R,7aR,12bS)-3-(cyclopropylmethyl)-4a,9-dihydroxy-2,3,4,4a,5,6,7,7a-octahydro-1H-4,12-methanobenzofuro[3,2-e]isoquinolin-7-yl)hexanamide (**92h**) (0.88 mg, 1.5 μ mol, 1.0 eq) in DMF (0.5 ml) was added DIPEA (0.78 μ l, 4.5 μ mol, 3.0 eq) followed by BODIPY 630/650-X NHS ester (1.0 mg, 1.5 μ mol, 1.0 eq) in DMF (0.5 ml). The reaction mixture was stirred at room temperature for 90 min. Solvent was removed under high vacuum and purification by reverse phase HPLC (system 3) yielded **99**, a blue solid (1.2 mg, 75%).

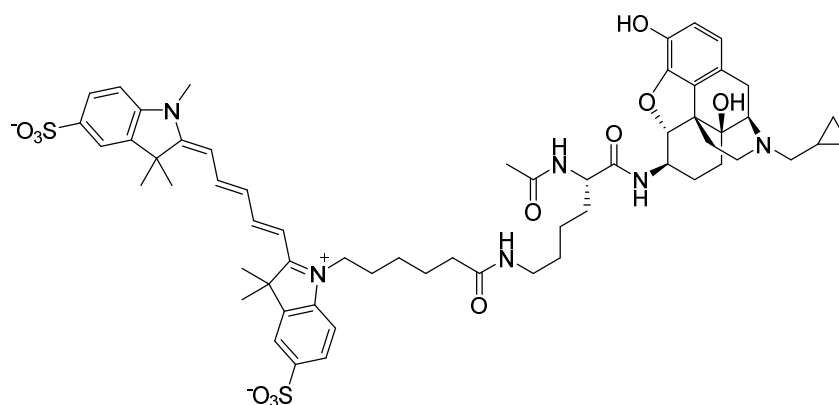
m/z: HRMS C₅₇H₆₆BF₂N₇O₈S [MH]⁺ calcd 1058.4827; found 1058.4837



(S)-2-Acetamido-N-((4R,4aS,7R,7aR,12bS)-3-(cyclopropylmethyl)-4a,9-dihydroxy-2,3,4,4a,5,6,7,7a-octahydro-1H-4,12-methanobenzofuro[3,2-e]isoquinolin-7-yl)-6-(2-(4-((E)-2-(5,5-difluoro-7-(thiophen-2-yl)-5H-4 λ ⁴,5 λ ⁴-dipyrrrolo[1,2-c:2',1'-f][1,3,2]diazaborinin-3-yl)vinyl)phenoxy)acetamido)hexanamide (100**)**

To BODIPY 630/650 (0.68 mg, 1.5 μ mol) in DMF (0.5 ml) was added PyBOP (0.78 mg, 1.5 μ mol, 1.0 eq) and DIPEA (1.30 μ l, 7.5 μ mol, 5.0 eq). The reaction mixture was stirred at room temperature for 15 min after which (S)-2-acetamido-6-amino-N-((4R,4aS,7R,7aR,12bS)-3-(cyclopropylmethyl)-4a,9-dihydroxy-2,3,4,4a,5,6,7,7a-octahydro-1H-4,12-methanobenzofuro[3,2-e]isoquinolin-7-yl)hexanamide (**92h**) (0.88 mg, 1.5 μ mol, 1.0 eq) in DMF (0.5 ml) was added. The reaction mixture was then stirred at room temperature for 90 min. Solvent was removed under high vacuum and purification by reverse phase HPLC (system 3) yielded **100**, a blue solid (0.6 mg, 42%).

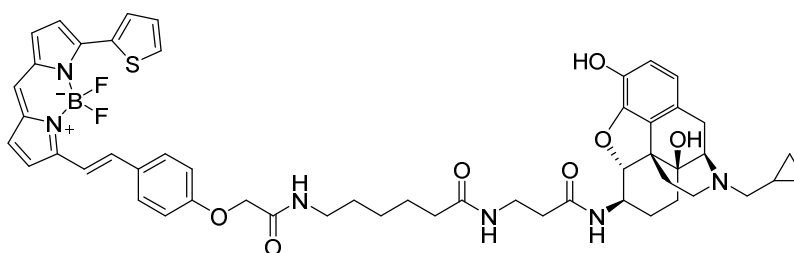
m/z: HRMS C₅₁H₅₅BF₂N₆O₇S [MH]⁺ calcd 945.3987; found 945.3982



1-(6-(((*S*)-5-Acetamido-6-(((4*R*,4*aS*,7*R*,7*aR*,12*bS*)-3-(cyclopropylmethyl)-4*a*,9-dihydroxy-2,3,4,4*a*,5,6,7,7*a*-octahydro-1*H*-4,12-methanobenzofuro[3,2-*e*]isoquinolin-7-yl)amino)-6-oxohexyl)amino)-6-oxohexyl)-3,3-dimethyl-2-((1*E*,3*E*)-5-((*E*)-1,3,3-trimethyl-5-sulfonatoindolin-2-ylidene)penta-1,3-dien-1-yl)-3*H*-indol-1-ium-5-sulfonate (101**)**

To (*S*)-2-acetamido-6-amino-*N*-((4*R*,4*aS*,7*R*,7*aR*,12*bS*)-3-(cyclopropylmethyl)-4*a*,9-dihydroxy-2,3,4,4*a*,5,6,7,7*a*-octahydro-1*H*-4,12-methanobenzofuro[3,2-*e*]isoquinolin-7-yl)hexanamide (**92h**) (0.88 mg, 1.5 μ mol, 1.0 eq) in DMF (0.5 ml) was added DIPEA (0.78 μ l, 4.5 μ mol, 3.0 eq) followed by sulfo-Cy5 NHS ester (1.17 mg, 1.5 μ mol, 1.0 eq) in DMF (0.5 ml). The reaction mixture was stirred at room temperature for 90 min. Solvent was removed under high vacuum and purification by reverse phase HPLC (system 3) yielded **101**, a blue solid (0.6 mg, 35%).

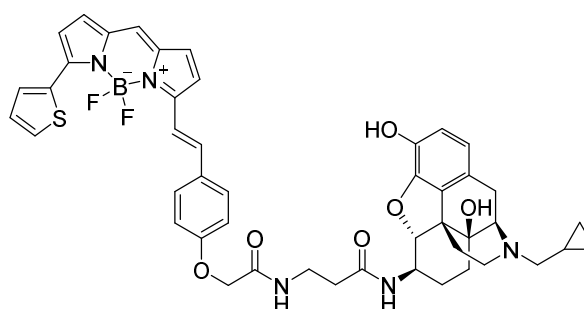
m/z: HRMS C₅₅H₆₆N₅O₁₁S₂⁻ [M]⁻ calcd 1135.4890; found 1135.4827



***N*-(3-(((4*R*,4*aS*,7*R*,7*aR*,12*bS*)-3-(Cyclopropylmethyl)-4*a*,9-dihydroxy-2,3,4,4*a*,5,6,7,7*a*-octahydro-1*H*-4,12-methanobenzofuro[3,2-*e*]isoquinolin-7-yl)amino)-3-oxopropyl)-6-(2-(4-((*E*)-2-(5,5-difluoro-7-(thiophen-2-yl)-5*H*-4*λ*⁴,5*λ*⁴-dipyrrolo[1,2-*c*:2',1'-*f*][1,3,2]diazaborinin-3-yl)vinyl)phenoxy)acetamido)hexanamide (102)**

To 3-amino-*N*-((4*R*,4*aS*,7*R*,7*aR*,12*bS*)-3-(cyclopropylmethyl)-4*a*,9-dihydroxy-2,3,4,4*a*,5,6,7,7*a*-octahydro-1*H*-4,12-methanobenzofuro[3,2-*e*]isoquinolin-7-yl)propanamide (**92i**) (0.73 mg, 1.5 μmol, 1.0 eq) in DMF (0.5 ml) was added DIPEA (0.78 μl, 4.5 μmol, 3.0 eq) followed by BODIPY 630/650-X NHS ester (1.0 mg, 1.5 μmol, 1.0 eq) in DMF (0.5 ml). The reaction mixture was stirred at room temperature for 90 min. Solvent was removed under high vacuum and purification by reverse phase HPLC (system 3) yielded **102**, a blue solid (1.2 mg, 83%).

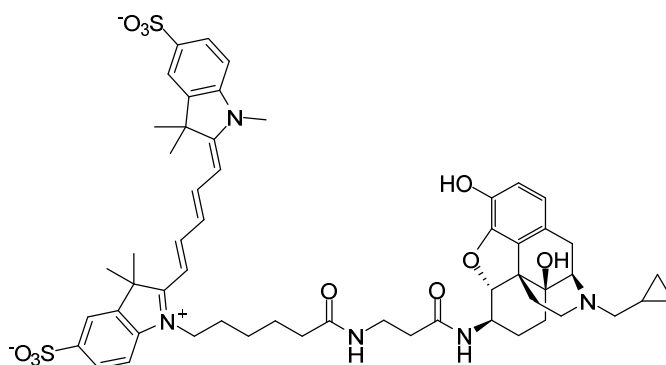
m/z: HRMS C₄₆H₄₆BF₂N₅O₆S [MH]⁺ calcd 846.3303; found 846.3286



***N*-((4*R*,4*aS*,7*R*,7*aR*,12*bS*)-3-(Cyclopropylmethyl)-4*a*,9-dihydroxy-2,3,4,4*a*,5,6,7,7*a*-octahydro-1*H*-4,12-methanobenzofuro[3,2-*e*]isoquinolin-7-yl)-3-(2-(4-((*E*)-2-(5,5-difluoro-7-(thiophen-2-yl)-5*H*-4*λ*⁴,5*λ*⁴-dipyrrolo[1,2-*c*:2',1'-*f*][1,3,2]diazaborinin-3-yl)vinyl)phenoxy)acetamido)propanamide (103)**

To BODIPY 630/650 (0.68 mg, 1.5 μmol) in DMF (0.5 ml) was added PyBOP (0.78 mg, 1.5 μmol , 1.0 eq) and DIPEA (1.30 μl , 7.5 μmol , 5.0 eq). The reaction mixture was stirred at room temperature for 15 min after which 3-amino-*N*-((4*R*,4*aS*,7*R*,7*aR*,12*bS*)-3-(cyclopropylmethyl)-4*a*,9-dihydroxy-2,3,4,4*a*,5,6,7,7*a*-octahydro-1*H*-4,12-methanobenzofuro[3,2-*e*]isoquinolin-7-yl)propanamide (**92i**) (0.73 mg, 1.5 μmol , 1.0 eq) in DMF (0.5 ml) was added. The reaction mixture was then stirred at room temperature for 90 min. Solvent was removed under high vacuum and purification by reverse phase HPLC (system 3) yielded **103**, a blue solid (0.6 mg, 47%).

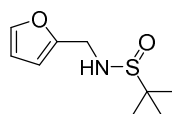
m/z: HRMS $\text{C}_{52}\text{H}_{57}\text{BF}_2\text{N}_6\text{O}_7\text{S}$ $[\text{MH}]^+$ calcd 959.4143; found 959.4143



1-(6-(((3-(((4*R*,4*aS*,7*R*,7*aR*,12*bS*)-3-(Cyclopropylmethyl)-4*a*,9-dihydroxy-2,3,4,4*a*,5,6,7,7*a*-octahydro-1*H*-4,12-methanobenzofuro[3,2-*e*]isoquinolin-7-yl)amino)-3-oxopropyl)amino)-6-oxohexyl)-3,3-dimethyl-2-((1*E*,3*E*)-5-((*E*)-1,3,3-trimethyl-5-sulfonatoindolin-2-ylidene)penta-1,3-dien-1-yl)-3*H*-1 λ^4 -indole-5-sulfonate (104**)**

To 3-amino-*N*-((4*R*,4*aS*,7*R*,7*aR*,12*bS*)-3-(cyclopropylmethyl)-4*a*,9-dihydroxy-2,3,4,4*a*,5,6,7,7*a*-octahydro-1*H*-4,12-methanobenzofuro[3,2-*e*]isoquinolin-7-yl)propanamide (**92i**) (0.73 mg, 1.5 μmol , 1.0 eq) in DMF (0.5 ml) was added DIPEA (0.78 μl , 4.5 μmol , 3.0 eq) followed by sulfo-Cy5 NHS ester (1.17 mg, 1.5 μmol , 1.0 eq) in DMF (0.5 ml). The reaction mixture was stirred at room temperature for 90 min. Solvent was removed under high vacuum and purification by reverse phase HPLC (system 3) yielded **104**, a blue solid (0.7 mg, 45%).

m/z : HRMS $C_{55}H_{66}N_5O_{11}S_2^- [M]^-$ calcd 1036.4211; found 1036.4231



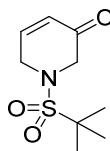
***N*-(Furfuryl)-*tert*-butylsulfonamide (148)**

To a solution of furfurylamine (3.5 g, 3.18 mL, 36.00 mmol) and triethylamine (10.9 g, 15.00 mL, 107.7 mmol, 3 eq) in dichloromethane (20 mL) at 0°C was added *tert*-butylsulfonyl chloride (5.0 g, 4.41 mL, 35.6 mmol, 1 eq) in dichloromethane (40 mL) dropwise over a period of 30 minutes. The mixture was stirred for a further 1 hour at 0°C and reaction completion was confirmed by thin layer chromatography (TLC) (50% EtOAc in petroleum ethers (PE)). The solution was diluted with further dichloromethane and washed with water (20 mL) and brine (20 mL). The organic phase was dried over magnesium sulfate and the solvent evaporated off under vacuum. Column chromatography (50% EtOAc in PE) afforded **148** as a yellow oil (6.5 g, 90%).

^1H NMR (CDCl_3): δ 1.21 (s, 9H, *t*-Bu CH_3), 3.46 (br t, $J = 6.26$ Hz, 1H, NH), 4.23 (dd, $J = 14.82/7.01$, 1H, CH_2), 4.33 (dd, $J = 14.82/5.22$, 1H, CH_2), 6.26 (dd, $J = 3.25/0.81$ Hz, 1H, furan 3-CH), 6.32 (dd, $J = 3.21/1.84$ Hz, 1H, furan 4-CH), 7.37 (dd, $J = 1.85/0.86$ Hz, 1H, furan 5-CH).

^{13}C NMR (CDCl_3): δ 22.5, 42.2, 56.0, 107.8, 110.3, 142.4, 151.9.

m/z : LCMS $C_9H_{15}NO_2S [MH]^+$ calcd 202.3, found 202.1 with t_R of 2.44 min.



***N*-(*tert*-Butylsulfonyl)-1,2-dihydropyridin-3-one (150)**

To a solution of *N*-(furfuryl)-*tert*-butylsulfonamide (**148**) (100 mg, 0.50 mmol, 1 eq) in dichloromethane (5 mL) at room temperature was added 3-chloroperbenzoic acid (*m*-CPBA) (86 mg, 0.50 mmol, 1 eq). After 20 minutes a further 1 molar equivalent of *m*-CPBA was added (86 mg, 0.50 mmol) and again

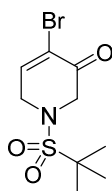
at 40 minutes and 60 minutes (total *m*-CPBA used was 344 mg, 2.00 mmol, 4 eq). The reaction was monitored throughout by TLC (50% EtOAc in PE) which showed that after 2 hours the reaction was complete. The mixture was diluted in dichloromethane (15 mL) and washed with saturated sodium bicarbonate solution (10 mL x2), water (10 mL) and brine (10 mL). The organic phase was dried over magnesium sulfate and the solvent evaporated until approximately 5 mL of solvent remained (note: this solution should not be evaporated to dryness as the product has been observed to decompose explosively¹). The solution was cooled to 0°C and triethylsilane (58 mg, 0.08 mL, 0.50 mmol, 1 eq) added with stirring. BF₃·OEt₂ (71 mg, 0.06 mL, 0.50 mmol, 1 eq) was then added dropwise and the reaction was stirred at 0°C for 3 hours. The mixture was diluted in dichloromethane (15 mL) and washed with saturated sodium bicarbonate solution/10% w/v sodium sulfite (1:1) (10 mL), saturated sodium bicarbonate solution (10 mL), water (10 mL) and brine (10 mL). The organic phase was dried over magnesium sulfate and the solvent evaporated off under vacuum. Column chromatography (20-50% EtOAc in PE) afforded **150** as an off-white solid (39 mg, 36%).

mp: 113-114°C

¹H NMR (CDCl₃): δ 1.39 (s, 9H, *t*-Bu CH₃), 4.06 (s, 2H, pyridinone 2-CH₂), 4.23 (s, 2H, pyridinone 6-CH₂), 6.25 (dt, *J* = 10.28/2.17 Hz, 1H, pyridinone 4-CH), 7.08 (dt, *J* = 10.30/3.62 Hz, 1H, pyridinone 5-CH).

¹³C NMR (CDCl₃): δ 24.4, 46.1, 54.4, 62.1, 128.3, 146.4, 192.2.

m/z: LCMS C₉H₁₅NO₃S [MH+MeCN]⁺ calc 259.3, found 259.2 with *t*_R of 2.30 min.



4-Bromo-*N*-(*tert*-butylsulfonyl)-1,2-dihydropyridin-3-one (151)

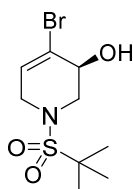
To a solution of *N*-(*tert*-butylsulfonyl)-1,2-dihydropyridin-3-one (**150**) (665 mg, 3.06 mmol) in dichloromethane (30 mL) at 0°C was added bromine (489 mg, 0.16 mL, 3.06 mmol, 1 eq) in dichloromethane (13.7 mL) dropwise. After 30 minutes the reaction was complete by TLC (50% EtOAc in PE). Triethylamine (310 mg, 0.43 mL, 3.06 mmol, 1 eq) was then added with further stirring at 0°C for 30 minutes. The mixture was diluted in dichloromethane (50 mL) and washed with water (30 mL x2), saturated sodium bicarbonate solution (30 mL) and brine (30 mL). The organic phase was dried over magnesium sulfate and the solvent evaporated off under vacuum. Recrystallization in methanol afforded **151** as colourless crystals (696 mg, 77%).

mp: 128-130°C.

¹H NMR (CDCl₃): δ 1.40 (s, 9H, *t*-Bu CH₃), 4.23 (s, 2H, pyridinone 2-CH₂), 4.27 (d, *J* = 3.9 Hz, 2H, pyridinone 6-CH₂), 7.47 (t, *J* = 3.9 Hz, 1H, pyridinone 5-CH).

¹³C NMR (CDCl₃): δ 24.3, 48.2, 54.7, 62.2, 122.2, 146.8, 185.0

m/z: LCMS C₉H₁₄NO₃BrS [MH]⁺ calc 295.0, found 295.1 with *t*_R of 2.59 min.



(S)-4-Bromo-*N*-(*tert*-butylsulfonyl)-1,2,3,6-tetrahydropyridin-3-ol (152**)**

To a solution of (*R*)-(+)-2-methyl-CBS-oxazaborolidine (263 mg, 0.95 mmol, 0.3 eq) in tetrahydrofuran (15 mL) at 0°C was added borane-*N,N*-diethylaniline (1.034 g, 1.13 mL, 6.34 mmol, 2 eq). 4-Bromo-*N*-(*tert*-butylsulfonyl)-1,2-dihydropyridin-3-one (**151**) (940 mg, 3.17 mmol) in tetrahydrofuran (30 mL) was then added dropwise over 15 minutes. The reaction was allowed to warm slowly to room temperature and was stirred for 16 hours. Excess borane was quenched with methanol (2.1 mL) and the solvents removed by evaporation. The resulting residue was re-dissolved in dichloromethane (50 mL) and washed with 1M HCl (20 mL x2), water (20 mL) and brine (20 mL). The organic phase

was dried over magnesium sulfate and the solvent evaporated off under vacuum. Column chromatography (30% EtOAc in PE) afforded **152** as an off-white solid (886 mg, 94%).

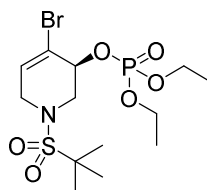
$[\alpha]_{\text{D}}^{19}$: -46.0 (MeOH, *c* 1.00).

mp: 120-122°C.

^1H NMR (CDCl_3) δ 1.42 (s, 9H, *t*-Bu CH_3), 2.75 (br s, 1H, OH), 3.68 (d, $J = 4.2$ Hz, 2H, pyridinol 6- CH_2), 3.86 (d, $J = 17.6$, 1H, pyridinol 2- CH_2), 4.04 (d, $J = 17.8$, 1H, pyridinol 2- CH_2), 4.23 (br s, 1H, pyridinol 3-CH), 6.25 (t, $J = 3.5$ Hz, 1H, pyridinol 5-CH).

^{13}C NMR (CDCl_3) δ 24.5, 47.8, 51.5, 62.0, 68.6, 124.1, 128.8

m/z: LCMS $\text{C}_9\text{H}_{16}\text{NO}_3\text{BrS}$ $[\text{MH}]^+$ calc 297.0, found 297.0 with t_{R} of 2.41 min.



(S)-4-Bromo-N-(tert-butylsulfonyl)-1,2,3,6-tetrahydropyridin-3-yl diethyl phosphate (153)

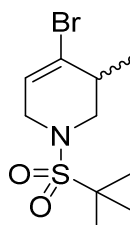
To a solution of (*S*)-4-bromo-*N*-(*tert*-butylsulfonyl)-1,2,3,6-tetrahydropyridin-3-ol (**152**) (1.265 g, 4.24 mmol) in dichloromethane (28 mL) at 0°C was added triethylamine (3.432 g, 4.73 mL, 33.92 mmol, 8 eq) and a catalytic amount of dimethylaminopyridine (26 mg, 5%). Chlorodiethylphosphate (2.195 g, 1.84 mL, 12.72 mmol, 3 eq) was added gradually over 2.5 hours. It was then allowed to warm to room temperature and left to stir overnight. It was then washed with brine (20 mL) and the aqueous layer extracted with dichloromethane (10 mL x3). The combined organic extracts had their solvent evaporated under vacuum before column chromatography (75% EtOAc in PE) afforded **153** as an orange oil (1.511 g, 82%).

$[\alpha]_{\text{D}}^{19}$: -19.0 (MeOH, *c* 1.00).

^1H NMR (CDCl_3): δ 1.37 (two overlapping quartets, $J = 7.0$ Hz, 6H, Et CH_3), 1.42 (s, 9H, *t*-Bu CH_3), 3.63 (dd, $J = 14.1/3.6$ Hz, 1H, pyridinol 2- CH_2), 3.85 (d, $J = 17.8$ Hz, 1H, pyridinol 6- CH_2), 3.95 (dd, $J = 14.5/3.6$ Hz, 1H, pyridinol 2- CH_2), 4.04 (d, $J = 17.7$, 1H, pyridinol 6- CH_2) 4.22 (two overlapping quintets, $J = 7.0$ Hz, 4H in total, Et CH_2), 4.88-4.92 (m, 1H, pyridinol 3-CH), 6.36 (t, $J = 3.5$ Hz, 1H, pyridinol 5-CH).

^{13}C NMR (CDCl_3): δ 16.0, 16.1, 24.5, 47.9, 50.4, 62.1, 64.4, 64.5, 73.3, 118.6, 131.4.

m/z : LCMS $\text{C}_{13}\text{H}_{25}\text{NO}_6\text{BrPS}$ $[\text{MH}]^+$ calc 433.0, found 433.1 with t_R of 2.76 min.



4-Bromo-*N*-(*tert*-butylsulfonyl)-3-methyl-1,2,3,6-tetrahydropyridine (**154**)

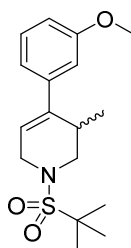
To a slurry of Copper (I) bromide dimethyl sulfide complex (103 mg, 0.50 mmol, 2 eq) in tetrahydrofuran (1 mL) at 0°C was added methyl magnesium bromide (0.17 mL of a 3.0 M solution in diethyl ether, 0.50 mmol, 2 eq). The mixture was stirred for 30 minutes before reducing the temperature to -40°C using a bath of dry ice and acetonitrile. (*S*)-4-Bromo-*N*-(*tert*-butylsulfonyl)-1,2,3,6-tetrahydropyridin-3-yl diethyl phosphate (**153**) (108 mg, 0.25 mmol) in tetrahydrofuran (1.5 mL) was then added dropwise over 15 minutes. The reaction conditions were maintained at -40°C until the reaction was complete by TLC (100% EtOAc). The reaction was quenched with saturated ammonium chloride solution (5 mL) and extracted with diethyl ether (5 mL x3) and the combined layers were washed with brine (5 mL). The organic phase was dried over magnesium sulfate and then filtered through Celite. Evaporation of the solvent under vacuum afforded **154** as an off-white solid (25 mg, 34%).

mp: $96-97^\circ\text{C}$.

^1H NMR (CDCl_3): δ 1.20 (d, $J = 7.0$ Hz, 3H, pyridine 3- CH_3), 1.37 (s, 9H, *t*Bu CH_3), 2.60 (d, $J = 7.2$ Hz, 1H, pyridine 3-CH), 3.29 (d, $J = 9.7$ Hz, 1H, pyridine 2- CH_2), 3.62 (dd, $J = 13.4/4.6$ Hz, 1H, pyridine 2- CH_2), 3.90 (t, $J = 19.5$ Hz, 2H, pyridine 6- CH_2), 6.01 (td, $J = 3.6/1.5$ Hz 1H, pyridine 5-CH).

^{13}C NMR (CDCl_3): δ 17.7, 24.6, 38.5, 47.9, 51.3, 61.8, 125.2, 127.0.

m/z : LCMS $\text{C}_{10}\text{H}_{18}\text{NO}_2\text{BrS}$ $[\text{MH}]^+$ calc 295.0, found 295.1 with t_R of 2.90 min.



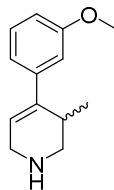
***N*-(*tert*-butylsulfonyl)-4-(3-methoxyphenyl)-3-methyl-1,2,3,6-tetrahydropyridine (155)**

To a solution of 4-Bromo-*N*-(*tert*-butylsulfonyl)-3-methyl-1,2,3,6-tetrahydropyridine (**154**) (15 mg, 0.05 mmol) in 1:1 ethanol-toluene (1.2 mL) were added 3-methoxybenzeneboronic acid (9 mg, 0.06 mmol, 1 eq) and sodium carbonate (1 M, 0.22 mL). A catalytic amount of tetrakis(triphenylphosphine)palladium(0) (5%) was added and the reaction heated to 100°C in a microwave for 30 minutes. The solvent was then removed by evaporation under vacuum and the resulting mixture partitioned between diethyl ether (5 mL) and water (5 mL) before the organic phase was washed with brine (5 mL). The organic phase was dried over magnesium sulfate and the solvent evaporated off under vacuum. Column chromatography (15-30% EtOAc in PE) afforded **155** as a pale yellow oil (12 mg, 73%).

^1H NMR (CDCl_3): δ 1.08 (d, $J = 6.9$ Hz, 3H, pyridine 3- CH_3), 1.45 (s, 9H, *t*Bu CH_3), 2.91 (br s, 1H, pyridine 3-CH), 3.55 (m, 2H, pyridine 6- CH_2), 3.85 (s, 3H, O- CH_3), 4.04 (d, $J = 17.7$ Hz, 1H, pyridine 2- CH_2), 4.19 (d, $J = 17.8$ Hz, 1H, pyridine 2- CH_2), 5.86 (dd, $J = 3.4/1.0$ Hz, 1H, pyridine 5- CH_2), 6.85 (dd, $J = 10.8/2.5$ Hz, 2H, phenol 2 and 6-CH), 6.92 (dt, $J = 7.7/1.3$ Hz, 1H, phenol 4-CH), 7.28 (t, $J = 7.7$ Hz, 1H, phenol 5-CH).

^{13}C NMR (CDCl_3): δ 18.0, 25.0, 32.4, 47.0, 51.1, 55.4, 61.9, 112.2, 112.7, 118.7, 120.8, 129.5, 141.8, 159.8.

m/z : LCMS $\text{C}_{17}\text{H}_{25}\text{NO}_3\text{S}$ $[\text{MH}]^+$ calc 324.2, found 324.4 with t_R of 2.20 min.

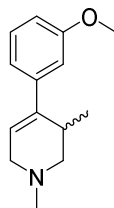


4-(3-methoxyphenyl)-3-methyl-1,2,3,6-tetrahydropyridine (**156**)

To a solution of *N*-(tert-butylsulfonyl)-4-(3-methoxyphenyl)-3-methyl-1,2,3,6-tetrahydropyridine (**155**) (323 mg, 1.00 mmol) and anisole (2.17 mL, 2.163 g, 20.00 mmol, 20 eq) in dichloromethane (30.1 mL) was added a solution of triflic acid (0.53 mL, 900 mg, 6.00 mmol, 6 eq) in dichloromethane (30.1 mL) dropwise at 0°C. The reaction was left to stir at 0°C until complete by TLC. The reaction was quenched by the addition of 2M NaOH (40 mL) and the organic and aqueous layers separated. The aqueous layer was extracted with dichloromethane (20 mL x3) and the combined organic phases dried over magnesium sulfate. Solvents were evaporated under vacuum. Column chromatography (10% 1M NH_3 / MeOH in dichloromethane) afforded **156** as a colourless oil (157 mg, 77%).

^1H NMR (CDCl_3) δ 1.02 (d, $J = 7.0$ Hz, 3H, pyridine 3- CH_3), 2.85 (m, 1H, pyridine 3-CH), 2.93 (dd, $J = 12.5/4.6$ Hz, 1H, pyridine 2- CH_2), 3.23 (dd, $J = 12.5/4.8$ Hz, 1H, pyridine 2- CH_2), 3.52 (s, 1H, NH), 3.57 (t, $J = 2.6$ Hz, 2H, pyridine 6- CH_2), 3.81 (s, 3H, O- CH_3), 5.89 (dd, $J = 3.4/2.3$ Hz, 1H, pyridine 5-CH), 6.81 (dd, $J = 8.0/2.1$ Hz, 1H, phenol 6-CH), 6.84 (t, $J = 2.0$ Hz, 1H, phenol 2-CH), 6.89 (dt, $J = 7.7/1.2$ Hz, 1H, phenol 4-CH), 7.24 (t, $J = 7.9$ Hz, 1H, phenol 5-CH)

^{13}C NMR (CDCl_3) δ 18.2, 30.2, 44.9, 49.7, 55.2, 112.0, 112.4, 118.6, 122.4, 129.3, 141.8, 142.2, 159.6.

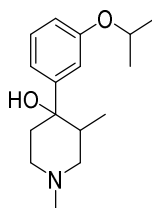


4-(3-methoxyphenyl)-1,3-dimethyl-1,2,3,6-tetrahydropyridine (157)

To a solution of 4-(3-methoxyphenyl)-3-methyl-1,2,3,6-tetrahydropyridine (**156**) (157 mg, 0.772 mmol) in dichloroethane (5.5 mL) was added 37% aqueous formaldehyde (23mg, 0.06 ml, 0.772 mmol, 1 eq) followed by the slow addition of sodium triacetoxyborohydride (665 mg, 3.089 mmol, 4 eq) at room temperature. After 90 minutes of stirring, acetic acid (0.04 mL, 43.4 mg, 0.723 mmol, 1 eq) was added and the reaction was left to stir for a further 30 minutes. The solution was basified by the addition of saturated sodium bicarbonate solution (10 mL) and extracted with dichloromethane (10 mL x3). The combined organic phases were dried with magnesium sulfate and solvents evaporated off under vacuum. Column chromatography (10% 1M NH₃/ MeOH in dichloromethane) afforded **157** as a yellow oil (149 mg, 89%).

¹H NMR (CDCl₃): δ 1.00 (d, *J* = 7.0 Hz, 3H, pyridine 3-CH₃), 2.38 (s, 3H, N-CH₃), 2.39 (dd, *J* = 11.2/5.2 Hz, 1H, pyridine 6-CH₂), 2.69 (dd, *J* = 11.2/4.9 Hz, 1H, pyridine 6-CH₂), 2.91 (m, 1H, pyridine 3-CH), 2.99 (dt, *J* = 16.8/3.0 Hz, 1H, pyridine 2-CH₂), 3.10 (dt, *J* = 16.8/3.0 Hz, 1H, pyridine 2-CH₂), 3.81 (s, 3H, O-CH₃), 5.85 (td, *J* = 3.6/1.2 Hz, 1H, pyridine 5-CH), 6.79 (ddd, *J* = 8.2/2.7/0.8 Hz, 1H, phenol 6-CH), 6.85 (t, *J* = 2.0 Hz, 1H, phenol 2-CH), 6.90 (dt, *J* = 7.7/1.2 Hz, 1H, phenol 4-CH), 7.22 (t, *J* = 8.0 Hz, 1H, phenol 5-CH).

¹³C NMR (CDCl₃): δ 18.8, 32.3, 45.9, 55.2, 55.5, 60.3, 112.0, 112.1, 118.8, 122.7, 129.1, 141.0, 142.6, 159.5.



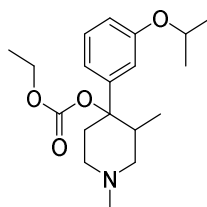
4-(3-isopropoxyphenyl)-1,3-dimethylpiperidin-4-ol (159)

To a solution of 1-bromo-3-isopropoxybenzene (3.76 mL, 5 g, 23.25 mmol, 1.35 eq) in tetrahydrofuran (50 mL) at -75°C was added *n*-butyllithium (1.48M in hexanes) (15.1 mL, 22.39 mmol, 1.3 eq). The reaction was allowed to stir at -75°C for 1 hr before the dropwise addition of 1,3-dimethyl-4-piperidone (2.30 mL, 2.187 g, 17.22 mmol, 1 eq). The reaction was left to stir at -75°C until complete by TLC. The reaction mixture was diluted with heptane (100 mL) followed by the addition of saturated ammonium chloride solution (50 mL). The layers were separated and the organic layer was washed with water (25 mL) and brine (25 mL). It was then dried with magnesium sulfate and solvents evaporated off under vacuum. Column chromatography (10% 1M NH₃/MeOH in EtOAc) afforded **159** as a colourless oil (4.099 g, 94%).

¹H NMR (CDCl₃): δ 0.65 (d, *J* = 6.8 Hz, 3H, piperidine 3-CH₃), 1.34 (d, *J* = 6.0 Hz, 6H, *i*-Pr CH₃), 1.72 (dt, *J* = 14.1, 2.5 Hz, 1H, piperidine 5-CH₂), 2.11-2.23 (m, 2H, piperidine 2-CH₂ and 5-CH₂), 2.23-2.33 (m, 1H, piperidine 3-CH), 2.36 (s, 3H, N-CH₃), 2.42 (dd, *J* = 12.9, 2.5 Hz, 1H, piperidine 6-CH₂), 2.70 (ddd, *J* = 11.2, 4.0, 1.6 Hz, 1H, piperidine 2-CH₂), 2.77 (ddt, *J* = 11.3, 4.3, 1.9 Hz, 1H, piperidine 6-CH₂), 4.56 (hept, *J* = 6.1 Hz, 1H, *i*-Pr CH), 6.78 (ddd, *J* = 8.2, 2.5, 1.0 Hz, 1H, phenol 6-CH), 7.01 (dt, *J* = 7.9, 1.5 Hz, 1H, phenol 2-CH), 7.04 (t, *J* = 2.1 Hz, 1H, phenol 4-CH), 7.25 (t, *J* = 7.9 Hz, 1H, phenol 5-CH).

¹³C NMR (CDCl₃): δ 12.3, 22.1, 22.1, 39.3, 40.6, 46.2, 51.5, 58.8, 69.8, 73.4, 112.7, 113.9, 116.9, 129.2, 149.0, 157.9.

m/z: LCMS C₁₆H₂₅NO₂ [MH]⁺ calc 264.2, found 264.2 with *t*_R of 2.48 min.



Ethyl (4-(3-isopropoxyphenyl)-1,3-dimethylpiperidin-4-yl) carbonate (160)

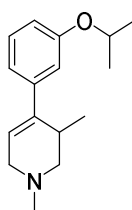
To a solution of 4-(3-isopropoxyphenyl)-1,3-dimethylpiperidin-4-ol (**159**) (4.000 g, 15.19 mmol) and triethylamine (2.96 mL, 2.151 g, 21.26 mmol, 1.4 eq)

in ethyl acetate (100 mL) at 0°C was added ethyl chloroformate (2.03 mL, 2.307 g, 21.26 mmol, 1.4 eq) dropwise over 15 minutes. The reaction was allowed to stir and warm to room temperature over 24 hrs. 2M NaOH (100 mL) and additional EtOAc (100 mL) were added and the layers separated. The aqueous layer was extracted with further EtOAc (2 x 50 mL). The combined organic phases were then washed with water (50 mL) and brine (50 mL). It was then dried with magnesium sulfate and solvents evaporated off under vacuum. Column chromatography (5-10% 1M NH₃/MeOH in EtOAc) afforded **160** as a colourless oil (4.044 g, 79%).

¹H NMR (CDCl₃): δ 0.75 (d, *J* = 6.8 Hz, 3H, piperidine 3-CH₃), 1.30 – 1.38 (m, 9H, *i*-Pr CH₃ and Et CH₃), 1.88 – 2.02 (m, 1H, piperidine 3-CH), 2.17 – 2.33 (m, 2H, piperidine 2-CH₂ and 6-CH₂), 2.36 (s, 3H, N-CH₃), 2.35 – 2.47 (m, 1H, piperidine 5-CH₂), 2.69 (ddd, *J* = 11.5, 4.1, 1.5 Hz, 1H, piperidine 2-CH₂), 2.83 (br d, *J* = 11.4 Hz, 1H, piperidine 6-CH₂), 3.00 (dt, *J* = 14.2, 2.5 Hz, 1H, piperidine 5-CH₂), 4.19 (ddq, *J* = 15.2, 10.7, 7.1 Hz, 2H, Et CH₂), 4.52 (hept, *J* = 6.0 Hz, 1H, *i*-Pr CH), 6.74 – 6.84 (m, 3H, Ph 2-CH, Ph 4-CH and Ph 6-CH), 7.24 (t, *J* = 7.9 Hz, 1H, Ph 5-CH).

¹³C NMR (CDCl₃): δ 12.6, 14.4, 22.0, 22.1, 32.8, 42.6, 45.9, 51.0, 58.8, 63.5, 69.9, 84.3, 113.2, 114.3, 117.3, 129.0, 143.4, 153.2, 157.7.

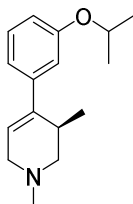
m/z: LCMS C₁₉H₂₉NO₄ [MH]⁺ calc 336.2, found 336.1 with *t*_R of 2.20 min.



4-(3-isopropoxyphenyl)-1,3-dimethyl-1,2,3,6-tetrahydropyridine (**161**)

To a two-neck flask containing ethyl (4-(3-isopropoxyphenyl)-1,3-dimethylpiperidin-4-yl) carbonate (**160**) (8.650 g, 25.79 mmol) was added anhydrous decalin (100 ml). The reaction was heated to reflux (195°C) for 24 hrs or until the reaction was complete by TLC. Ethanol produced in the reaction was removed by evaporation under vacuum. The decalin was washed with 2M

HCl (4 x 25 mL) and the combined aqueous phases were basified with 2M NaOH (200 mL) and the product extracted with EtOAc (3 x 50 mL). The organic phase was finally washed with water (50 mL) and brine (50 mL), dried with magnesium sulfate and solvents evaporated off under vacuum. Column chromatography (5% 1M NH₃/MeOH in EtOAc) afforded **161** as a pale yellow oil (6.248 g, 99%).



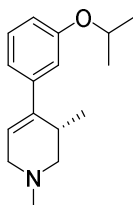
(R)-4-(3-isopropoxyphenyl)-1,3-dimethyl-1,2,3,6-tetrahydropyridine (161a)

[α]¹⁹_D: -79.7 (MeOH, c 1.00).

¹H NMR (CDCl₃): δ 1.00 (d, J = 6.9 Hz, 3H, piperidine 3-CH₃), 1.33 (d, J = 6.1 Hz, 6H, *i*-Pr CH₃), 2.38 (s, 3H, N-CH₃), 2.39 (dd, J = 10.9, 5.1 Hz, 1H, piperidine 2-CH₂), 2.68 (dd, J = 11.2, 4.9 Hz, 1H, piperidine 2-CH₂), 2.87 – 2.97 (m, 1H, piperidine 3-CH), 2.98 (dt, J = 16.8, 3.0 Hz, 1H, piperidine 6-CH₂), 3.09 (dt, J = 16.8, 3.0 Hz, 1H, piperidine 6-CH₂), 4.55 (hept, J = 6.0 Hz, 1H, *i*-Pr CH), 5.86 (td, J = 3.6, 1.2 Hz, 1H, piperidine 5-CH), 6.76 (ddd, 8.2, 2.5, 0.9 Hz, 1H, phenol 6-CH), 6.83 (t, J = 2.1 Hz, 1H phenol 2-CH), 6.87 (dt, J = 7.7, 1.2 Hz, 1H, phenol 4-CH), 7.20 (t, J = 7.9 Hz, 1H, phenol 5-CH).

¹³C NMR (CDCl₃): δ 18.9, 22.2, 22.3, 32.4, 46.1, 55.6, 60.4, 69.9, 114.2, 114.2, 118.7, 122.7, 129.3, 141.2, 142.7, 158.0.

m/z : LCMS C₁₆H₂₃NO [MH]⁺ calc 246.2, found 246.2 with t_R of 2.07 min.



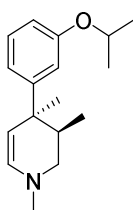
(S)-4-(3-isopropoxyphenyl)-1,3-dimethyl-1,2,3,6-tetrahydropyridine (161b)

[α]¹⁹_D: +79.7 (MeOH, c 1.00).

¹H NMR (CDCl₃): δ 1.00 (d, *J* = 6.9 Hz, 3H, piperidine 3-CH₃), 1.33 (d, *J* = 6.1 Hz, 6H, *i*-Pr CH₃), 2.38 (s, 3H, N-CH₃), 2.39 (dd, *J* = 10.9, 5.1 Hz, 1H, piperidine 2-CH₂), 2.68 (dd, *J* = 11.2, 4.9 Hz, 1H, piperidine 2-CH₂), 2.87 – 2.97 (m, 1H, piperidine 3-CH), 2.98 (dt, *J* = 16.8, 3.0 Hz, 1H, piperidine 6-CH₂), 3.09 (dt, *J* = 16.8, 3.0 Hz, 1H, piperidine 6-CH₂), 4.55 (hept, *J* = 6.0 Hz, 1H, *i*-Pr CH), 5.86 (td, *J* = 3.6, 1.2 Hz, 1H, piperidine 5-CH), 6.76 (ddd, 8.2, 2.5, 0.9 Hz, 1H, phenol 6-CH), 6.83 (t, *J* = 2.1 Hz, 1H phenol 2-CH), 6.87 (dt, *J* = 7.7, 1.2 Hz, 1H, phenol 4-CH), 7.20 (t, *J* = 7.9 Hz, 1H, phenol 5-CH).

¹³C NMR (CDCl₃): δ 18.9, 22.2, 22.3, 32.4, 46.1, 55.6, 60.4, 69.9, 114.2, 114.2, 118.7, 122.7, 129.3, 141.2, 142.7, 158.0.

m/z: LCMS C₁₆H₂₃NO [MH]⁺ calc 246.2, found 246.2 with *t_R* of 2.07 min.



(3*R*,4*S*)-4-(3-isopropoxyphenyl)-1,3,4-trimethyl-1,2,3,4-tetrahydropyridine (162a)

To a solution of 1-(4-(3-isopropoxyphenyl)-1,3-dimethyl-1,2,3,6-tetrahydropyridine) (**161a**) (588 mg, 2.40 mmol) in THF (10 ml) at -10°C was added *n*-Butyllithium (1.56 ml of a 1.48M solution in hexanes, 3.59 mmol, 1.5 eq) dropwise. The dark red solution was allowed to stir at -10°C for 30 minutes. The flask was then cooled to -50°C and dimethylsulphate (0.25 ml, 332 mg, 2.636 mmol, 1.1 eq) was added dropwise over 15 minutes. The reaction was then allowed to stir at -50°C until complete by TLC and LCMS (1 hour). A dilute solution of ammonium hydroxide (1:3 35% NH₄OH/water, 5 ml) and heptane (5 ml) were added at 0°C and stirred for a further 1 hour, allowing the solution to warm to room temperature. The layers were then separated and the aqueous phase extracted with EtOAc (25 mL). The combined organic phases were washed with water (10 mL) and brine (10 mL), dried over MgSO₄ and

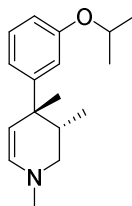
evaporated under vacuum. Column chromatography (1% 1M NH₃/MeOH in EtOAc) afforded **162a** as a pale yellow oil (481 mg, 77%).

[α]_D¹⁹: -59.7 (MeOH, c 1.00).

¹H NMR (CDCl₃): δ 0.60 (d, *J* = 7.0 Hz, 3H, piperidine 3-CH₃), 1.34 (d, *J* = 6.1 Hz, 6H, *i*-Pr CH₃), 1.44 (s, 3H, piperidine 4-CH₃), 1.92 (dq, *J* = 10.5, 6.9, 3.4 Hz, 1H, piperidine 3-CH), 2.47 (dd, *J* = 11.6, 10.4 Hz, 1H, piperidine 2-CH₂), 2.67 (dd, *J* = 11.5, 3.6 Hz, 1H, piperidine 2-CH₂), 2.67 (s, 3H, N-CH₃), 4.34 (d, *J* = 7.8 Hz, 1H, piperidine 5-CH), 4.53 (hept, *J* = 6.0 Hz, 1H *i*-Pr CH), 5.98 (d, *J* = 7.8 Hz, 1H, piperidine 6-CH), 6.72 (ddd, *J* = 8.2, 2.5, 1.1 Hz, 1H, phenol 6-CH), 6.94 – 6.98 (m, 2H, phenol 2-CH, 4-CH), 7.17 (t, *J* = 8.2 Hz, 1H, phenol 5-CH).

¹³C NMR (CDCl₃): δ 15.2, 22.3, 22.3, 28.2, 38.9, 40.3, 42.6, 52.9, 69.9, 106.3, 112.8, 117.4, 121.4, 127.9, 135.3, 148.1, 157.1.

m/z: LCMS C₁₇H₂₅NO [MH]⁺ calc 260.2, found 260.3 with *t*_R of 2.12 min.



(3S,4R)-4-(3-isopropoxyphenyl)-1,3,4-trimethyl-1,2,3,4-tetrahydropyridine (162b)

Experimental method unchanged from that described for the synthesis of (3R,4S)-4-(3-isopropoxyphenyl)-1,3,4-trimethyl-1,2,3,4-tetrahydropyridine (**162a**) yielding **162b** as a pale yellow oil (78%).

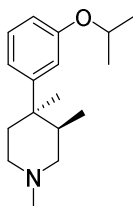
[α]_D¹⁹: +59.7 (MeOH, c 1.00).

¹H NMR (CDCl₃): δ 0.60 (d, *J* = 7.0 Hz, 3H, piperidine 3-CH₃), 1.34 (d, *J* = 6.1 Hz, 6H, *i*-Pr CH₃), 1.44 (s, 3H, piperidine 4-CH₃), 1.92 (dq, *J* = 10.5, 6.9, 3.4 Hz, 1H, piperidine 3-CH), 2.47 (dd, *J* = 11.6, 10.4 Hz, 1H, piperidine 2-CH₂), 2.67 (dd, *J* = 11.5, 3.6 Hz, 1H, piperidine 2-CH₂), 2.67 (s, 3H, N-CH₃), 4.34 (d, *J* = 7.8 Hz, 1H, piperidine 5-CH), 4.53 (hept, *J* = 6.0 Hz, 1H *i*-Pr CH), 5.98 (d, *J* = 7.8 Hz, 1H,

piperidine 6-CH), 6.72 (ddd, $J = 8.2, 2.5, 1.1$ Hz, 1H, phenol 6-CH), 6.94 – 6.98 (m, 2H, phenol 2-CH, 4-CH), 7.17 (t, $J = 8.2$ Hz, 1H, phenol 5-CH).

^{13}C NMR (CDCl_3): δ 15.2, 22.3, 22.3, 28.2, 38.9, 40.3, 42.6, 52.9, 69.9, 106.3, 112.8, 117.4, 121.4, 127.9, 135.3, 148.1, 157.1.

m/z : LCMS $\text{C}_{17}\text{H}_{25}\text{NO}$ $[\text{MH}]^+$ calc 260.2, found 260.3 with t_R of 2.12 min.



(3R,4R)-4-(3-isopropoxyphenyl)-1,3,4-trimethylpiperidine (163a)

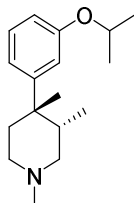
To a solution of (3R,4S)-4-(3-isopropoxyphenyl)-1,3,4-trimethyl-1,2,3,4-tetrahydropyridine (**162a**) (465 mg, 1.79 mmol) in methanol (10 mL) at 0°C was added sodium borohydride (109 mg, 2.87 mmol, 1.6 eq). It was stirred while warming to room temperature until complete by TLC. The solution was quenched with 1:1 acetone/sat. NaHCO_3 solution (10 mL). The solvents were evaporated off under vacuum and the remaining mixture re-dissolved in EtOAc (20 mL). This was then washed with water (10 mL) and brine (10 mL), dried over MgSO_4 and evaporated under vacuum. Column chromatography (5% 1M NH_3/MeOH in EtOAc) afforded **163a** as a pale yellow oil (332 mg, 71%).

$[\alpha]_D^{19}$: -69.4 (MeOH, c 1.00).

^1H NMR (CDCl_3): δ 0.80 (d, $J = 7.0$ Hz, 3H, piperidine 3- CH_3), 1.31 (s, 3H, piperidine 4- CH_3), 1.34 (dd, $J = 6.0, 1.9$ Hz, 6H, *i*-Pr CH_3), 1.60 (ddd, $J = 10.3, 3.4, 1.7$ Hz, 1H, piperidine 6- CH_2), 1.94-2.05 (m, 1H, piperidine 3-CH), 2.28 (s, 3H, N- CH_3), 2.32 (dt, $J = 9.0, 3.1$ Hz, 2H, piperidine 5- CH_2), 2.53 (d, $J = 2.9$ Hz, 2H, piperidine 2- CH_2), 2.76-2.82 (m, 1H, piperidine 6- CH_2), 4.54 (hept, $J = 6.1$ Hz, 1H, *i*-Pr CH), 6.70 (dd, $J = 8.2, 2.2$ Hz, 1H, phenol 4-CH), 6.82 (t, $J = 2.2$ Hz, 1H, phenol 2-CH), 6.86 (ddd, $J = 7.8, 1.8, 0.9$ Hz, 1H, phenol 6-CH), 7.20 (t, $J = 8.0$ Hz, 1H, phenol 5-CH).

^{13}C NMR (CDCl_3): δ 16.5, 22.1, 22.2, 27.6, 38.0, 38.8, 46.7, 52.3, 58.6, 69.7, 112.1, 114.4, 118.1, 128.9, 151.9, 157.8.

LCMS m/z for $\text{C}_{17}\text{H}_{27}\text{NO}$ $[\text{MH}]^+$ calc 262.2, found 262.2 with t_R of 2.14 min.



(3S,4S)-4-(3-isopropoxyphenyl)-1,3,4-trimethylpiperidine 163

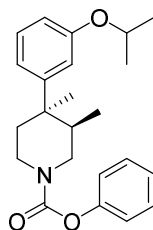
Experimental method unchanged from that described for the synthesis of (3R,4R)-4-(3-isopropoxyphenyl)-1,3,4-trimethylpiperidine (**163a**) yielding **163b** as a pale yellow oil (69%).

$[\alpha]^{19}_D$: +69.4 (MeOH, c 1.00).

^1H NMR (CDCl_3): δ 0.80 (d, $J = 7.0$ Hz, 3H, piperidine 3- CH_3), 1.31 (s, 3H, piperidine 4- CH_3), 1.34 (dd, $J = 6.0, 1.9$ Hz, 6H, *i*-Pr CH_3), 1.60 (ddd, $J = 10.3, 3.4, 1.7$ Hz, 1H, piperidine 6- CH_2), 1.94-2.05 (m, 1H, piperidine 3-CH), 2.28 (s, 3H, N- CH_3), 2.32 (dt, $J = 9.0, 3.1$ Hz, 2H, piperidine 5- CH_2), 2.53 (d, $J = 2.9$ Hz, 2H, piperidine 2- CH_2), 2.76-2.82 (m, 1H, piperidine 6- CH_2), 4.54 (hept, $J = 6.1$ Hz, 1H, *i*-Pr CH), 6.70 (dd, $J = 8.2, 2.2$ Hz, 1H, phenol 4-CH), 6.82 (t, $J = 2.2$ Hz, 1H, phenol 2-CH), 6.86 (ddd, $J = 7.8, 1.8, 0.9$ Hz, 1H, phenol 6-CH), 7.20 (t, $J = 8.0$ Hz, 1H, phenol 5-CH).

^{13}C NMR (CDCl_3): δ 16.5, 22.1, 22.2, 27.6, 38.0, 38.8, 46.7, 52.3, 58.6, 69.7, 112.1, 114.4, 118.1, 128.9, 151.9, 157.8.

m/z : LCMS $\text{C}_{17}\text{H}_{27}\text{NO}$ $[\text{MH}]^+$ calc 262.2, found 262.2 with t_R of 2.14 min.



Phenyl (3R,4R)-4-(3-isopropoxyphenyl)-3,4-dimethylpiperidine-1-carboxylate (164a)

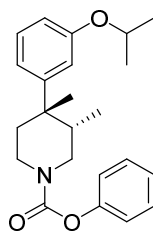
To a solution of (3R,4R)-4-(3-isopropoxyphenyl)-1,3,4-trimethylpiperidine (**163a**) (403 mg, 1.542 mmol) in anhydrous toluene (20 mL) at 85°C was added phenyl chloroformate (0.23 mL, 290 mg, 1.850 mmol, 1.2 eq) dropwise. The solution was heated to reflux and stirred for 2 hours. It was then cooled to 45°C and quenched with 1.4 M NaOH (5 mL) before allowing it to cool to room temperature. The layers were partitioned and the organic washed with 1:1 MeOH/1M HCl (10 mL x3), 1:1 MeOH/1M NaOH (10 mL), water (10 mL) and brine (10 mL), dried over MgSO₄ and evaporated under vacuum. Column chromatography (5% 1M NH₃/MeOH in EtOAc) afforded phenyl **164a** as an orange oil (423 mg, 75%).

[α]¹⁹_D: -65.1 (MeOH, c 1.00).

¹H NMR (CDCl₃): δ 0.71-0.82 (m, 3H, piperidine 3-CH₃), 1.35 (d, *J* = 6.1 Hz, 6H, *i*-Pr CH₃), 1.42 (s, 3H, piperidine 4-CH₃), 1.61-1.70 (m, 1H, piperidine 5-CH₂), 2.00-2.15 (m, 1H, piperidine 3-CH), 2.32 (dd, *J* = 13.0, 5.0 Hz, 1H, piperidine 5-CH₂), 3.13-3.60 (m, 2H, piperidine 2-CH₂, piperidine 6-CH₂), 3.94- 4.14 (m, 1H, piperidine 2-CH₂), 4.25-4.39 (m, 1H, piperidine 6-CH₂), 4.56 (septet, *J* = 6.1 Hz, 1H, *i*-Pr CH), 6.74 (ddd, *J* = 8.2, 2.5, 0.8 Hz, 1H, phenol 4-CH), 6.82 (t, *J* = 3.6 Hz, 1H, phenol 2-CH), 6.85 (d, *J* = 8.1 Hz, 1H, phenol 6-CH), 7.06 – 7.31 (m, 3H, phenol 5-CH, phenyl 2-CH, phenyl 6-CH), 7.32 – 7.48 (m, 3H, phenyl 3-CH, phenyl 4-CH, phenyl 5-CH).

¹³C NMR (CDCl₃): δ 14.3, 22.0, 26.4, 29.1, 29.6, 38.3, 38.4, 38.7, 40.3, 40.7, 45.9, 46.5, 69.6, 112.1, 112.2, 113.9, 117.5, 120.8, 121.6, 125.0, 126.2, 129.1, 129.4, 150.9, 157.8.

m/z: LCMS C₂₃H₂₉NO₃ [MH]⁺ calc 368.5, found 368.3 with *t*_R of 2.30 min.



Phenyl (3*S*,4*S*)-4-(3-isopropoxyphenyl)-3,4-dimethylpiperidine-1-carboxylate (164b)

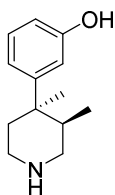
Experimental method unchanged from that described for the synthesis of phenyl (3*R*,4*R*)-4-(3-isopropoxyphenyl)-3,4-dimethylpiperidine-1-carboxylate (164a) yielding phenyl **164b** as an orange oil (74%).

$[\alpha]_D^{19}$: +65.1 (MeOH, *c* 1.00).

^1H NMR (CDCl_3): δ 0.71-0.82 (m, 3H, piperidine 3- CH_3), 1.35 (d, $J = 6.1$ Hz, 6H, *i*-Pr CH_3), 1.42 (s, 3H, piperidine 4- CH_3), 1.61-1.70 (m, 1H, piperidine 5- CH_2), 2.00-2.15 (m, 1H, piperidine 3-CH), 2.32 (dd, $J = 13.0, 5.0$ Hz, 1H, piperidine 5- CH_2), 3.13-3.60 (m, 2H, piperidine 2- CH_2 , piperidine 6- CH_2), 3.94- 4.14 (m, 1H, piperidine 2- CH_2), 4.25-4.39 (m, 1H, piperidine 6- CH_2), 4.56 (septet, $J = 6.1$ Hz, 1H, *i*-Pr CH), 6.74 (ddd, $J = 8.2, 2.5, 0.8$ Hz, 1H, phenol 4-CH), 6.82 (t, $J = 3.6$ Hz, 1H, phenol 2-CH), 6.85 (d, $J = 8.1$ Hz, 1H, phenol 6-CH), 7.06 – 7.31 (m, 3H, phenol 5-CH, phenyl 2-CH, phenyl 6-CH), 7.32 – 7.48 (m, 3H, phenyl 3-CH, phenyl 4-CH, phenyl 5-CH).

^{13}C NMR (CDCl_3): δ 14.3, 22.0, 26.4, 29.1, 29.6, 38.3, 38.4, 38.7, 40.3, 40.7, 45.9, 46.5, 69.6, 112.1, 112.2, 113.9, 117.5, 120.8, 121.6, 125.0, 126.2, 129.1, 129.4, 150.9, 157.8.

m/z : LCMS $\text{C}_{23}\text{H}_{29}\text{NO}_3$ $[\text{MH}]^+$ calc 368.5, found 368.3 with t_R of 2.30 min.



3-((3*R*,4*R*)-3,4-dimethylpiperidin-4-yl)phenol (146a)

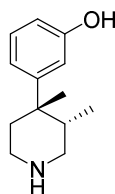
A solution of phenyl (3*R*,4*R*)-4-(3-isopropoxyphenyl)-3,4-dimethylpiperidine-1-carboxylate (**15a**) (500 mg, 1.36 mmol) in glacial acetic acid (0.84 ml) and 48% hydrobromic acid (0.84 ml) were heated to reflux for 16 hours. The solution was cooled to room temperature and extracted with methyl *tert*-butyl ether (x3) to remove any phenol by-product. The aqueous phase was titrated to pH 10 and extracted with 1:3 toluene/butan-1-ol until no further compound could be detected in the extracts. The combined extracts were evaporated under vacuum. Column chromatography (30% 1M NH₃/MeOH in EtOAc) afforded **146a** as an orange oil (240 mg, 86%) which dried into a foam at room temperature.

$[\alpha]_D^{19}$: +118.7 (MeOH, *c* 1.00).

¹H NMR (MeOD): δ 0.84 (d, *J* = 7.3 Hz, 3H, piperidine 3-CH₃), 1.44 (s, 3H, piperidine 4-CH₃), 1.86 (dt, *J* = 14.0, 3.6 Hz, 1H, piperidine 5-CH₂), 2.26 – 2.34 (m, 1H, piperidine 3-CH), 2.39 (ddd, *J* = 14.5, 11.1, 6.2 Hz, 1H, piperidine 5-CH₂), 3.16 (dd, *J* = 13.1, 3.2 Hz, 1H, piperidine 6-CH₂), 3.26 – 3.39 (m, 2H, piperidine 2-CH₂), 3.50 (dd, *J* = 13.0, 3.8 Hz, 1H, piperidine 6-CH₂), 6.66 (dd, *J* = 7.9, 2.2 Hz, 1H, phenol 6-CH), 6.76 (t, *J* = 2.1 Hz, 1H, phenol 2-CH), 6.80 (dd, *J* = 8.0, 1.7 Hz, 1H, phenol 4-CH), 7.16 (t, *J* = 7.9 Hz, 1H, phenol 5-CH).

¹³C NMR (MeOD): δ 14.8, 24.2, 27.4, 37.4, 38.8, 41.7, 47.2, 113.5, 114.1, 117.5, 130.6, 150.2, 158.8.

m/z: LCMS C₁₃H₁₉NO [MH]⁺ calc 206.3, found 206.3 with *t_R* of 0.84 min.



3-((3*S*,4*S*)-3,4-dimethylpiperidin-4-yl)phenol (**146b**)

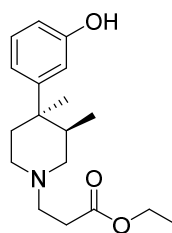
Experimental method unchanged from that described for the synthesis of 3-((3*R*,4*R*)-3,4-dimethylpiperidin-4-yl)phenol (**146a**) yielding **146b** as an orange oil (82%) which dried into a foam at room temperature.

$[\alpha]_{\text{D}}^{19}$: -118.7 (MeOH, c 1.00).

^1H NMR (MeOD): δ 0.84 (d, J = 7.3 Hz, 3H, piperidine 3- CH_3), 1.44 (s, 3H, piperidine 4- CH_3), 1.86 (dt, J = 14.0, 3.6 Hz, 1H, piperidine 5- CH_2), 2.26 – 2.34 (m, 1H, piperidine 3-CH), 2.39 (ddd, J = 14.5, 11.1, 6.2 Hz, 1H, piperidine 5- CH_2), 3.16 (dd, J = 13.1, 3.2 Hz, 1H, piperidine 6- CH_2), 3.26 – 3.39 (m, 2H, piperidine 2- CH_2), 3.50 (dd, J = 13.0, 3.8 Hz, 1H, piperidine 6- CH_2), 6.66 (dd, J = 7.9, 2.2 Hz, 1H, phenol 6-CH), 6.76 (t, J = 2.1 Hz, 1H, phenol 2-CH), 6.80 (dd, J = 8.0, 1.7 Hz, 1H, phenol 4-CH), 7.16 (t, J = 7.9 Hz, 1H, phenol 5-CH).

^{13}C NMR (MeOD): δ 14.8, 24.2, 27.4, 37.4, 38.8, 41.7, 47.2, 113.5, 114.1, 117.5, 130.6, 150.2, 158.8.

m/z : LCMS $\text{C}_{13}\text{H}_{19}\text{NO}$ $[\text{MH}]^+$ calc 206.3, found 206.3 with t_{R} of 0.84 min.



Ethyl 3-((3R,4R)-4-(3-hydroxyphenyl)-3,4-dimethylpiperidin-1-yl)propanoate (167a)

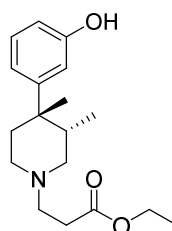
To a solution of 3-((3R,4R)-3,4-dimethylpiperidin-4-yl)phenol (**146a**) (240 mg, 1.17 mmol) in anhydrous tetrahydrofuran (10 mL) at 50 °C was added ethyl acrylate (0.25 mL, 235 mg, 2.33 mmol, 2 eq) dropwise. The reaction was left to stir for 20 hours at 50°C. The solution was cooled to room temperature and filtered through celite, washing with MeOH before the solvents were evaporated under vacuum. Column chromatography (5% 1M NH_3/MeOH in EtOAc) afforded **167a** as a white solid (300 mg, 84%).

^1H NMR (CDCl_3) δ 0.73 (d, J = 7.0 Hz, 3H, piperidine 3- CH_3), 1.25 (t, J = 7.2 Hz, 3H, Et- CH_3), 1.30 (s, 3H, piperidine 4- CH_3), 1.58 (d, J = 12.9 Hz, 1H, piperidine 5- CH_2), 1.93 – 2.01 (m, 1H, piperidine 3-CH), 2.29 (td, J = 12.4, 4.6 Hz, 1H, piperidine 5- CH_2), 2.41 (td, J = 11.5, 2.6 Hz, 1H, piperidine 6- CH_2), 2.51 (t, J = 7.1 Hz, 2H, propanoate α - CH_2), 2.58 (t, J = 3.4 Hz, 2H, piperidine 2- CH_2), 2.61-2.80

(m, 2H, propanoate β -CH₂), 2.85 (dt, $J = 10.8, 3.7$ Hz, 1H, piperidine 6-CH₂), 4.13 (qd, $J = 7.1, 2.0$ Hz, 2H, Et-CH₂), 6.63 (dd, $J = 7.8, 2.3$ Hz, 1H, phenol 4-CH), 6.74 (t, $J = 2.1$ Hz, 1H, phenol 2-CH), 6.83 (d, $J = 8.0$ Hz, 1H, phenol 6-CH), 7.16 (t, $J = 7.9$ Hz, 1H, phenol 5-CH).

¹³C NMR (CDCl₃) δ 16.1, 27.5, 30.8, 32.0, 38.4, 38.9, 49.9, 51.7, 53.9, 55.8, 112.6, 113.2, 117.7, 129.2, 151.6, 156.1, 173.4.

m/z : LCMS C₁₈H₂₇NO₃ [MH]⁺ calc 306.4, found 306.2 with t_R of 1.89 min.



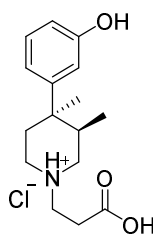
Ethyl 3-((3S,4S)-4-(3-hydroxyphenyl)-3,4-dimethylpiperidin-1-yl)propanoate (167b)

Experimental method unchanged from that described for the synthesis of ethyl 3-((3R,4R)-4-(3-hydroxyphenyl)-3,4-dimethylpiperidin-1-yl)propanoate (**167a**) yielding **167b** as a white solid (84%).

¹H NMR (CDCl₃): δ 0.73 (d, $J = 7.0$ Hz, 3H, piperidine 3-CH₃), 1.25 (t, $J = 7.2$ Hz, 3H, Et-CH₃), 1.30 (s, 3H, piperidine 4-CH₃), 1.58 (d, $J = 12.9$ Hz, 1H, piperidine 5-CH₂), 1.93 – 2.01 (m, 1H, piperidine 3-CH), 2.29 (td, $J = 12.4, 4.6$ Hz, 1H, piperidine 5-CH₂), 2.41 (td, $J = 11.5, 2.6$ Hz, 1H, piperidine 6-CH₂), 2.51 (t, $J = 7.1$ Hz, 2H, propanoate α -CH₂), 2.58 (t, $J = 3.4$ Hz, 2H, piperidine 2-CH₂), 2.61-2.80 (m, 2H, propanoate β -CH₂), 2.85 (dt, $J = 10.8, 3.7$ Hz, 1H, piperidine 6-CH₂), 4.13 (qd, $J = 7.1, 2.0$ Hz, 2H, Et-CH₂), 6.63 (dd, $J = 7.8, 2.3$ Hz, 1H, phenol 4-CH), 6.74 (t, $J = 2.1$ Hz, 1H, phenol 2-CH), 6.83 (d, $J = 8.0$ Hz, 1H, phenol 6-CH), 7.16 (t, $J = 7.9$ Hz, 1H, phenol 5-CH).

¹³C NMR (CDCl₃): δ 16.1, 27.5, 30.8, 32.0, 38.4, 38.9, 49.9, 51.7, 53.9, 55.8, 112.6, 113.2, 117.7, 129.2, 151.6, 156.1, 173.4

m/z : LCMS C₁₈H₂₇NO₃ [MH]⁺ calc 306.4, found 306.2 with t_R of 1.89 min.



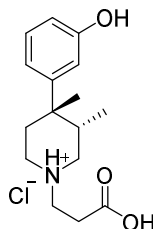
3-((3R,4R)-4-(3-hydroxyphenyl)-3,4-dimethylpiperidin-1-yl)propanoic acid hydrochloride (165a)

To a solution of ethyl 3-((3R,4R)-4-(3-hydroxyphenyl)-3,4-dimethylpiperidin-1-yl)propanoate (**167a**) (40 mg, 0.913 mmol) in dioxane (1 mL) was added 4M HCl (in dioxane and water) (0.5 mL) and heated to reflux (105°C) for 2 hours. Once cooled to room temperature the solvents were evaporated *in vacuo* to give **165a** as a white solid (39 mg, 95%).

¹H NMR (MeOD): δ 0.83 (d, *J* = 7.3 Hz, 3H, piperidine 3-CH₃), 1.45 (s, 3H, piperidine 4-CH₃), 1.93 (d, *J* = 14.8 Hz, 1H, piperidine 5-CH₂), 2.34 – 2.44 (m, 1H, piperidine 3-CH), 2.49 (td, *J* = 14.1, 4.4 Hz, 1H, piperidine 5-CH₂), 2.91 (t, *J* = 7.0 Hz, 2H, propanoate α-CH₂), 3.42 (dt, *J* = 14.2, 2.7 Hz, 1H, piperidine 6-CH₂), 3.49 (t, *J* = 7.1 Hz, 2H, propanoate β-CH₂), 3.53 – 3.62 (m, 3H, piperidine 2-CH₂, piperidine 6-CH₂), 6.66 (dd, *J* = 8.0, 2.4 Hz, 1H, phenol 6-CH), 6.73 (t, *J* = 2.1 Hz, 1H, phenol 2-CH), 6.77 (dd, *J* = 7.7, 1.8 Hz, 1H, phenol 4-CH), 7.16 (t, *J* = 7.8 Hz, 1H, phenol 5-CH).

¹³C NMR (MeOD): δ 15.1, 27.0, 28.7, 29.3, 38.3, 38.4, 43.7, 50.9, 54.1, 56.0, 113.27, 114.2, 117.3, 130.7, 150.2, 158.8, 173.6.

m/z: HRMS C₁₆H₂₃NO₃ [MH]⁺ calc 278.1751, found 278.1755.



3-((3S,4S)-4-(3-hydroxyphenyl)-3,4-dimethylpiperidin-1-yl)propanoic acid hydrochloride (165b)

Experimental method unchanged from that described for the synthesis of 3-((3*R*,4*R*)-4-(3-hydroxyphenyl)-3,4-dimethylpiperidin-1-yl)propanoic acid hydrochloride (**165a**) yielding **165b** as a white solid (98%).

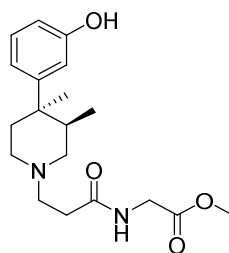
¹H NMR (MeOD): δ 0.83 (d, *J* = 7.3 Hz, 3H, piperidine 3-CH₃), 1.45 (s, 3H, piperidine 4-CH₃), 1.93 (d, *J* = 14.8 Hz, 1H, piperidine 5-CH₂), 2.34 – 2.44 (m, 1H, piperidine 3-CH), 2.49 (td, *J* = 14.1, 4.4 Hz, 1H, piperidine 5-CH₂), 2.91 (t, *J* = 7.0 Hz, 2H, propanoate α-CH₂), 3.42 (dt, *J* = 14.2, 2.7 Hz, 1H, piperidine 6-CH₂), 3.49 (t, *J* = 7.1 Hz, 2H, propanoate β-CH₂), 3.53 – 3.62 (m, 3H, piperidine 2-CH₂, piperidine 6-CH₂), 6.66 (dd, *J* = 8.0, 2.4 Hz, 1H, phenol 6-CH), 6.73 (t, *J* = 2.1 Hz, 1H, phenol 2-CH), 6.77 (dd, *J* = 7.7, 1.8 Hz, 1H, phenol 4-CH), 7.16 (t, *J* = 7.8 Hz, 1H, phenol 5-CH).

¹³C NMR (MeOD): δ 15.1, 27.0, 28.7, 29.3, 38.3, 38.4, 43.7, 50.9, 54.1, 56.0, 113.27, 114.2, 117.3, 130.7, 150.2, 158.8, 173.6.

m/z: HRMS C₁₆H₂₃NO₃ [MH]⁺ calc 278.1751, found 278.1754.

General procedure 2 – amide coupling of 3-(4-(3-hydroxyphenyl)-3,4-dimethylpiperidin-1-yl)propanoic acids to amino acid methyl esters

To a solution of a 3-(4-(3-hydroxyphenyl)-3,4-dimethylpiperidin-1-yl)propanoic acid (**165a** or **165b**) (1 eq) in DMF was added HBTU (0.5 eq), HOBT (1 eq) and amino acid methyl ester hydrochloride (1 eq). TEA (4 eq) was then added dropwise and the solution was stirred at room temperature for 24 hours. The DMF was evaporated off under vacuum and before re-dissolving in toluene and further evaporation under vacuum to remove any residual DMF. Column chromatography (5% 1M NH₃/MeOH in EtOAc) of the product afforded the product. Where necessary, further purification was carried out using reverse phase HPLC (system 3).

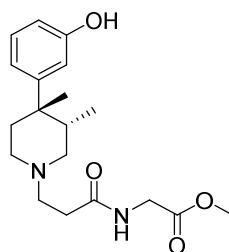


Methyl (3-((3R,4R)-4-(3-hydroxyphenyl)-3,4-dimethylpiperidin-1-yl)propanoyl)glycinate (166a)

The title compound was synthesised as described in general procedure 2, using 3-((3R,4R)-4-(3-hydroxyphenyl)-3,4-dimethylpiperidin-1-yl)propanoic acid hydrochloride (**165a**) (23 mg, 0.072 mmol, 1 eq) and glycine methyl ester hydrochloride (9 mg, 0.072 mmol, 1 eq) to give **166a** as a white solid (4 mg, 16%).

^1H NMR (MeOD) δ 0.77 (d, J = 7.0 Hz, 3H, piperidine 3-CH₃), 1.32 (s, 3H, piperidine 4-CH₃), 1.63 (d, J = 13.2 Hz, 1H, piperidine 5-CH₂), 2.02 – 2.10 (m, 1H, piperidine 3-CH), 2.35 (td, J = 12.6, 4.2 Hz, 1H, piperidine 5-CH₂), 2.41 – 2.51 (m, 1H, piperidine 6-CH₂), 2.47 (t, J = 6.6 Hz, 2H, propanamide α -CH₂), 2.61 – 2.77 (m, 4H, piperidine 2-CH₂, propanamide β -CH₂), 2.93 (dt, J = 11.0, 4.0 Hz, 1H, piperidine 6-CH₂), 3.71 (s, 3H, O-CH₃), 3.92 (d, J = 17.8 Hz, 1H, glycine CH₂), 3.99 (d, J = 17.8 Hz, 1H, glycine CH₂), 6.59 (dd, J = 8.0, 2.4 Hz, 1H, phenol 6-CH), 6.75 (d, J = 2.2 Hz, 1H, phenol 2-CH), 6.78 (d, J = 8.4 Hz, 1H, phenol 4-CH), 7.11 (t, J = 7.9 Hz, 1H, phenol 5-CH).

m/z : HRMS C₁₉H₂₈N₂O₄ [MH]⁺ calc 349.2122, found 349.2116.



Methyl (3-((3S,4S)-4-(3-hydroxyphenyl)-3,4-dimethylpiperidin-1-yl)propanoyl)glycinate (166b)

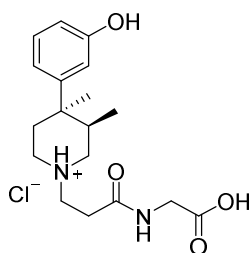
The title compound was synthesised as described in general procedure 2, using 3-((3*S*,4*S*)-4-(3-hydroxyphenyl)-3,4-dimethylpiperidin-1-yl)propanoic acid hydrochloride (**146b**) (23 mg, 0.072 mmol, 1 eq) and glycine methyl ester hydrochloride (9 mg, 0.072 mmol, 1 eq) to give **166b** as a white solid (4 mg, 16%).

¹H NMR (MeOD) δ 0.77 (d, $J = 7.0$ Hz, 3H, piperidine 3-CH₃), 1.32 (s, 3H, piperidine 4-CH₃), 1.63 (d, $J = 13.2$ Hz, 1H, piperidine 5-CH₂), 2.02 – 2.10 (m, 1H, piperidine 3-CH), 2.35 (td, $J = 12.6, 4.2$ Hz, 1H, piperidine 5-CH₂), 2.41 – 2.51 (m, 1H, piperidine 6-CH₂), 2.47 (t, $J = 6.6$ Hz, 2H, propanamide α -CH₂), 2.61 – 2.77 (m, 4H, piperidine 2-CH₂, propanamide β -CH₂), 2.93 (dt, $J = 11.0, 4.0$ Hz, 1H, piperidine 6-CH₂), 3.71 (s, 3H, O-CH₃), 3.92 (d, $J = 17.8$ Hz, 1H, glycine CH₂), 3.99 (d, $J = 17.8$ Hz, 1H, glycine CH₂), 6.59 (dd, $J = 8.0, 2.4$ Hz, 1H, phenol 6-CH), 6.75 (d, $J = 2.2$ Hz, 1H, phenol 2-CH), 6.78 (d, $J = 8.4$ Hz, 1H, phenol 4-CH), 7.11 (t, $J = 7.9$ Hz, 1H, phenol 5-CH).

m/z : HRMS C₁₉H₂₈N₂O₄ [MH]⁺ calc 349.2122, found 349.2112.

General procedure 3 – Ester hydrolysis of 3-(4-(3-hydroxyphenyl)-3,4-dimethylpiperidin-1-yl)propanoylamido methyl esters

To a solution of the 3-(4-(3-hydroxyphenyl)-3,4-dimethylpiperidin-1-yl)propanoylamido methyl ester in dioxane (0.5 mL) was added 4M HCl (in dioxane and water) (0.1 mL) and heated to reflux (105°C) for 2 hours. Once cooled to room temperature the solvents were evaporated to give the 3-(4-(3-hydroxyphenyl)-3,4-dimethylpiperidin-1-yl)propanoylamido acid hydrochloride product.

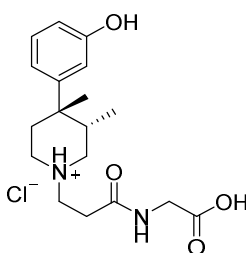


(3-((3*R*,4*R*)-4-(3-hydroxyphenyl)-3,4-dimethylpiperidin-1-yl)propanoyl)glycine hydrochloride (**136a**)

The title compound was synthesised as described in general procedure 3, using methyl (3-((3*R*,4*R*)-4-(3-hydroxyphenyl)-3,4-dimethylpiperidin-1-yl)propanoyl)glycinate (**166a**) (5 mg, 0.014 mmol) to give **136a** as a white solid (5 mg, 100%).

¹H NMR (MeOD) δ 0.82 (d, *J* = 7.4 Hz, 3H, piperidine 3-CH₃), 1.45 (s, 3H, piperidine 4-CH₃), 1.94 (d, *J* = 14.8 Hz, 1H, piperidine 5-CH₂), 2.35 – 2.44 (m, 1H, piperidine 3-CH), 2.49 (td, *J* = 14.1, 4.5 Hz, 1H, piperidine 5-CH₂), 2.85 (t, *J* = 6.4 Hz, 2H, propanamide α-CH₂), 3.38 – 3.70 (m, 5H, propanamide β-CH₂, piperidine 2-CH₂, piperidine 6-CH₂), 3.75 (dd, *J* = 11.4, 6.4 Hz, 1H, piperidine 6-CH₂), 6.66 (dd, *J* = 8.0, 2.3 Hz, 1H, phenol 6-CH), 6.73 (t, *J* = 2.2 Hz, 1H, phenol 2-CH), 6.78 (d, *J* = 7.8 Hz, 1H, phenol 4-CH), 7.17 (t, *J* = 7.9 Hz, 1H, phenol 5-CH).

m/z HRMS C₁₈H₂₆N₂O₄ [MH]⁺ calc 335.1965, found 335.1955.

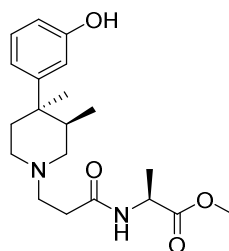


(3-((3*S*,4*S*)-4-(3-hydroxyphenyl)-3,4-dimethylpiperidin-1-yl)propanoyl)glycine hydrochloride (136b**)**

The title compound was synthesised as described in general procedure 3, using methyl (3-((3*S*,4*S*)-4-(3-hydroxyphenyl)-3,4-dimethylpiperidin-1-yl)propanoyl)glycinate (**166b**) (5 mg, 0.014 mmol) to give **136b** as a white solid (5 mg, 100%).

¹H NMR (MeOD) δ 0.82 (d, *J* = 7.4 Hz, 3H, piperidine 3-CH₃), 1.45 (s, 3H, piperidine 4-CH₃), 1.94 (d, *J* = 14.8 Hz, 1H, piperidine 5-CH₂), 2.35 – 2.44 (m, 1H, piperidine 3-CH), 2.49 (td, *J* = 14.1, 4.5 Hz, 1H, piperidine 5-CH₂), 2.85 (t, *J* = 6.4 Hz, 2H, propanamide α-CH₂), 3.38 – 3.70 (m, 5H, propanamide β-CH₂, piperidine 2-CH₂, piperidine 6-CH₂), 3.75 (dd, *J* = 11.4, 6.4 Hz, 1H, piperidine 6-CH₂), 6.66 (dd, *J* = 8.0, 2.3 Hz, 1H, phenol 6-CH), 6.73 (t, *J* = 2.2 Hz, 1H, phenol 2-CH), 6.78 (d, *J* = 7.8 Hz, 1H, phenol 4-CH), 7.17 (t, *J* = 7.9 Hz, 1H, phenol 5-CH).

m/z HRMS $C_{18}H_{26}N_2O_4$ $[MH]^+$ calc 335.1965, found 335.1958.



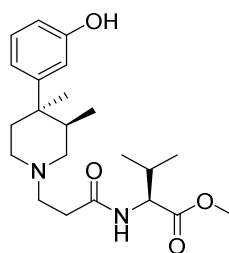
Methyl (3-((3R,4R)-4-(3-hydroxyphenyl)-3,4-dimethylpiperidin-1-yl)propanoyl)-L-alaninate (166c)

The title compound was synthesised as described in general procedure 2, using 3-((3R,4R)-4-(3-hydroxyphenyl)-3,4-dimethylpiperidin-1-yl)propanoic acid hydrochloride (**165a**) (25 mg, 0.080 mmol, 1 eq) and *L*-alanine methyl ester hydrochloride (11 mg, 0.080 mmol, 1 eq) to give **166c** as a white solid (4 mg, 14%).

1H NMR (DMSO- d_6): δ 0.67 (d, J = 6.9 Hz, 3H, piperidine 3- CH_3), 1.22 (s, 3H, piperidine 4- CH_3), 1.23 (d, J = 7.6 Hz, 3H, alanine CH_3), 1.51 (d, J = 12.8 Hz, 1H, piperidine 5- CH_2), 1.96 (d, J = 7.3 Hz, 1H, piperidine 3-CH), 2.14 (dt, J = 12.7, 6.4 Hz, 1H, piperidine 5- CH_2), 2.22 – 2.35 (m, 2H, piperidine 2- CH_2 , piperidine 6- CH_2), 2.28 (t, J = 6.9 Hz, 2H, propanamide α - CH_2), 2.47 – 2.58 (m, 3H, propanamide β - CH_2 , piperidine 2- CH_2), 2.82 (d, J = 10.7 Hz, 1H, piperidine 6- CH_2), 3.62 (s, 3H, O- CH_3), 4.29 (p, J = 7.2 Hz, 1H, alanine α -CH), 6.55 (dd, J = 7.7, 2.3 Hz, 1H, phenol 6-CH), 6.66 (t, J = 2.1 Hz, 1H, phenol 2-CH), 6.71 (d, J = 8.0 Hz, 1H, phenol 4-CH), 7.08 (t, J = 7.9 Hz, 1H, phenol 5-CH), 8.21 (s, 1H, phenol OH), 8.55 (d, J = 7.3 Hz, 1H, amide NH).

^{13}C NMR (DMSO- d_6): δ 16.1, 17.4, 27.2, 29.1, 32.6, 37.9, 47.2, 49.0, 50.9, 53.5, 54.7, 112.2, 112.4, 116.0, 128.8, 157.1, 163.8, 171.2, 173.2.

m/z : HRMS $C_{20}H_{30}N_2O_4$ $[MH]^+$ calc 363.2278, found 363.2288.



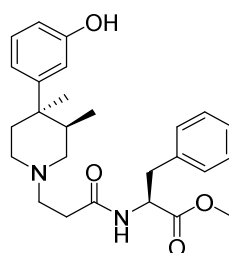
Methyl (3-((3R,4R)-4-(3-hydroxyphenyl)-3,4-dimethylpiperidin-1-yl)propanoyl)-L-valinate (166d)

The title compound was synthesised as described in general procedure 2, using 3-((3R,4R)-4-(3-hydroxyphenyl)-3,4-dimethylpiperidin-1-yl)propanoic acid hydrochloride (**165a**) (25 mg, 0.080 mmol, 1 eq) and *L*-valine methyl ester hydrochloride (13 mg, 0.080 mmol, 1 eq) to give **166d** as a white solid (5 mg, 16%).

^1H NMR (MeOD): δ 0.85 (d, $J = 7.3$ Hz, 3H, piperidine 3-CH₃), 0.97 (dd, $J = 6.8, 1.0$ Hz, 6H, valine CH₃), 1.42 (s, 3H, piperidine 4-CH₃), 1.89 (dt, $J = 13.6, 3.8$ Hz, 1H, piperidine 5-CH₂), 2.15 (dp, $J = 7.0, 6.6$ Hz, 1H, valine β -CH), 2.27 – 2.37 (m, 1H, piperidine 3-CH), 2.46 (ddd, $J = 15.6, 12.1, 4.3$ Hz, 1H, piperidine 5-CH₂), 2.80 (t, $J = 6.7$ Hz, 2H, propanamide α -CH₂), 3.13 – 3.31 (m, 2H, piperidine 2-CH₂, piperidine 6-CH₂), 3.32 – 3.41 (m, 3H, propanamide β -CH₂, piperidine 2-CH₂), 3.45 (d, $J = 12.4$ Hz, 1H, piperidine 6-CH₂), 3.72 (s, 3H, O-CH₃), 4.35 (d, $J = 5.9$ Hz, 1H, valine α -CH), 6.65 (ddd, $J = 8.1, 2.4, 0.9$ Hz, 1H, phenol 6-CH), 6.75 (t, $J = 2.1$ Hz, 1H, phenol 2-CH), 6.79 (dt, $J = 7.8, 1.5$ Hz, 1H, phenol 4-CH), 7.16 (t, $J = 7.9$ Hz, 1H, phenol 5-CH), 8.45 (s, 1H, phenol OH).

^{13}C NMR (MeOD): δ 15.2, 18.5, 19.4, 27.6, 30.0, 30.7, 38.8, 38.9, 50.6, 52.5, 54.6, 55.9, 59.4, 113.7, 114.1, 117.7, 130.6, 158.7, 169.0, 173.1, 173.5.

m/z : HRMS C₂₂H₃₄N₂O₄ [MH]⁺ calc 391.2591, found 391.2593.



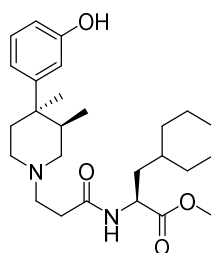
Methyl (3-((3*R*,4*R*)-4-(3-hydroxyphenyl)-3,4-dimethylpiperidin-1-yl)propanoyl)-*L*-phenylalaninate (166e)

The title compound was synthesised as described in general procedure 2, using 3-((3*R*,4*R*)-4-(3-hydroxyphenyl)-3,4-dimethylpiperidin-1-yl)propanoic acid hydrochloride (**165a**) (25 mg, 0.080 mmol, 1 eq) and *L*-phenylalanine methyl ester hydrochloride (17 mg, 0.080 mmol, 1 eq) to give **166e** as a white solid (6 mg, 17%).

¹H NMR (CDCl₃): δ 0.60 (d, *J* = 7.0 Hz, 3H, piperidine 3-CH₃), 1.28 (s, 3H, piperidine 4-CH₃), 1.58 (dd, *J* = 10.5, 3.9 Hz, 1H, piperidine 5-CH₂), 1.87 – 2.02 (m, 1H, piperidine 3-CH), 2.21 – 2.36 (m, 2H, piperidine 5-CH₂, piperidine 6-CH₂), 2.40 (qt, *J* = 16.7, 5.4 Hz, 2H, propanamide β-CH₂), 2.50 – 2.62 (m, 4H, propanamide α-CH₂, piperidine 2-CH₂), 2.88 – 2.97 (m, 1H, piperidine 6-CH₂), 3.00 (dd, *J* = 13.9, 6.9 Hz, 1H, phenylalanine CH₂), 3.11 (dd, *J* = 13.9, 6.1 Hz, 1H, phenylalanine CH₂), 3.68 (s, 3H, O-CH₃), 4.92 (dt, *J* = 8.2, 6.5 Hz, 1H, phenylalanine α-CH), 6.67 (dd, *J* = 7.9, 2.4 Hz, 1H, phenol 6-CH), 6.77 (t, *J* = 2.1 Hz, 1H, phenol 2-CH), 6.80 (dd, *J* = 7.9, 1.7 Hz, 1H, phenol 4-CH), 7.06 – 7.11 (m, 2H, phenylalanine *ortho*-CH), 7.13 – 7.25 (m, 3H, phenylalanine *para*-CH, phenylalanine *meta*-CH), 7.16 (t, *J* = 7.9 Hz, 1H, phenol 5-CH), 9.10 (d, *J* = 8.4 Hz, 1H, amide NH).

¹³C NMR (CDCl₃): δ 16.3, 27.6, 30.4, 31.9, 38.3, 38.6, 38.6, 49.2, 52.3, 53.2, 54.3, 56.1, 112.6, 113.1, 117.8, 127.0, 128.5, 129.3, 129.4, 136.6, 151.7, 156.2, 172.2, 172.8.

m/z: HRMS C₂₆H₃₄N₂O₄ [MH]⁺ calc 439.2591, found 439.2597.



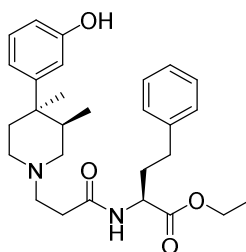
Methyl (S)-3-cyclohexyl-2-(3-((3*R*,4*R*)-4-(3-hydroxyphenyl)-3,4-dimethylpiperidin-1-yl)propanamido)propanoate (166f)

The title compound was synthesised as described in general procedure 2, using 3-((3*R*,4*R*)-4-(3-hydroxyphenyl)-3,4-dimethylpiperidin-1-yl)propanoic acid hydrochloride (**165a**) (25 mg, 0.080 mmol, 1 eq) and *L*-cyclohexylalanine methyl ester hydrochloride (18 mg, 0.080 mmol, 1 eq) to give **166f** as a white solid (6 mg, 17%).

¹H NMR (MeOD): δ 0.85 (d, *J* = 7.4 Hz, 3H, piperidine 3-CH₃), 0.88 – 1.05 (m, 2H, cyclohexyl 2-CH₂, cyclohexyl 6-CH₂), 1.14 – 1.40 (m, 4H, cyclohexyl 3-CH₂, cyclohexyl 4-CH₂, cyclohexyl 5-CH₂), 1.42 (s, 3H, piperidine 4-CH₃), 1.50 – 1.82 (m, 7H, cyclohexylalanine β-CH₂, cyclohexyl 1-CH, cyclohexyl 2-CH₂, cyclohexyl 3-CH₂, cyclohexyl 5-CH₂, cyclohexyl 6-CH₂), 1.88 (d, *J* = 14.5 Hz, 1H, piperidine 5-CH₂), 2.26 – 2.37 (m, 1H, piperidine 3-CH), 2.46 (td, *J* = 12.6, 4.2 Hz, 1H, piperidine 5-CH₂), 2.76 (t, *J* = 6.6 Hz, 2H, propanamide α-CH₂), 3.10 – 3.24 (m, 2H, piperidine 2-CH₂, piperidine 6-CH₂), 3.24 – 3.40 (m, 3H, piperidine 2-CH₂, propanamide β-CH₂), 3.44 (d, *J* = 12.0 Hz, 1H, piperidine 6-CH₂), 3.70 (s, 3H, O-CH₃), 4.48 (dd, *J* = 9.9, 5.1 Hz, 1H, cyclohexylalanine α-CH), 6.65 (ddd, *J* = 8.1, 2.4, 0.8 Hz, 1H, phenol 6-CH), 6.75 (t, *J* = 2.1 Hz, 1H, phenol 2-CH), 6.79 (dt, *J* = 7.9, 1.3 Hz, 1H, phenol 4-CH), 7.16 (t, *J* = 7.9 Hz, 1H, phenol 5-CH), 8.43 (s, 1H, OH)

¹³C NMR (MeOD): δ 15.3, 27.1, 27.3, 27.5, 30.2, 30.7, 33.2, 34.7, 35.4, 38.8, 39.0, 40.0, 50.7, 51.6, 52.7, 54.5, 55.9, 113.7, 114.1, 117.7, 130.5, 158.7, 168.7, 173.1, 174.7.

m/z: HRMS C₂₆H₄₀N₂O₄ [MH]⁺ calc 445.3061, found 445.3058.



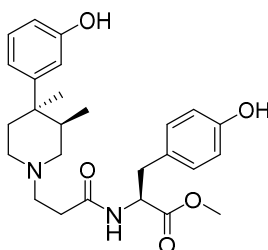
Ethyl (S)-2-(3-((3*R*,4*R*)-4-(3-hydroxyphenyl)-3,4-dimethylpiperidin-1-yl)propanamido)-4-phenylbutanoate (166g)

The title compound was synthesised as described in general procedure 2, using 3-((3*R*,4*R*)-4-(3-hydroxyphenyl)-3,4-dimethylpiperidin-1-yl)propanoic acid hydrochloride (**165a**) (25 mg, 0.080 mmol, 1 eq) and *L*-homophenylalanine ethyl ester hydrochloride (18 mg, 0.080 mmol, 1 eq) to give **166g** as a white solid (6 mg, 16%).

¹H NMR (DMSO-*d*₆): δ 0.67 (d, *J* = 6.9 Hz, 3H, piperidine 3-CH₃), 1.15 (t, *J* = 6.3 Hz, 3H, Et-CH₃) 1.22 (s, 3H, piperidine 4-CH₃), 1.51 (d, *J* = 12.7 Hz, 1H, piperidine 5-CH₂), 1.74 (m, 4H, homophenylalanine β-CH₂, propanamide α-CH₂), 2.05 – 2.10 (m, 1H, piperidine 3-CH), 2.15 (td, *J* = 12.7, 4.2 Hz, 1H, piperidine 5-CH₂), 2.22 – 2.41 (m, 4H, propanamide β-CH₂, piperidine 2-CH₂, piperidine 6-CH₂), 2.44 – 2.68 (m, homophenylalanine γ-CH₂, piperidine 2-CH₂), 2.85 (d, *J* = 11.1 Hz, 1H, piperidine 6-CH₂), 4.09 (qd, *J* = 6.3, 2.2 Hz, 2H, Et-CH₂), 4.26 (td, *J* = 8.7, 4.8 Hz, 1H, homophenylalanine α-CH), 6.54 (dd, *J* = 7.9, 1.6 Hz, 1H, phenol 6-CH), 6.64 – 6.71 (m, 2H, phenol 2-CH, phenol 4-CH), 7.07 (t, *J* = 7.8 Hz, 1H, phenol 5-CH), 7.13 – 7.21 (m, 3H, phenyl *ortho*-CH, phenyl *para*-CH), 7.22 – 7.30 (m, 2H, phenyl *meta*-CH), 8.27 (s, 1H, phenol OH), 8.58 (d, *J* = 7.9 Hz, 1H, amide NH)

¹³C NMR (DMSO-*d*₆): δ 15.4, 16.6, 27.7, 31.7, 33.3, 33.6, 38.4, 49.1, 49.6, 51.5, 52.3, 54.5, 55.6, 56.0, 112.6, 112.9, 116.5, 126.4, 128.8, 129.4, 141.3, 152.1, 157.6, 172.1, 173.1.

m/z: HRMS C₂₇H₃₆N₂O₄ [MH]⁺ calc 467.2904, found 466.2901.



Methyl (3-((3*R*,4*R*)-4-(3-hydroxyphenyl)-3,4-dimethylpiperidin-1-yl)propanoyl)-L-tyrosinate (166h**)**

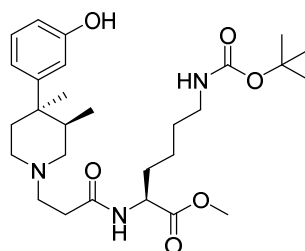
The title compound was synthesised as described in general procedure 2, using 3-((3*R*,4*R*)-4-(3-hydroxyphenyl)-3,4-dimethylpiperidin-1-yl)propanoic acid

hydrochloride (**165a**) (25 mg, 0.080 mmol, 1 eq) and *L*-tyrosine methyl ester hydrochloride (19 mg, 0.080 mmol, 1 eq) to give **166g** as a white solid (5 mg, 14%).

¹H NMR (MeOD): δ 0.76 (d, *J* = 7.2 Hz, 3H, piperidine 3-CH₃), 1.37 (s, 3H, piperidine 4-CH₃), 1.80 (d, *J* = 14.1 Hz, 1H, piperidine 5-CH₂), 2.22 (d, *J* = 7.7 Hz, 1H, piperidine 3-CH), 2.37 (td, *J* = 14.0, 10.1 Hz, 1H, piperidine 5-CH₂), 2.52 – 2.71 (m, 2H, propanamide α-CH₂), 2.84 (dd, *J* = 14.0, 9.2 Hz, 1H, tyrosine β-CH₂), 2.91 – 3.05 (m, 2H, piperidine 2-CH₂, piperidine 6-CH₂), 3.07 – 3.19 (m, 4H, tyrosine β-CH₂, piperidine 2-CH₂, propanamide β-CH₂), 3.24 (d, *J* = 14.6 Hz, 1H, piperidine 6-CH₂), 3.70 (s, 3H, O-CH₃), 4.69 (ddd, *J* = 9.3, 5.3, 2.1 Hz, 1H, tyrosine α-CH), 6.64 (ddd, *J* = 8.1, 2.4, 0.8 Hz, 1H, phenol 6-CH), 6.67 – 6.77 (m, 3H, phenol 2-CH, tyrosine phenol *ortho*-CH), 6.78 (dd, *J* = 8.1, 1.9 Hz, 1H, phenol 4-CH), 7.02 (d, *J* = 8.5 Hz, 2H, tyrosine *meta*-CH), 7.15 (t, *J* = 7.9 Hz, 1H, phenol 5-CH).

¹³C NMR (MeOD): δ 15.4, 27.6, 30.5, 31.6, 36.9, 37.8, 38.9, 50.5, 52.8, 54.5, 55.3, 56.0, 113.7, 114.0, 116.3, 116.3, 117.8, 128.6, 130.5, 131.3, 151.1, 157.5, 158.6, 169.4, 173.0, 173.5.

m/z: HRMS C₂₆H₃₄N₂O₅ [MH]⁺ calc 455.2640, found 455.2548.

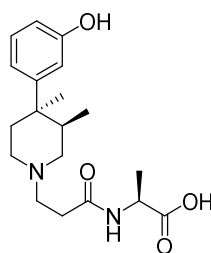


Methyl N⁶-(tert-butoxycarbonyl)-N²-(3-((3*R*,4*R*)-4-(3-hydroxyphenyl)-3,4-dimethylpiperidin-1-yl)propanoyl)-L-lysinate (168i**)**

The title compound was synthesised as described in general procedure 2, using 3-((3*R*,4*R*)-4-(3-hydroxyphenyl)-3,4-dimethylpiperidin-1-yl)propanoic acid hydrochloride (**165a**) (25 mg, 0.080 mmol, 1 eq) and *N*_ε-Boc-*L*-lysine methyl ester hydrochloride (24 mg, 0.080 mmol, 1 eq) to give **166g** as a white solid (5 mg, 12%).

^1H NMR (MeOD): δ 0.81 (d, $J = 7.3$ Hz, 3H, piperidine 3-CH₃), 1.34 – 1.54 (m, 4H, lysine γ -CH₂, lysine δ -CH₂), 1.43 (s, 9H, *t*Bu-CH₃), 1.45 (s, 3H, piperidine 4-CH₃), 1.65 – 1.78 (m, 1H, lysine β -CH₂), 1.79 – 1.91 (m, 1H, lysine β -CH₂), 1.95 (d, $J = 14.5$ Hz, 1H, piperidine 5-CH₂), 2.36 – 2.53 (m, 2H, piperidine 5-CH₂, piperidine 3-CH), 2.83 (t, $J = 6.7$ Hz, 2H, propanamide α -CH₂), 3.02 (t, $J = 6.8$ Hz, 2H, lysine ε -CH₂), 3.29 – 3.38 (m, 1H, piperidine 6-CH₂), 3.40 – 3.56 (m, 4H, piperidine 2-CH₂, propanamide β -CH₂), 3.60 (d, $J = 14.4$ Hz, 1H, piperidine 6-CH₂), 3.73 (s, 3H, O-CH₃), 4.41 (dd, $J = 8.8, 5.1$ Hz, 1H, lysine α -CH), 6.66 (ddd, $J = 8.1, 2.4, 0.8$ Hz, 1H, phenol 6-CH), 6.73 (t, $J = 2.1$ Hz, 1H, phenol 2-CH), 6.78 (dt, $J = 7.9, 1.5$ Hz, 1H, phenol 4-CH), 7.17 (t, $J = 7.9$ Hz, 1H, phenol 5-CH).

^{13}C NMR (MeOD): δ 13.4, 22.7, 25.6, 27.4, 27.7, 29.1, 30.6, 36.8, 37.1, 39.6, 49.3, 51.5, 52.4, 53.1, 54.1, 78.5, 111.8, 112.8, 115.9, 129.3, 148.9, 157.4, 171.4, 172.7.



(3-((3R,4R)-4-(3-Hydroxyphenyl)-3,4-dimethylpiperidin-1-yl)propanoyl)-L-alanine (136c)

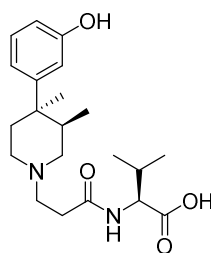
The title compound was synthesised as described in general procedure 3, using methyl (3-((3R,4R)-4-(3-hydroxyphenyl)-3,4-dimethylpiperidin-1-yl)propanoyl)-L-alaninate (**166c**) (3 mg, 0.008 mmol) to give **136c** as a white solid (3 mg, 100%).

^1H NMR (DMSO-*d*₆): δ 0.67 (d, $J = 6.9$ Hz, 3H, piperidine 3-CH₃), 1.22 (s, 3H, piperidine 4-CH₃), 1.23 (d, $J = 7.6$ Hz, 3H, alanine CH₃), 1.51 (d, $J = 12.8$ Hz, 1H, piperidine 5-CH₂), 1.96 (d, $J = 7.3$ Hz, 1H, piperidine 3-CH), 2.14 (dt, $J = 12.7, 6.4$ Hz, 1H, piperidine 5-CH₂), 2.22 – 2.35 (m, 2H, piperidine 2-CH₂, piperidine 6-CH₂), 2.28 (t, $J = 6.9$ Hz, 2H, propanamide α -CH₂), 2.47 – 2.58 (m, 3H, propanamide β -CH₂, piperidine 2-CH₂), 2.82 (d, $J = 10.7$ Hz, 1H, piperidine 6-

CH₂), 4.29 (p, *J* = 7.2 Hz, 1H, alanine α-CH), 6.55 (dd, *J* = 7.7, 2.3 Hz, 1H, phenol 6-CH), 6.66 (t, *J* = 2.1 Hz, 1H, phenol 2-CH), 6.71 (d, *J* = 8.0 Hz, 1H, phenol 4-CH), 7.08 (t, *J* = 7.9 Hz, 1H, phenol 5-CH), 8.21 (s, 1H, phenol OH), 8.55 (d, *J* = 7.3 Hz, 1H, amide NH).

¹³C NMR (DMSO-d₆): δ 16.1, 17.4, 27.2, 29.1, 32.6, 37.9, 47.2, 49.0, 53.5, 54.7, 112.2, 112.4, 116.0, 128.8, 157.1, 163.8, 171.2, 173.2.

m/z: HRMS C₁₉H₂₈N₂O₄ [MH]⁺ calc 349.2122, found 349.2130.



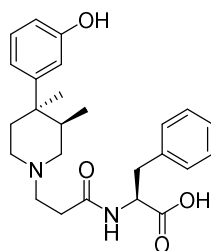
(3-((3*R*,4*R*)-4-(3-Hydroxyphenyl)-3,4-dimethylpiperidin-1-yl)propanoyl)-*L*-valine (136d)

The title compound was synthesised as described in general procedure 3, using methyl (3-((3*R*,4*R*)-4-(3-hydroxyphenyl)-3,4-dimethylpiperidin-1-yl)propanoyl)-*L*-valinate (**166d**) (3 mg, 0.008 mmol) to give **136d** as a white solid (3 mg, 100%).

¹H NMR (DMSO-d₆): δ 0.68 (d, *J* = 7.0 Hz, 3H, piperidine 3-CH₃), 0.85 (dd, *J* = 6.8, 3.5 Hz, 6H, valine CH₃), 1.23 (s, 3H, piperidine 4-CH₃), 1.51 (d, *J* = 12.6 Hz, 1H, piperidine 5-CH₂), 1.91 – 2.09 (m, 2H, valine β-CH, piperidine 3-CH), 2.18 (td, *J* = 12.7, 4.2 Hz, 1H, piperidine 5-CH₂), 2.24 – 2.43 (m, 3H, propanamide α-CH₂, piperidine 6-CH₂), 2.52 – 2.63 (m, 4H, propanamide β-CH₂, piperidine 2-CH₂), 2.87 (d, *J* = 11.8 Hz, 1H, piperidine 6-CH₂), 4.17 (dd, *J* = 8.7, 5.6 Hz, 1H), 6.55 (dd, *J* = 7.9, 2.3 Hz, 1H, phenol 6-CH), 6.66 (t, *J* = 2.1 Hz, 1H, phenol 2-CH), 6.70 (d, *J* = 7.9 Hz, 1H, phenol 4-CH), 7.08 (t, *J* = 7.9 Hz, 1H, phenol 5-CH), 8.19 (s, 1H, phenol OH), 8.31 (d, *J* = 8.7 Hz, 1H, amide NH).

¹³C NMR (DMSO-d₆): δ 16.6, 18.5, 19.6, 27.7, 30.3, 30.7, 33.0, 38.4, 38.4, 49.5, 54.7, 55.7, 57.4, 112.6, 113.0, 116.5, 129.4, 152.0, 157.6, 164.0, 171.9, 173.7.

m/z : HRMS $C_{21}H_{32}N_2O_4$ $[MH]^+$ calc 377.2435, found 377.2427.



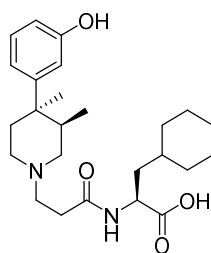
(3-((3R,4R)-4-(3-Hydroxyphenyl)-3,4-dimethylpiperidin-1-yl)propanoyl)-L-phenylalanine (136e)

The title compound was synthesised as described in general procedure 3, using methyl (3-((3R,4R)-4-(3-hydroxyphenyl)-3,4-dimethylpiperidin-1-yl)propanoyl)-L-phenylalaninate (**166e**) (5 mg, 0.011 mmol) to give **136e** as a white solid (5 mg, 100%).

1H NMR (MeOD): δ 0.77 (d, J = 7.3 Hz, 3H, piperidine 3-CH₃), 1.42 (s, 3H, piperidine 4-CH₃), 1.90 (d, J = 10.5 Hz, 1H, piperidine 5-CH₂), 2.30 – 2.47 (m, 2H, piperidine 3-CH, piperidine 5-CH₂), 2.69 (dt, J = 17.0, 6.7 Hz, 1H, phenylalanine β -CH₂), 2.79 (dt, J = 16.9, 6.4 Hz, 1H, phenylalanine β -CH₂), 2.94 (dd, J = 13.9, 9.9 Hz, 2H, propanamide α -CH₂), 3.20 – 3.29 (m, 1H, piperidine 6-CH₂), 3.36 – 3.42 (m, 2H, propanamide β -CH₂), 3.43 – 3.52 (m, 2H, piperidine 2-CH₂), 3.61 – 3.73 (m, 1H, piperidine 6-CH₂), 4.72 (dd, J = 9.7, 4.7 Hz, 1H, phenylalanine α -CH), 6.66 (dd, J = 8.1, 2.3 Hz, 1H, phenol 6-CH), 6.72 (d, J = 2.3 Hz, 1H, phenol 2-CH), 6.76 (d, J = 7.8 Hz, 1H, phenol 4-CH), 7.17 (t, J = 7.9 Hz, 1H, phenol 5-CH), 7.19 – 7.35 (m, 5H, phenyl CH).

^{13}C NMR (DMSO- d_6): δ 15.2, 26.4, 26.9, 29.3, 36.3, 36.6, 37.0, 43.6, 60.2, 70.5, 72.2, 112.2, 122.8, 115.7, 126.5, 128.2, 129.1, 129.3, 137.7, 149.5, 157.4, 169.2, 172.9.

m/z : HRMS $C_{25}H_{32}N_2O_4$ $[MH]^+$ calc 425.2435, found 425.2425.



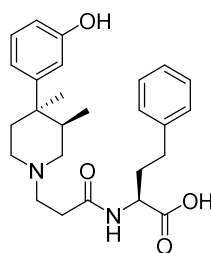
(S)-3-cyclohexyl-2-(3-((3R,4R)-4-(3-hydroxyphenyl)-3,4-dimethylpiperidin-1-yl)propanamido)propanoic acid (136f)

The title compound was synthesised as described in general procedure 3, using methyl (S)-3-cyclohexyl-2-(3-((3R,4R)-4-(3-hydroxyphenyl)-3,4-dimethylpiperidin-1-yl)propanamido)propanoate (**166f**) (5 mg, 0.011 mmol) to give **136f** as a white solid (5 mg, 100%).

^1H NMR (DMSO- d_6): δ 0.77 (d, $J = 7.3$ Hz, 3H, piperidine 3- CH_3), 0.80 – 0.99 (m, 2H, cyclohexyl 2- CH_2 , cyclohexyl 6- CH_2), 1.05 – 1.31 (m, 4H, cyclohexyl 3- CH_2 , cyclohexyl 4- CH_2 , cyclohexyl 5- CH_2), 1.35 (s, 3H, piperidine 4- CH_3), 1.47 – 1.72 (m, 7H, cyclohexylalanine β - CH_2 , cyclohexyl 1- CH , cyclohexyl 2- CH_2 , cyclohexyl 3- CH_2 , cyclohexyl 5- CH_2 , cyclohexyl 6- CH_2), 1.76 (d, $J = 14.2$ Hz, 1H, piperidine 5- CH_2), 2.20 – 2.29 (m, 1H, piperidine 3- CH), 2.26 (td, $J = 14.1, 3.0$ Hz, 1H, piperidine 5- CH_2), 2.80 (t, $J = 7.5$ Hz, 2H, propanamide α - CH_2), 3.19 – 3.43 (m, 6H, propanamide α - CH_2 , piperidine 2- CH_2 , piperidine 6- CH_2), 4.25 (q, $J = 7.6$ Hz, 1H, cyclohexylalanine α - CH), 6.61 (dd, $J = 7.9, 2.2$ Hz, 1H, phenol 6- CH), 6.66 (t, $J = 2.0$ Hz, 1H, phenol 2- CH), 6.70 (d, $J = 8.1$ Hz, 1H, phenol 4- CH), 7.12 (t, $J = 7.9$ Hz, 1H, phenol 5- CH), 8.48 (d, $J = 7.8$ Hz, 1H, amide NH).

^{13}C NMR (DMSO- d_6): δ 15.1, 25.6, 25.8, 26.0, 26.4, 27.0, 29.2, 31.5, 33.1, 33.6, 36.3, 37.1, 38.3, 43.6, 48.6, 49.7, 52.3, 53.3, 112.2, 112.8, 115.7, 129.2, 149.4, 157.4, 169.2, 174.0.

m/z : HRMS $\text{C}_{25}\text{H}_{38}\text{N}_2\text{O}_4$ $[\text{MH}]^+$ calc 431.2904, found 431.2894.



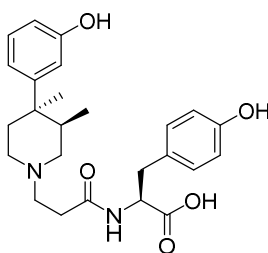
(S)-2-(3-((3R,4R)-4-(3-Hydroxyphenyl)-3,4-dimethylpiperidin-1-yl)propanamido)-4-phenylbutanoic acid (136g)

The title compound was synthesised as described in general procedure 3, using ethyl (S)-2-(3-((3R,4R)-4-(3-hydroxyphenyl)-3,4-dimethylpiperidin-1-yl)propanamido)-4-phenylbutanoate (**166g**) (5 mg, 0.011 mmol) to give **136g** as a white solid (5 mg, 100%).

¹H NMR (DMSO-d₆): δ 0.67 (d, *J* = 6.9 Hz, 3H, piperidine 3-CH₃), 1.22 (s, 3H, piperidine 4-CH₃), 1.51 (d, *J* = 12.7 Hz, 1H, piperidine 5-CH₂), 1.74 (m, 4H, homophenylalanine β-CH₂, propanamide α-CH₂), 2.05 – 2.10 (m, 1H, piperidine 3-CH), 2.15 (td, *J* = 12.7, 4.2 Hz, 1H, piperidine 5-CH₂), 2.22 – 2.41 (m, 4H, propanamide β-CH₂, piperidine 2-CH₂, piperidine 6-CH₂), 2.44 – 2.68 (m, homophenylalanine γ-CH₂, piperidine 2-CH₂), 2.85 (d, *J* = 11.1 Hz, 1H, piperidine 6-CH₂), 4.26 (td, *J* = 8.7, 4.8 Hz, 1H, homophenylalanine α-CH), 6.54 (dd, *J* = 7.9, 1.6 Hz, 1H, phenol 6-CH), 6.64 – 6.71 (m, 2H, phenol 2-CH, phenol 4-CH), 7.07 (t, *J* = 7.8 Hz, 1H, phenol 5-CH), 7.13 – 7.21 (m, 3H, phenyl *ortho*-CH, phenyl *para*-CH), 7.22 – 7.30 (m, 2H, phenyl *meta*-CH), 8.27 (s, 1H, phenol OH), 8.58 (d, *J* = 7.9 Hz, 1H, amide NH)

¹³C NMR (DMSO-d₆): δ 16.6, 27.7, 31.7, 33.3, 33.6, 38.4, 49.1, 49.6, 51.5, 52.3, 54.5, 55.6, 112.6, 112.9, 116.5, 126.4, 128.8, 129.4, 141.3, 152.1, 157.6, 172.1, 173.1.

m/z: HRMS C₂₆H₃₄N₂O₄ [MH]⁺ calc 439.2591, found 439.2594.



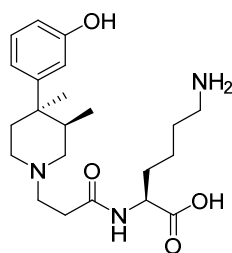
(3-((3R,4R)-4-(3-hydroxyphenyl)-3,4-dimethylpiperidin-1-yl)propanoyl)-L-tyrosine (136h)

The title compound was synthesised as described in general procedure 3, using methyl (3-((3R,4R)-4-(3-hydroxyphenyl)-3,4-dimethylpiperidin-1-yl)propanoyl)-L-tyrosinate (**166h**) (4 mg, 0.009 mmol) to give **136h** as a white solid (4 mg, 100%).

^1H NMR (DMSO- d_6): δ 0.59 (d, J = 7.0 Hz, 3H, piperidine 3- CH_3), 1.22 (s, 3H, piperidine 4- CH_3), 1.50 (d, J = 13.3 Hz, 1H, piperidine 5- CH_2), 1.85 – 1.99 (m, 1H, piperidine 3-CH), 2.15 (td, J = 12.8, 4.4 Hz, 1H, piperidine 5- CH_2), 2.24 – 2.42 (m, 3H, propanamide α - CH_2 , piperidine 6- CH_2), 2.52 – 2.65 (m, 3H, propanamide β - CH_2 , piperidine 2- CH_2), 2.72 (dd, J = 13.8, 8.4 Hz, 1H, tyrosine β - CH_2), 2.86 (d, J = 11.4 Hz, 1H, piperidine 6- CH_2), 2.91 (dd, J = 13.9, 5.0 Hz, 1H, tyrosine β - CH_2), 4.38 (td, J = 8.2, 5.0 Hz, 1H, tyrosine α -CH), 6.55 (dd, J = 7.9, 1.6 Hz, 1H, phenol 6-CH), 6.59 – 6.67 (m, phenol 2-CH, tyrosine phenol *ortho*-CH), 6.69 (d, J = 8.6 Hz, 1H, phenol 4-CH), 6.92 – 7.01 (m, 2H, tyrosine phenol *meta*-CH), 7.08 (t, J = 7.9 Hz, 1H, phenol 5-CH), 8.18 (s, 1H, phenol OH), 8.42 (d, J = 8.1 Hz, 1H, amide NH).

^{13}C NMR (DMSO- d_6): δ 15.7, 27.2, 29.5, 32.1, 36.3, 37.7, 37.8, 48.9, 53.6, 53.8, 54.9, 112.2, 112.5, 114.9, 116.1, 127.5, 129.0, 130.0, 151.3, 155.9, 157.1, 163.4, 170.8, 173.2.

m/z : HRMS $\text{C}_{26}\text{H}_{34}\text{N}_2\text{O}_4$ $[\text{MH}]^+$ calc 441.2384, found 441.2390.



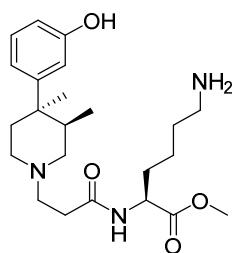
(3-((3R,4R)-4-(3-hydroxyphenyl)-3,4-dimethylpiperidin-1-yl)propanoyl)-L-lysine (136i)

The title compound was synthesised as described in general procedure 3, using methyl *N*⁶-(tert-butoxycarbonyl)-*N*²-(3-((3R,4R)-4-(3-hydroxyphenyl)-3,4-dimethylpiperidin-1-yl)propanoyl)-L-lysinate (**168i**) (4 mg, 0.009 mmol) to give **136i** as a white solid (2 mg, 50%).

¹H NMR (DMSO-*d*₆): δ 0.67 (d, *J* = 6.9 Hz, 3H, piperidine 3-CH₃), 1.23 (s, 3H, piperidine 4-CH₃), 1.32 (tq, *J* = 13.7, 8.5 Hz, 2H, lysine γ-CH₂), 1.43 – 1.60 (m, 4H, lysine δ-CH₂, lysine β-CH₂, piperidine 5-CH₂), 1.67 (ddt, *J* = 11.4, 9.6, 5.5 Hz, 1H, lysine β-CH₂), 1.91 – 2.00 (m, 1H, piperidine 3-CH), 2.13 (td, *J* = 12.6, 4.3 Hz, 1H, piperidine 5-CH₂), 2.22 – 2.34 (m, 3H, propanamide α-CH₂, piperidine 6-CH₂), 2.47 – 2.57 (m, 4H, lysine ε-CH₂, piperidine 2-CH₂), 2.69 (t, *J* = 7.6 Hz, 2H, propanamide β-CH₂), 2.82 (dd, *J* = 9.9, 5.7 Hz, 1H, piperidine 6-CH₂), 4.27 (ddd, *J* = 9.1, 7.8, 5.0 Hz, 1H, lysine α-CH), 6.55 (ddd, *J* = 8.0, 2.4, 0.8 Hz, 1H, phenol 6-CH), 6.68 (t, *J* = 2.1 Hz, 1H, phenol 2-CH), 6.71 (dt, *J* = 7.9, 1.2 Hz, 1H, phenol 4-CH), 7.09 (t, *J* = 7.9 Hz, 1H, phenol 5-CH), 8.39 (s, 1H, phenol OH), 8.56 (d, *J* = 7.9 Hz, 1H, amide NH).

¹³C NMR (DMSO-*d*₆): δ 16.6, 22.8, 27.7, 27.8, 30.3, 31.3, 33.2, 38.4, 38.4, 39.1, 49.6, 51.9, 54.5, 55.5, 112.7, 112.9, 116.4, 129.4, 152.2, 157.7, 165.5, 172.1, 173.1.

m/z: HRMS C₂₃H₃₇N₃O₄ [MH]⁺ calc 420.2857, found 420.2861.



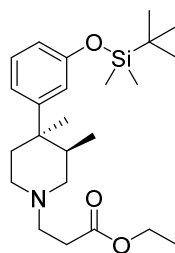
Methyl (3-((3R,4R)-4-(3-hydroxyphenyl)-3,4-dimethylpiperidin-1-yl)propanoyl)-L-lysinate (166i)

The title compound was synthesised as described in general procedure 3, using methyl *N*⁶-(tert-butoxycarbonyl)-*N*²-(3-((3R,4R)-4-(3-hydroxyphenyl)-3,4-dimethylpiperidin-1-yl)propanoyl)-L-lysinate (**168i**) (4 mg, 0.009 mmol) to give **166i**, a white solid as a biproduct of **136i** (2 mg, 50%).

¹H NMR (DMSO-*d*₆): δ 0.67 (d, *J* = 6.9 Hz, 3H, piperidine 3-CH₃), 1.23 (s, 3H, piperidine 4-CH₃), 1.32 (tq, *J* = 13.7, 8.5 Hz, 2H, lysine γ-CH₂), 1.43 – 1.60 (m, 4H, lysine δ-CH₂, lysine β-CH₂, piperidine 5-CH₂), 1.67 (ddt, *J* = 11.4, 9.6, 5.5 Hz, 1H, lysine β-CH₂), 1.91 – 2.00 (m, 1H, piperidine 3-CH), 2.13 (td, *J* = 12.6, 4.3 Hz, 1H, piperidine 5-CH₂), 2.22 – 2.34 (m, 3H, propanamide α-CH₂, piperidine 6-CH₂), 2.47 – 2.57 (m, 4H, lysine ε-CH₂, piperidine 2-CH₂), 2.69 (t, *J* = 7.6 Hz, 2H, propanamide β-CH₂), 2.82 (dd, *J* = 9.9, 5.7 Hz, 1H, piperidine 6-CH₂), 3.63 (s, 3H, O-CH₃), 4.27 (ddd, *J* = 9.1, 7.8, 5.0 Hz, 1H, lysine α-CH), 6.55 (ddd, *J* = 8.0, 2.4, 0.8 Hz, 1H, phenol 6-CH), 6.68 (t, *J* = 2.1 Hz, 1H, phenol 2-CH), 6.71 (dt, *J* = 7.9, 1.2 Hz, 1H, phenol 4-CH), 7.09 (t, *J* = 7.9 Hz, 1H, phenol 5-CH), 8.39 (s, 1H, phenol OH), 8.56 (d, *J* = 7.9 Hz, 1H, amide NH).

¹³C NMR (DMSO-*d*₆): δ 16.6, 22.8, 27.7, 27.8, 30.3, 31.3, 33.2, 38.4, 38.4, 39.1, 49.6, 51.9, 52.3, 54.5, 55.5, 112.7, 112.9, 116.4, 129.4, 152.2, 157.7, 165.5, 172.1, 173.1.

m/z: HRMS C₂₃H₃₇N₃O₄ [MH]⁺ calc 420.2857, found 420.2861.



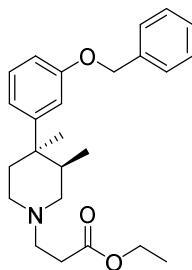
Ethyl 3-((3R,4R)-4-(3-((tert-butyldimethylsilyl)oxy)phenyl)-3,4-dimethylpiperidin-1-yl)propanoate (179)

To ethyl 3-((3R,4R)-4-(3-hydroxyphenyl)-3,4-dimethylpiperidin-1-yl)propanoate (**167**) (278 mg, 0.91 mmol) and imidazole (124 mg, 1.820 mmol, 2 eq) in DMF (25 ml) was added tert-butyldimethylsilyl chloride (206 mg, 1.365 mmol, 1.5 eq) and stirred at rt for 4 hours. The solution was diluted with water (200 ml) and extracted with EtOAc (3 x 50 ml). The combined organics were washed with brine (50 ml) and dried over Na₂SO₄. Column chromatography (5% MeOH in EtOAc) yielded **179** as a pale orange oil (344 mg, 90%)

¹H NMR (CDCl₃): δ 0.18 (s, 6H, silyl CH₃), 0.74 (d, *J* = 7.0 Hz, 3H, piperidine 3-CH₃), 0.98 (s, 9H, *t*Bu CH₃), 1.25 (t, *J* = 7.1 Hz, 3H, Et CH₃), 1.29 (s, 3H, piperidine 4-CH₃), 1.56 (d, *J* = 12.3 Hz, 1H, piperidine 5-CH₂), 1.91 – 1.99 (m, 1H, piperidine 3-CH), 2.26 (td, *J* = 12.4, 4.3 Hz, 1H, piperidine 5-CH₂), 2.40 (td, *J* = 11.7, 2.3 Hz, 1H, piperidine 6-CH₂), 2.49 (t, *J* = 7.2 Hz, 2H, propanoate α-CH₂), 2.54 – 2.58 (m, 2H, piperidine 2-CH₂), 2.70 (ddt, *J* = 26.5, 12.4, 7.1 Hz, 2H, propanoate β-CH₂), 2.83 (dd, *J* = 7.6, 3.6 Hz, 1H, piperidine 6-CH₂), 4.13 (qd, *J* = 7.1, 2.6 Hz, 2H, Et CH₂), 6.65 (ddd, *J* = 8.0, 2.4, 0.8 Hz, 1H, phenol 6-CH), 6.75 (t, *J* = 2.0 Hz, 1H, phenol 2-CH), 6.86 (ddd, *J* = 7.9, 1.7, 0.9 Hz, 1H, phenol 4-CH), 7.14 (t, *J* = 7.9 Hz, 1H, phenol 5-CH).

¹³C NMR (CDCl₃): δ -4.2, 14.4, 16.2, 18.4, 25.9, 27.6, 30.8, 32.8, 38.5, 39.0, 50.1, 54.0, 55.7, 60.5, 117.2, 117.9, 118.8, 129.0, 152.0, 155.6, 172.9.

m/z: LCMS C₂₄H₄₁NO₃Si [MH]⁺ calc 420.7, found 420.1 with *t_R* of 4.62 min.



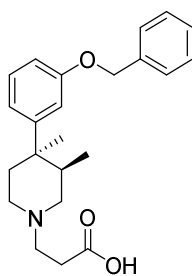
Ethyl 3-((3R,4R)-4-(3-(benzyloxy)phenyl)-3,4-dimethylpiperidin-1-yl)propanoate (180)

To ethyl 3-((3R,4R)-4-(3-hydroxyphenyl)-3,4-dimethylpiperidin-1-yl)propanoate (**167**) (88 mg, 0.288 mmol) and K_2CO_3 (119 mg, 0.864 mmol, 3 eq) under N_2 was added dry DMF (10 ml) and stirred at rt for 10 mins. Benzyl bromide (38 μ l, 0.317 mmol, 1.1 eq) was added dropwise and the reaction was left to stir at rt overnight. Solvent was removed under high vacuum and the residue was partitioned between water (50 ml) and EtOAc (50 ml). The organic was washed with brine (20 ml) and dried over Na_2SO_4 . Column chromatography (5% MeOH in EtOAc) yielded **180** as an orange oil (80 mg, 70%).

1H NMR ($CDCl_3$): δ 0.66 (d, $J = 7.0$ Hz, 3H, piperidine 3- CH_3), 1.16 (t, $J = 7.1$ Hz, 3H, Et CH_3), 1.21 (s, 3H, piperidine 4- CH_3), 1.50 (d, $J = 11.3$ Hz, 1H, piperidine 5- CH_2), 1.85 – 1.94 (m, 1H, piperidine 3-CH), 2.19 (td, $J = 12.4, 4.4$ Hz, 1H, piperidine 5- CH_2), 2.33 (td, $J = 11.5, 2.7$ Hz, 1H, piperidine 6- CH_2), 2.41 (t, $J = 7.2$ Hz, 2H, propanoate α - CH_2), 2.44 – 2.53 (m, 2H, piperidine 2- CH_2), 2.53 – 2.70 (m, 2H, propanoate β - CH_2), 2.74 (dt, $J = 10.8, 4.1$ Hz, 1H, piperidine 6- CH_2), 4.04 (qd, $J = 7.1, 2.3$ Hz, 2H, Et CH_2), 4.96 (s, 2H, benzyl CH_2), 6.71 (dd, $J = 8.4, 2.5$ Hz, 1H, phenol 6-CH), 6.77 – 6.85 (m, 2H, phenol 2-CH, phenol 4-CH), 7.14 (t, $J = 7.9$ Hz, 1H, phenol 5-CH), 7.19 – 7.42 (m, 5H, benzyl CH).

^{13}C NMR ($CDCl_3$): δ 14.3, 16.2, 27.7, 30.9, 32.7, 38.7, 38.9, 50.1, 53.9, 55.7, 60.4, 70.1, 111.1, 113.5, 118.6, 127.7, 128.0, 128.7, 129.1, 137.3, 152.0, 158.8, 172.9.

m/z : LCMS $C_{25}H_{33}NO_3$ $[MH]^+$ calc 396.6, found 396.2 with t_R of 3.60 min.



3-((3R,4R)-4-(3-(benzyloxy)phenyl)-3,4-dimethylpiperidin-1-yl)propanoic acid (182)

To a solution of ethyl 3-((3R,4R)-4-(3-(benzyloxy)phenyl)-3,4-dimethylpiperidin-1-yl)propanoate (**180**) (72 mg, 0.182 mmol) in dioxane (5 mL) was added 4M HCl (in dioxane and water) (2.5 mL) and heated to reflux (105°C) for 2 hours. Once cooled to room temperature the solvents were evaporated *in vacuo* to give **182** as a white solid (70 mg, 100%).

¹H NMR (CDCl₃): δ 0.76 (d, *J* = 7.1 Hz, 3H, piperidine 3-CH₃), 1.30 (s, 3H, piperidine 4-CH₃), 1.71 (d, *J* = 13.9 Hz, 1H, piperidine 5-CH₂), 2.01 – 2.15 (m, 1H, piperidine 3-CH), 2.34 (td, *J* = 11.8 Hz, 1H, piperidine 5-CH₂), 2.41 (t, *J* = 7.2 Hz, 2H, propanoate α-CH₂), 2.33 (td, *J* = 11.5, 2.7 Hz, 1H, piperidine 6-CH₂), 2.73 – 2.95 (m, 4H, piperidine 2-CH₂, propanoate β-CH₂), 3.09 (s, 1H, piperidine 6-CH₂), 4.04 (qd, *J* = 7.1, 2.3 Hz, 2H, Et CH₂), 4.98 (s, 2H, benzyl CH₂), 6.72 – 6.83 (m, 3H, phenol 6-CH, phenol 2-CH, phenol 4-CH), 7.14 (t, *J* = 8.2 Hz, 1H, phenol 5-CH), 7.22 – 7.41 (m, 5H, benzyl CH).

¹³C NMR (CDCl₃): δ 15.8, 29.2, 29.8, 38.3, 48.8, 53.8, 55.2, 70.2, 111.7, 127.7, 128.2, 128.7, 129.6, 137.1, 159.0, 174.0.

m/z: LCMS C₂₃H₂₉NO₃ [MH]⁺ calc 368.5, found 368.2 with *t_R* of 2.85 min.

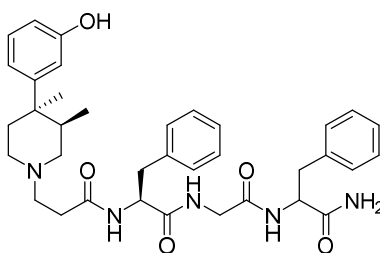
General procedure 4 – solid phase peptide synthesis.

Novagel rink amide resin (0.69 mmol/g) (290 mg, 0.2 mmol) was swelled in DMF in a filtered column for 1 hour before draining. 20% *v/v* piperidine in DMF (5 ml) was added and the column gently agitated over 1 hour. The column was drained and then washed with DMF (3 x 5 ml). Separately, a coupling solution of HCTU (414 mg, 1.0 mmol, 5 eq), Fmoc-amino acid (1.0 mmol, 5 eq) and DIPEA

(174 μ l, 1.0 mmol, 5 eq) were stirred in DMF for 15 min at rt. The coupling solution was added to the column and the column gently agitated over 4 hours. The resin was drained, washed with DMF (3 x 5 ml), a 3:2 v/v mixture of acetic anhydride/pyridine (5 ml) was added and the column was gently agitated over 1 hour. The column was drained and then washed with DMF (3 x 5 ml). The Fmoc-deprotection in 20% v/v piperidine in DMF, Fmoc-amino acid coupling, and capping steps were repeated twice more, with DMF washing (3 x 5ml) between each step. This was followed by washing in DMF (3 x 5 ml), Fmoc-deprotection in 20% v/v piperidine in DMF (5 ml), and further washing in DMF (3 x 5 ml). A coupling mixture of HCTU (414 mg, 1.0 mmol, 5 eq), acrylic acid (69 μ l, 1.0 mmol, 5 eq) and DIPEA (174 μ l, 1.0 mmol, 5 eq) were stirred in DMF for 15 min at rt. This coupling mixture was then added to the column and the column gently agitated over 4 hours. Washing in DMF (3 x 5 ml) was followed by washing with DCM (3 x 5 ml) and the resin was dried under a stream of nitrogen. The product was cleaved from the resin using an 18:1:1 v/v/v mixture of TFA, TIPS and water (5 ml). The filtrate solvent was evaporated *in vacuo*. Column chromatography (10% MeOH in EtOAc) yielded the product as a pale yellow oil.

General procedure 5 – Michael addition of 3-((3*R*,4*R*)-3,4-dimethylpiperidin-4-yl)phenol (146a**) to acrylamido tripeptides.**

3-((3*R*,4*R*)-3,4-dimethylpiperidin-4-yl)phenol (**146a**) (5 eq) and acrylamido tripeptide (1 eq) were dissolved in minimal NMP and stirred at 85°C until complete by TLC or LCMS (2-3 days). NMP was removed under high vacuum and the residue was taken up in a 20% v/v solution of MeOH/EtOAc. It was then passed through a silica plug with additional washing with EtOAc and purified by HPLC (system 3), to give the product as a pale yellow oil. Unreacted **146a** was recovered by washing the silica with MeOH.



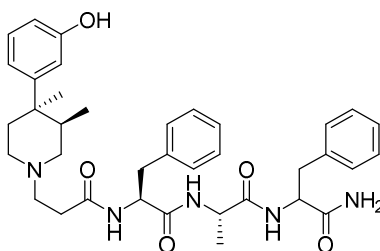
(2S)-N-(2-((1-amino-1-oxo-3-phenylpropan-2-yl)amino)-2-oxoethyl)-2-(3-((3R,4R)-4-(3-hydroxyphenyl)-3,4-dimethylpiperidin-1-yl)propanamido)-3-phenylpropanamide (170a)

The title compound was synthesised as described in general procedure 5, using *N*-((2S)-1-((2-((1-amino-1-oxo-3-phenylpropan-2-yl)amino)-2-oxoethyl)amino)-1-oxo-3-phenylpropan-2-yl)acrylamide (**177a**) (5 mg, 0.01 mmol), which was synthesised using general procedure 4. This yielded **170a** as a white solid (7 mg, 100%).

¹H NMR (DMSO-*d*₆): δ 0.62 (d, *J* = 6.9 Hz, 3H, piperidine 3-CH₃), 1.19 (s, 3H, piperidine 4-CH₃), 1.45 (d, *J* = 12.5 Hz, 1H piperidine 5-CH₂), 1.85 – 1.96 (m, 1H, piperidine 3-CH), 2.08 (td, *J* = 12.6, 4.2 Hz, 1H, piperidine 5-CH₂), 2.13 – 2.30 (m, 3H, propanamide α-CH₂, piperidine 6-CH₂), 2.34 – 2.46 (m, 4H, propanamide β-CH₂, piperidine 2-CH₂), 2.69 – 2.77 (m, 1H, piperidine 6-CH₂), 2.73 (dd, *J* = 13.7, 9.6 Hz, 1H, Phe³ β-CH₂), 2.81 (dd, *J* = 13.8, 9.6 Hz, 1H, Phe¹ β-CH₂), 3.00 (dd, *J* = 14.4, 5.2 Hz, 1H, Phe³ β-CH₂), 3.04 (dd, *J* = 14.1, 4.9 Hz, 1H, Phe¹ β-CH₂), 3.55 (dd, *J* = 16.6, 5.4 Hz, 1H, Gly² CH₂), 3.78 (dd, *J* = 16.7, 6.1 Hz, 1H, Gly² CH₂), 4.41 (td, *J* = 9.0, 4.5 Hz, 1H, Phe¹ α-CH), 4.50 (td, *J* = 8.9, 4.5 Hz, 1H, Phe³ α-CH), 6.55 (dd, *J* = 8.0, 2.3 Hz, 1H, phenol 6-CH), 6.66 (s, 1H, phenol 2-CH), 6.69 (d, *J* = 8.0 Hz, 1H, phenol 4-CH), 7.08 (t, *J* = 7.9 Hz, 1H, phenol 5-CH), 7.12 (s, 1H, amide NH₂), 7.15 – 7.30 (m, 10H, phenyl CH), 7.43 (s, 1H, amide NH₂), 8.02 (d, *J* = 8.5 Hz, 1H, Pr-Phe¹ amide NH), 8.26 (t, *J* = 5.8 Hz, 1H, Phe¹-Gly² amide NH), 8.41 (s, 1H, phenol OH), 8.46 (d, *J* = 8.0 Hz, 1H, Gly²-Phe³ amide NH).

¹³C NMR (DMSO-*d*₆): δ 16.1, 27.3, 29.9, 32.8, 37.5, 37.6, 37.9, 40.4, 42.0, 49.0, 53.9, 54.0, 55.1, 112.1, 112.5, 116.1, 126.3, 128.0, 128.1, 128.9, 129.1, 129.1, 137.9, 138.1, 151.7, 157.2, 165.1, 168.5, 171.6, 172.9.

m/z: HRMS C₃₆H₄₅N₅O₅ [MH]⁺ calc 628.3493, found 628.3492.



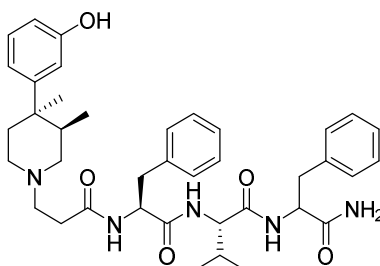
(2S)-N-((2S)-1-(((1-amino-1-oxo-3-phenylpropan-2-yl)amino)-1-oxopropan-2-yl)-2-(3-((3R,4R)-4-(3-hydroxyphenyl)-3,4-dimethylpiperidin-1-yl)propanamido)-3-phenylpropanamide (170b)

The title compound was synthesised as described in general procedure 5, using *N*-((2S)-1-(((2S)-1-(((1-amino-1-oxo-3-phenylpropan-2-yl)amino)-1-oxopropan-2-yl)amino)-1-oxo-3-phenylpropan-2-yl)acrylamide (**177b**) (5 mg, 0.01 mmol), which was synthesised using general procedure 4. This yielded **170b** as a white solid (7 mg, 100%).

¹H NMR (DMSO-*d*₆): δ 0.61 (d, *J* = 6.9 Hz, 3H, piperidine 3-CH₃), 1.16 (d, *J* = 7.1 Hz, 3H, Ala² β-CH₃), 1.19 (s, 3H, piperidine 4-CH₃), 1.45 (d, *J* = 12.2 Hz, 1H piperidine 5-CH₂), 1.84 – 1.95 (m, 1H, piperidine 3-CH), 2.08 (td, *J* = 12.5, 4.0 Hz, 1H, piperidine 5-CH₂), 2.13 – 2.27 (m, 3H, propanamide α-CH₂, piperidine 6-CH₂), 2.29 – 2.45 (m, 4H, propanamide β-CH₂, piperidine 2-CH₂), 2.66 (dd, *J* = 13.9, 10.1 Hz, 1H, Phe³ β-CH₂), 2.73 (d, *J* = 10.8 Hz, 1H, piperidine 6-CH₂), 2.83 (dd, *J* = 13.8, 8.6 Hz, 1H, Phe¹ β-CH₂), 2.96 (dd, *J* = 14.4, 5.2 Hz, 1H, Phe³ β-CH₂), 3.01 (dd, *J* = 14.1, 4.9 Hz, 1H, Phe¹ β-CH₂), 4.21 (p, *J* = 7.0 Hz, 1H, Ala² α-CH), 4.40 (td, *J* = 8.4, 5.0 Hz, 1H, Phe¹ α-CH), 4.54 (td, *J* = 9.7, 4.1 Hz, 1H, Phe³ α-CH), 6.54 (dd, *J* = 8.0, 2.3 Hz, 1H, phenol 6-CH), 6.65 (t, *J* = 2.0 Hz, 1H, phenol 2-CH), 6.68 (d, *J* = 8.0 Hz, 1H, phenol 4-CH), 7.07 (t, *J* = 7.8 Hz, 1H, phenol 5-CH), 7.09 (s, 1H, Phe³ amide NH₂), 7.11 – 7.26 (m, 10H, phenyl CH), 7.36 (s, 1H, Phe³ amide NH₂), 7.84 (d, *J* = 8.2 Hz, 1H, Pr-Phe¹ amide NH), 8.18 (d, *J* = 7.2 Hz, 1H, Phe¹-Ala² amide NH), 8.30 (s, 1H, phenol OH), 8.33 (d, *J* = 8.4 Hz, 1H, Ala²-Phe³ amide NH).

^{13}C NMR (DMSO- d_6): δ 16.1, 18.0, 27.3, 29.9, 32.8, 37.4, 37.6, 37.9, 40.2, 48.5, 49.0, 53.3, 53.6, 54.0, 55.1, 112.2, 112.5, 116.0, 126.2, 126.2, 127.9, 128.0, 128.9, 129.1, 129.2, 137.8, 137.9, 151.7, 157.1, 171.1, 171.3, 171.8, 172.6.

m/z : HRMS $\text{C}_{36}\text{H}_{42}\text{N}_5\text{O}_5$ $[\text{MH}]^+$ calc 642.3650, found 642.3660.



(2S)-N-(1-amino-1-oxo-3-phenylpropan-2-yl)-2-((S)-2-(3-((3R,4R)-4-(3-hydroxyphenyl)-3,4-dimethylpiperidin-1-yl)propanamido)-3-phenylpropanamido)-3-methylbutanamide (170c)

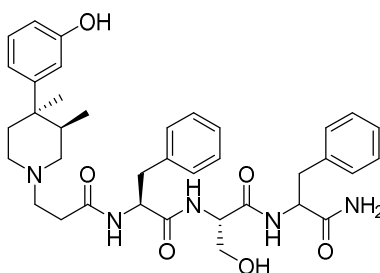
The title compound was synthesised as described in general procedure 5, using (2S)-2-((S)-2-acrylamido-3-phenylpropanamido)-N-(1-amino-1-oxo-3-phenylpropan-2-yl)-3-methylbutanamide (**177c**) (5 mg, 0.01 mmol), which was synthesised using general procedure 4. This yielded **170c** as a white solid (7 mg, 100%).

^1H NMR (DMSO- d_6): δ 0.62 (d, J = 7.0 Hz, 3H, piperidine 3- CH_3), 0.76 (dd, J = 6.7, 2.4 Hz, 6H, Val² CH_3), 1.19 (s, 3H, piperidine 4- CH_3), 1.45 (d, J = 12.4 Hz, 1H piperidine 5- CH_2), 1.86 – 1.98 (m, 3H, Val² β -CH, piperidine 3-CH), 2.08 (td, J = 12.5, 4.2 Hz, 1H, piperidine 5- CH_2), 2.13 – 2.27 (m, 3H, propanamide α - CH_2 , piperidine 6- CH_2), 2.33 – 2.46 (m, 4H, propanamide β - CH_2 , piperidine 2- CH_2), 2.68 (dd, J = 14.1, 10.1 Hz, 1H, Phe³ β - CH_2), 2.73 (dt, J = 11.4, 3.6 Hz, 1H, piperidine 6- CH_2), 2.81 (dd, J = 13.9, 9.0 Hz, 1H, Phe¹ β - CH_2), 2.95 (dd, J = 14.0, 4.3 Hz, 1H, Phe³ β - CH_2), 2.99 (dd, J = 13.8, 5.2 Hz, 1H, Phe¹ β - CH_2), 4.11 (dd, J = 8.8, 6.8 Hz, 1H, Val² α -CH), 4.48 (td, J = 8.6, 5.2 Hz, 1H, Phe¹ α -CH), 4.61 (td, J = 9.2, 4.2 Hz, 1H, Phe³ α -CH), 6.55 (dd, J = 7.9, 2.5 Hz, 1H, phenol 6-CH), 6.64 – 6.72 (m, 2H, phenol 2-CH, phenol 4-CH), 7.06 (s, 1H, Phe³ amide NH_2), 7.08 (t, J = 7.8 Hz, 1H, phenol 5-CH), 7.12 – 7.27 (m, 10H, phenyl CH), 7.35 (s, 1H, Phe³ amide NH_2), 7.92 (d, J = 9.0 Hz, 1H, Phe¹-Ala² amide NH), 8.00 (d, J = 8.3 Hz, 1H,

Pr-Phe¹ amide NH), 8.35 (d, $J = 8.5$ Hz, 1H, Ala²-Phe³ amide NH), 8.43 (s, 1H, phenol OH).

¹³C NMR (DMSO-d₆): δ 14.4, 16.1, 18.1, 19.1, 26.5, 27.3, 29.3, 30.6, 32.9, 37.5, 37.6, 38.0, 38.3, 49.0, 53.3, 53.6, 54.0, 55.1, 112.2, 112.5, 116.0, 126.2, 126.2, 127.9, 128.0, 128.9, 129.1, 129.2, 137.8, 137.9, 151.7, 157.1, 171.1, 171.3, 171.8, 172.6.

m/z : HRMS C₃₉H₅₁N₅O₅ [MH]⁺ calc 670.3963, found 670.3957.



(2S)-N-(1-amino-1-oxo-3-phenylpropan-2-yl)-3-hydroxy-2-((S)-2-(3-((3R,4R)-4-(3-hydroxyphenyl)-3,4-dimethylpiperidin-1-yl)propanamido)-3-phenylpropanamido)propanamide (170d)

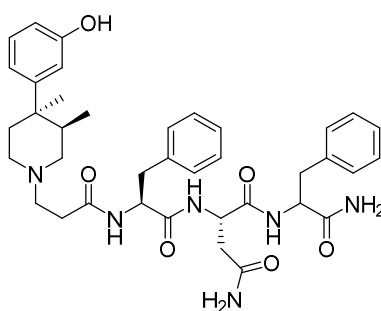
The title compound was synthesised as described in general procedure 5, using *N*-((2S)-1-(((2S)-1-((1-amino-1-oxo-3-phenylpropan-2-yl)amino)-3-hydroxy-1-oxopropan-2-yl)amino)-1-oxo-3-phenylpropan-2-yl)acrylamide (**177d**) (5 mg, 0.01 mmol), which was synthesised using general procedure 4. This yielded **170d** as a white solid (7 mg, 100%).

¹H NMR (DMSO-d₆): δ 0.62 (d, $J = 6.9$ Hz, 3H, piperidine 3-CH₃), 1.19 (s, 3H, piperidine 4-CH₃), 1.46 (d, $J = 12.3$ Hz, 1H piperidine 5-CH₂), 1.85 – 1.94 (m, 1H, piperidine 3-CH), 2.10 (td, $J = 12.5, 4.0$ Hz, 1H, piperidine 5-CH₂), 2.14 – 2.27 (m, 3H, propanamide α -CH₂, piperidine 6-CH₂), 2.29 – 2.47 (m, 4H, propanamide β -CH₂, piperidine 2-CH₂), 2.68 (dd, $J = 14.1, 10.1$ Hz, 1H, Phe³ β -CH₂), 2.74 (d, $J = 11.2$ Hz, 1H, piperidine 6-CH₂), 2.84 (dd, $J = 13.9, 9.2$ Hz, 1H, Phe¹ β -CH₂), 2.97 (dd, $J = 13.9, 4.1$ Hz, 1H, Phe³ β -CH₂), 3.08 (dd, $J = 14.0, 4.5$ Hz, 1H, Phe¹ β -CH₂), 3.48 (dd, $J = 10.9, 6.2$ Hz, 1H, Ser² β -CH₂), 3.59 (dd, $J = 10.7, 6.0$ Hz, 1H, Ser² CH₂), 4.27 (q, $J = 6.4$ Hz, 1H, Ser² α -CH), 4.41 (td, $J = 8.7, 4.5$ Hz,

¹H, Phe¹ α-CH), 4.59 (td, *J* = 9.2, 4.0 Hz, 1H, Phe³ α-CH), 6.56 (dd, *J* = 8.0, 2.3 Hz, 1H, phenol 6-CH), 6.65 – 6.72 (m, 2H, phenol 2-CH, phenol 4-CH), 7.08 (t, *J* = 7.8 Hz, 1H, phenol 5-CH), 7.12 – 7.29 (m, 11H, Phe³ amide NH₂, phenyl CH), 7.40 (s, 1H, Phe³ amide NH₂), 8.06 (d, *J* = 8.2 Hz, 1H, Pr-Phe¹ amide NH), 8.19 (d, *J* = 7.5 Hz, 1H, Phe¹-Ala² amide NH), 8.37 (d, *J* = 8.4 Hz, 1H, Ala²-Phe³ amide NH), 8.44 (s, 1H, phenol OH).

¹³C NMR (DMSO-d₆): δ 16.1, 27.3, 32.9, 37.0, 37.8, 37.9, 37.9, 49.0, 53.4, 54.0, 54.0, 55.1, 55.1, 61.7, 112.2, 112.5, 116.0, 126.1, 126.2, 127.9, 128.0, 128.9, 129.1, 129.1, 137.9, 138.0, 151.7, 157.2, 165.6, 169.8, 171.3, 171.5, 172.8.

m/z: HRMS C₃₇H₄₇N₅O₆ [MH]⁺ calc 658.3599, found 658.3604.



(2S)-N¹-(1-amino-1-oxo-3-phenylpropan-2-yl)-2-((S)-2-(3-((3R,4R)-4-(3-hydroxyphenyl)-3,4-dimethylpiperidin-1-yl)propanamido)-3-phenylpropanamido)succinamide (170e)

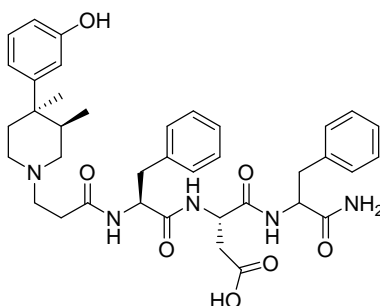
The title compound was synthesised as described in general procedure 5, using (2S)-2-((S)-2-acrylamido-3-phenylpropanamido)-N¹-(1-amino-1-oxo-3-phenylpropan-2-yl)succinimide (**177e**) (6 mg, 0.01 mmol), which was synthesised using general procedure 4. This yielded **170e** as a white solid (8 mg, 100%).

¹H NMR (DMSO-d₆): δ 0.63 (d, *J* = 6.9 Hz, 3H, piperidine 3-CH₃), 1.20 (s, 3H, piperidine 4-CH₃), 1.46 (d, *J* = 11.8 Hz, 1H piperidine 5-CH₂), 1.85 – 1.96 (m, 1H, piperidine 3-CH), 2.03 – 2.30 (m, 4H, propanamide α-CH₂, piperidine 5-CH₂, piperidine 6-CH₂), 2.31 – 2.46 (m, 5H, propanamide β-CH₂, piperidine 2-CH₂, Asn² β-CH₂), 2.52 – 2.66 (m, 2H, Asn² β-CH₂, Phe³ β-CH₂), 2.73 (d, *J* = 10.5 Hz, 1H, piperidine 6-CH₂), 2.82 (dd, *J* = 14.2, 9.7 Hz, 1H, Phe¹ β-CH₂), 2.87 (dd, *J* =

13.9, 3.9 Hz, 1H, Phe³ β-CH₂), 3.11 (dd, *J* = 14.1, 4.2 Hz, 1H, Phe¹ β-CH₂), 4.34 (td, *J* = 8.9, 4.1 Hz, 1H, Phe¹ α-CH), 4.44 – 4.58 (m, 2H, Asn² α-CH, Phe³ α-CH), 6.55 (dd, *J* = 7.9, 2.3 Hz, 1H, phenol 6-CH), 6.67 (t, *J* = 2.1 Hz, 1H, phenol 2-CH), 6.70 (d, *J* = 7.8 Hz, 1H, phenol 4-CH), 6.99 (s, 1H, Asn² NH₂), 7.09 (t, *J* = 7.9 Hz, 1H, phenol 5-CH), 7.13 – 7.30 (m, 11H, Phe³ amide NH₂, phenyl CH), 7.43 (s, 1H, Phe³ amide NH₂), 7.47 (s, 1H, Asn² NH₂), 8.06 (d, *J* = 8.3 Hz, 1H, Pr-Phe¹ amide NH), 8.30 (s, 1H, phenol OH), 8.33 (d, *J* = 7.8 Hz, 1H, Phe¹-Ala² amide NH), 8.36 (d, *J* = 8.4 Hz, 1H, Ala²-Phe³ amide NH).

¹³C NMR (DMSO-d₆): δ 16.1, 27.3, 29.9, 32.8, 36.8, 36.9, 37.8, 37.9, 37.9, 40.2, 48.9, 49.7, 53.4, 54.0, 55.2, 112.2, 112.5, 116.1, 126.1, 126.2, 127.9, 128.1, 128.9, 129.0, 129.1, 137.8, 138.2, 151.7, 157.1, 170.5, 171.3, 171.3, 171.9, 172.8.

m/z: HRMS C₃₈H₄₈N₆O₆ [MH]⁺ calc 685.3708, found 685.3705.



(3S)-4-((1-amino-1-oxo-3-phenylpropan-2-yl)amino)-3-((S)-2-(3-((3R,4R)-4-(3-hydroxyphenyl)-3,4-dimethylpiperidin-1-yl)propanamido)-3-phenylpropanamido)-4-oxobutanoic acid (170f)

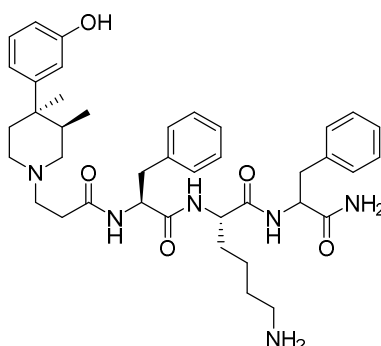
The title compound was synthesised as described in general procedure 5, using (3S)-3-((S)-2-acrylamido-3-phenylpropanamido)-4-((1-amino-1-oxo-3-phenylpropan-2-yl)amino)-4-oxobutanoic acid (**177f**) (6 mg, 0.01 mmol), which was synthesised using general procedure 4. This yielded **170f** as a white solid (8 mg, 100%).

¹H NMR (DMSO-d₆): δ 0.63 (d, *J* = 6.9 Hz, 3H, piperidine 3-CH₃), 1.20 (s, 3H, piperidine 4-CH₃), 1.46 (d, *J* = 12.1 Hz, 1H piperidine 5-CH₂), 1.86 – 1.96 (m, 1H, piperidine 3-CH), 2.06 – 2.31 (m, 4H, propanamide α-CH₂, piperidine 5-CH₂,

piperidine 6-CH₂), 2.34 – 2.49 (m, 5H, propanamide β-CH₂, piperidine 2-CH₂, Asn² β-CH₂), 2.52 – 2.70 (m, 2H, Asp² β-CH₂, Phe³ β-CH₂), 2.77 (d, *J* = 10.8 Hz, 1H, piperidine 6-CH₂), 2.83 (dd, *J* = 13.9, 9.2 Hz, 1H, Phe¹ β-CH₂), 2.92 (dd, *J* = 14.0, 4.2 Hz, 1H, Phe³ β-CH₂), 3.06 (dd, *J* = 14.0, 4.5 Hz, 1H, Phe¹ β-CH₂), 4.34 (td, *J* = 8.7, 4.4 Hz, 1H, Phe¹ α-CH), 4.45 (q, *J* = 7.0 Hz, 1H, Asn² α-CH), 4.51 (td, *J* = 9.6, 4.2 Hz, 1H, Phe³ α-CH), 6.54 (dd, *J* = 8.8, 1.9 Hz, 1H, phenol 6-CH), 6.64 – 6.72, phenol 2-CH, phenol 4-CH), 7.00 – 7.29 (m, 12H, phenol 5-CH, Phe³ amide NH₂, phenyl CH), 7.40 (s, 1H, Phe³ amide NH₂), 8.02 (d, *J* = 8.2 Hz, 1H, Pr-Phe¹ amide NH), 8.30 (s, 1H, phenol OH), 8.37 (d, *J* = 7.6 Hz, 1H, Phe¹-Ala² amide NH), 8.41 (d, *J* = 8.4 Hz, 1H, Ala²-Phe³ amide NH).

¹³C NMR (DMSO-d₆): δ 16.1, 27.2, 29.8, 32.6, 37.0, 37.3, 37.6, 37.9, 40.2, 48.9, 50.0, 53.5, 53.8, 54.0, 55.1, 112.2, 112.6, 116.1, 126.1, 126.2, 128.0, 128.1, 128.9, 129.1, 129.1, 137.9, 138.1, 151.5, 157.2, 170.6, 171.2, 171.2, 171.4, 172.6, 172.8.

m/z: HRMS C₃₈H₄₈N₆O₆ [MH]⁺ calc 686.3548, found 686.3544.



(2S)-6-amino-N-(1-amino-1-oxo-3-phenylpropan-2-yl)-2-((S)-2-(3-((3R,4R)-4-(3-hydroxyphenyl)-3,4-dimethylpiperidin-1-yl)propanamido)-3-phenylpropanamido)hexanamide (170g)

The title compound was synthesised as described in general procedure 5, using (2S)-2-((S)-2-acrylamido-3-phenylpropanamido)-6-amino-N-(1-amino-1-oxo-3-phenylpropan-2-yl)hexanamide (**177g**) (7 mg, 0.015 mmol), which was synthesised using general procedure 4. This yielded **170g** as a white solid (10 mg, 100%).

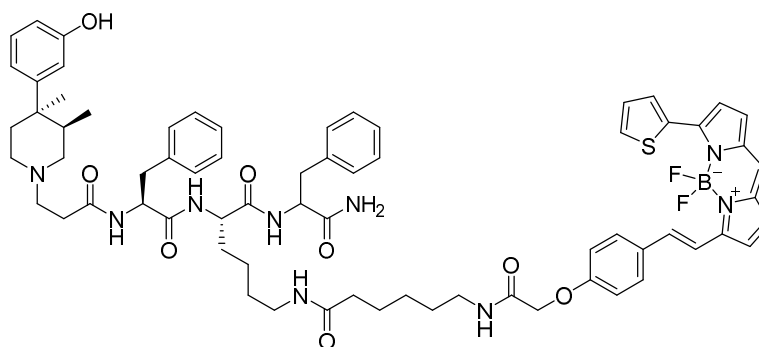
(2S)-N-(1-amino-1-oxo-3-phenylpropan-2-yl)-5-guanidino-2-((S)-2-(3-((3R,4R)-4-(3-hydroxyphenyl)-3,4-dimethylpiperidin-1-yl)propanamido)-3-phenylpropanamido)pentanamide (170h)

The title compound was synthesised as described in general procedure 5, using (2S)-2-((S)-2-acrylamido-3-phenylpropanamido)-N-(1-amino-1-oxo-3-phenylpropan-2-yl)-5-guanidinopentanamide (**177h**) (7 mg, 0.015 mmol), which was synthesised using general procedure 4. This yielded **170h** as a white solid (10 mg, 100%).

¹H NMR (DMSO-d₆): δ 0.61 (d, *J* = 6.9 Hz, 3H, piperidine 3-CH₃), 1.19 (s, 3H, piperidine 4-CH₃), 1.32 – 1.42 (m, 2H, Arg² γ-CH₂), 1.45 (d, *J* = 12.6 Hz, 1H, piperidine 5-CH₂), 1.40 – 1.71 (m, 2H, Arg² β-CH₂), 1.83 – 1.95 (m, 1H, piperidine 3-CH), 2.08 (td, *J* = 13.1, 6.5 Hz, 1H, piperidine 5-CH₂), 2.12 – 2.30 (m, 3H, propanamide α-CH₂, piperidine 6-CH₂), 2.34 – 2.45 (m, 4H, propanamide β-CH₂, piperidine 2-CH₂), 2.64 – 2.77 (m, 2H, Phe³ β-CH₂, piperidine 6-CH₂), 2.82 (dd, *J* = 13.8, 9.0 Hz, 1H, Phe¹ β-CH₂), 2.92 – 3.09 (m, 4H, Arg² δ-CH₂, Phe¹ β-CH₂, Phe³ β-CH₂), 4.19 (td, *J* = 8.0, 5.1 Hz, 1H, Arg² α-CH), 4.42 (td, *J* = 8.5, 4.9 Hz, 1H, Phe¹ α-CH), 4.53 (ddd, *J* = 9.8, 8.1, 4.2 Hz, 1H, Phe³ α-CH), 6.55 (dd, *J* = 8.0, 2.2 Hz, 1H, phenol 6-CH), 6.63 – 6.73, phenol 2-CH, phenol 4-CH), 7.07 (t, *J* = 7.8 Hz, 1H, phenol 5-CH), 7.09 (s, 1H, Phe³ amide NH₂), 7.10 – 7.27 (m, 10H, phenyl CH), 7.37 (s, 1H, Phe³ amide NH₂), 8.00 (d, *J* = 8.2 Hz, 1H, Pr-Phe¹ amide NH), 8.36 (d, *J* = 7.5 Hz, 1H, Phe¹-Ala² amide NH), 8.37 (s, 1H, phenol OH), 8.42 (d, *J* = 8.0 Hz, 1H, Ala²-Phe³ amide NH), 8.65 (t, *J* = 5.1 Hz, 1H, Arg² δ-NH).

¹³C NMR (DMSO-d₆): δ 16.1, 24.6, 27.3, 28.8, 29.9, 32.9, 37.5, 37.5, 37.9, 49.0, 51.4, 53.7, 53.8, 54.0, 55.1, 112.2, 112.5, 116.0, 126.2, 128.0, 128.0, 128.9, 129.1, 129.1, 137.8, 137.9, 151.7, 157.2, 157.3, 165.8, 171.0, 171.5, 171.6, 172.7.

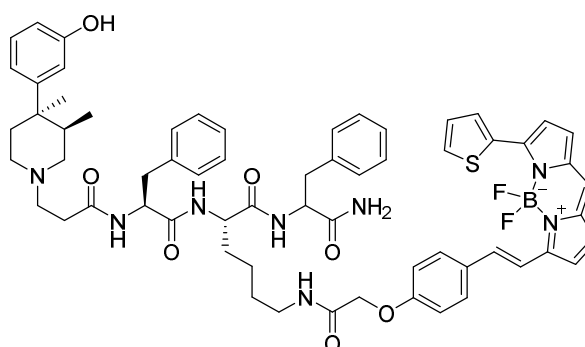
m/z: HRMS C₄₀H₅₄N₈O₅ [MH₂]²⁺ calc 364.2182, found 364.2189.



(2S)-N-(1-amino-1-oxo-3-phenylpropan-2-yl)-6-(6-(2-(4-((E)-2-(5,5-difluoro-7-(thiophen-2-yl)-5H-4 λ^4 ,5 λ^4 -dipyrrolo[1,2-c:2',1'-f][1,3,2]diazaborinin-3-yl)vinyl)phenoxy)acetamido)hexanamido)-2-((S)-2-(3-((3R,4R)-4-(3-hydroxyphenyl)-3,4-dimethylpiperidin-1-yl)propanamido)-3-phenylpropanamido)hexanamide (192)

To (2S)-6-amino-N-(1-amino-1-oxo-3-phenylpropan-2-yl)-2-((S)-2-(3-((3R,4R)-4-(3-hydroxyphenyl)-3,4-dimethylpiperidin-1-yl)propanamido)-3-phenylpropanamido)hexanamide (**170g**) (1.17 mg, 1.5 μ mol, 1.0 eq) in DMF (0.5 ml) was added BODIPY 630/650-X NHS ester (1.0 mg, 1.5 μ mol, 1.0 eq) in DMF (0.5 ml). The reaction mixture was stirred at room temperature for 90 min. Solvent was removed under high vacuum and purification by reverse phase HPLC (system 3) yielded **192**, a blue solid (1.0 mg, 53%).

m/z: HRMS C₆₉H₈₀BF₂N₉O₈S [MH]⁺ calcd 1244.5984; found 1244.5992.

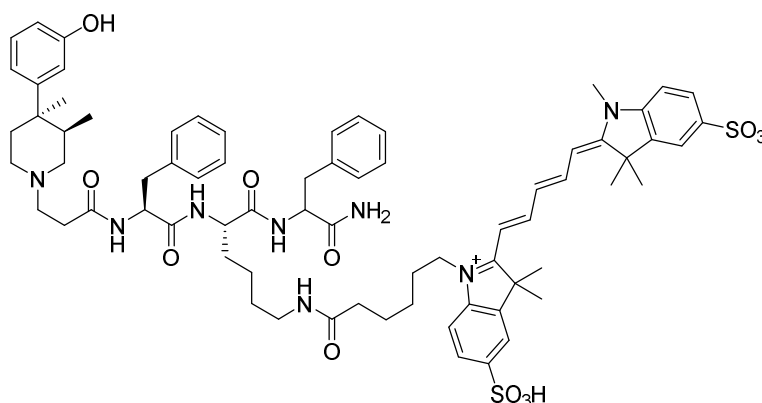


(2S)-N-(1-amino-1-oxo-3-phenylpropan-2-yl)-6-(2-(4-((E)-2-(5,5-difluoro-7-(thiophen-2-yl)-5H-4 λ^4 ,5 λ^4 -dipyrrolo[1,2-c:2',1'-f][1,3,2]diazaborinin-3-yl)vinyl)phenoxy)acetamido)-2-((S)-2-(3-((3R,4R)-4-(3-hydroxyphenyl)-3,4-

**dimethylpiperidin-1-yl)propanamido)-3-phenylpropanamido)hexanamide
(193)**

To BODIPY 630/650 (0.68 mg, 1.5 μ mol) in DMF (0.5 ml) was added PyBOP (0.78 mg, 1.5 μ mol, 1.0 eq) and DIPEA (0.26 μ l, 1.5 μ mol, 1.0 eq). The reaction mixture was stirred at room temperature for 15 min after which (2*S*)-6-amino-*N*-(1-amino-1-oxo-3-phenylpropan-2-yl)-2-((*S*)-2-(3-((3*R*,4*R*)-4-(3-hydroxyphenyl)-3,4-dimethylpiperidin-1-yl)propanamido)-3-phenylpropanamido)hexanamide (**170g**) (0.73 mg, 1.5 μ mol, 1.0 eq) in DMF (0.5 ml) was added. The reaction mixture was then stirred at room temperature for 90 min. Solvent was removed under high vacuum and purification by reverse phase HPLC (system 3) yielded **193**, a blue solid (0.6 mg, 35%).

m/z: HRMS C₆₃H₆₉BF₂N₈O₇S [MH]⁺ calcd 1131.5144; found 1131.5148.



(*E*)-2-((2*E*,4*E*)-5-(1-(6-(((5*S*)-6-((1-amino-1-oxo-3-phenylpropan-2-yl)amino)-5-((*S*)-2-(3-((3*R*,4*R*)-4-(3-hydroxyphenyl)-3,4-dimethylpiperidin-1-yl)propanamido)-3-phenylpropanamido)-6-oxohexyl)amino)-6-oxohexyl)-3,3-dimethyl-5-sulfo-3*H*-indol-1-ium-2-yl)penta-2,4-dien-1-ylidene)-1,3,3-trimethylindoline-5-sulfonate (194**)**

To (2*S*)-6-amino-*N*-(1-amino-1-oxo-3-phenylpropan-2-yl)-2-((*S*)-2-(3-((3*R*,4*R*)-4-(3-hydroxyphenyl)-3,4-dimethylpiperidin-1-yl)propanamido)-3-phenylpropanamido)hexanamide (**170g**) (1.05 mg, 1.5 μ mol, 1.0 eq) in DMF (0.5 ml) was added sulfo-Cy5 NHS ester (1.17 mg, 1.5 μ mol, 1.0 eq) in DMF (0.5 ml). The reaction mixture was stirred at room temperature for 90 min. Solvent

was removed under high vacuum and purification by reverse phase HPLC (system 3) yielded **194**, a blue solid (0.8 mg, 40%).

m/z: HRMS C₇₂H₉₀N₈O₁₂S₂ [M-H]⁻ calcd 1321.6047; found 1321.6037.

5.2 General pharmacology

Cell culture

MOR-expressing HEK293 cells and SNAP-MOR-expressing HEK293 cells were obtained from Dr Arisbel Gondin, who performed the transfections and isolated stable clones as described in Gondin *et al.*¹⁴⁹ Cells were grown in Dulbecco's modified Eagle's medium (DMEM) supplemented with 10% fetal calf serum (FCS) and maintained at 37 °C in a humidified incubator containing 5% CO₂.

Cells were grown to confluence in 75 cm² tissue culture treated flasks (T75s). Passaging of cells proceeded with removal of the DMEM and washing with phosphate buffered saline (PBS). Cells were lifted from the flask by 1 mL 1x trypsin-EDTA and removed from the flask with PBS. Following this, the cells were centrifuged at 1000 rpm for 5 min and the supernatant discarded. The pellet was resuspended in DMEM and a portion (typically 1/5 or 1/10) transferred into a new T75 flask containing DMEM.

Preparation of Lumi4-Tb-labelled membranes

SNAP-MOR-expressing HEK293 cells were seeded into poly-*D*-Lysine-coated 175 cm² tissue culture treated flasks (T175s) and grown to confluence. DMEM was aspirated and the cells were washed with PBS. SNAP tag labelling was performed by addition of 12 ml of 100 nM Lumi4-Tb (CisBio, Bagnols-sur-Ce'ze, France) in Tag-lite labelling medium to the cells and the cells incubated at 37 °C in a humidified incubator containing 5% CO₂ for 1 hour. The labelling solution was removed, and the cells washed with PBS. Cells were then removed from the flask by scraping and washing with further PBS. The cells were transferred

to a 50 ml tube and centrifuged at 1500 rpm for 10 min. The supernatant was removed, and the resulting pellets stored at -80°C.

Membranes were prepared from the defrosted cell pellets which were resuspended in 20 ml PBS and homogenised using an electrical homogeniser in 20 × 2 sec bursts. The resultant homogenate was centrifuged at 1500 x *g* for 20 min to remove unbroken cells and nuclei. The supernatant was decanted and subsequently centrifuged at 41415 x *g* for 30 min, the supernatant discarded, and the pellet resuspended in PBS. Further homogenisation was carried out by 20 passes of a glass homogeniser. Protein concentration was determined using a BCA protein assay and membranes were stored at -80 °C until required.

Whole cell competition binding assays

Cells were seeded into poly-*D*-Lysine-coated thin clear bottomed black wall 96 well plates (Greiner Bio-One Ltd, Stonehouse, UK) 24 hours prior to the assay. On the day of the experiment, DMEM was aspirated and the cells washed with room temperature PBS. The cells were incubated in duplicate with increasing concentrations of unlabelled ligand and 50 nM fluorescent ligand **51** in a final volume of 100 µl of HEPES-buffered saline solution (HBSS: 145 mmol/L NaCl, 5 mmol/L KCl, 1.7 mmol/L CaCl₂, 1 mmol/L MgSO₄, 10 mmol/L HEPES, 2 mmol/L sodium pyruvate, 1.5 mmol/L NaHCO₃, 10 mmol/L *D*-glucose, pH 7.4) for 1 hour at 37 °C in a humidified incubator. Plates were imaged using an ImageXpress Ultra confocal plate reader which captured four images per well. Excitation of **51** used a 635 nm laser (20 % laser power) with emission collected through a 640-685 nm bandpass filter. The focus and laser gain settings used were adjusted for each plate. Values for fluorescence intensity were obtained using a multi-wavelength cell scoring algorithm within the MetaXpress software, normalised as a percentage of maximal integrated intensity per plate (where fluorescence intensity in the absence of unlabelled competitor was defined at 100%) from mean total well intensity.

Results were fitted to a competition binding curve in GraphPad Prism 8.4.3 using non-linear regression analysis (variable slope – four parameters). IC₅₀ values were used to determine K_i using the Cheng-Prusoff equation:¹²²

$$K_i = \frac{IC_{50}}{1 + \frac{[\text{fluorescent ligand}]}{K_D}}$$

Where [fluorescent ligand] = concentration of free fluorescent ligand used in the assay. K_D = the dissociation constant of the fluorescent ligand for the receptor. IC₅₀ = the concentration of unlabelled ligand that displaces 50% of the specific binding of the fluorescent ligand.

Membrane-based competition binding assays

To each well of an opaque bottomed 96-well plate were added increasing concentrations of unlabelled ligand and fluorescent ligand at a concentration equal to its K_D, followed by 2.5 µg of Lumi4-Tb-labelled SNAP-MOR-expressing HEK293 cell membrane, in a final volume of 100 µl of HBSS. Membranes were incubated in duplicate or triplicate for 90 mins at 37 °C, after which plates were read in a TR-FRET competition binding assay using a PHERAstar FS plate reader (BMG Labtech, Offenberg, Germany) with the terbium (donor) excited with 30 flashes of laser at 337 nm and emission collected at 620 nm (terbium) and 665 nm (Cy5/BY630) 400 ms after excitation.

Competition binding curves were fitted from the percentage of maximal measured HTRF emission ratio (665/620 nm) (where HTRF emission ratio in the absence of unlabelled competitor was defined at 100%, and the mean of the lowest duplicate or triplicate sample set on the plate was defined as 0%) in GraphPad Prism 8.4.3 using non-linear regression analysis. IC₅₀ values were used to determine K_i using the Cheng-Prusoff equation (see above).¹²²

Saturation binding assays

Saturation binding assays were carried out using Lumi4-Tb-labelled SNAP-MOR-expressing HEK293 cell membranes. Increasing concentrations of fluorescent ligand followed 2.5 µg of membrane were added to each well of an opaque bottomed 96-well plate in HBSS, both in the absence (total binding)

and presence (non-specific binding) of 10 μ M naloxone, in a final volume of 100 μ l of HBSS. Membranes were incubated in duplicate or triplicate for 90 mins at 37 °C, after which plates were read in a TR-FRET saturation binding assay using a PHERAstar FS plate reader as described above.

Total and non-specific binding curves were fitted from the measured HTRF emission ratio (665/620 nm) (where HTRF emission ratio in the absence of unlabelled competitor was defined at 100%, and the mean of the lowest duplicate or triplicate sample set on the plate was defined as 0%) in GraphPad Prism 8.4.3 using a one site – total and non-specific binding model, from which K_D of specific binding curve was determined.

Statistical analysis

Statistical analysis was carried out using GraphPad Prism 8.4.3 software by one-way ANOVA and post-hoc analysis as described.

5.3 *In silico* modelling

The three dimensional model of MOR (PDB: 4DKL)³³ was obtained from GPCRdb (<https://www.gpcrdb.org>) and loaded into the online docking software DockingServer (<http://www.dockingserver.com/web>). Prior to docking, the binding site was established using the bound ligand β -FNA (**74**). Compounds of the structures **92** (**Figure 2-15**) and **93** (**Figure 2-20**) were drawn and docked. Twenty docking poses of each congener which visually met the criteria described in **Figure 2-16**, were inspected for 6-substituent interactions. Outputs were visualised on DockingServer as no export file was available.

6. References

1. Alberts, B.; Johnson, A.; Lewis, J.; Raff, M.; Roberts, K.; Walter, P., *Molecular Biology of the Cell*. 5th ed.; Garland Science: 2008.
2. Congreve, M.; Langmead, C. J.; Mason, J. S.; Marshall, F. H., Progress in Structure Based Drug Design for G Protein-Coupled Receptors. *J. Med. Chem.* **2011**, *54* (13), 4283-4311.
3. Rosenbaum, D. M.; Rasmussen, S. G. F.; Kobilka, B. K., The structure and function of G-protein-coupled receptors. *Nature* **2009**, *459* (7245), 356-363.
4. Hamm, H. E., The Many Faces of G Protein Signaling. *J. Biol. Chem.* **1998**, *273* (2), 669-672.
5. Stein, C., Opioid Receptors. *Annu. Rev. Med.* **2016**, *67* (1), 433-451.
6. Endres-Becker, J.; Heppenstall, P. A.; Mousa, S. A.; Labuz, D.; Oksche, A.; Schäfer, M.; Stein, C.; Zöllner, C., μ -Opioid Receptor Activation Modulates Transient Receptor Potential Vanilloid 1 (TRPV1) Currents in Sensory Neurons in A Model of Inflammatory Pain. *Mol. Pharmacol.* **2007**, *71* (1), 12-18.
7. Nockemann, D.; Rouault, M.; Labuz, D.; Hublitz, P.; McKnelly, K.; Reis, F. C.; Stein, C.; Heppenstall, P. A., The K⁺ channel GIRK2 is both necessary and sufficient for peripheral opioid-mediated analgesia. *EMBO Mol. Med.* **2013**, *5* (8), 1263-1277.
8. Tedford, H. W.; Zamponi, G. W., Direct G Protein Modulation of Cav2 Calcium Channels. *Pharmacol. Rev.* **2006**, *58* (4), 837-862.
9. Waldhoer, M.; Bartlett, S. E.; Whistler, J. L., Opioid Receptors. *Ann. Rev. Biochem.* **2004**, *73* (1), 953-990.
10. Law, P.-Y.; Reggio, P. H.; Loh, H. H., Opioid receptors: toward separation of analgesic from undesirable effects. *Trends Biochem Sci* **2013**, *38* (6), 275-282.
11. Pradhan, A. A.; Smith, M. L.; Kieffer, B. L.; Evans, C. J., Ligand-directed signalling within the opioid receptor family. *Br. J. Pharmacol.* **2012**, *167* (5), 960-969.
12. Ramoutsaki, I. A.; Askitopoulou, H.; Konsolaki, E., Pain relief and sedation in Roman Byzantine texts: Mandragoras officinarum, Hyoscyamos niger and Atropa belladonna. *International Congress Series* **2002**, *1242*, 43-50.
13. Markham, A., Naldemedine: First Global Approval. *Drugs* **2017**, *77* (8), 923-927.
14. Mordecai, L.; Reynolds, C.; Donaldson, L. J.; de C Williams, A. C., Patterns of regional variation of opioid prescribing in primary care in England: a retrospective observational study. *Br. J. Gen. Pract.* **2018**, *68* (668), e225-e233.
15. Spetea, M.; Asim, M. F.; Wolber, G.; Schmidhammer, H., The μ Opioid Receptor and Ligands Acting at the μ Opioid Receptor, as Therapeutics and Potential Therapeutics. *Curr. Pharm. Des.* **2013**, *19* (42), 7415-7434.
16. Pathan, H.; Williams, J., Basic opioid pharmacology: an update. *Br J Pain* **2012**, *6* (1), 11-16.
17. Nelson, A. D.; Camilleri, M., Opioid-induced constipation: advances and clinical guidance. *Ther. Adv. Chronic Dis.* **2016**, *7* (2), 121-134.
18. Viscusi, E. R.; Gan, T. J.; Leslie, J. B.; Foss, J. F.; Talon, M. D.; Du, W.; Owens, G., Peripherally Acting Mu-Opioid Receptor Antagonists and Postoperative Ileus: Mechanisms of Action and Clinical Applicability. *Anesth. Analg.* **2009**, *108* (6), 1811-1822.
19. Lutfy, K.; Cowan, A., Buprenorphine: a unique drug with complex pharmacology. *Curr. Neuropharmacol.* **2004**, *2* (4), 395-402.

20. Welsh, C.; Valadez-Meltzer, A., Buprenorphine: a (relatively) new treatment for opioid dependence. *Psychiatry (Edgmont)* **2005**, *2* (12), 29-39.
21. Polakiewicz, R. D.; Schieferl, S. M.; Gingras, A.-C.; Sonenberg, N.; Comb, M. J., μ -Opioid Receptor Activates Signaling Pathways Implicated in Cell Survival and Translational Control*. *J. Biol. Chem.* **1998**, *273* (36), 23534-23541.
22. Gupta, K.; Kshirsagar, S.; Chang, L.; Schwartz, R.; Law, P.-Y.; Yee, D.; Hebbel, R. P., Morphine Stimulates Angiogenesis by Activating Proangiogenic and Survival-promoting Signaling and Promotes Breast Tumor Growth. *Cancer Res.* **2002**, *62* (15), 4491-4498.
23. Boehncke, S.; Hardt, K.; Schadendorf, D.; Henschler, R.; Boehncke, W.-H.; Duthey, B., Endogenous μ -opioid peptides modulate immune response towards malignant melanoma. *Exp. Dermatol.* **2011**, *20* (1), 24-28.
24. Nguyen, J.; Luk, K.; Vang, D.; Soto, W.; Vincent, L.; Robiner, S.; Saavedra, R.; Li, Y.; Gupta, P.; Gupta, K., Morphine stimulates cancer progression and mast cell activation and impairs survival in transgenic mice with breast cancer. *Br. J. Anaesth.* **2014**, *113*, i4-i13.
25. Mathew, B.; Lennon, F. E.; Siegler, J.; Mirzapioazova, T.; Mambetsariev, N.; Sammani, S.; Gerhold, L. M.; LaRiviere, P. J.; Chen, C.-T.; Garcia, J. G. N.; Salgia, R.; Moss, J.; Singleton, P. A., The Novel Role of the Mu Opioid Receptor in Lung Cancer Progression: A Laboratory Investigation. *Anesth. Analg.* **2011**, *112* (3), 558-567.
26. Singleton, P. A.; Mirzapioazova, T.; Hasina, R.; Salgia, R.; Moss, J., Increased μ -opioid receptor expression in metastatic lung cancer. *Br. J. Anaesth.* **2014**, *113*, i103-i108.
27. Lennon, F. E.; Mirzapioazova, T.; Mambetsariev, B.; Poroyko, V. A.; Salgia, R.; Moss, J.; Singleton, P. A., The Mu Opioid Receptor Promotes Opioid and Growth Factor-Induced Proliferation, Migration and Epithelial Mesenchymal Transition (EMT) in Human Lung Cancer. *PLoS One* **2014**, *9* (3), e91577.
28. Singleton, P. A.; Moss, J.; Karp, D. D.; Atkins, J. T.; Janku, F., The mu opioid receptor: A new target for cancer therapy? *Cancer* **2015**, *121* (16), 2681-2688.
29. Zylla, D.; Gourley, B. L.; Vang, D.; Jackson, S.; Boatman, S.; Lindgren, B.; Kuskowski, M. A.; Le, C.; Gupta, K.; Gupta, P., Opioid requirement, opioid receptor expression, and clinical outcomes in patients with advanced prostate cancer. *Cancer* **2013**, *119* (23), 4103-4110.
30. Bortsov, Andrey V.; Millikan, Robert C.; Belfer, I.; Boortz-Marx, Richard L.; Arora, H.; McLean, Samuel A., μ -Opioid Receptor Gene A118G Polymorphism Predicts Survival in Patients with Breast Cancer. *Anesthesiology* **2012**, *116* (4), 896-902.
31. Wang, S.; Li, Y.; Liu, X.-D.; Zhao, C.-X.; Yang, K.-Q., Polymorphism of A118G in μ -opioid receptor gene is associated with risk of esophageal squamous cell carcinoma in a Chinese population. *Int. J. Clin. Oncol.* **2013**, *18* (4), 666-669.
32. de Graaf, C.; Rognan, D., Customizing G Protein-coupled receptor models for structure-based virtual screening. *Curr. Pharm. Des.* **2009**, *15* (35), 4026-4048.
33. Manglik, A.; Kruse, A. C.; Kobilka, T. S.; Thian, F. S.; Mathiesen, J. M.; Sunahara, R. K.; Pardo, L.; Weis, W. I.; Kobilka, B. K.; Granier, S., Crystal structure of the μ -opioid receptor bound to a morphinan antagonist. *Nature* **2012**, *485* (7398), 321-326.
34. Granier, S.; Manglik, A.; Kruse, A. C.; Kobilka, T. S.; Thian, F. S.; Weis, W. I.; Kobilka, B. K., Structure of the δ -opioid receptor bound to naltrindole. *Nature* **2012**, *485* (7398), 400-404.
35. Wu, H.; Wacker, D.; Mileni, M.; Katritch, V.; Han, G. W.; Vardy, E.; Liu, W.; Thompson, A. A.; Huang, X.-P.; Carroll, F. I.; Mascarella, S. W.; Westkaemper, R. B.;

- Mosier, P. D.; Roth, B. L.; Cherezov, V.; Stevens, R. C., Structure of the human κ -opioid receptor in complex with JDTic. *Nature* **2012**, *485* (7398), 327-332.
36. Schneider, G.; Clark, D. E., Automated De Novo Drug Design: Are We Nearly There Yet? *Angew. Chem. Int. Ed.* **2019**, *58* (32), 10792-10803.
37. Mok, N. Y.; Chadwick, J.; Kellett, K. A. B.; Casas-Arce, E.; Hooper, N. M.; Johnson, A. P.; Fishwick, C. W. G., Discovery of Biphenylacetamide-Derived Inhibitors of BACE1 Using de Novo Structure-Based Molecular Design. *J. Med. Chem.* **2013**, *56* (5), 1843-1852.
38. Perna, A. M.; Rodrigues, T.; Schmidt, T. P.; Böhm, M.; Stutz, K.; Reker, D.; Pfeiffer, B.; Altmann, K.-H.; Backert, S.; Wessler, S.; Schneider, G., Fragment-Based De Novo Design Reveals a Small-Molecule Inhibitor of Helicobacter Pylori HtrA. *Angew. Chem. Int. Ed.* **2015**, *54* (35), 10244-10248.
39. de Jong, L. A. A.; Uges, D. R. A.; Franke, J. P.; Bischoff, R., Receptor–ligand binding assays: Technologies and Applications. *J. Chromatogr. B* **2005**, *829* (1), 1-25.
40. Stoddart, L. A.; Kilpatrick, L. E.; Briddon, S. J.; Hill, S. J., Probing the pharmacology of G protein-coupled receptors with fluorescent ligands. *Neuropharmacology* **2015**, *98*, 48-57.
41. Vernall, A. J.; Hill, S. J.; Kellam, B., The evolving small-molecule fluorescent-conjugate toolbox for Class A GPCRs. *Br. J. Pharmacol.* **2014**, *171* (5), 1073-1084.
42. Kozma, E.; Suresh Jayasekara, P.; Squarcialupi, L.; Paoletta, S.; Moro, S.; Federico, S.; Spalluto, G.; Jacobson, K. A., Fluorescent ligands for adenosine receptors. *Bioorg. Med. Chem. Lett.* **2013**, *23* (1), 26-36.
43. McGrath, J. C.; Arribas, S.; Daly, C. J., Fluorescent ligands for the study of receptors. *Trends Pharmacol. Sci.* **1996**, *17* (11), 393-399.
44. Baidur, N.; Triggle, D. J., Selective fluorescent ligands for pharmacological receptors. *Drug Dev. Res.* **1994**, *33* (4), 373-398.
45. Tahtaoui, C.; Parrot, I.; Klotz, P.; Guillier, F.; Galzi, J.-L.; Hibert, M.; Ilien, B., Fluorescent Pirenzepine Derivatives as Potential Bitopic Ligands of the Human M1 Muscarinic Receptor. *J. Med. Chem.* **2004**, *47* (17), 4300-4315.
46. Jacobson, K. A.; Ukena, D.; Padgett, W.; Kirk, K. L.; Daly, J. W., Molecular probes for extracellular adenosine receptors. *Biochem. Pharmacol.* **1987**, *36* (10), 1697-1707.
47. Middleton, R. J.; Kellam, B., Fluorophore-tagged GPCR ligands. *Curr. Opin. Chem. Biol.* **2005**, *9* (5), 517-525.
48. Li, L.; Kracht, J.; Peng, S.; Bernhardt, G.; Elz, S.; Buschauer, A., Synthesis and pharmacological activity of fluorescent histamine H2 receptor antagonists related to potentidine1. *Bioorg. Med. Chem. Lett.* **2003**, *13* (10), 1717-1720.
49. Buschmann, V.; Weston, K. D.; Sauer, M., Spectroscopic Study and Evaluation of Red-Absorbing Fluorescent Dyes. *Bioconjugate Chemistry* **2003**, *14* (1), 195-204.
50. Vernall, A. J.; Stoddart, L. A.; Briddon, S. J.; Ng, H. W.; Laughton, C. A.; Doughty, S. W.; Hill, S. J.; Kellam, B., Conversion of a non-selective adenosine receptor antagonist into A3-selective high affinity fluorescent probes using peptide-based linkers. *Org. Biomol. Chem.* **2013**, *11* (34), 5673-5682.
51. Jacobson, K. A.; Kirk, K. L.; Padgett, W. L.; Daly, J. W., A functionalized congener approach to adenosine receptor antagonists: amino acid conjugates of 1,3-dipropylxanthine. *Mol. Pharmacol.* **1986**, *29* (2), 126-133.
52. Stoddart, L. A.; Vernall, A. J.; Bouzo-Lorenzo, M.; Bosma, R.; Kooistra, A. J.; de Graaf, C.; Vischer, H. F.; Leurs, R.; Briddon, S. J.; Kellam, B.; Hill, S. J., Development of novel fluorescent histamine H(1)-receptor antagonists to study ligand-binding kinetics in living cells. *Sci. Rep.* **2018**, *8* (1), 1572-1572.

53. Rose, R. H.; Briddon, S. J.; Hill, S. J., A novel fluorescent histamine H1 receptor antagonist demonstrates the advantage of using fluorescence correlation spectroscopy to study the binding of lipophilic ligands. *Br. J. Pharmacol.* **2012**, *165* (6), 1789-1800.
54. Cooper, A. G.; MacDonald, C.; Glass, M.; Hook, S.; Tyndall, J. D. A.; Vernall, A. J., Alkyl indole-based cannabinoid type 2 receptor tools: Exploration of linker and fluorophore attachment. *Eur. J. Med. Chem.* **2018**, *145*, 770-789.
55. Singh, S.; Cooper, Samantha L.; Glenn, J. R.; Beresford, J.; Percival, L. R.; Tyndall, J. D. A.; Hill, S. J.; Kilpatrick, L. E.; Vernall, A. J., Synthesis of novel (benzimidazolyl)isoquinolinols and evaluation as adenosine A1 receptor tools. *RSC Advances* **2018**, *8* (29), 16362-16369.
56. Falck, B.; Hillarp, N.-Å.; Thieme, G.; Torp, A., Fluorescence of Catechol Amines and Related Compounds Condensed with Formaldehyde. *J. Histochem. Cytochem.* **1962**, *10* (3), 348-354.
57. Schembri, L. S.; Stoddart, L. A.; Briddon, S. J.; Kellam, B.; Canals, M.; Graham, B.; Scammells, P. J., Synthesis, Biological Evaluation, and Utility of Fluorescent Ligands Targeting the μ -Opioid Receptor. *J. Med. Chem.* **2015**, *58* (24), 9754-9767.
58. Briddon, S. J.; Hill, S. J., Pharmacology under the microscope: the use of fluorescence correlation spectroscopy to determine the properties of ligand-receptor complexes. *Trends Pharmacol. Sci.* **2007**, *28* (12), 637-645.
59. Fournie-Zaluski, M. C.; Gacel, G.; Roques, B. P.; Senault, B.; Lecomte, J. M.; Malfroy, B.; Swerts, J. P.; Schwartz, J. C., Fluorescent enkephalin derivatives with biological activity. *Biochem. Biophys. Res. Commun.* **1978**, *83* (1), 300-305.
60. Hazum, E.; Chang, K. J.; Shechter, Y.; Wilkinson, S.; Cuatrecasas, P., Fluorescent and photo-affinity enkephalin derivatives: Preparation and interaction with opiate receptors. *Biochem. Biophys. Res. Commun.* **1979**, *88* (3), 841-846.
61. Mihara, H.; Lee, S.; Shimohigashi, Y.; Aoyagi, H.; Kato, T.; Izumiya, N.; Costa, T., δ and μ opiate receptor probes: fluorescent enkephalins with high receptor affinity and specificity. *FEBS Lett.* **1985**, *193* (1), 35-38.
62. Mihara, H.; Lee, S.; Shimohigashi, Y.; Aoyagi, H.; Kato, T.; Izumiya, N.; Costa, T., Tyr1-substituted and fluorescent Pya1-enkephalins bind strongly and selectively to μ and δ opiate receptors. *Biochem. Biophys. Res. Commun.* **1986**, *136* (3), 1170-1176.
63. Berezowska, I.; Chung, N. N.; Lemieux, C.; Zelent, B.; Szeto, H. H.; Schiller, P. W., Highly potent fluorescent analogues of the opioid peptide [Dmt1]DALDA. *Peptides* **2003**, *24* (8), 1195-1200.
64. Balboni, G.; Salvadori, S.; Dal Piaz, A.; Bortolotti, F.; Argazzi, R.; Negri, L.; Lattanzi, R.; Bryant, S. D.; Jinsmaa, Y.; Lazarus, L. H., Highly Selective Fluorescent Analogue of the Potent δ -Opioid Receptor Antagonist Dmt-Tic. *J. Med. Chem.* **2004**, *47* (26), 6541-6546.
65. Shi, M.; Bennett, T. A.; Cimino, D. F.; Maestas, D. C.; Foutz, T. D.; Gurevich, V. V.; Sklar, L. A.; Prossnitz, E. R., Functional Capabilities of an N-Formyl Peptide Receptor-Gai2 Fusion Protein: Assemblies with G Proteins and Arrestins. *Biochemistry* **2003**, *42* (24), 7283-7293.
66. Josan, J. S.; Morse, D. L.; Xu, L.; Trissal, M.; Baggett, B.; Davis, P.; Vagner, J.; Gillies, R. J.; Hruby, V. J., Solid-phase synthetic strategy and bioevaluation of a labeled delta-opioid receptor ligand Dmt-Tic-Lys for in vivo imaging. *Org. Lett.* **2009**, *11* (12), 2479-2482.
67. Kolb, V. M.; Koman, A.; Terenius, L., Fluorescent probes for opioid receptors. *Life Sci.* **1983**, *33*, 423-426.

68. Kolb, V. M.; Koman, A. D. o. P. P.; Neil, A., Synthesis and Pharmacological Characterization of Fluorescent Opioid Receptor Probes. *Pharm. Res.* **1985**, *2* (6), 266-271.
69. Archer, S.; Medzhradsky, F.; Seyed-Mozaffari, A.; Emmerson, P. J., Synthesis and characterization of 7-nitrobenzo-2-oxa-1,3-diazole (NBD)-labeled fluorescent opioids. *Biochem. Pharmacol.* **1992**, *43* (2), 301-306.
70. Emmerson, P. J.; Archer, S.; El-Hamouly, W.; Mansour, A.; Akil, H.; Medzhradsky, F., Synthesis and Characterization of 4,4-Difluoro-4-bora-3a,4a-Diazas-Indacene (BODIPY)-Labeled Fluorescent Ligands for the Mu Opioid Receptor. *Biochem. Pharmacol.* **1997**, *54* (12), 1315-1322.
71. Lam, R.; Gondin, A. B.; Canals, M.; Kellam, B.; Briddon, S. J.; Graham, B.; Scammells, P. J., Fluorescently Labeled Morphine Derivatives for Bioimaging Studies. *J. Med. Chem.* **2018**, *61* (3), 1316-1329.
72. Drakopoulos, A.; Decker, M., Development and Biological Applications of Fluorescent Opioid Ligands. *ChemPlusChem* **2020**, *85* (6), 1354-1364.
73. Lipkowski, A. W.; Tam, S. W.; Portoghese, P. S., Peptides as receptor selectivity modulators of opiate pharmacophores. *J. Med. Chem.* **1986**, *29* (7), 1222-1225.
74. Hedberg, M. H.; Johansson, A. M.; Fowler, C. J.; Terenius, L.; Hacksell, U., Palladium-catalyzed synthesis of C3-substituted 3-deoxymorphines. *Bioorg. Med. Chem. Lett.* **1994**, *4* (21), 2527-2532.
75. Wentland, M. P.; Lou, R.; Dehnhardt, C. M.; Duan, W.; Cohen, D. J.; Bidlack, J. M., 3-Carboxamido analogues of morphine and naltrexone: synthesis and opioid receptor binding properties. *Bioorg. Med. Chem. Lett.* **2001**, *11* (13), 1717-1721.
76. Mignat, C.; Wille, U.; Ziegler, A., Affinity profiles of morphine, codeine, dihydrocodeine and their glucuronides at opioid receptor subtypes. *Life Sci.* **1995**, *56* (10), 793-799.
77. Smith, H. S., Opioid metabolism. *Mayo Clin. Proc.* **2009**, *84* (7), 613-624.
78. Klous, M. G.; Brink, W. V. d.; Ree, J. M. V.; Beijnen, J. H., Development of pharmaceutical heroin preparations for medical co-prescription to opioid dependent patients. *Drug Alcohol Depend.* **2005**, *80* (3), 283-295.
79. Stinchcomb, A. L.; Swaan, P. W.; Ekabo, O.; Harris, K. K.; Browe, J.; Hammell, D. C.; Cooperman, T. A.; Pearsall, M., Straight-Chain Naltrexone Ester Prodrugs: Diffusion and Concurrent Esterase Biotransformation in Human Skin. *J. Pharm. Sci.* **2002**, *91* (12), 2571-2578.
80. Wang, J.-J.; Sung, K. C.; Huang, J.-F.; Yeh, C.-H.; Fang, J.-Y., Ester prodrugs of morphine improve transdermal drug delivery: a mechanistic study. *J. Pharm. Pharmacol.* **2007**, *59* (7), 917-925.
81. Leppert, W.; Woron, J., The role of naloxegol in the management of opioid-induced bowel dysfunction. *Therap. Adv. Gastroenterol.* **2016**, *9* (5), 736-746.
82. Fürst, S.; Friedmann, T.; Tóth, Z.; Hosztafi, S.; Simon, C.; Makleit, S., The pharmacological significance of the spatial orientation of C-6-OH group in ring C of morphine. *Regul. Pept.* **1994**, *54* (1), 99-100.
83. Chatterjie, N.; Inturrisi, C. E.; Dayton, H. B.; Blumberg, H., Stereospecific synthesis of the 6 β -hydroxy metabolites of naltrexone and naloxone. *J. Med. Chem.* **1975**, *18* (5), 490-492.
84. Jiang, J. B.; Hanson, R. N.; Portoghese, P. S.; Takemori, A. E., Stereochemical studies on medicinal agents. 23. Synthesis and biological evaluation of 6-amino derivatives of naloxone and naltrexone. *J. Med. Chem.* **1977**, *20* (8), 1100-1102.
85. Obeng, S.; Wang, H.; Jali, A.; Stevens, D. L.; Akbarali, H. I.; Dewey, W. L.; Selley, D. E.; Zhang, Y., Structure–Activity Relationship Studies of 6 α - and 6 β -

- Indolylacetamidonaltrexamine Derivatives as Bitopic Mu Opioid Receptor Modulators and Elaboration of the “Message-Address Concept” To Comprehend Their Functional Conversion. *ACS Chem. Neurosci.* **2019**, *10* (3), 1075-1090.
86. Ma, H.; Obeng, S.; Wang, H.; Zheng, Y.; Li, M.; Jali, A. M.; Stevens, D. L.; Dewey, W. L.; Selley, D. E.; Zhang, Y., Application of Bivalent Bioisostere Concept on Design and Discovery of Potent Opioid Receptor Modulators. *J. Med. Chem.* **2019**, *62* (24), 11399-11415.
87. Cami-Kobeci, G.; Neal, A. P.; Bradbury, F. A.; Purington, L. C.; Aceto, M. D.; Harris, L. S.; Lewis, J. W.; Traynor, J. R.; Husbands, S. M., Mixed κ/μ Opioid Receptor Agonists: The 6 β -Naltrexamines. *J. Med. Chem.* **2009**, *52* (6), 1546-1552.
88. Nagase, H.; Hayakawa, J.; Kawamura, K.; Kawai, K.; Takezawa, Y.; Matsuura, H.; Tajima, C.; Endo, T., DISCOVERY OF A STRUCTURALLY NOVEL OPIOID K-AGONIST DERIVED FROM 4, 5-EPOXYMORPHINAN. *Chem. Pharm. Bull. (Tokyo)* **1998**, *46* (2), 366-369.
89. Derrick, I.; Lewis, J. W.; Moynihan, H. A.; Broadbear, J.; Woods, J. H., Potential irreversible ligands for opioid receptors. Cinnamoyl derivatives of beta-naltrexamine. *J Pharm Pharmacol* **1996**, *48* (2), 192-6.
90. Derrick, I.; Moynihan, H. A.; Broadbear, J.; Woods, J. H.; Lewis, J. W., 6N-Cinnamoyl- β -naltrexamine and its *p*-nitro derivative. High efficacy κ -opioid agonists with weak antagonist actions. *Bioorg. Med. Chem. Lett.* **1996**, *6* (2), 167-172.
91. Takemori, A. E.; Larson, D. L.; Portoghese, P. S., The irreversible narcotic antagonistic and reversible agonistic properties of the fumaramate methyl ester derivative of naltrexone. *Eur. J. Pharmacol.* **1981**, *70* (4), 445-451.
92. Takemori, A. E.; Portoghese, P. S., Affinity Labels for Opioid Receptors. *Annual Review of Pharmacology and Toxicology* **1985**, *25* (1), 193-223.
93. Werner, L.; Machara, A.; Adams, D. R.; Cox, D. P.; Hudlicky, T., Synthesis of Buprenorphine from Oripavine via N-Demethylation of Oripavine Quaternary Salts. *J. Org. Chem.* **2011**, *76* (11), 4628-4634.
94. Lewis, J. W.; Husbands, S. M., The orvinols and related opioids--high affinity ligands with diverse efficacy profiles. *Curr. Pharm. Des.* **2004**, *10* (7), 717-32.
95. Cueva, J. P.; Roche, C.; Ostovar, M.; Kumar, V.; Clark, M. J.; Hillhouse, T. M.; Lewis, J. W.; Traynor, J. R.; Husbands, S. M., C7 β -Methyl Analogues of the Orvinols: The Discovery of Kappa Opioid Antagonists with Nociceptin/Orphanin FQ Peptide (NOP) Receptor Partial Agonism and Low, or Zero, Efficacy at Mu Opioid Receptors. *J. Med. Chem.* **2015**, *58* (10), 4242-4249.
96. Bentley, K. W.; Hardy, D. G., Novel analgesics and molecular rearrangements in the morphine-thebaine group. III. Alcohols of the 6,14-endo-ethenotetrahydrooripavine series and derived analogs of N-allylnormorphine and -norcodeine. *J. Am. Chem. Soc.* **1967**, *89* (13), 3281-3292.
97. Krüll, J.; Fehler, S. K.; Hofmann, L.; Nebel, N.; Maschauer, S.; Prante, O.; Gmeiner, P.; Lanig, H.; Hübner, H.; Heinrich, M. R., Synthesis, Radiosynthesis and Biological Evaluation of Buprenorphine-Derived Phenylazocarboxamides as Novel μ -Opioid Receptor Ligands. *ChemMedChem* **2020**, *15* (13), 1175-1186.
98. Cami-Kobeci, G.; Polgar, W. E.; Khroyan, T. V.; Toll, L.; Husbands, S. M., Structural Determinants of Opioid and NOP Receptor Activity in Derivatives of Buprenorphine. *J. Med. Chem.* **2011**, *54* (19), 6531-6537.
99. Rennison, D.; Neal, A. P.; Cami-Kobeci, G.; Aceto, M. D.; Martinez-Bermejo, F.; Lewis, J. W.; Husbands, S. M., Cinnamoyl Derivatives of 7 α -Aminomethyl-6,14-endo-ethanotetrahydrothebaine and 7 α -Aminomethyl-6,14-endo-ethanotetrahydrooripavine and Related Opioid Ligands. *J. Med. Chem.* **2007**, *50* (21), 5176-5182.

100. Shafiee, A.; Amanlou, M.; Farsam, H.; Dehpour, A. R.; Mir-Ershadi, F.; Mani, A. R., Synthesis and pharmacological activity of thebaine-derived μ -opioid receptor agonists. *Pharm. Acta Helv.* **1999**, *73* (5), 251-254.
101. Loew, G. H.; Berkowitz, D. S., Quantum chemical studies of N-substituent variation in the oxymorphone series of opiate narcotics. *J. Med. Chem.* **1978**, *21* (1), 101-106.
102. Ben Haddou, T.; Béni, S.; Hosztafi, S.; Malfacini, D.; Calo, G.; Schmidhammer, H.; Spetea, M., Pharmacological investigations of N-substituent variation in morphine and oxymorphone: opioid receptor binding, signaling and antinociceptive activity. *PLoS One* **2014**, *9* (6), e99231.
103. Yuan, C.-S.; Israel, R. J., Methylnaltrexone, a novel peripheral opioid receptor antagonist for the treatment of opioid side effects. *Expert Opin. Investig. Drugs* **2006**, *15* (5), 541-552.
104. Feinberg, A. P.; Creese, I.; Snyder, S. H., The Opiate Receptor: A Model Explaining Structure-Activity Relationships of Opiate Agonists and Antagonists. *Proc. Natl. Acad. Sci. U. S. A.* **1976**, *73* (11), 4215-4219.
105. Lattanzi, R.; Spetea, M.; Schüllner, F.; Rief, S. B.; Krassnig, R.; Negri, L.; Schmidhammer, H., Synthesis and Biological Evaluation of 14-Alkoymorphinans. 22. Influence of the 14-Alkoxy Group and the Substitution in Position 5 in 14-Alkoymorphinan-6-ones on in Vitro and in Vivo Activities. *J. Med. Chem.* **2005**, *48* (9), 3372-3378.
106. Greiner, E.; Spetea, M.; Krassnig, R.; Schüllner, F.; Aceto, M.; Harris, L. S.; Traynor, J. R.; Woods, J. H.; Coop, A.; Schmidhammer, H., Synthesis and Biological Evaluation of 14-Alkoymorphinans. 18. N-Substituted 14-Phenylpropyloxymorphinan-6-ones with Unanticipated Agonist Properties: Extending the Scope of Common Structure-Activity Relationships. *J. Med. Chem.* **2003**, *46* (9), 1758-1763.
107. Husbands, S. M.; Sadd, J.; Broadbear, J. H.; Woods, J. H.; Martin, J.; Traynor, J. R.; Aceto, M. D.; Bowman, E. R.; Harris, L. S.; Lewis, J. W., 3-Alkyl Ethers of Cloccinamox: Delayed Long-Term μ -Antagonists with Variable μ Efficacy. *J. Med. Chem.* **1998**, *41* (18), 3493-3498.
108. Raynor, K.; Kong, H.; Chen, Y.; Yasuda, K.; Yu, L.; Bell, G. I.; Reisine, T., Pharmacological characterization of the cloned kappa-, delta-, and mu-opioid receptors. *Mol. Pharmacol.* **1994**, *45* (2), 330-334.
109. Kelly, E.; Mundell, S. J.; Sava, A.; Roth, A. L.; Felici, A.; Maltby, K.; Nathan, P. J.; Bullmore, E. T.; Henderson, G., The opioid receptor pharmacology of GSK1521498 compared to other ligands with differential effects on compulsive reward-related behaviours. *Psychopharmacology* **2015**, *232* (1), 305-314.
110. Zimmerman, D. M.; Gidda, J. S.; Cantrell, B. E.; Schoepp, D. D.; Johnson, B. G.; Leander, J. D., Discovery of a Potent, Peripherally Selective trans-3,4-Dimethyl-4-(3-hydroxyphenyl)piperidine Opioid Antagonist for the Treatment of Gastrointestinal Motility Disorders. *J. Med. Chem.* **1994**, *37* (15), 2262-2265.
111. Le Bourdonnec, B.; Belanger, S.; Cassel, J. A.; Stabley, G. J.; DeHaven, R. N.; Dolle, R. E., trans-3,4-dimethyl-4-(3-carboxamidophenyl)piperidines: a novel class of micro-selective opioid antagonists. *Bioorg. Med. Chem. Lett.* **2003**, *13* (24), 4459-4462.
112. Stefanucci, A.; Dimmito, M. P.; Macedonio, G.; Ciarlo, L.; Pieretti, S.; Novellino, E.; Lei, W.; Barlow, D.; Houseknecht, K. L.; Streicher, J. M.; Mollica, A., Potent, Efficacious, and Stable Cyclic Opioid Peptides with Long Lasting Antinociceptive Effect after Peripheral Administration. *J. Med. Chem.* **2020**, *63* (5), 2673-2687.

113. Ananthan, S.; Kezar, H. S.; Carter, R. L.; Saini, S. K.; Rice, K. C.; Wells, J. L.; Davis, P.; Xu, H.; Dersch, C. M.; Bilsky, E. J.; Porreca, F.; Rothman, R. B., Synthesis, Opioid Receptor Binding, and Biological Activities of Naltrexone-Derived Pyrido- and Pyrimidomorphinans. *J. Med. Chem.* **1999**, *42* (18), 3527-3538.
114. Portoghese, P. S.; Nagase, H.; MaloneyHuss, K. E.; Lin, C. E.; Takemori, A. E., Role of spacer and address components in peptidomimetic .delta.-opioid receptor antagonists related to naltrindole. *J. Med. Chem.* **1991**, *34* (5), 1715-1720.
115. Spetea, M.; Schüllner, F.; Moisa, R. C.; Berzetei-Gurske, I. P.; Schraml, B.; Dörfler, C.; Aceto, M. D.; Harris, L. S.; Coop, A.; Schmidhammer, H., Synthesis and Biological Evaluation of 14-Alkoymorphinans. 21. Novel 4-Alkoxy and 14-Phenylpropoxy Derivatives of the μ Opioid Receptor Antagonist Cyprodime. *J. Med. Chem.* **2004**, *47* (12), 3242-3247.
116. Comer, S. D.; Burke, T. F.; Lewis, J. W.; Woods, J. H., Clocinnamox: a novel, systemically-active, irreversible opioid antagonist. *J. Pharmacol. Exp. Ther.* **1992**, *262* (3), 1051-1056.
117. Zernig, G.; Burke, T.; Lewis, J. W.; Woods, J. H., Mechanism of clocinnamox blockade of opioid receptors: evidence from in vitro and ex vivo binding and behavioral assays. *J. Pharmacol. Exp. Ther.* **1996**, *279* (1), 23-31.
118. Nieland, N. P. R.; Moynihan, H. A.; Carrington, S.; Broadbear, J.; Woods, J. H.; Traynor, J. R.; Husbands, S. M.; Lewis, J. W., Structural Determinants of Opioid Activity in Derivatives of 14-Aminomorphinones: Effect of Substitution in the Aromatic Ring of Cinnamoylaminomorphinones and Codeinones. *J. Med. Chem.* **2006**, *49* (17), 5333-5338.
119. Filer, C. N.; Seguin, R. J., Synthesis of [15, 16-3H] beta-funaltrexamine. *J. Label. Compd. Radiopharm.* **2013**, *56* (5), 310-311.
120. Abdel-Magid, A. F.; Carson, K. G.; Harris, B. D.; Maryanoff, C. A.; Shah, R. D., Reductive Amination of Aldehydes and Ketones with Sodium Triacetoxyborohydride. Studies on Direct and Indirect Reductive Amination Procedures1. *J. Org. Chem.* **1996**, *61* (11), 3849-3862.
121. Benoiton, N. L., *Chemistry of Peptide Synthesis*. Taylor and Francis Group: 2006.
122. Yung-Chi, C.; Prusoff, W. H., Relationship between the inhibition constant (KI) and the concentration of inhibitor which causes 50 per cent inhibition (I50) of an enzymatic reaction. *Biochem. Pharmacol.* **1973**, *22* (23), 3099-3108.
123. Goodman, A. J.; Le Bourdonnec, B.; Dolle, R. E., Mu Opioid Receptor Antagonists: Recent Developments. *ChemMedChem* **2007**, *2* (11), 1552-1570.
124. Ziauddeen, H.; Nestor, L. J.; Subramaniam, N.; Dodds, C.; Nathan, P. J.; Miller, S. R.; Sarai, B. K.; Maltby, K.; Fernando, D.; Warren, L.; Hosking, L. K.; Waterworth, D.; Korzeniowska, A.; Win, B.; Richards, D. B.; Vasist Johnson, L.; Fletcher, P. C.; Bullmore, E. T., Opioid Antagonists and the A118G Polymorphism in the μ -Opioid Receptor Gene: Effects of GSK1521498 and Naltrexone in Healthy Drinkers Stratified by OPRM1 Genotype. *Neuropsychopharmacology* **2016**, *41* (11), 2647-2657.
125. Ignar, D. M.; Goetz, A. S.; Noble, K. N.; Carballo, L. H.; Stroup, A. E.; Fisher, J. C.; Boucheron, J. A.; Brainard, T. A.; Larkin, A. L.; Epperly, A. H.; Shearer, T. W.; Sorensen, S. D.; Speake, J. D.; Hommel, J. D., Regulation of Ingestive Behaviors in the Rat by GSK1521498, a Novel μ -Opioid Receptor-Selective Inverse Agonist. *J. Pharmacol. Exp. Ther.* **2011**, *339* (1), 24-34.
126. Zimmerman, D. M.; Nickander, R.; Horng, J. S.; Wong, D. T., New structural concepts for narcotic antagonists defined in a 4-phenylpiperidine series. *Nature* **1978**, *275* (5678), 332-334.

127. Mitch, C. H.; Leander, J. D.; Mendelsohn, L. G.; Shaw, W. N.; Wong, D. T.; Cantrell, B. E.; Johnson, B. G.; Reel, J. K.; Snoddy, J. D., 3,4-Dimethyl-4-(3-hydroxyphenyl)piperidines: opioid antagonists with potent anorectant activity. *J. Med. Chem.* **1993**, *36* (20), 2842-2850.
128. Thomas, J. B.; Zheng, X.; Mascarella, S. W.; Rothman, R. B.; Dersch, C. M.; Partilla, J. S.; Flippen-Anderson, J. L.; George, C. F.; Cantrell, B. E.; Zimmerman, D. M.; Carroll, F. I., N-Substituted 9 β -Methyl-5-(3-hydroxyphenyl)morphans Are Opioid Receptor Pure Antagonists. *J. Med. Chem.* **1998**, *41* (21), 4143-4149.
129. Hashimoto, A.; Jacobson, A. E.; Rothman, R. B.; Dersch, C. M.; George, C.; Flippen-Anderson, J. L.; Rice, K. C., Probes for Narcotic Receptor Mediated Phenomena. Part 28: New Opioid Antagonists from Enantiomeric Analogues of 5-(3-Hydroxyphenyl)-N-phenylethylmorphans. *Bioorg. Med. Chem.* **2002**, *10* (10), 3319-3329.
130. Long, D. D.; Armstrong, S. R.; Beattie, D. T.; Campbell, C. B.; Church, T. J.; Colson, P.-J.; Dalziel, S. M.; Jacobsen, J. R.; Jiang, L.; Obedencio, G. P.; Rapta, M.; Saito, D.; Stergiades, I.; Tsuruda, P. R.; Van Dyke, P. M.; Vickery, R. G., Discovery of Axelopropran (TD-1211): A Peripherally Restricted μ -Opioid Receptor Antagonist. *ACS Med. Chem. Lett.* **2019**, *10* (12), 1641-1647.
131. Jiang, L.; Beattie, D. T.; Jacobsen, J. R.; Kintz, S.; Obedencio, G. P.; Saito, D.; Stergiades, I.; Vickery, R. G.; Long, D. D., Discovery of N-substituted-endo-3-(8-azabicyclo[3.2.1]oct-3-yl)-phenol and -phenyl carboxamide series of μ -opioid receptor antagonists. *Bioorg. Med. Chem. Lett.* **2017**, *27* (13), 2926-2930.
132. Díaz, N.; Benvenga, M.; Emmerson, P.; Favours, R.; Mangold, M.; McKinzie, J.; Patel, N.; Peters, S.; Quimby, S.; Shannon, H.; Siegel, M.; Statnick, M.; Thomas, E.; Woodland, J.; Surface, P.; Mitch, C., SAR and biological evaluation of novel trans-3,4-dimethyl-4-arylpiperidine derivatives as opioid antagonists. *Bioorg. Med. Chem. Lett.* **2005**, *15* (17), 3844-3848.
133. Kormos, C. M.; Gichinga, M. G.; Maitra, R.; Runyon, S. P.; Thomas, J. B.; Brieady, L. E.; Mascarella, S. W.; Navarro, H. A.; Carroll, F. I., Design, Synthesis, and Biological Evaluation of (3R)-1,2,3,4-Tetrahydro-7-hydroxy-N-[(1S)-1-[(3R,4R)-4-(3-hydroxyphenyl)-3,4-dimethyl-1-piperidinyl]methyl]-2-methylpropyl]-3-isoquinolinecarboxamide (JDTic) Analogues: In Vitro Pharmacology and ADME Profile. *J. Med. Chem.* **2014**, *57* (17), 7367-7381.
134. Cai, T. B.; Zou, Z.; Thomas, J. B.; Brieady, L.; Navarro, H. A.; Carroll, F. I., Synthesis and In Vitro Opioid Receptor Functional Antagonism of Analogues of the Selective Kappa Opioid Receptor Antagonist (3R)-7-Hydroxy-N-[(1S)-1-[(3R,4R)-4-(3-hydroxyphenyl)-3,4-dimethyl-1-piperidinyl]methyl]-2-methylpropyl]-1,2,3,4-tetrahydro-3-isoquinolinecarboxamide (JDTic). *J. Med. Chem.* **2008**, *51* (6), 1849-1860.
135. Zimmerman, D. M.; Leander, J. D.; Cantrell, B. E.; Reel, J. K.; Snoddy, J.; Mendelsohn, L. G.; Johnson, B. G.; Mitch, C. H., Structure-activity relationships of trans-3,4-dimethyl-4-(3-hydroxyphenyl)piperidine antagonists for μ - and κ -opioid receptors. *J. Med. Chem.* **1993**, *36* (20), 2833-2841.
136. Le Bourdonnec, B.; Goodman, A. J.; Michaut, M.; Ye, H.-F.; Graczyk, T. M.; Belanger, S.; Herbertz, T.; Yap, G. P. A.; DeHaven, R. N.; Dolle, R. E., Elucidation of the Bioactive Conformation of the N-Substituted trans-3,4-Dimethyl-4-(3-hydroxyphenyl)piperidine Class of μ -Opioid Receptor Antagonists. *J. Med. Chem.* **2006**, *49* (25), 7278-7289.
137. Le Bourdonnec, B.; Goodman, A. J.; Graczyk, T. M.; Belanger, S.; Seida, P. R.; DeHaven, R. N.; Dolle, R. E., Synthesis and Pharmacological Evaluation of Novel

- Octahydro-1H-pyrido[1,2-a]pyrazine as μ -Opioid Receptor Antagonists. *J. Med. Chem.* **2006**, *49* (25), 7290-7306.
138. Thomas, J. B.; Mascarella, S. W.; Rothman, R. B.; Partilla, J. S.; Xu, H.; McCullough, K. B.; Dersch, C. M.; Cantrell, B. E.; Zimmerman, D. M.; Carroll, F. I., Investigation of the N-Substituent Conformation Governing Potency and μ Receptor Subtype-Selectivity in (+)-(3R,4R)-Dimethyl-4-(3-hydroxyphenyl)- piperidine Opioid Antagonists. *J. Med. Chem.* **1998**, *41* (11), 1980-1990.
139. Le Bourdonnec, B.; Barker, W. M.; Belanger, S.; Wiant, D. D.; Conway-James, N. C.; Cassel, J. A.; O'Neill, T. J.; Little, P. J.; DeHaven, R. N.; DeHaven-Hudkins, D. L.; Dolle, R. E., Novel trans-3,4-dimethyl-4-(3-hydroxyphenyl)piperidines as μ opioid receptor antagonists with improved opioid receptor selectivity profiles. *Bioorg. Med. Chem. Lett.* **2008**, *18* (6), 2006-2012.
140. Le Bourdonnec, B.; Goodman, A. J.; Michaut, M.; Ye, H.-F.; Graczyk, T. M.; Belanger, S.; DeHaven, R. N.; Dolle, R. E., Synthesis and structure-activity relationships of a new series of 2 α -substituted trans-4,5-dimethyl-4-(3-hydroxyphenyl)piperidine as μ -selective opioid antagonists. *Bioorg. Med. Chem. Lett.* **2006**, *16* (4), 864-868.
141. Werner, J. A.; Cerbone, L. R.; Frank, S. A.; Ward, J. A.; Labib, P.; Tharp-Taylor, R. W.; Ryan, C. W., Synthesis of trans-3,4-Dimethyl-4-(3-hydroxyphenyl)piperidine Opioid Antagonists: Application of the Cis-Thermal Elimination of Carbonates to Alkaloid Synthesis. *J. Org. Chem.* **1996**, *61* (2), 587-597.
142. Mitch, C. H.; Zimmerman, D. M.; Snoddy, J. D.; Reel, J. K.; Cantrell, B. E., Synthesis and absolute configuration of LY255582, a potent opioid antagonist. *J. Org. Chem.* **1991**, *56* (4), 1660-1663.
143. Zimmerman, D. M.; Cantrell, B. E.; Reel, J. K.; Hemrick-Luecke, S. K.; Fuller, R. W., Characterization of the neurotoxic potential of m-methoxy-MPTP and the use of its N-ethyl analog as a means of avoiding exposure to a possible Parkinson-causing agent. *J. Med. Chem.* **1986**, *29* (8), 1517-1520.
144. Furkert, D. P.; Husbands, S. M., First Asymmetric Synthesis of trans-3,4-Dimethyl-4-arylpiperidines. *Org. Lett.* **2007**, *9* (19), 3769-3771.
145. Stress, C. J.; Sauter, B.; Schneider, L. A.; Sharpe, T.; Gillingham, D., A DNA-Encoded Chemical Library Incorporating Elements of Natural Macrocycles. *Angew. Chem. Int. Ed.* **2019**, *58* (28), 9570-9574.
146. Pícha, J.; Buděšínský, M.; Macháčková, K.; Collinsová, M.; Jiráček, J., Optimized syntheses of Fmoc azido amino acids for the preparation of azidopeptides. *J. Pept. Sci.* **2017**, *23* (3), 202-214.
147. Zhou, R.; Basile, F., Convective-heating thermal decomposition/digestion of peptides and proteins on surfaces. *J. Anal. Appl. Pyrolysis* **2017**, *127*, 451-460.
148. Cohen, S. L.; Price, C.; Vlasak, J., β -Elimination and Peptide Bond Hydrolysis: Two Distinct Mechanisms of Human IgG1 Hinge Fragmentation upon Storage. *J. Am. Chem. Soc.* **2007**, *129* (22), 6976-6977.
149. Gondin, A. B.; Halls, M. L.; Canals, M.; Briddon, S. J., GRK Mediates μ -Opioid Receptor Plasma Membrane Reorganization. *Front. Mol. Neurosci.* **2019**, *12* (104).